International
Progress Report

IPR-02-37

Äspö Hard Rock Laboratory

Fracman modelling of geochemical end-member transport pathways Äspö HRL, Äspö Sweden

Task 5

Bill Dershowitz
Dawn Shuttle
Kate Klise
Golder Associates Inc

Masahiro Uchida
JNC

Richard Metcalfe
JNC-Tono

Mark Cave
British Geological Survey

November 2000

Svensk Kärnbränslehantering AB
Swedish Nuclear Fuel
and Waste Management Co
Box 5864
SE-102 40 Stockholm Sweden
Tel +46 8 459 84 00
Fax +46 8 661 57 19

Äspö Hard Rock
Laboratory

Report no.	No.
IPR-02-37	F65K
Author	Date
Dershowitz, Shuttle, Uchida, Metcalfe, Cave, Klise	00-11-01
Checked by	Date
M. Uchida	01-06-14
Approved	Date
Christer Svemar	02-11-19

Äspö Hard Rock Laboratory

Fracman modelling of geochemical end-member transport pathways Äspö HRL, Äspö Sweden

Task 5

Bill Dershowitz
Dawn Shuttle
Kate Klise
Golder Associates Inc

Masahiro Uchida
JNC

Richard Metcalfe
JNC-Tono

Mark Cave
British Geological Survey

November 2000

Keywords: Discrete fracture modelling, groundwater flow, solute transport, coupled hydrogeochemistry, pathways analysis, Äspö, Task 5

ABSTRACT

This report describes the participation of the JNC/Golder team in the coupled hydrogeological/geochemical pathway modeling of the construction of the Äspö Hard Rock Laboratory during the period 1990 through 1996. Modeling was carried out to the specifications of the Äspö Task Force on Modeling of Groundwater Flow and Transport of Solutes, Task 5.

The modeling was carried out using the discrete feature network/channel network approach (DFN/CN). In this approach, both major deterministic fracture zones and background fracturing was modeled explicitly as two-dimensional discrete features using FracMan/FracWorks. Deterministic fracture zones were based on the zone specifications of Rhén (1999), with the addition of a northwest trending feature to explain the step drawdown responses observed during shaft construction.

Flow and transport were modeled by transforming the fracture network to a topologically equivalent pipe network using FracMan/PAWorks.

The purpose of the modeling was to demonstrate the value of geochemical data for construction and validation of hydrogeological and pathway models. This investigation was undertaken in three separate stages.

- Stage 1: Calibrate and Predict Based on Hydrological Data Only (Results Presented 4/99);
- Stage 1.5: Improve the Calibration and Prediction for Stage 1 Based on Hydrological Data Only (10/99);
- Stage 2: Update based on Geochemical Data, Repeat Predictions (10/99); and
- Stage 3: Complementary Analysis to Address Uncertainty Issues (11/00).

The modeling approach was updated during the project. For Stages 1 and 2 hydrological and geochemical initial conditions for the model were provided by Rhén (1998). The transport calculations were made using transport pathways defined by graph theory searches through the channel network model. Flow velocities were adjusted to account for the effect of salinity on density and flow (Bear, 1972). The salinity-adjusted transport was expressed in terms of travel times and proportions of four geochemical end member water compositions: meteoric, glacial, marine, and brine. These compositions of end-members were calculated by SKB using the computer code Multivariate Mixing and Mass balance, referred to as M3 in this document (Rhén et al. 1997; Laaksoharju, 1999a; Laaksoharju et al. 1999b). These compositions and mixing proportions were presented in Data Delivery 19, released by SKB on 15th December 1999 (delivery reference F65H). Oxygen-18 and chloride were back calculated from the geochemical end members. The modeled period was from 1990 through 1996.

For Stage 3 of the Task 5 modeling, two major changes were adopted. Firstly, the geochemical initial conditions for the model were adapted to enable consideration of all the chemical variability in the measured data. Several possible alternative combinations of input data were considered, in addition to the data used in the original M3 modeling. The second change was that the methodology for finding the source locations of the water types was changed from a graph theory search to a particle tracking approach. The latter provides a more accurate measure of the proportion of mass originating in a given location.

The stages of the modeling process achieved differing levels of success. The purely hydrogeological models constructed in Stages 1 and 1.5 were very successful in matching the head distribution, but did not provide optimum geochemical predictions. These data provided sufficient information to predict the likely existence of the additional "mystery" feature.

The Stage 2 geochemical calibration resulted in both lower head and geochemical error measures. These analyses, using the M3 chemistry and the original pathway algorithm, involved additional changes to the boundary conditions and connectivity. Many of these changes were subsequently seen to be the result of a poor geochemical conceptual model. The deficiencies of the pathway-tracking algorithm compounded the required changes.

However, the most interesting results from the modeling occurred during the Stage 3 analysis. This model used an improved chemistry model and pathways algorithm, but was run using the hydrogeologically calibrated fracture model and boundary conditions. Fits between the measured and modeled chemistry were very good: the deficiencies primarily being related to travel velocities, not spatial location. The results from this set of simulations indicate that for a large modeled region the initial geochemical spatial variation used in the model is very important. The travel velocities were then calibrated by varying the storativities of specific large scale features, further improving the fits.

In conclusion, the authors believe that the specific objectives of Task 5 were met. The first objective, "to assess the consistency of groundwater flow models and hydrochemical mixing-reaction models through the integration and comparison of hydraulic and hydrochemical data obtained before, during and after tunnel construction" was addressed. The model derived from purely hydrogeological considerations was adequate for determining the major connectivity of the system. However, the geochemical response was strongly influenced by the geochemical interpretation and optimization required additional calibration. The use of geochemical data was also required to calibrate the model aperture and storage parameters.

The second Task 5 objective, "to develop a procedure for integration of hydrological and hydrochemical information which could be used for assessment of potential repository sites" is discussed in detail in Sections 5-5 and 6. The approach is based on sequential use of hydrogeological and geochemical data. Based on the Task 5 modeling of the Äspö site this approach worked well. It was found that the calibration to measured heads provided a reasonable calibration to the general water sources, but that the travel velocity was poorly predicted. The chemistry data provided a data set from which to refine these velocities. Chemistry data also reduced the non-uniqueness of the system.

SAMMANFATTNING

Rapporten beskriver JNC/Golders deltagande i den kopplade hydrogeologiska/geokemiska kanalmodelleringen av tillredningen av Äspö HRL under perioden 1990 till 1996. Modellering genomfördes i enlighet med de specifikationer som lämnats av Äspö Task Force för modellering av grundvattenflöde och transport av lösningar i Task 5.

Modelleringen genomfördes med den diskreta spricknätverks/kanalnätverksmetoden (DFN/CN). Med denna metod modellerades både stora deterministiska sprickzoner och bakgrundssprickor uttryckligen som 2-dimensionella diskreta strukturer med hjälp av FracMan/FracWorks. Deterministiska sprickzoner baserades på zonspecifikationer från Rhén (1999) med tillägg av en nordvästligt riktad zon för att förklara de stegvisa avsänkningar som observerades under tillredningen av schaktet.

Flöde och transport modellerades genom omvandling av spricknätverket till ett topologiskt, ekvivalent kanalnätverk med hjälp av FracMan/PAWorks.

Syftet med modelleringen var att demonstrera betydelsen av geokemiska data för sammanställning och validering av hydrogeologiska modeller och kanalmodeller. Undersökningen genomfördes i tre separata steg:

- Steg 1: Kalibrering och prediktering med hjälp av enbart hydrologiska data (resultat presenterat 4/99).
- Steg 1.5: Förbättra kalibreringen och prediktionen från Steg 1 med hjälp av enbart hydrologiska data (10/99).
- Steg 2: Uppdatera med hjälp av geokemiska data, upprepa prediktionen (10/))).
- Steg 3: Kompletterande analyser som fokuseras på osäkerhetsfrågor (11/00).

Modelleringsmetoden uppdaterades under projektets gång. Hydrologisk och geokemiskt initialtillstånd till modellerna lämnades av Rhén (1998) i Steg 1 och 2. Transportberäkningarna förutsatte transportkanaler som definierades av kurvteoretisk sökning i kanalnätverkets model. Flödeshastigheter justerades med hänsyn till salthaltens påverkan på täthet och flöde (Bear, 1972). Den salthaltsjusterade transporten uttrycktes som transporttider och proportioner av fyra geokemiskt slutgiltiga vattentypers sammansättning: meteoriskt, glacialt, marint och saltlake. Dessa sammansättningar av slutliga vattentyper beräknades av SKB med hjälp av beräkningskoden Multivariate Mixing and Mass balance (M3). Dessa sammansättningar och blandningsproportioner presenterades i Dataleverans 19, som släpptes av SKB den 15:e december 1999 (Leveransreferens: F65H). Syre-18 och klorid beräknades baklänges från de geokemiska slutprodukterna. Modelleringsperioden sträckte sig från 1990 till 1996.

Vid modellering av Steg 3 i Task 5 gjordes två stora ändringar. Den första rörde anpassning av de initiala geokemiska förhållandena till all den förekommande kemiska variationen i mätdata. Flera möjliga alternativa kombinationer av ingående data beaktades förutom data som användes i den ursprungliga M3-modelleringen. Den andra rörde metodiken att bestämma källtermer för vattentyper, vilken ändrades från kurvteoretisk sökning till en metod för beständig partikelspårning. Den senare ger en mer noggrann mätning av massproportioner, som kommer från en given plats.

Stegen i modelleringsprocessen nådde olika grad av succé. Den rena hydrologiska modellen som sammanställts i Steg 1 och 1.5 blev lyckad rörande jämförelse av tryckfördelningen, men lämnade inte optimala geokemiska prediktioner. Dessa data gav tillräcklig information för prediktion av den troliga förekomsten av ytterligare ”okända” strukturer.

Steg 2s geokemiska kalibrering resulterade i både lägre tryck och geokemiska felindikationer. Dessa analyser, som använde M3-kemin och den ursprungliga kanalalgoritmen, inkluderade ytterligare ändringar i randvillkor och konnektivitet. Många av dessa ändringar betraktades följaktligen som ett resultat av en undermålig geokemisk modell. Bristerna i algoritmen för kanalvägsspårning utgjorde tillsammans de erforderliga justeringarna.

Men, de mest intressanta resultaten från modelleringen erhölls under analysen i Steg 3. Modellen använde en förbättrad kemisk modell och kanalvägsalgoritm, men kördes under användning av hydrologiskt kalibrerad sprickmodell och randvillkor. Överensstämmelsen mellan modellerad och uppmätt kemi var mycket bra med brister i primärt bara transporthastigheter, ej rumslig lokalisering. Resultatet från denna uppsättning simuleringar indikerar att för en stor modellerad region är den ursprungliga geokemiska fördelningen i rummet, som används i modellen, viktig. Transporthastigheten kalibrerades sedan genom variation av magasinskoefficienten hos stor-skaliga strukturer för att ytterligare förbättra överensstämmelsen.

Sammanfattningsvis anser författarna att de specifika målen med Task 5 har uppfyllts. Det första målet var att ”analysera stabiliteten hos grundvattenflödesmodeller och modeller för hydrokemiska blandningsreaktioner genom integrering och jämförelse av hydrauliska och hydrokemiska data, som genererats före, under och efter tunneldrivningen” Modellen som utvecklats med enbart hänsyn tagen till ren hydrokemi var tillräcklig för bestämning av den mest betydelsefulla konnektiviteten i systemet. Men, den geokemiska responsen påverkades starkt av den geokemiska tolkningen, och optimering krävde ytterligare kalibrering. Användning av geokemiska data erfordrades också för kalibrering av modellens sprickvidder och magasinsparametrar.

Det andra målet för Task 5 ”att utveckla ett sätt att integrera hydraulisk och hydrokemisk information , som kan användas vid analys av en potentiell djupförvarsplats” diskuteras i detalj i sektion 5-5 och kapitel 6. Tillvägagångssättet baseras på sekventiell användning av hydrogeologiska och geokemiska data. . Denna modellering i Task 5, applicerad på Äspö, fungerad väl. Ett resultat var också att kalibreringen mot uppmätta grundvattentryck presenterade en rimlig kalibrering för de allmänna vattenkällorna, men att transporthastigheten predikterades dåligt. Kemiska data gav en datauppsättning med vilken hastigheterna kan förfinas. Kemiska data gjorde även systemets mindre unikt.

TABLE OF CONTENTS

LIST OF FIGURES

LIST OF TABLES

LIST OF APPENDICES

EXECUTIVE SUMMARY

This report describes the participation of the JNC/Golder team in the coupled hydrogeological/geochemical pathway modeling of the construction of the Äspö Hard Rock Laboratory during the period 1990 through 1996. Modeling was carried out to the specifications of the Äspö Task Force on Modeling of Groundwater Flow and Transport of Solutes, Task 5. In order to demonstrate the value of geochemical data in hydrogeological modeling, models were calibrated separately to hydrogeological data and geochemical data. Both of these calibrated models were then used in predictive simulations.

Following these simulations an additional set of complimentary analyses were undertaken to address issues of uncertainty related to the geochemical methodology. Concurrently, the algorithm used to compute the source locations of the waters infiltrating into the tunnels was improved.

The modeling was carried out using the discrete feature network/channel network approach (DFN/CN). In this approach, both major deterministic fracture zones and background fracturing was modeled explicitly as two-dimensional discrete features using FracMan/FracWorks. Deterministic fracture zones were based on the zone specifications of Rhén (1999), with the addition of a northwest trending feature to explain the step drawdown responses observed during shaft construction.

Flow and transport were modeled by transforming the fracture network to a topologically equivalent pipe network using FracMan/PAWorks.

For the main simulations hydrological and geochemical initial conditions for the model were provided by SKB. All transport calculations were made using transport pathways defined by graph theory searches through the channel network model. The flow velocities were adjusted to account for the effect of salinity on density and flow (Bear, 1972). This density-corrected transport was expressed in terms of travel times and proportions of four geochemical end member water geochemistries: meteoric, glacial, marine, and brine. Oxygen-18 and chloride were back calculated from the geochemical end members. The modeled period was from 1990 through 1996.

For the additional complimentary Task 5 analyses, two major changes were adopted. Firstly, the geochemical initial conditions for the model were adapted to enable consideration of all the chemical variability in the measured data. Several possible alternative combinations of input data were considered. The second change was that the methodology for finding the source locations of the water types was changed from a graph theory search to a particle tracking approach. The latter provides a more accurate measure of the proportion of mass originating in a given location.

The three stages of the modeling process achieved differing levels of success. The purely hydrogeological model constructed in Stage 1 was very successful in matching the head distribution, but did not provide optimum geochemical predictions.

The Stage 2 geochemical calibration, using the M3 chemistry and the original pathway algorithm, involved additional changes to the boundary conditions and connectivity. In particular the geochemical data provided information on model where the model required additional/lower connectivity. The addition of geochemical information resulted in both lower head and geochemical error measures.

However, the most interesting results from the modeling occurred during the Stage 3 analysis. This model used an improved chemistry model and pathways algorithm, but was only run using the hydrogeologically calibrated fracture model and boundary conditions. Fits between the measured and modeled chemistry were very good: the deficiencies primarily being related to travel velocities, not spatial location. The results from this set of simulations indicate that for a large modeled region the initial geochemical spatial variation used in the model is very important.

In conclusion, the authors believe that the specific objectives of Task 5 were met. The first objective, "to assess the consistency of groundwater flow models and hydrochemical mixing-reaction models through the integration and comparison of hydraulic and hydrochemical data obtained before, during and after tunnel construction" was addressed. The model derived from purely hydrogeological considerations was adequate for determining the major connectivity of the system. However, the geochemical response was strongly influenced by the geochemical interpretation and optimization required additional calibration. The use of a geochemical conceptual model improved the geochemical interpretation. The use of geochemical data was also required to calibrate the model aperture and storage parameters.

The second Task 5 objective, "to develop a procedure for integration of hydrological and hydrochemical information which could be used for assessment of potential repository sites" is discussed in detail in Section 5-5 and 6. The approach is based on sequential use of the hydrogeological and geochemical data. The phases could be summarized as:

- Develop a regional model of the site including only the large scale features
- Develop a conceptual model for the background fractures. For a DFN idealization this included the orientation, size, intensity, and transmissivity of the non-regional features.
- Develop boundary conditions for the modeled region.
- Create a finite element model including the major features, background features, and boundary conditions. Calibrate this model to the measured head distribution by varying the fracture properties and boundary conditions.
- Use this calibrated model to predict chemistry distributions. Calibrate this model to the measured chemistry and head distribution by varying the fracture properties and boundary conditions.

Based on the Task 5 modeling of the Äspö site this approach worked well. It was found that the calibration to measured heads provided a reasonable calibration to the general water sources, but that the travel velocity was poorly predicted. The chemistry data provided a data set from which to refine these velocities. Chemistry data also reduced the non-uniqueness of the system.

It should be noted, however, that the goodness-of-fits achieved were also sensitive to the methodology used to compute the geochemical distribution across the site. The hydrogeology and the geology at the Äspö site are consistent with the major features dominating mixing and flows. Therefore it was necessary to distribute chemistry based on the major features, rather than assuming a continuum. The strong influence of the Baltic/Äspö Island boundary on the chemistry also markedly affected the interpretation. For a different site, this means that the modelers would need to ascertain the structures, geology and/or major processes affecting the chemistry prior to setting up the geochemical spatial distribution. Similarly, the interpretation scheme should also account for the hydrogeological conditions.

1. INTRODUCTION

This report describes the participation of the JNC/Golder team in coupled hydrogeological/geochemical pathway modeling of the construction of the Äspö Hard Rock Laboratory during the period 1990 through 1996. Modeling was carried out to the specifications of the Äspö Task Force on Modeling of Groundwater Flow and Transport of Solutes, Task 5 during the period June through October 1999.

The aim of Task 5 is to compare, and ultimately integrate, site scale hydrogeology and hydrochemistry by evaluating the large scale groundwater flow pathways activated by construction of the Äspö tunnels (Wikberg, 1998). This integration is expected to benefit underground radioactive waste repository performance assessment by providing a better understanding of transport pathways at the site scale.

JNC/Golder has defined an additional goal for this task, to demonstrate quantitatively the value of geochemical data for hydrogeological model development. In order to meet this goal, JNC/Golder carried out model calibration and prediction in three stages.

In the first stage, we developed and calibrated a model based solely on hydrogeological data, and used this model to predict end-member geochemical breakthroughs to predictive points defined by Rhén et al. (1998). In the second stage, this model was refined using geochemical data, and a second prediction was made. It is hoped that comparison of these two predictive stages will provide quantitative support to the increased use of geochemical data in hydrogeological modeling.

In the third stage additional complementary analyses were undertaken to address uncertainty issues. Uncertainty exists in the interpretation of the initial spatial variation of chemical compositions. Therefore the initial conditions for the geochemical model were adapted to enable consideration of all the chemical variability in the measured data. Additionally the methodology for finding the source locations of the water types was changed from a graph theory search to a particle tracking approach. The latter provides a more accurate measure of the proportion of mass originating in a given location.

These three stages are documented in the following reports:
- Approaches, Algorithms, and Demonstration Report Dated 12/98;
- Hydrological and Geochemical Calibrations and Predictions Report Dated 12/99;
- Complementary Analysis to Address Uncertainty Issues Report Dated 12/00 (current report).

This report is organized as follows: Chapter 2 describes the hydrogeological model used by the JNC/Golder team. Phase 1 (hydrogeological) model calibration and prediction are presented in Chapter 3. Chapter 4 presents Phase 2 (geochemical) model calibration and prediction. The modeling and analysis approaches used for Task 5 by the JNC/Golder team is described in a companion report, Dershowitz et al. (1998a). The additional complementary analyses undertaken to address uncertainty issues are described in Section 5.

2. HYDROGEOLOGICAL/PATHWAY MODEL

This section describes the initial hydrogeological model used for the calibrations and modeling presented in this report. Variants to this model for model calibration and prediction are described in Chapters 3 and 4. Additional variants related to Stage 3 uncertainty issues are described in Section 5.

2.1 DISCRETE FEATURES

The Task 5 modeling region is 2 km by 2 km, with a depth of 1 km (Figure 2-1). This scale was selected to include the Äspö tunnels and extend the boundaries as far as possible given computation time constraints. The structural model used for these analyses is based on the discrete fracture network (DFN) approach, in which all fluid storage, flow, and transport occurs through a limited subset of "conductive structures" represented by polygonal plates. The DFN approach assumes that there is no advective flow in the matrix. In the Task 5 implementation of the DFN approach the majority of fluid measured at the monitoring borehole locations was assumed to have originated in the fractures (not matrix). Hence any effect of matrix storage was accounted for implicitly in the fracture storativity values.

Task 5 is based on SKB's "SR-97" geological/structural model for Äspö Island. This model (Rhén et al., 1997) was distributed to modeling teams as a Task 5 data delivery. The Task 5 structural model is illustrated in Figure 2-2. Dershowitz et al. (1998) used an earlier version of this structural model, which may explain some of the differences between the results of the current and previous JNC/Golder Task 5 modeling. In addition, while Dershowitz et al. (1998) simulations generally used only the deterministic structural features, the current modeling includes a stochastic background fracture model. Background fracturing included in the current model is illustrated in Figure 2-3.

The model is summarized in Table 2-1.

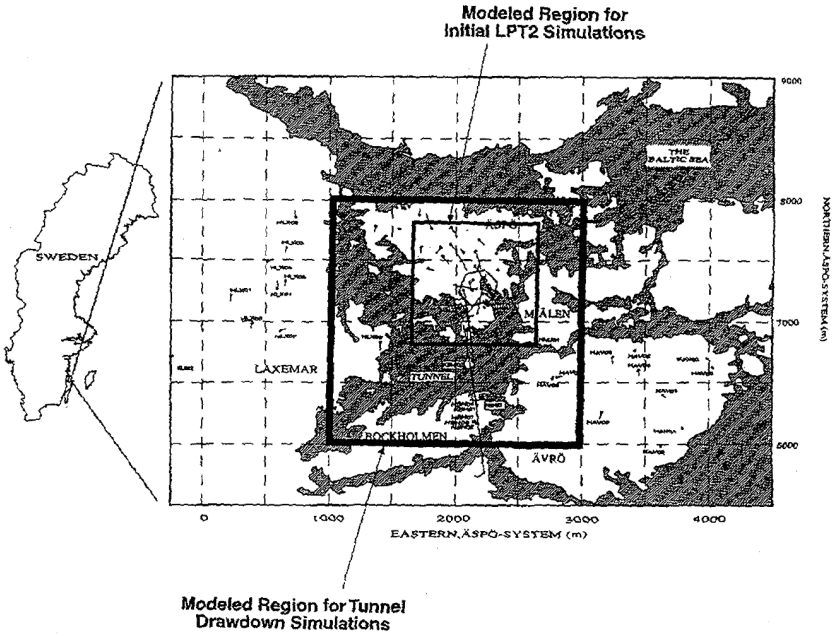

Figure 2-1 *Äspö Task 5 Modeling Region*

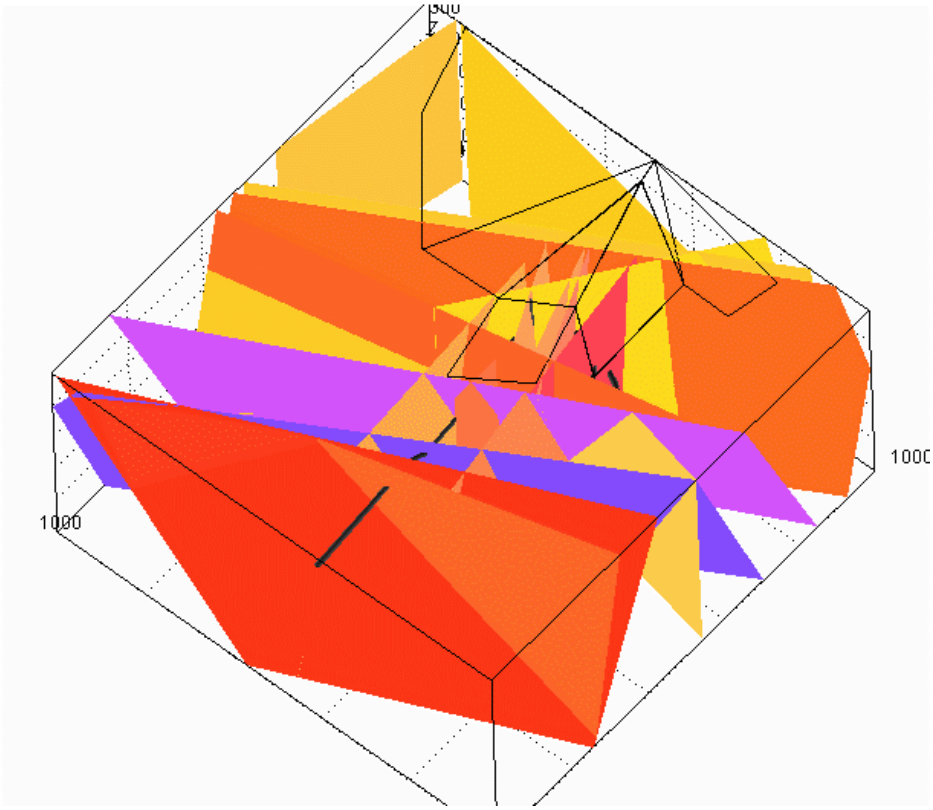

Figure 2-2 *DFN Structural Model*

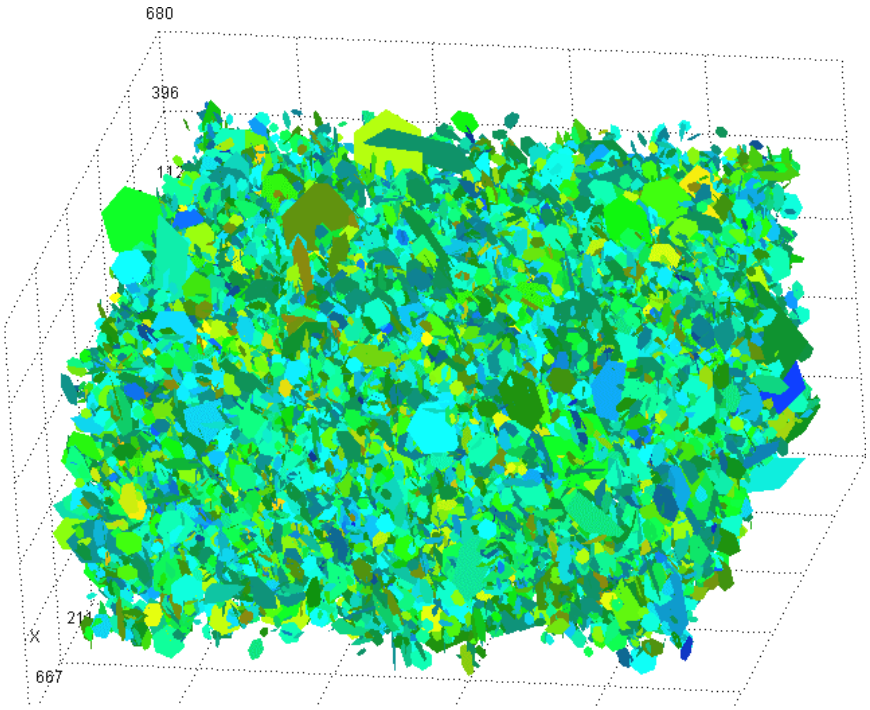

Figure 2-3 *Background Fracturing*

Table 2-1 Structural Model Parameters

Fracture Set	Deterministic Fracture Zones	Background Fracture Properties
Name	Fracture Zone Fractures	Background fractures
Location	22 Planar Homogeneous Zones (Rhén et al., 1997)	Baecher/Bart Model
Size	Surface Traces Mean = 1420 m	LogNormal (μ = 13.7 m, σ = 12.7 m)
Orientation	3 Point Solution	Bootstrap SKB, 1994 Fractures Mapped in Tunnels
Transmissivity	Rhén et al., 1997	LogNormal ($\mu = 9 \times 10^{-7}$ m^2/s, $\sigma = 5 \times 10^{-6}$ m^2/s)
Storativity	$0.001\ T^{1/2}$	$0.001\ T^{1/2}$
Intensity	Rhén et al., 1997	$P_{32} = 0.020214$ (m^2/m^3) (22704 fractures)
Transport Aperture	$2\ T^{0.5}$	$2\ T^{0.5}$

Since Task 5 requires calibration and evaluation of drawdown response to tunnel construction, conditioned discrete features were included in this model. These features were installed perpendicular to each of the monitoring intervals considered in boreholes KAS02 to KAS09, KAS12, and KAS14. The conditioned discrete features do not have the exact location or transmissivity of specific measured fractures within the boreholes, as this information was not available. The purpose of these features was purely to improve the connectivity between the borehole sections and the DFN, thereby increasing the number of locations in the DFN at which computed heads could be measured. These conditioned features are illustrated in Figure 2-4.

Uchida et al. (1997) carried out extensive simulations of drawdowns due to tunnel construction as part of Task 3 of the Äspö Task Force on Modeling of Groundwater Flow and Transport of Solutes. They identified step drawdown responses due to tunnel construction as one of the key factors contributing to difficulties in matching measured and observed drawdowns (Figure 2-5). Uchida et al. (1997) ascribed this to a discrete feature and was able to localize this feature by plotting the location of exceptionally fast, strong hydraulic responses to tunnel construction. These responses occur on a single plane, as illustrated in Figure 2-6. This previously undetected feature has been modeled as two fractures: the plane containing the step responses, and a small connecting feature to ensure connection to the shafts. The “Mystery Feature” is located between features NNW1and NNW7. The tunnel sections shown in green on Figure 2-7 are sections containing a step response (Uchida et. al, 1997). The shafts are depicted in red.

JNC/Golder are not asserting that an undiscovered fracture zone exists in this location, but only that discrete features providing the connectivity of the features illustrated in Figure 2-7 are potentially useful to explain observed hydraulic responses to the shaft construction. This could be provided, for example, by particular "background" features which happen to intersect the shaft and monitoring sections at the location shown in Figure 2-7. The step drawdown responses observed, however, are indicative of isolated hydraulic connections rather than extensive background fracture connections.

2.2 BOUNDARY AND INITIAL CONDITIONS

For modeling purposes, Äspö Island and the Baltic were discretized into triangles as illustrated in Figure 2-8. Task 5 simulations required boundary and initial conditions for the head distribution and geochemistry.

2.2.1 Initial Head Conditions

Initial head boundary conditions are shown in Figure 2-9. The base of the model was assigned as a "no flow" boundary. The sides of the model were specified as constant head values interpolated from the values of Svensson (1999). The surface of Äspö Island was specified to have a constant infiltration rate of either 0.0 mm/year or 30.0 mm/year. Infiltration of 30 mm/year is equivalent to precipitation of approximately 650 mm/year assuming no runoff so that infiltration is equal to precipitation minus evapotranspiration). An infiltration of 0.0 mm/year was used for the hydrogeological calibrations. The Baltic seabed was modeled using a constant head boundary condition of 0.0 m. For some simulations, a 1 m thick skin was provided at the base of the Baltic to represent the influence of sea-bottom sediments (see Section 4).

Task 5 simulations were run over the time period from October 1, 1990 through November 28, 1996. October 1, 1990 through January 24, 1994 was used for calibrations to 2900 m tunnel face, and January 25, 1994 through November 28, 1996 were used for predictive simulations. Äspö tunnels were treated as time varying group flux boundary conditions. Therefore, for any individual section of tunnel, prior to its construction had a net flux of zero: after construction its flux was equal to the measured flow into that tunnel section from weir data. Weir data was provided by SKB for tunnel construction to 3600 m tunnel face. The weir flux boundary condition is illustrated in Figure 2-10.

The alternative tunnel boundary condition would have been an "internal" (i.e. no effect) boundary condition at early times, changing to a constant head condition once the tunnel was constructed. The most obvious head assumption at the tunnel wall, that of atmospheric pressure in the tunnel, is problematic however. This is because significant head loss will occur in the few meters behind the tunnel wall due to combined effect of grouting behind the tunnel lining and the tunnel lining itself. Any other head assumption is essentially a calibration parameter, not a constraint.

2.2.2 Initial Geochemical Conditions

Initial geochemical conditions were provided at 98 locations, in Appendix 14 of Data Delivery 7, as illustrated in Figure 2-11. These initial conditions utilized end-member definitions and proportions calculated using the program M^3 (Laaksoharju et. al., 1999b). These values were extrapolated by SKB (Rhén, 1998) using Kriging to a grid of 1000 locations (Figure 2-12). The extrapolation used a simple data-smoothing algorithm, and did not consider structural geologic issues, even through the majority of the measurement points are in fracture zones, at locations. Metcalfe (1999) has addressed the data quality issues and modeling implications associated with these initial geochemical conditions.

The JNC/Golder FracMan/PAWorks modeling for Stages 1 and 2 used a distance-weighted interpolation of the 1000 point grided initial geochemical conditions to define the initial conditions in each fracture in the DFN model.

At each point in the model, $P_I(x, y, z)$, the percentage geochemical end member "I" was calculated by a distance-weighted interpolation in the x, y, and z directions as follows:

$$P_I(x,y,z) = RelY1 + z*(RelY2-RelY1)$$

where RelY1 and RelY2 reflect interpolation in the Y direction,

$$RelY1 = RelX1 + y * (RelX3-RelX1)$$
$$RelY2 = RelX2 + y * (RelX4-RelX2)$$

and RelX1 through RelX4 reflect interpolation in the X direction,

$$RelX1 = P(X_i,Y_i,Z_i) + x * (P(X_{i+1},Y_i,Z_i)- P(X_i,Y_i,Z_i))$$
$$RelX2 = P(X_i,Y_i,Z_{i+1}) + x * (P(X_{i+1},Y_i,Z_{i+1})-P(X_i,Y_i,Z_{i+1}))$$
$$RelX3 = P(X_i,Y_{i+1},Z_i) + x * (P(X_{i+1},Y_{i+1},Z_i)-P(X_i,Y_{i+1},Z_i))$$
$$RelX4 = P(X_i,Y_{i+1},Z_{i+1})+ x*(P(X_{i+1},Y_{i+1},Z_{i+1})-P(X_i,Y_{i+1},Z_{i+1}))$$

Initial geochemical conditions at the edges of the model were assigned based on those at the closest grid point.

The updated approach used for the Stage 3 complimentary analyses are described in Section 5.

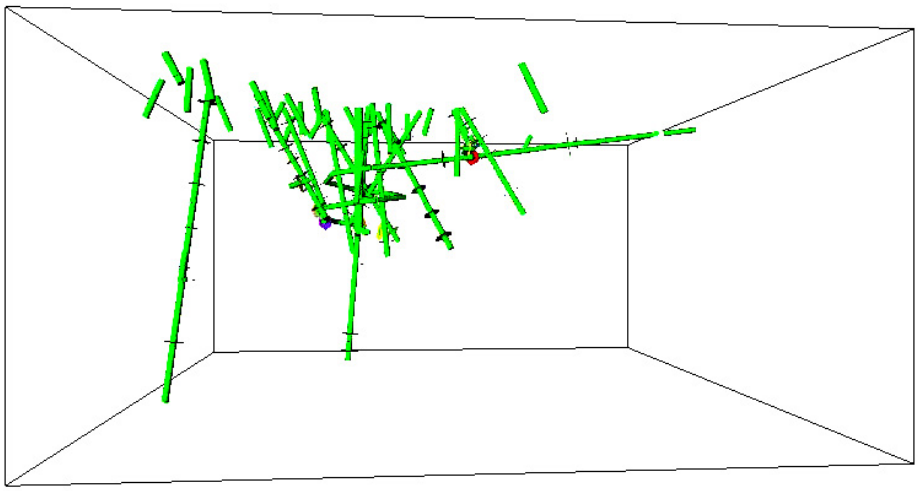

Figure 2-4 *Conditioned Fracturing*

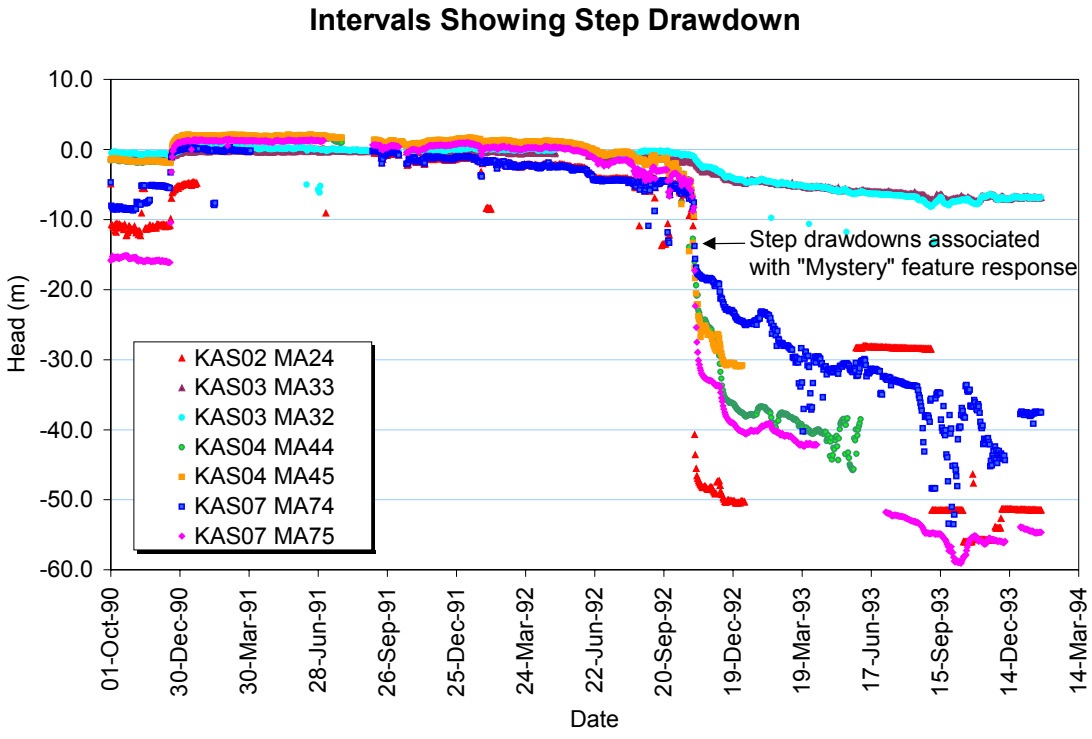

Figure 2-5 *Mystery Feature Responses*

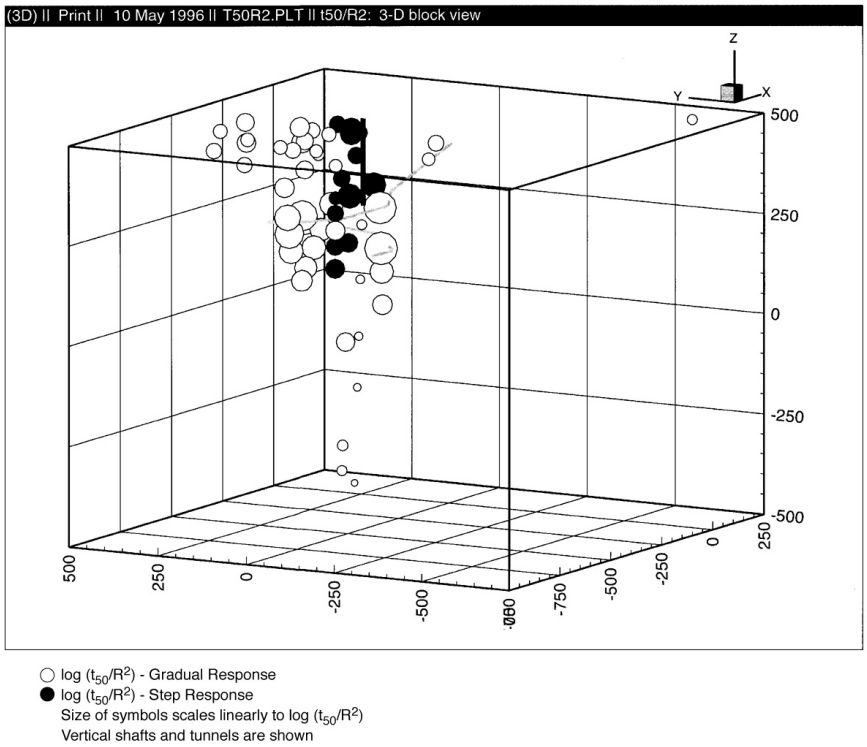

Figure 2-6 *Mystery Feature Location*

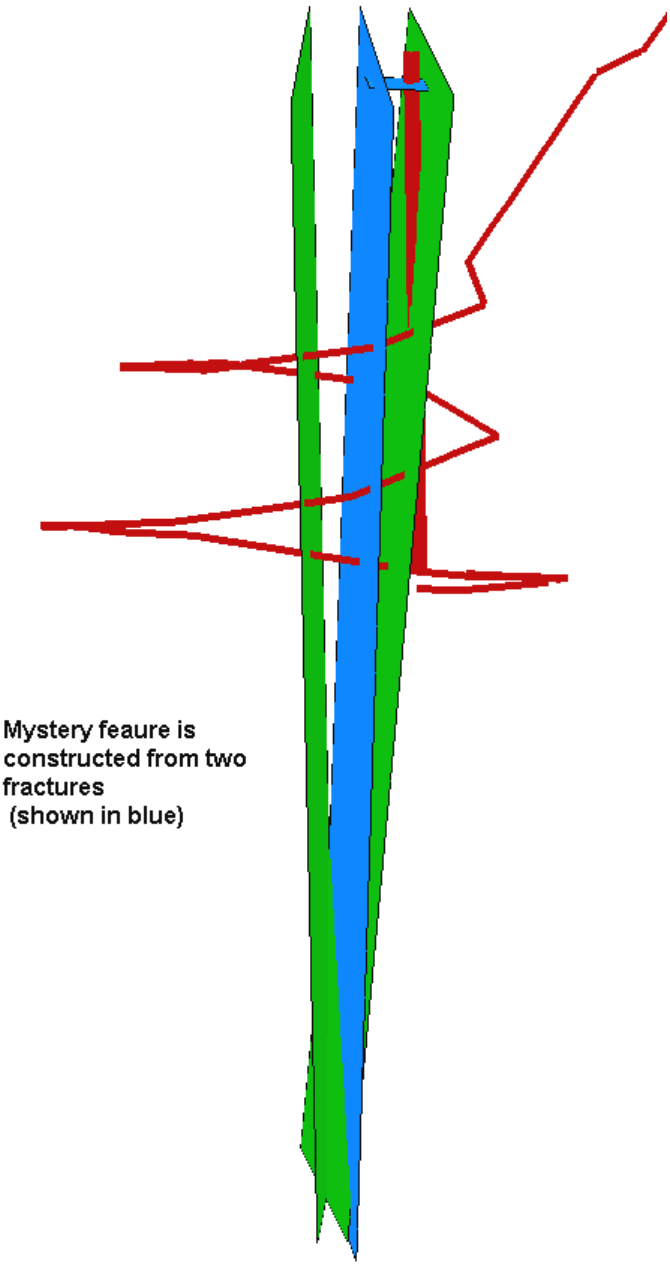

Figure 2-*7 Mystery Feature comparison to SR-97 Structural Model*

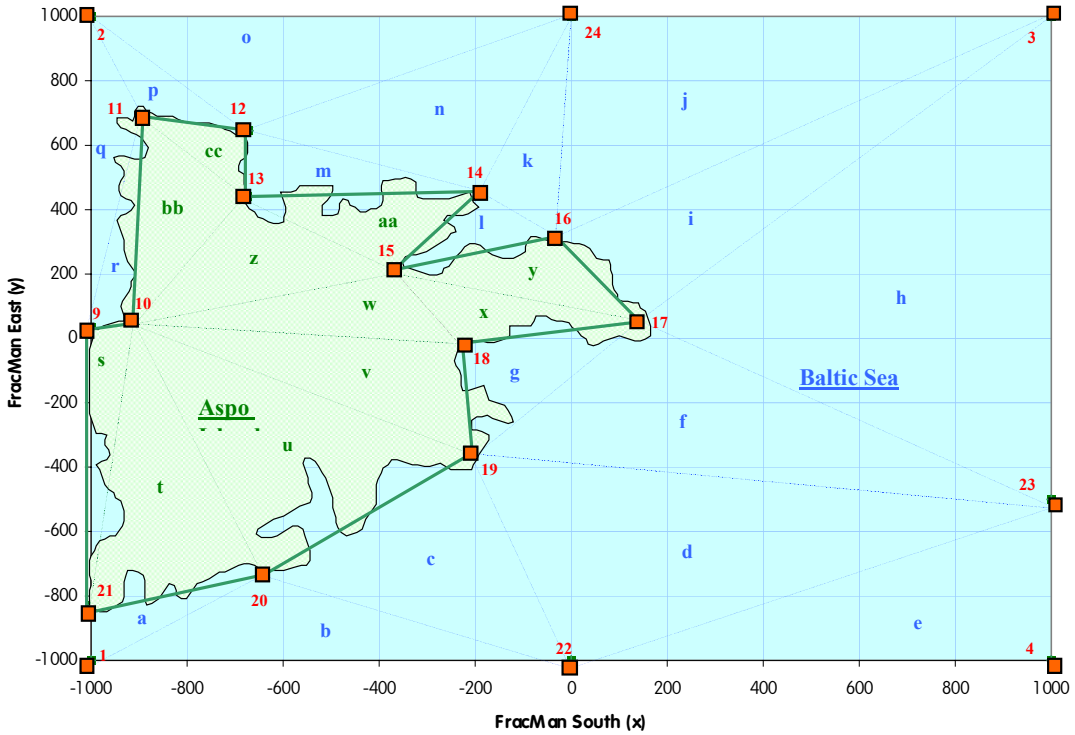

Figure 2-8 *Model Boundary Discretization*

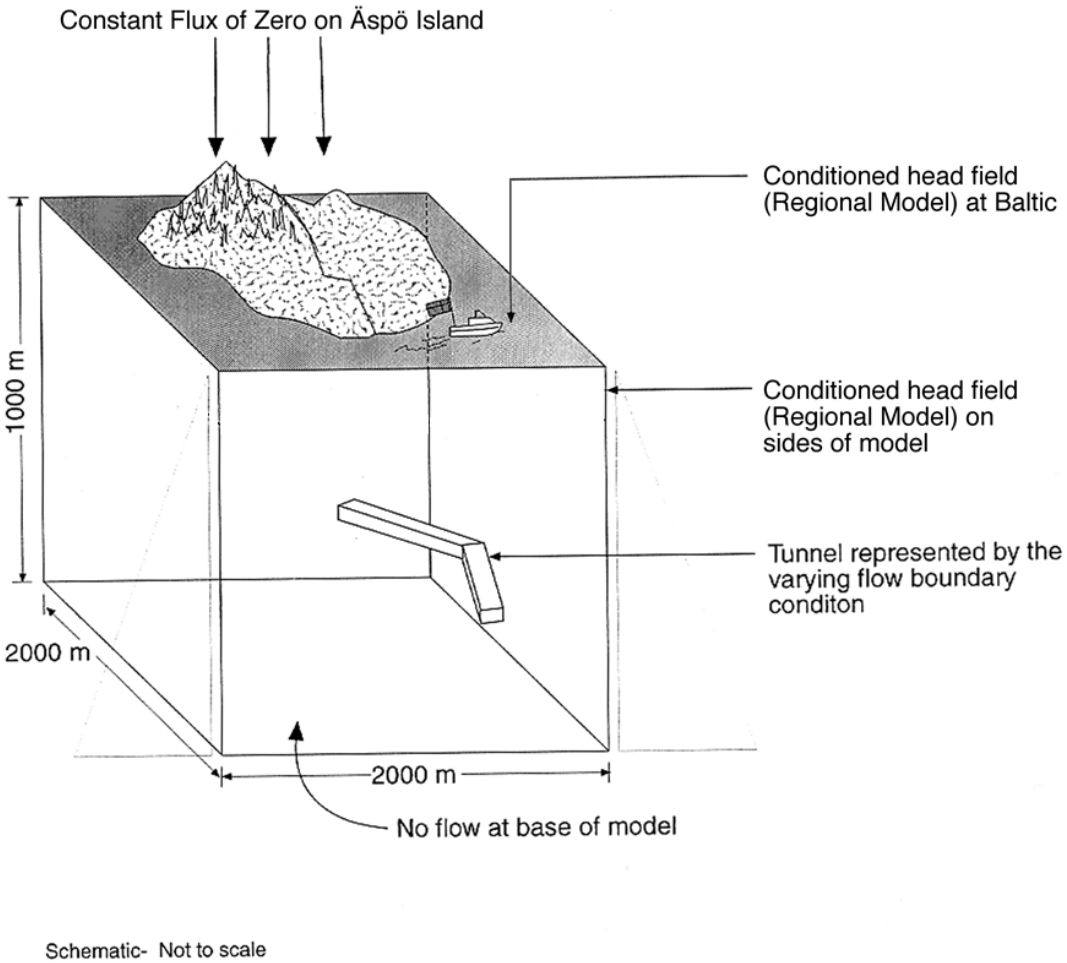

Figure 2-9 *Boundary Conditions*

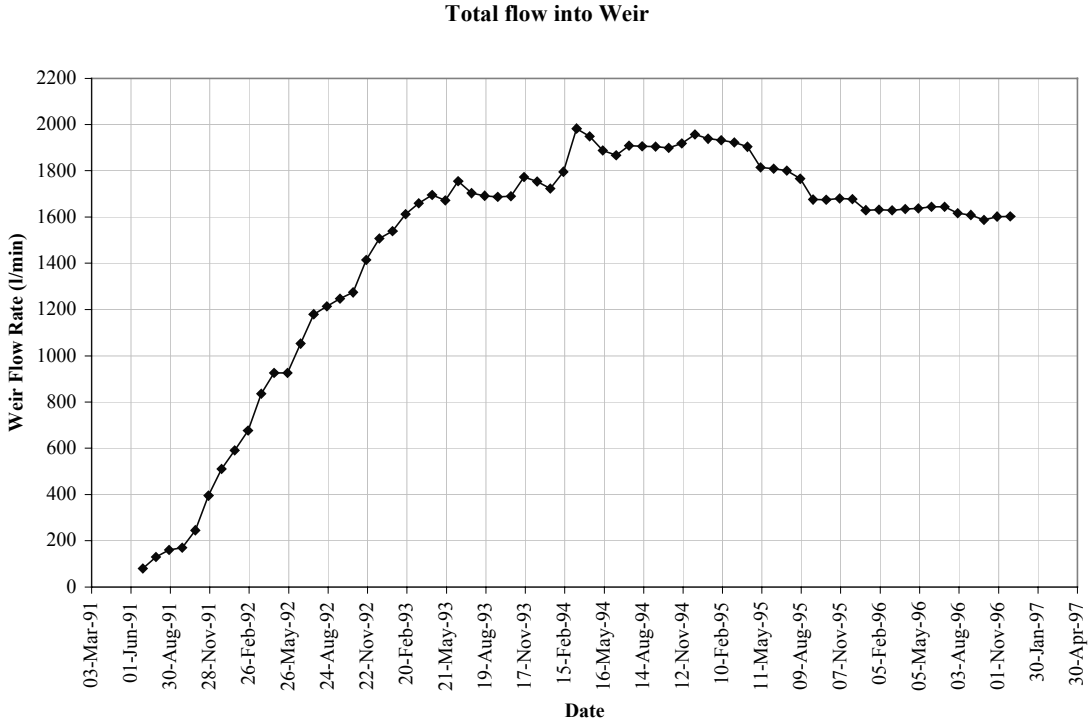

Figure 2-10 *Weir Fluxes to June 4, 1996*

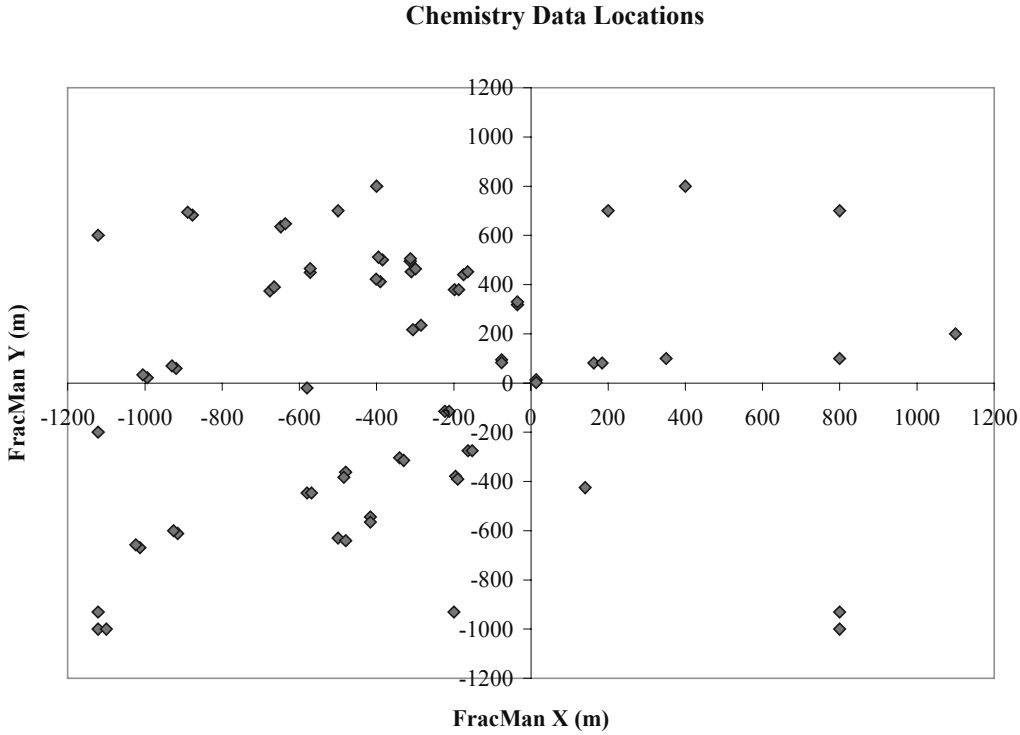

Figure 2-11 *Geochemical End-Member Data Points*

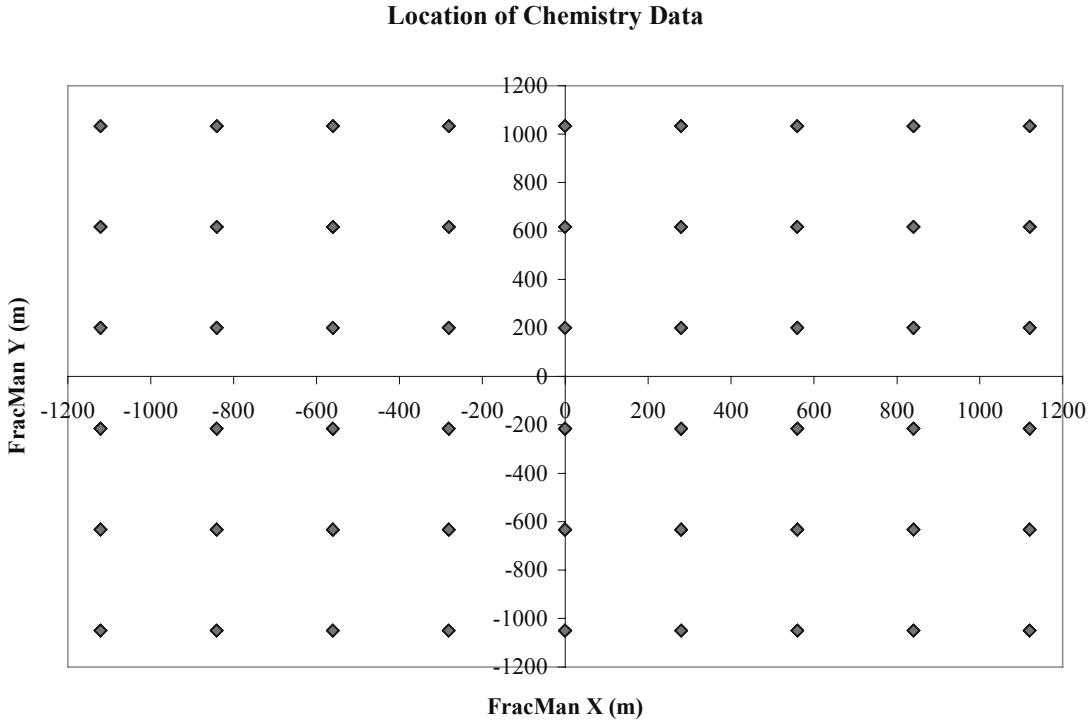

Figure 2-12 *Geochemical End-Member Data Grid*

2.3 MEASURES OF ERROR

In order to determine which hydrogeological DFN model provides the best idealization of the true groundwater system at Äspö the following error terms were used (Rhén et al., 1998).

Mean Error, dh

$$dh = \frac{\sum_{i=1}^{n} (h_i^m - h_i^c)}{n}$$

$$dh(abs) = \frac{\sum_{i=1}^{n} \left| h_i^m - h_i^c \right|}{n}$$

Accuracy

$$Dh = \sqrt{\frac{\sum_{i=1}^{n} (h_i^m - h_i^c - dh)^2}{n - 1}}$$

where

n is the number of borehole intervals at which a head is measured. For the modeling results this is typically equal to the number of borehole intervals connected to the fracture network.

h: Piezometric level (freshwater head) in meters above sea level (masl).

m index to represent measured values

c index to represent calculated values

For time dependent simulations the time-averaged value of mean error is used as an assessment of the error bias. This is the defined as ∑(dh)/(number of time measurements).

A similar error measure was used to provide an indication of the bias of the geochemical fit, the "geochemical absolute average error". The number is given as a percentage. The value is defined as:

$$dg(abs) = \frac{\sum_{i=1}^{n} \left| g_i^m - g_i^c \right|}{n}$$

where g are the percentages of measured (m) and calculated (c) Brine, Glacial, Meteoric and Baltic. The number of measured values is limited therefore all the measured values are used. Therefore the "n" is the total number of measurements.

2.4 SOFTWARE

The FracMan discrete feature network model was used for this analysis. In particular, FracMan/FracWorks was used for generation of background discrete fractures, FracMan/MAFIC was used for steady state and transient flow simulations, and FracMan/PAWorks pathway analysis was used to define pathways. FracMan is described in Appendix A of SKB 97-03 (Uchida et al, 1997) and in more detail in the FracMan manual (Dershowitz et al., 1998a), MAFIC manual (Miller et al., 1998) and PAWorks manual (Dershowitz et al., 1998b).

FracMan/PAWorks is a suite of analysis codes that represent fracture networks as a 3-D pipe network, with nodes defined by fracture intersection traces. The advantage of using pipe elements, as opposed to plate elements, is that there is a vast saving in memory and computation time requirements. In PAWorks, the pipes are generated to maintain the connectivity structure of the 3-D discrete fracture network, with approximately equivalent conductances and surface areas (Figure 2-13).

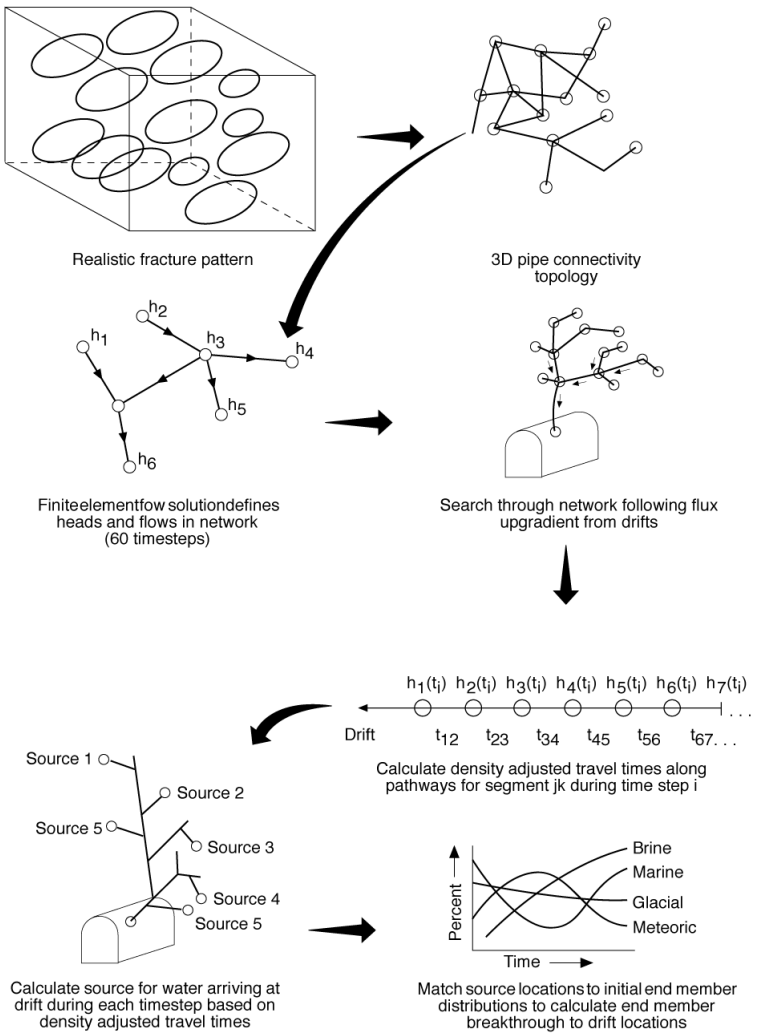

Figure 2-13 *PAWorks Pipe Networks from Fractures*

3. STAGE 1: HYDROGEOLOGICAL MODELING

JNC/Golder carried out the first modeling phase considering only hydraulic data for our calibrations. The hydrogeological calibration exercise took approximately one month. Calibration considered only the head values in the monitoring sections, and did not make use of any geochemical information.

Since one of JNC/Golder's goals for this task was to increase modeling transparency, the following section provides a record of the process of hydrogeological model calibration. The following section summarizes the results of the calibrated Stage 1 model. Detailed Stage 1 model results are provided as Appendix A.

3.1 HYDROGEOLOGICAL CALIBRATION

The hydrogeological model calibration for Task 5 started with the initial Task 3 model (Uchida et al., 1997), and was extended during preliminary Task 5 modeling in 1998 (Dershowitz et al., 1999) and in modeling for the Äspö Task Force meeting in April, 1999. The formal modeling for Task 5 was initiated in September 1999. The progress of hydrogeological calibration for the Task 5 simulations is illustrated in Figure 3-1. The hydrogeological model simulations are summarized in Table 3-1. In Table 3-1 the number of borehole sections being intersected varies with simulation. This number is defined as the minimum of the number of borehole sections connected to the DFN and the number of in situ measurements taken. It is defined at a specific time because the number of borehole sections at which in situ measurements were taken varied over time.

Initial modeling was carried out based on fracture zones alone (H-1). This model is very fast, and produced very good results, with an average error of only about 5 m. The success of this initial model can be attributed in part to the fact that this model benefits from the previous "Task 5" model of Uchida et al. (1997), which determined the appropriate skin value for the soils under the Baltic to be 0.01x.

The majority of the error in head predictions for the H-1 model arose from the lack of fit for the extreme drawdown responses to shaft construction (Figure 3-2). Therefore, the first change to the hydrogeologic model was to add the "mystery feature" to explain this response. As described in Section 2.1 above, these features were placed to connect the shaft to the locations at which anomalous large, steep drawdowns had been observed. The mystery feature does not necessarily correspond to a single fracture zone, but may instead comprise a set of individual conductive features.

Table 3-1: Hydrogeological Calibration

Sim	Stage I: Head Calibration	Features	# of BH Sections 1st Oct 1990	Time Average dh	dh on 13th Jan 1994
H-1 20-Sep	Zones Only	Pipe network created from DFN model of 22 deterministic fracture zones. Baltic Sea skin applied to reduce T in upper 10m to a multiple of 0.01 times the original value.	14	4.94	6.31
H-2 23-Sep	add Mystery Feature	Two fractures added to explain mystery response	14	5.30	6.61
H-3 8-Oct	Zones and Background	First iteration with 22704 background fractures	14	4.20	
H-4 10-Oct	Background Fracs, Mystery Feature	Model includes two fractures to explain mystery response	14	2.74	
H-5 11-Oct	Background Fracs and Conditioned Features	161 deterministic fractures with T=10^-6 added at head calibration sections in order to ensure that all calibration sections are connected	45	9.45	25.66
H-6 14-Oct	Background Fractures, Mystery Feature, Conditioned Fractures	Model includes two fractures to explain mystery response	45	10.18	26.03
H-7 21-Oct	Adjust Conditioned Fractures	Number of deterministic fractures at head calibration sections reduced to 69 and transmissivity of remaining fractures decreased to 10^-8 to reduce excessive drawdowns	45	10.05	25.28
H-8 22-Oct	Remove Baltic Skin	Baltic Sea skin removed in order to reduce excessive drawdowns	45	5.13	13.46

The first model including the "mystery feature" is H-2. This model did in fact improve the drawdown response to shaft construction (Figure 3-3). However, it did not have a significant influence on the average error. In addition, the model still only provides connection with 14 monitoring sections. Models H-3 and H-4 add background fractures to models H-1 and H-2 respectively. However, these stochastic background fractures did not increase the number of monitored sections, although they do decrease the average error.

Conditioned features intersecting each of the monitoring sections were added to models H-3 and H-4, respectively in simulations H-5 and H-6. (Figure 2-4). These models significantly worsened the average error, since they produced drawdown in many sections which were not in fact hydrogeologically connected (Figure 3-4). The match was improved in model H-7, which removed conditioned fractures from non-responding sections, and reduced the transmissivity of the conditioned fractures from 10^{-6} to 10^{-8} m^2/s. This only made minor improvement to the average drawdown measure dh, and the average drawdown in the model remained too high. Therefore, to reduce the average drawdown in the model, the low permeability skin was removed from the Baltic for model H-8.

Table 3-2 Summary of Model H-8

Property	Description
Fracture Model	
Major Discrete Features	22 Planar Homogeneous Zones (Rhén et al., 1997). See Table 2-1 for details.
Background Fractures	22704 features described in Table 2-1.
Mystery Feature	Addition an additional feature located between features NNW1and NNW7. Constructed from two fractures as shown in Figure 2-7.
Conditioned fractures intersecting tunnel sections.	Deterministic fractures added at 69 head calibration sections. Transmissivity of these deterministic fractures set at 10^-8 m^2/s to reduce excessive drawdowns.
Transport Aperture	Aperture = 2 * Transmissivity$^{0.5}$
Boundary Conditions	
North, South, East & West sides	Conditioned to the values reported in Svensson (1999).
Base	No flow boundary assigned to each node.
Baltic Sea	Head of 0.0 m.
Äspö Island	No flow boundary assigned to each node.
Geochemistry	
Chemical Composition	End-member definitions and proportions calculated using the program M^3 (Laaksoharju, M., 1999).
Interpolation Scheme	Linear interpolation from a grid of 1000 locations provided in Data Delivery No.4

It is interesting to note that a skin was required for model H-1, but gave excessive drawdowns in model H-7. The likely reason for this effect is that the addition of background fractures and conditioned features affects the connectivity of the DFN. This effect is magnified by the use of group flow boundary conditions for the tunnel sections: the number of tunnel sections connected into the DFN increases as the background fractures and conditioned features are added, and at each connected tunnel section water is removed from the finite element model.

This effect has implications for DFN model calibration. To provide a calibration that is insensitive to stochastic changes for a DFN model that contains non-zero flow boundary conditions, or in which the total flow through the model is critical to the understanding, the majority of flowing features must be included. For the Äspö site, although the major features may dominate the flow regime, the background fractures are a necessary part of the model connecting the tunnel sections to the major zones or the outer boundary.

The last model in this series, model H-8, was used as the "hydrogeologic only" head and geochemical response prediction. The parameters defining the H-8 model are summarized in Table 3-2. However, the calibration of this model was somewhat limited by a decision to not change the assigned values of fracture zone transmissivity provided by SKB. The SKB transmissivity values were typically based on a small number of hydrogeological tests with wide variability. Therefore, to improve the calibration the major feature transmissivities were changed as part of the Stage 2 geochemical calibration.

3.2 PREDICTIVE SIMULATIONS

Hydrogeological performance measures for the hydrological prediction Model H-8 are presented in Appendix A. Figure 3-5 through Figure 3-8 present example hydrogeological results for model H-8.

As discussed earlier in the document, the predictions H-1 through H-8 were undertaken using only head data. The final prediction, H-8, provided the smallest time average head error and was selected as a baseline model for the geochemical calibrations, and a geochemical simulation was carried out.

Figure 3-9 though Figure 3-13 shows a comparison between the geochemical calibration control points and simulated results using Model H-8. This model resulted in a geochemical absolute average error of 14.4%. The poor quality of the fit to the measured head data and particularly the inaccurate geochemical results indicate that significant improvements could be made to the numerical model.

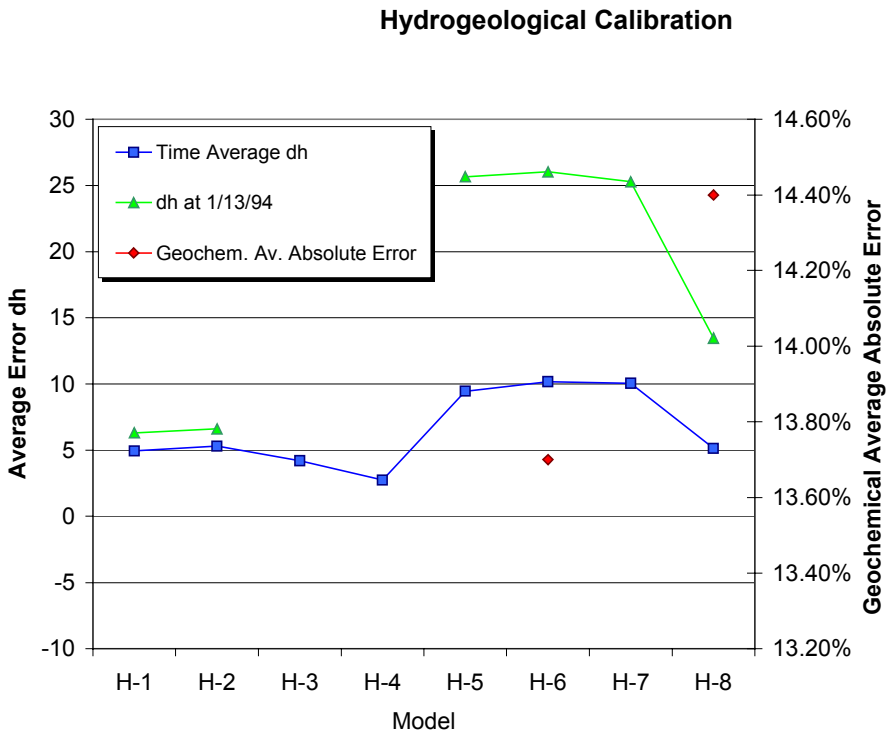

Figure 3-1 *Error Associated with Hydrogeological Calibration*

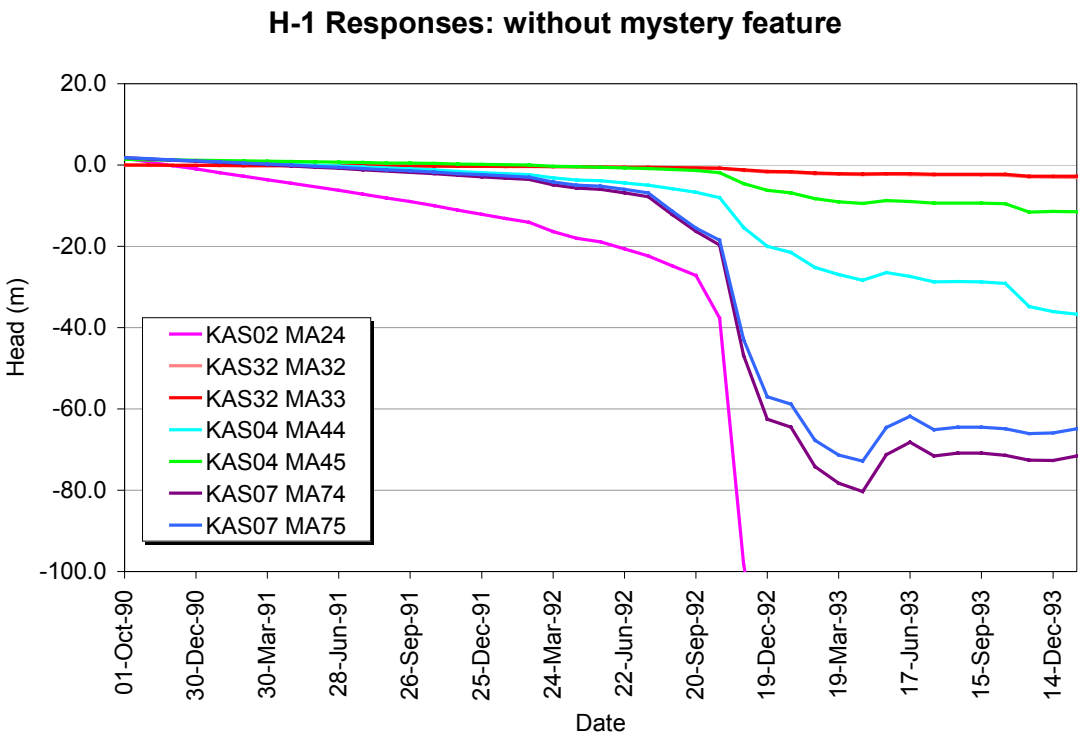

Figure 3-2 *Responses to Shaft Construction in Model H-1*

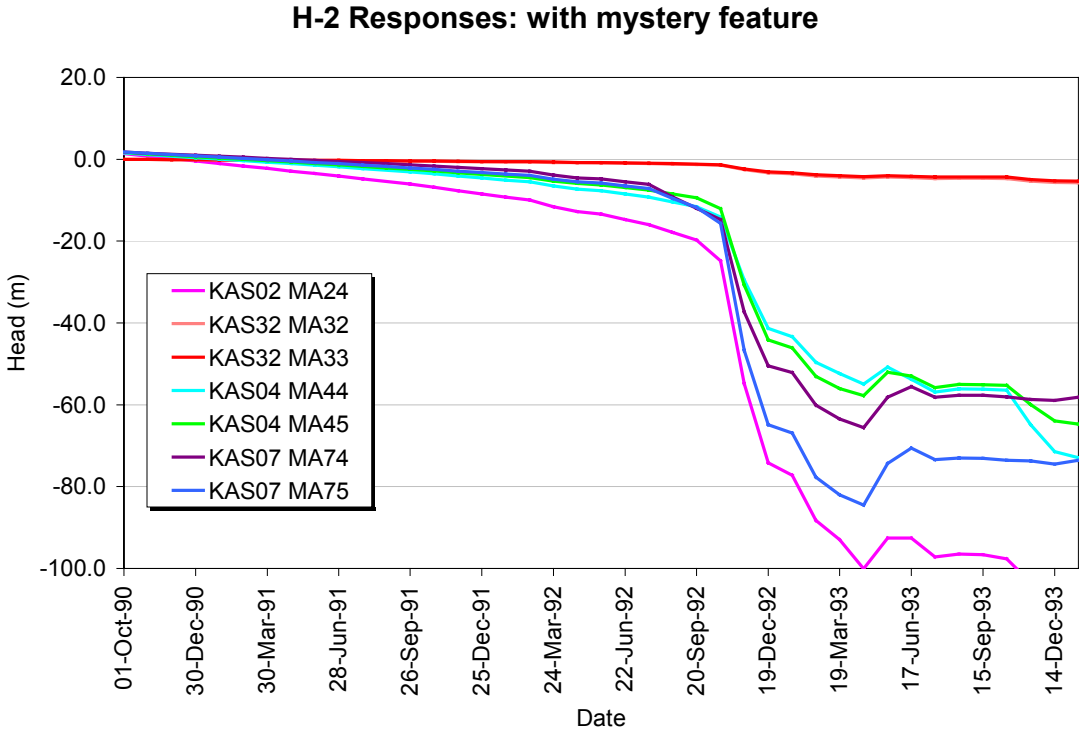

Figure 3-3 *Zone-only Model H-2 including "Mystery Feature"*

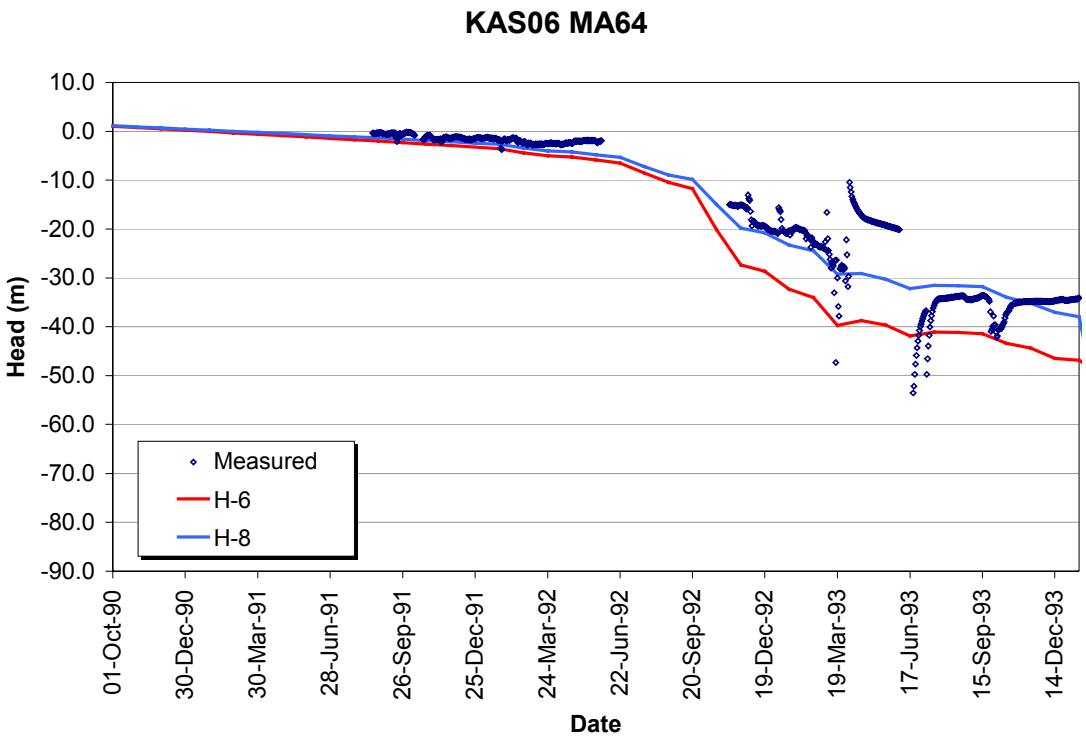

Figure 3-4 *Example Drawdown, KAS06 MA64 in Model H-6*

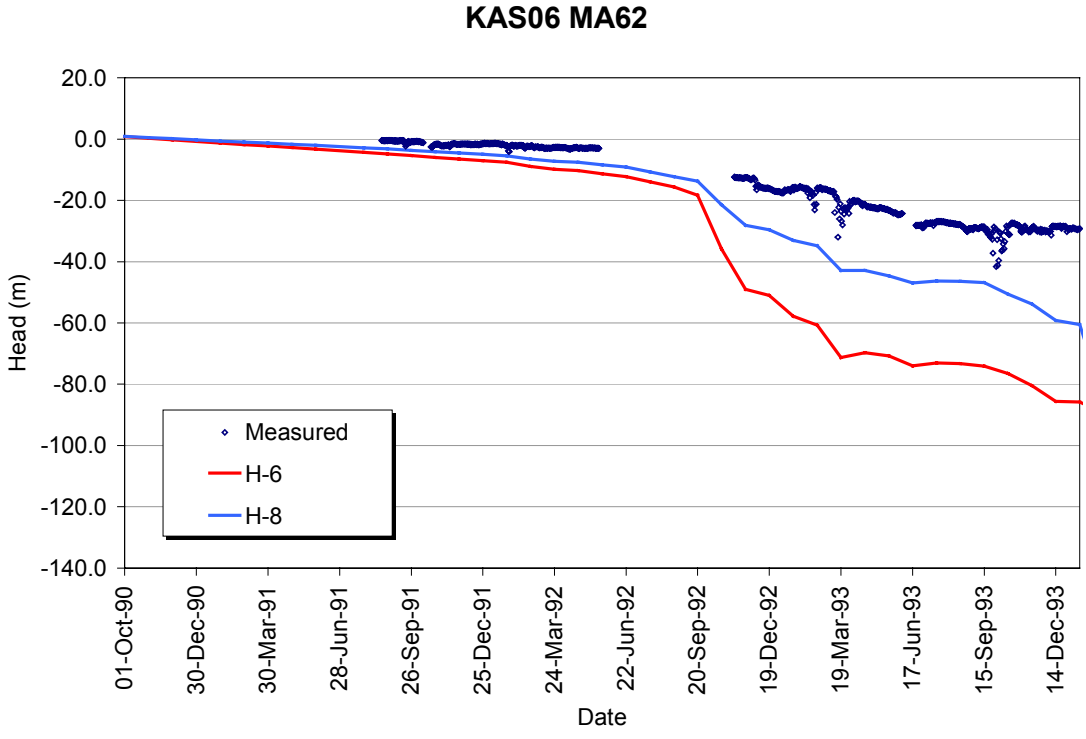

Figure 3-5 *Drawdown Response of KAS06 MA62 in Model H-8*

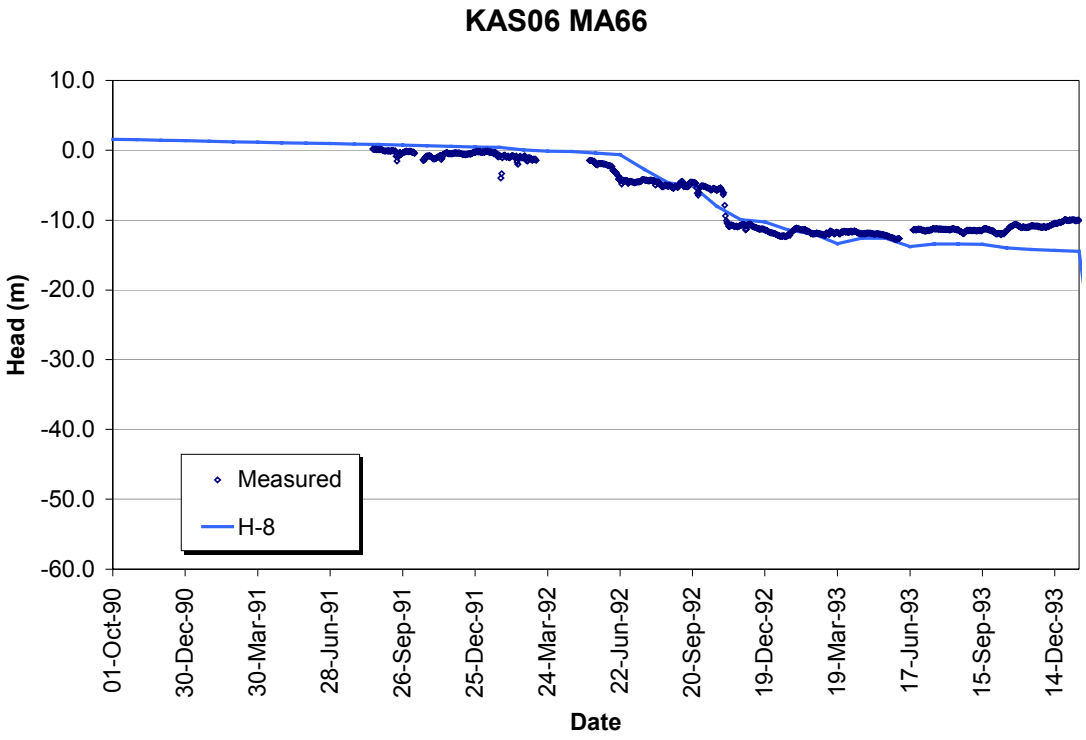

Figure 3-6 *Drawdown Response of KAS06 MA66 in Model H-8*

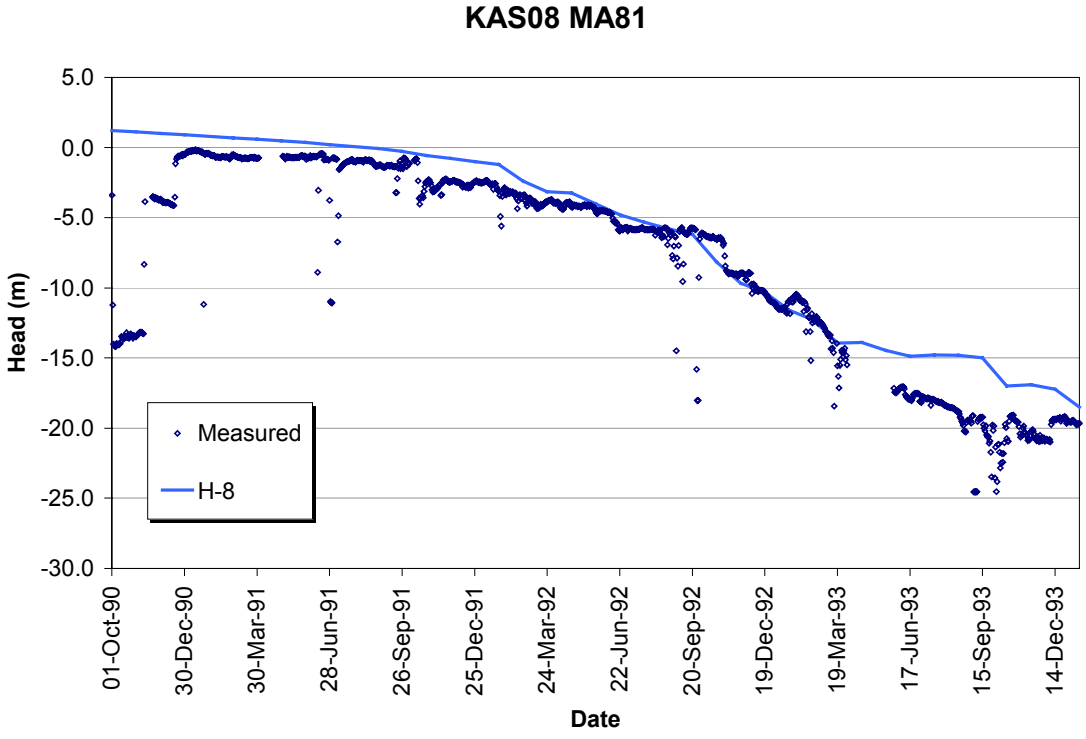

Figure 3-7 *Drawdown Response of KAS08 MA81 in Model H-8*

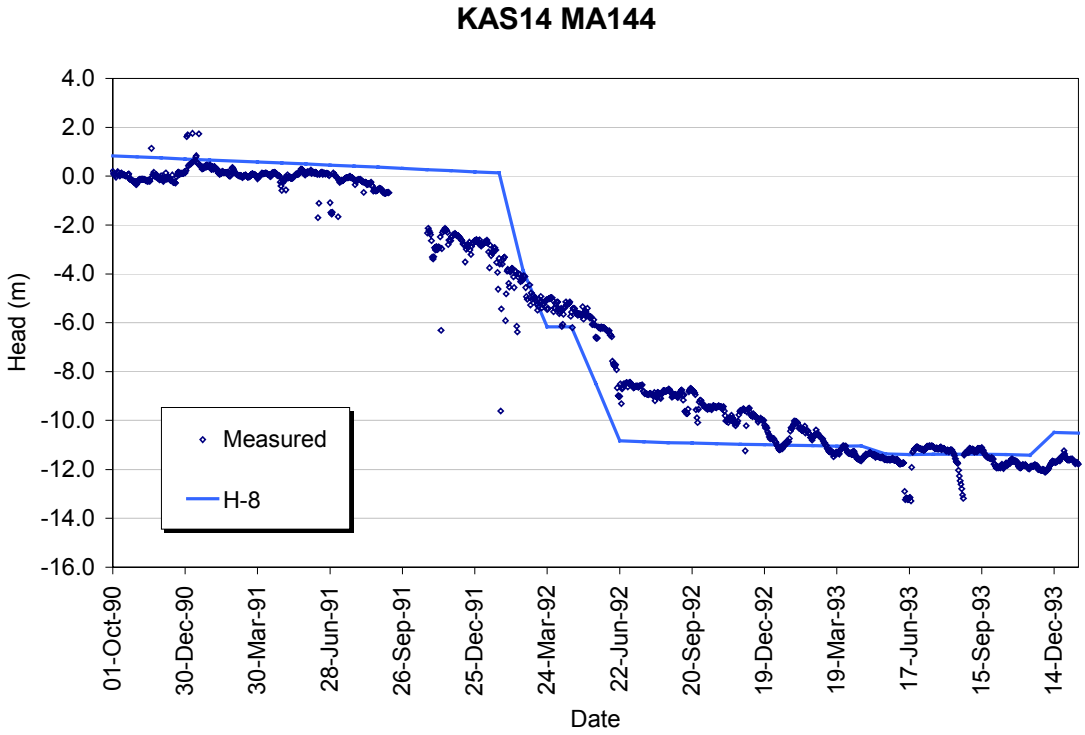

Figure 3-8 *Drawdown Response of KAS14 MA144 in Model H-8*

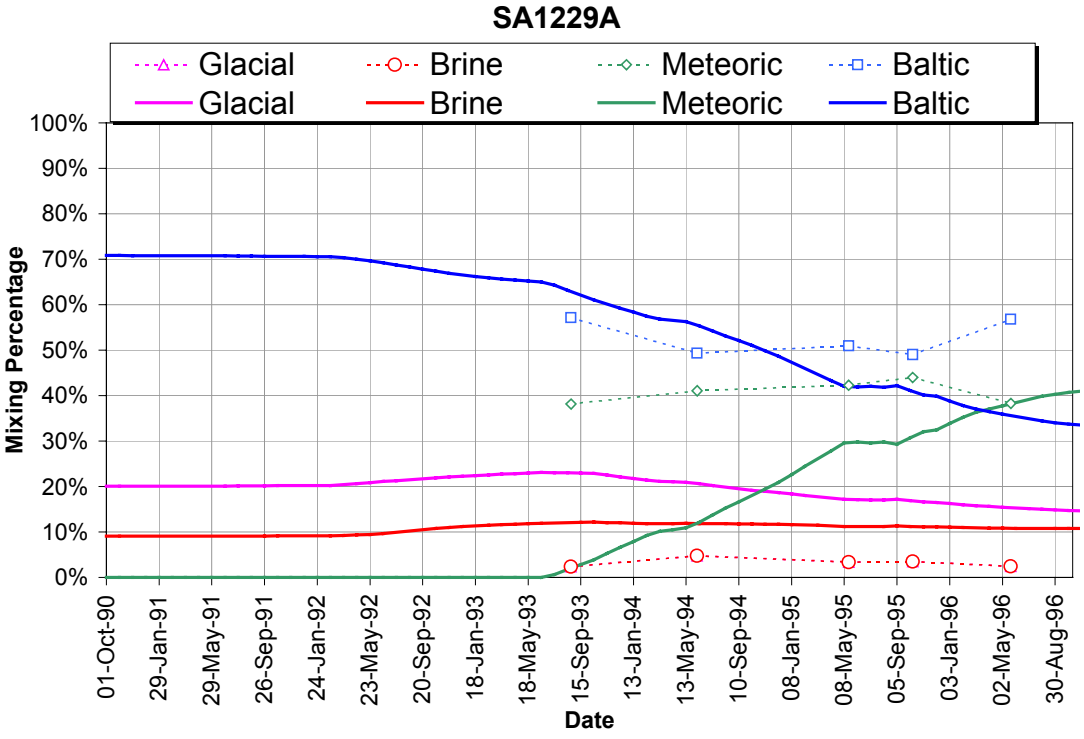

Figure 3-9 *Geochemical Response of SA1229A in Model H-8*

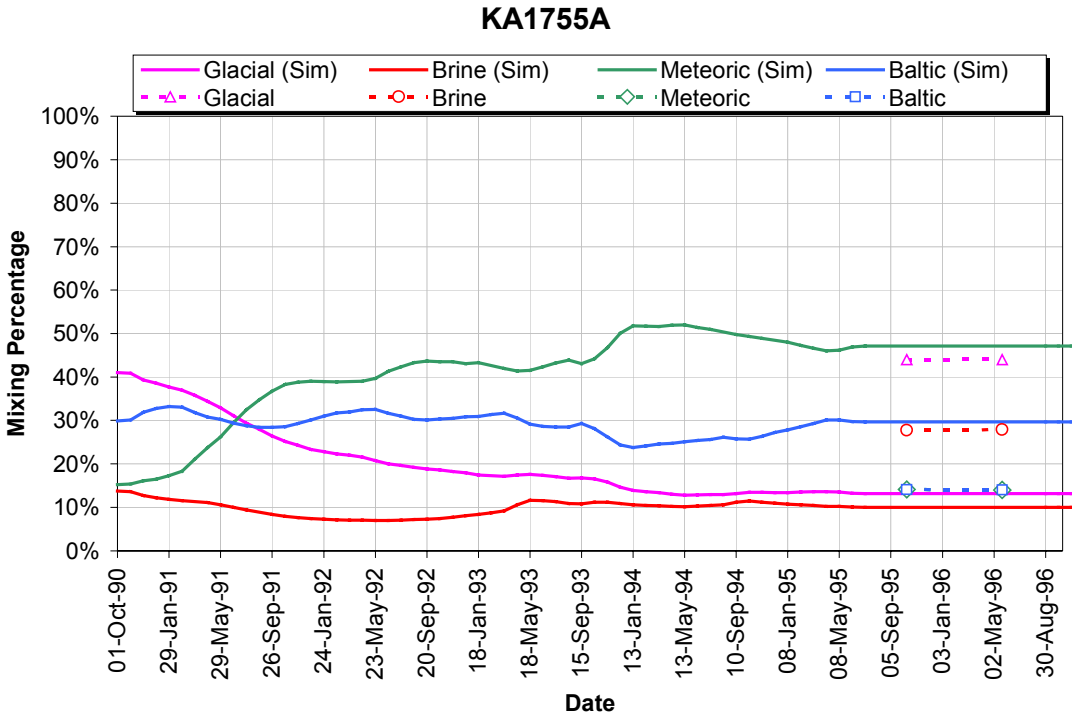

Figure 3-10 *Geochemical Response of KA1775A in Model H-8*

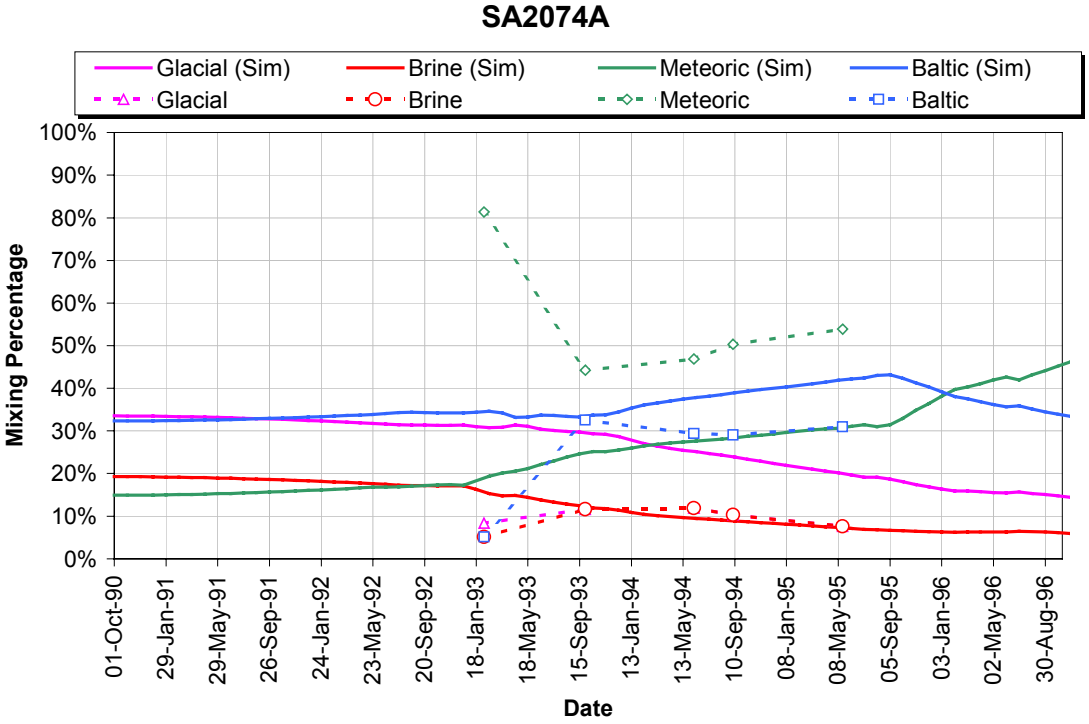

Figure 3-11 *Geochemical Response of SA2074A in Model H-8*

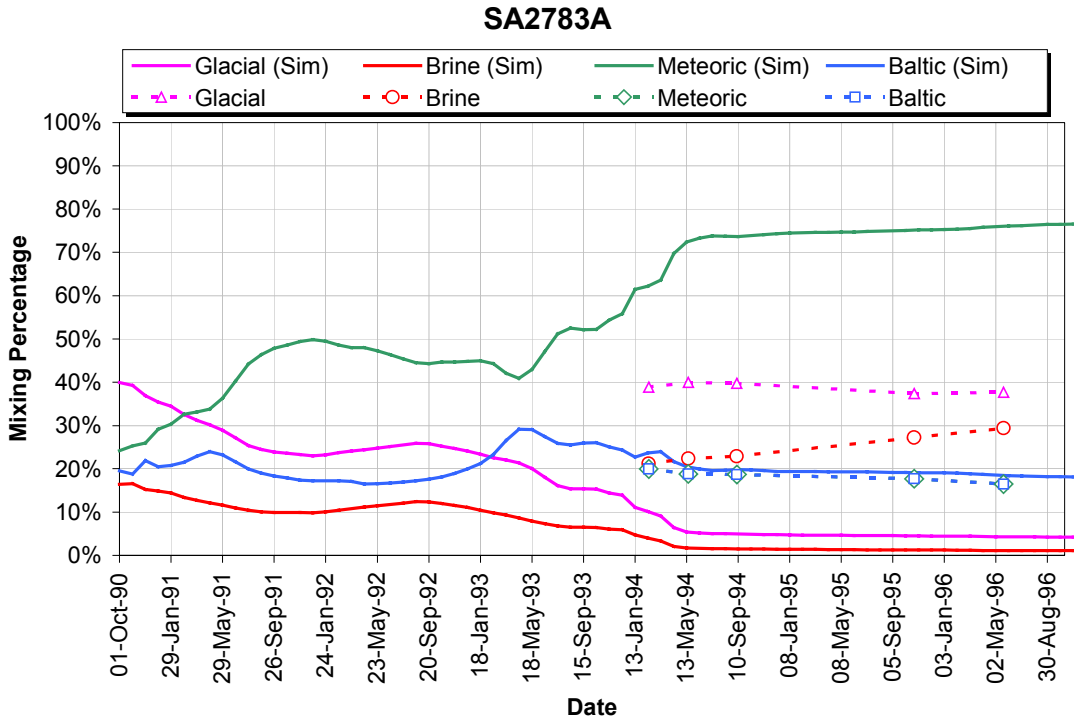

Figure 3-12 *Geochemical Response of SA2783A in Model H-8*

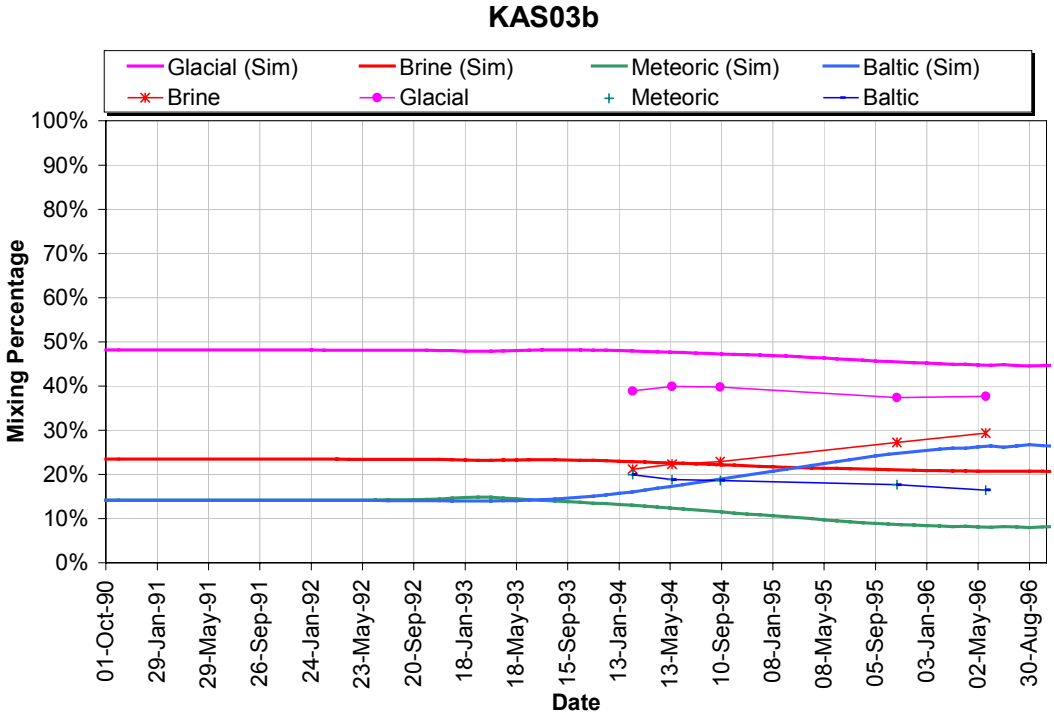

Figure 3-13 *Geochemical Response of KAS03b in Model H-8*

4. STAGE 2: GEOCHEMICAL CALIBRATION

In the second modeling phase JNC/Golder adjusted the Task 5 hydrogeological model to match the geochemical observations. The modeling was primarily focused on improving the calibration to geochemical end members collected at the control points. Of particular interest was the glacial component, which was lacking in the modeling from the hydrogeological calibration.

The following section provides a record of the process of geochemical model calibration and summarizes the results of the calibrated Stage 2 model. Detailed Stage 2 model results are provided as Appendix B.

4.1 GEOCHEMICAL CALIBRATION

The geochemical model calibration for Task 5 started from model H-8 developed in the previous section. The geochemical model calibration simulations are summarized in Table 4-1 and the progress of geochemical calibration is illustrated in Figure 4-1.

The first step for the geochemical calibration was to compare the geochemical results from the hydrogeological calibration H-8 to measured values. Although the average absolute error in the end-member fit was not bad, many deep control points have large measured influxes of glacial water end-members (Figure 4-2).

Since there are no connections to significant glacial water reserves (Figure 4-3), it was necessary to add fracture connections to the north to provide those connections. The structural connection added to the north is illustrated in Figure 4-4. The resulting transport pathways are shown in Figure 4-5.

Another problem with the model H-8 was that it did not provide sufficient meteoric water, as illustrated in Figure 4-6. To solve this problem, the surface boundary condition was changed from no-flow on Äspö Island to a constant infiltration.

The resulting model, G-1, provided a better match for glacial water and meteoric water. Model G-1 constituted the geochemical model prediction as presented to the Task Force in November 1999.

Comparison of end-member breakthrough at control points shows that Model G-1 still had too much Baltic seawater, as shown in Figure 4-7. To solve this, it was necessary to add the Baltic Sea skin back into the model. This skin had been removed to decrease the average drawdown and improve the hydrogeological model for simulation H-8. However, the geochemical evidence indicates that the Baltic Sea skin effect is real. Therefore, to compensate for the increased drawdown due to reinstatement of the Baltic Sea skin, the transmissivity of all fractures, including the deterministic fracture zones, was increased by a factor of 3. Example results from this model are shown in Figure 4-8.

Results from Model G-2 indicated that the introduction of a 3-fold increase in fracture transmissivity was too much, as the model drawdowns are very sensitive to the fracture transmissivity due to the flow boundary conditions. The change in head is approximately linearly related to the change in transmissivity; therefore the transmissivity was decreased by a factor of 1.6 for Model G-3. Model G-3 showed a much better balance of glacial, meteoric, and Baltic water. However, the Baltic seawater boundary still arrives to the tunnel much to fast. Therefore, the effective transport aperture for model G-4 was increased by a factor of 5. Example results from model G-4 are provided in Figure 4-9 and Figure 4-10.

Table 4-1 Geochemical Calibration Simulations

Sim	Stage II: Geochem Calibration	Features	# of Sections at first time	Time Average dh	dh at 1/13/94	Geochem Fit Average ABS
H-8	No geochemical calibration	Final hydrogeological model.	45	5.13	13.46	14.4%
G-1 28-Oct	chem2: H-8 model with connection added to north, modify boundary condition on Äspö Island	Connection to north added in order to draw in more Glacial-rich water to deeper control points. Äspö Island boundary condition changed from no flow to 30 mm/year infiltration. No low transmissivity skin over Baltic.	45	3.75	9.74	15.6%
G-2 1-Nov	chem3: Baltic skin, change zone transmissivity	Baltic Skin of T=0.01x reintroduced, All fractures (incl. deterministic frac. zones) T= 3x	45	-4.11	-9.13	13.1%
G-3 2-Nov	chem3-2 s1	G-2, with all fractures (incl. deterministic frac. zones)T=1.6x	45	-0.49	0.25	13.3%
G-4 3-Nov	chem3-2 s5	G-3, with transport aperture increased to 5x to increase travel time	45	-0.49	0.25	12.7%

Table 4-2 Summary of Model G-4

Property	Description
Fracture Model	
Major Discrete Features	22 Planar Homogeneous Zones (Rhén et al., 1997). See Table 2-1 for details. Fracture transmissivities increased by a factor of 1.6.
Background Fractures	22704 features described in Table 2-1. Fracture transmissivities increased by a factor of 1.6.
Mystery Feature	Addition an additional feature located between features NNW1and NNW7. Constructed from two fractures as shown in Figure 2-7.
Conditioned fractures intersecting tunnel sections.	Deterministic fractures added at 69 head calibration sections. Transmissivity of these deterministic fractures set at 1.6×10^{-8} m^2/s to reduce excessive drawdowns.
Connection to North	Connection to north added in order to draw in more Glacial-rich water to deeper control points.
Transport Aperture	Aperture = 10 * Transmissivity$^{0.5}$
Boundary Conditions	
North, South, East & West sides	Conditioned to the values reported in Svensson (1999).
Base	No flow boundary assigned to each node.
Baltic Sea	Head of 0.0 m. Skin of $0.01*T_{original}$ added to upper 10m.
Äspö Island	Group flow boundary condition added equivalent to net infiltration of 30 mm/year.
Geochemistry	
Chemical Composition	End-member definitions and proportions calculated using the program M^3 (Laaksoharju, M., 1999).
Interpolation Scheme	Linear interpolation from a grid of 1000 locations provided in Data Delivery No. 4

4.2 PREDICTIVE SIMULATIONS

The G-3 geochemical model was then used as the basis for the Stage 2, geochemical model predictions. The model predictions are reported in Appendix B.

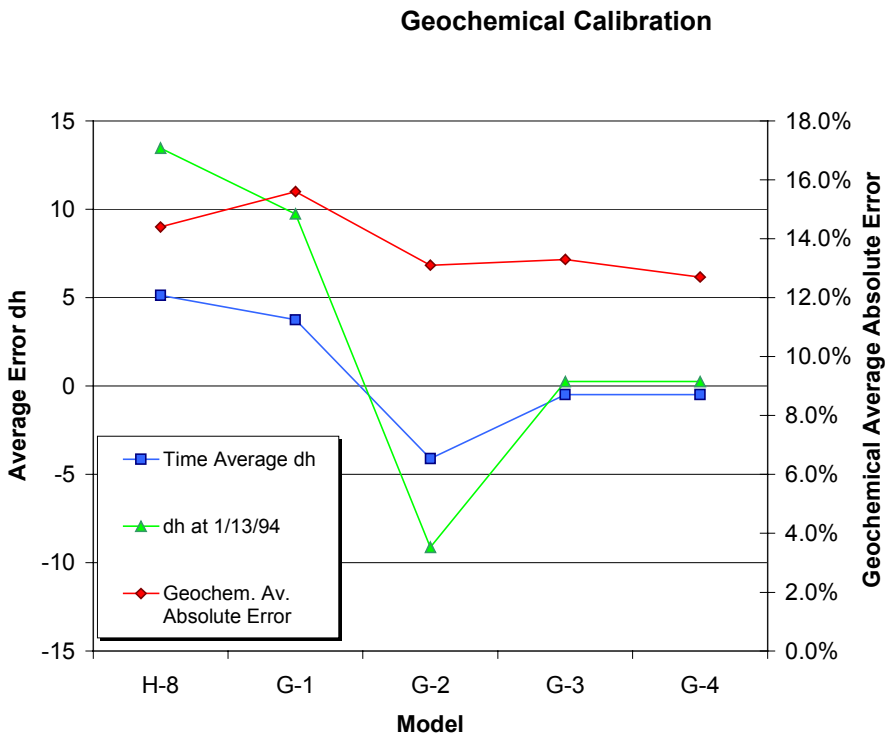

Figure 4-1 *Progress of Geochemical Calibration*

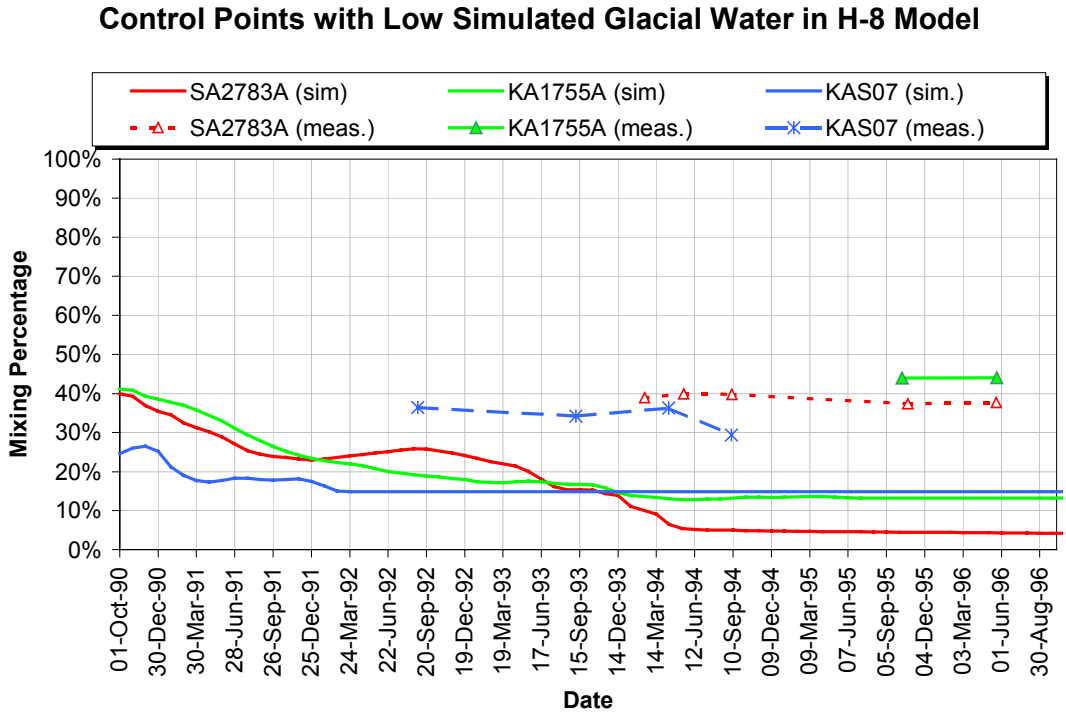

Figure 4-2 *Glacial Water in Model H-8*

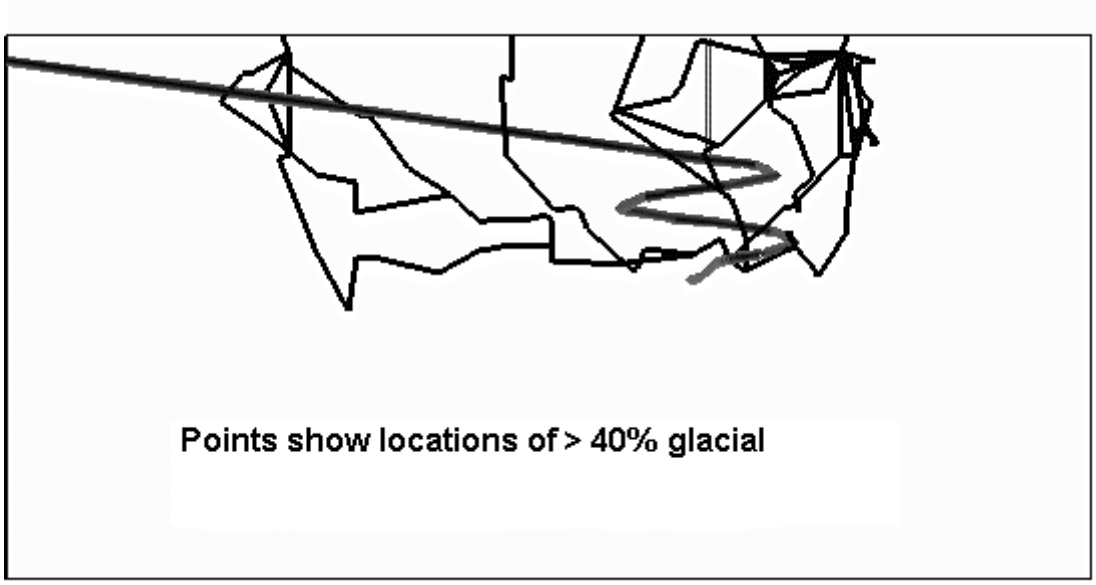

Figure 4-3 *Pathways to Glacial Water in Model H-8*

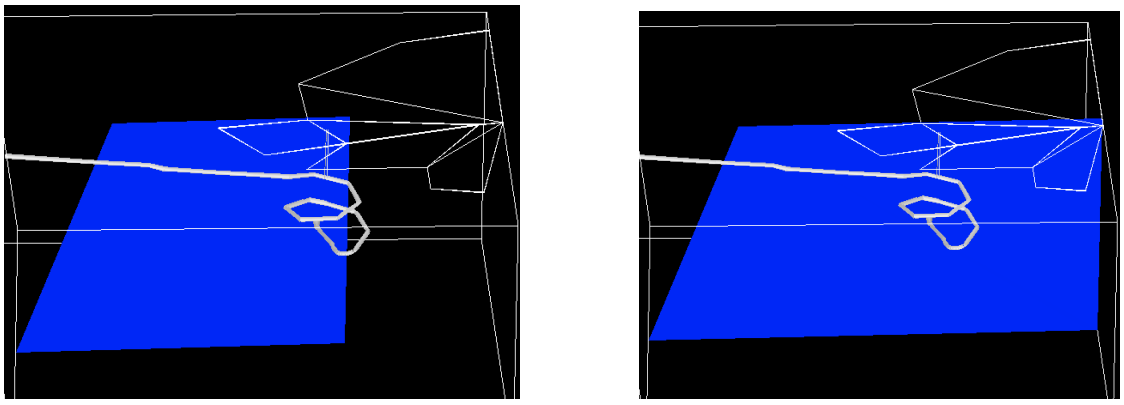

Figure 4-4 *Modification to Structural Model for Geochemical Calibration. Figure on top shows original structural model with NNW-5 truncating near the latitude of the tunnel. Figure on the bottom shows the extension of this feature north, into the glacially rich groundwater zone.*

(a) Model G-1: No pathway to Glacial water

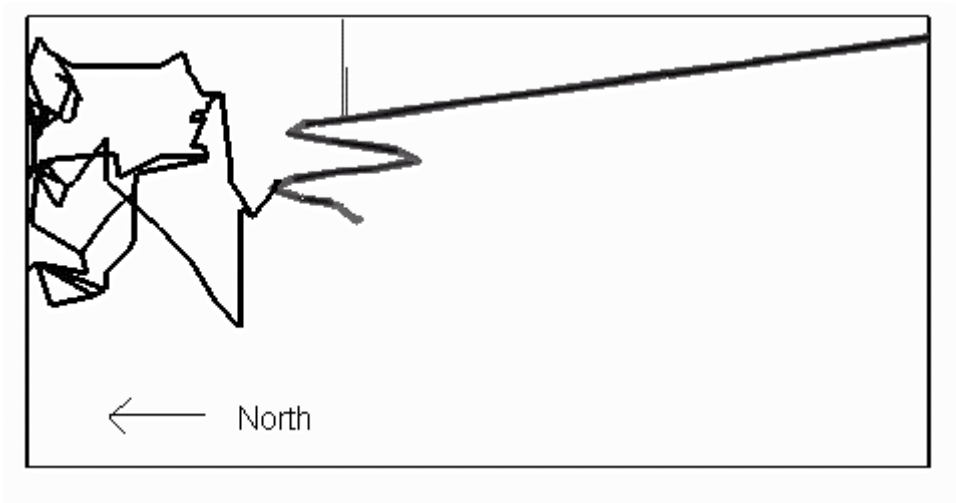

(b) Model G-3: Pathways to Glacial water at north

Figure 4-5 *Pathways to Glacial Water in Model G-1*

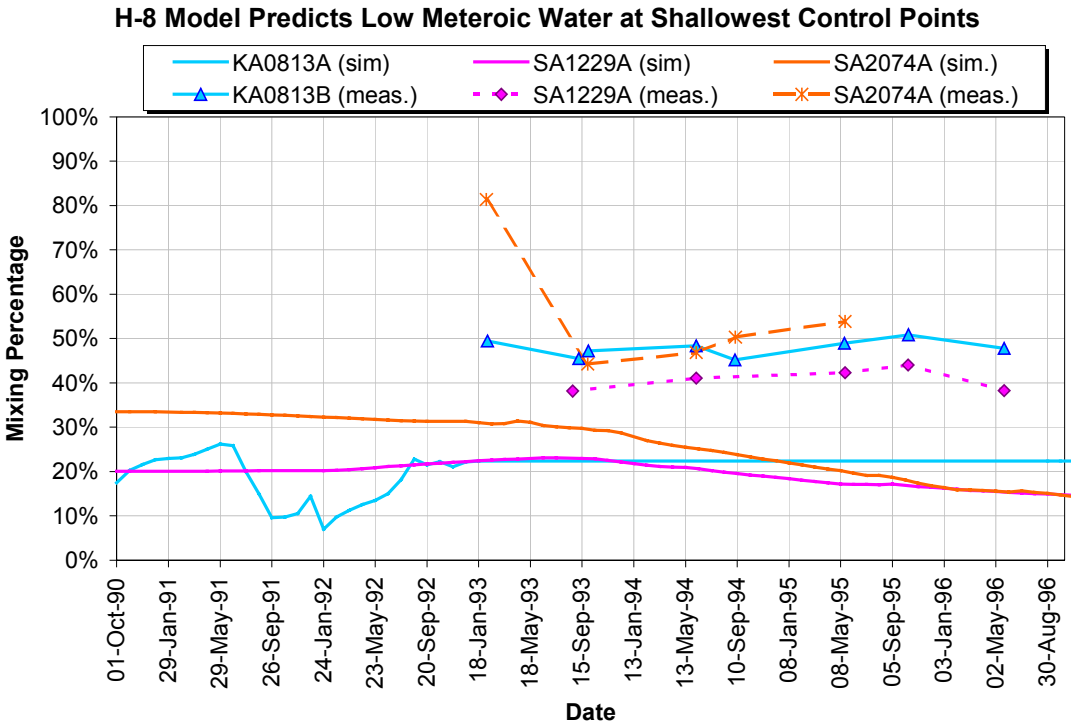

Figure 4-6 *Meteoric Water in Model H-8*

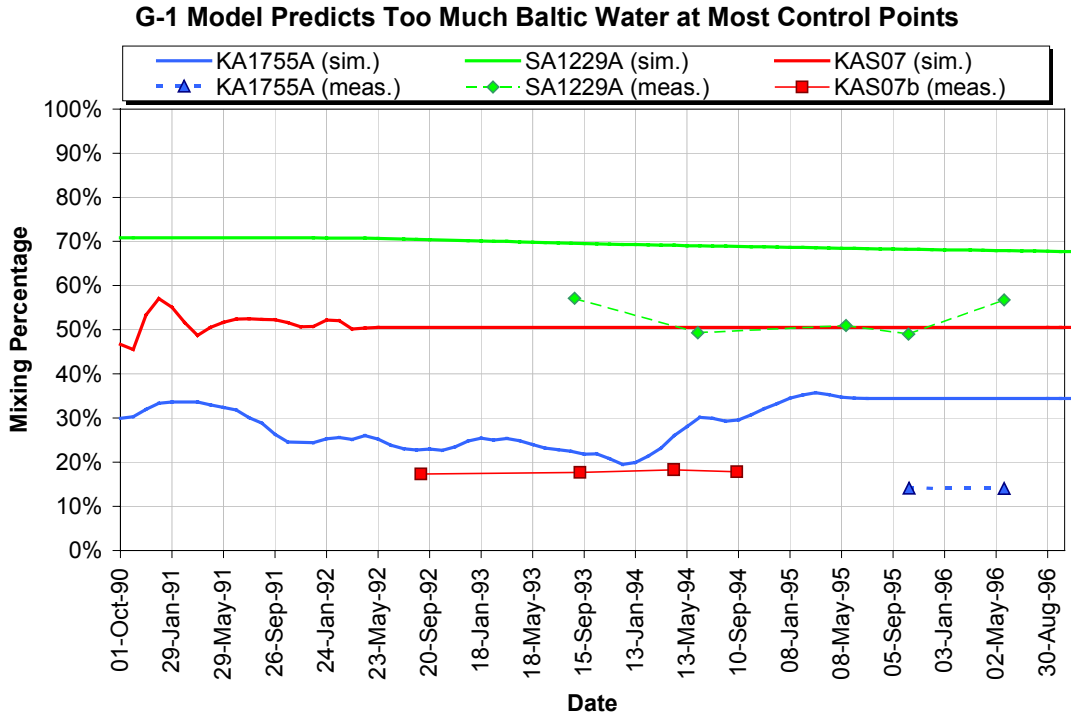

Figure 4-7 *Baltic Sea Water in Model G-1*

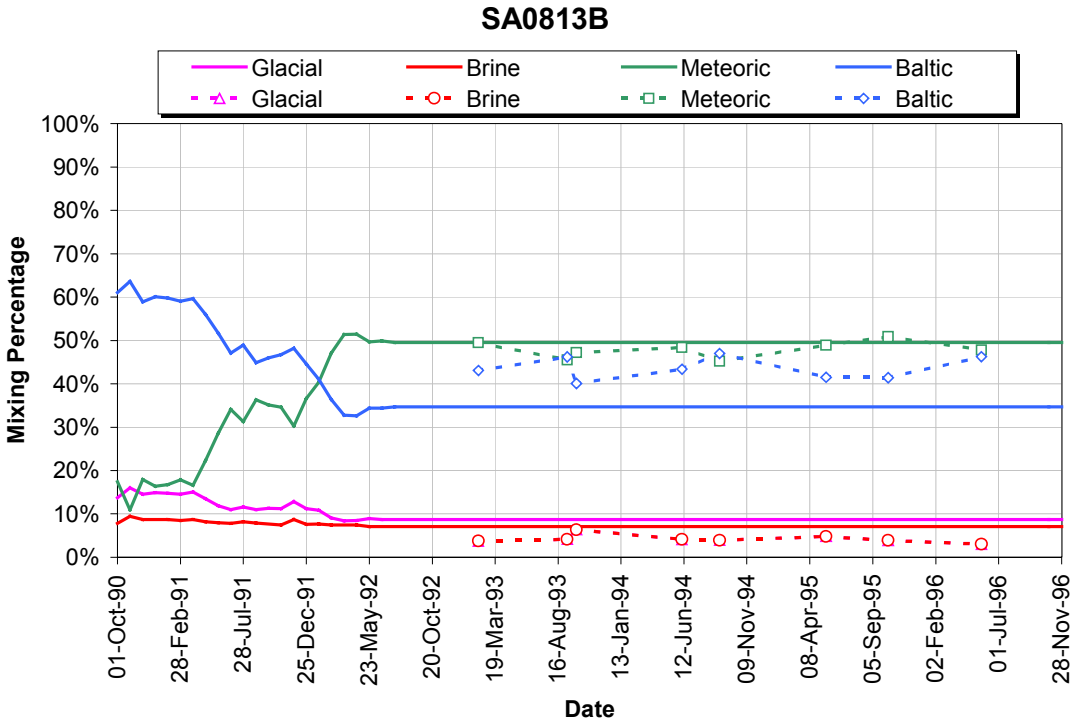

Figure 4-8 *Geochemical Calibration, SA0813B of Model G-2*

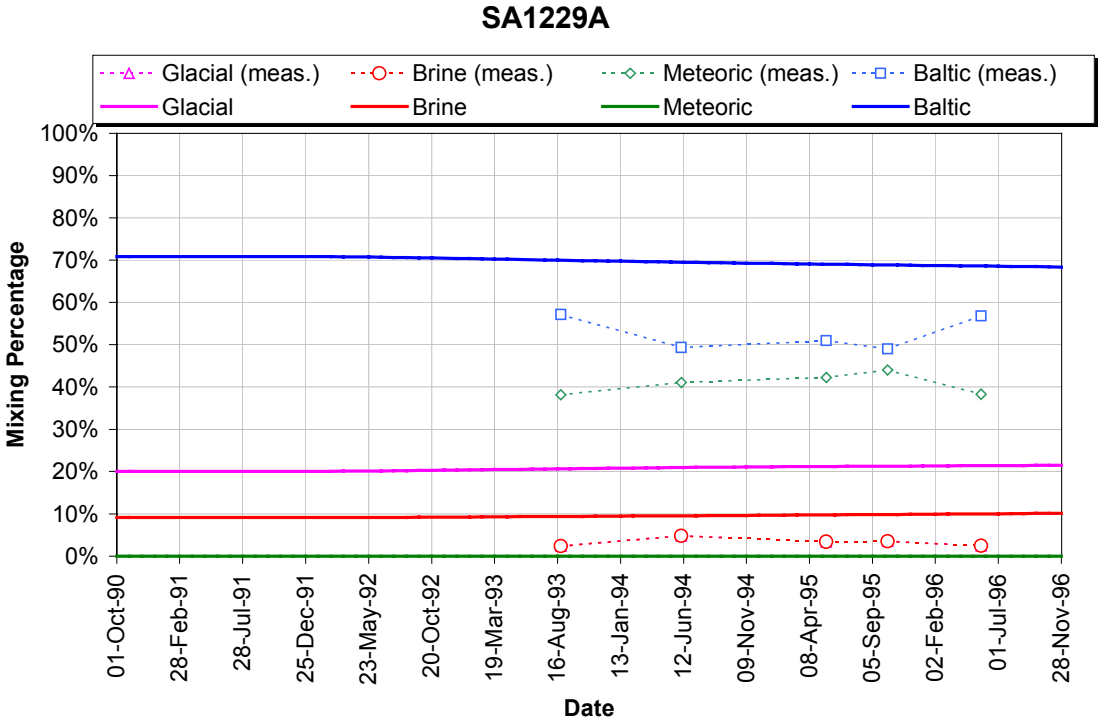

Figure 4-9 *Geochemical Prediction, SA1229A of Model G-4*

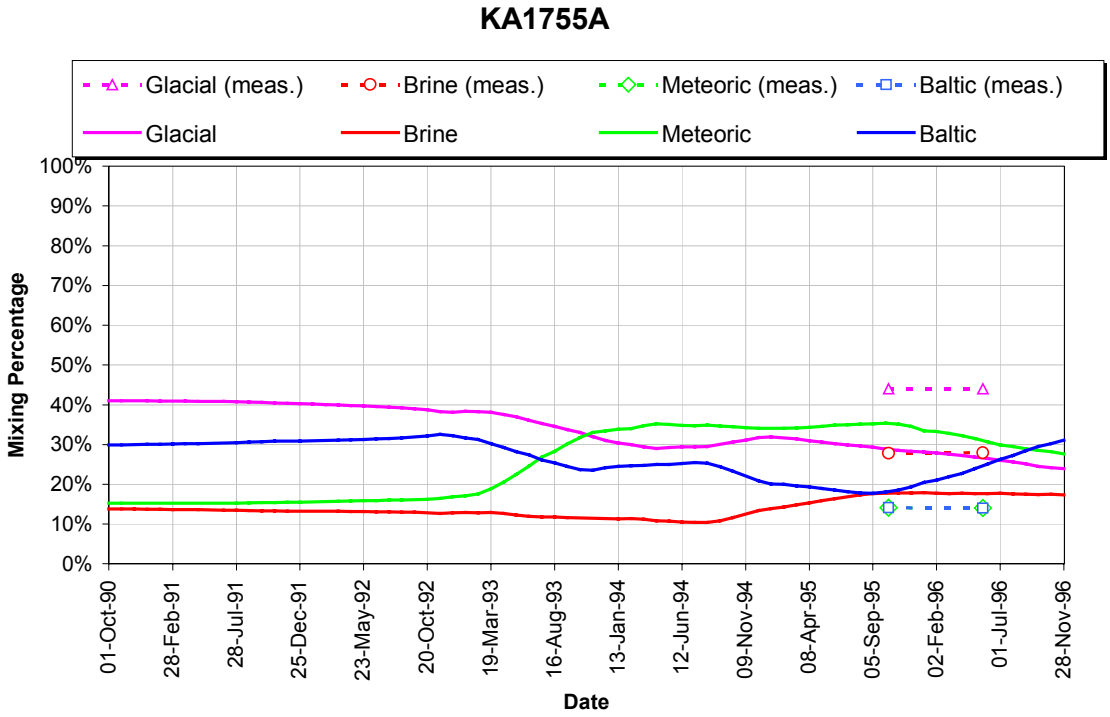

Figure 4-10 *Geochemical Prediction, KA1755A of Model G-4*

5. EVALUATION

A demonstration of consistency between physical hydrogeological models and hydrogeochemical models is a key goal of Task 5. Such a demonstration builds general confidence in the models. The smaller the uncertainties in models that are shown to be consistent, the greater will be the improvement in this confidence.

In the modeling approach adopted by JNC/Golder two main groups of hydrogeochemical uncertainties are important:

- Uncertainties in the initial spatial distributions of chemically distinct groundwaters;
- Uncertainties in the chemistry and mixing proportions of different end-members.

This section is concerned with the second group of hydrogeochemical uncertainties.

To represent this uncertainty additional numerical analysis was undertaken considering three issues:

Issue 1: Uncertainty introduced to the analysis by the use of the four M3 geochemical end members.
This was addressed by using a multivariate analysis for end members with lower residual error.

Issue 2: Pathway analysis limitations related to using a graph theory algorithm.
This was addressed by replacing the graph theory pathway analysis with a new particle backtracking algorithm to improve pathway identification

Issue 3: Spatial interpolation of initial conditions.
This was addressed by using an interpolation scheme that was weighted to reflect fracture zone geochemistry patterns, and to distinguish between waters under Äspö island from those beneath the Baltic.

The details of this analysis are presented in Sections 5-1 to 5-5.

5.1 GEOCHEMICAL ISSUES

5.1.1 Importance of Uncertainties in End-Member Compositions and Mixing Proportions

A demonstration of consistency between physical hydrogeological models and hydrogeochemical models is a key goal of Task 5. Such a demonstration builds general confidence in the models. The smaller the uncertainties in models that are shown to be consistent, the greater will be the improvement in this confidence.

In the modeling approach adopted by JNC/Golder two main groups of hydrogeochemical uncertainties are important:

- Uncertainties in the initial spatial distributions of chemically distinct groundwaters;
- Uncertainties in the chemistry and mixing proportions of different end-members.

This section is concerned with the second group of hydrogeochemical uncertainties.

5.1.2 Definitions

Three definitions in particular are important in the following discussion:

- **End-member:** In the present context, this term simply means a water at the extreme of a compositional range (c.f. Bates and Jackson, 1980). Thus, the definition of an end-member depends upon the precise compositional range of interest and does not necessarily imply anything about the origin of the water; an "end-member" may be a mixture of other waters, which have simply not been identified.
- **Principal Component:** This term refers to a mathematical component derived during Principal Component Analysis (PCA). Each principal component is an eigenvector of a variance-covariance or correlation matrix and represents an independent contribution to the variability of the system being analyzed (e.g. Davis, 1986).
- **Chemical component:** This term refers to any chemical entity used to describe the chemistry of a system. Unlike phases (gas, liquid etc) or species (Fe^{2+}, Cl^- etc), which are real entities, chemical components are abstract quantities that may be defined in any convenient manner (Nordstrom and Munoz, 1994). For example, the formation of water, H_2O can be described in terms of the components H and O ($2H + O = H_2O$), or in terms of the components H2 and O2 ($H_2 + 0.5O_2 = H_2O$). While chemical components are often selected to be *real* chemical entities within a system (e.g. H_2O), this is not always the case.

Thus, in the present report a principal component derived from a set of chemical data always corresponds to a chemical component. However, the reverse is not true and there is not always a principal component that corresponds to a chemical component.

5.1.3 Justification for End-Member Modeling

Task 5 aims to predict the chemistry of water flowing into the Äspö tunnel, using knowledge of the initial spatial distributions of chemically distinct groundwaters and simulations of mixing based upon an understanding of physical hydrogeology. Therefore, it is required to:

- Distinguish variations in chemical components that reflect only mixing over the time-scale of the investigations at Äspö (i.e. to neglect the effects of variations caused by water/rock interactions); and
- Reduce the number of alternative interpretations of mixing (ideally a unique interpretation of mixing is sought, though in practice this may not be possible).

By modeling based upon PCA it is possible in principle to meet both goals. This approach can distinguish correlations between several chemical components that reflect only mixing. Then, by identifying these correlations with variations in the proportions of end-members, it is possible to interpret groundwater mixing based upon a range of chemical components. This interpretation is likely to be less ambiguous than one based upon only a single chemical component, such as chloride (for example).

5.1.4 Approach to Evaluation

The initial modeling conducted by JNC/Golder used the compositions of end-members and mixing proportions of these end-members calculated by SKB using the computer code Multivariate Mixing and Mass balance (M3; Rhén et al. 1997; Laaksoharju, 1999a; Laaksoharju et al. 1999b). These compositions and mixing proportions were presented in Data Delivery 19, released by SKB on 15th December 1999 (delivery reference F65H).

The initial evaluation involved reviewing the M3 methodology; to identify and evaluate uncertainties of particular relevance to JNC/Golder's modeling approach. As part of this review, a series of questions were written concerning M3 and submitted to SKB. These questions were answered in Laaksoharju (2000).

From this initial evaluation it was apparent that the M3 approach did not consider all the variability in the chemical data (see below). Additionally, it was not clear to what extent the method would be generally applicable to groundwater systems other than systems like the one at Äspö, within which saline waters and brines occur. Therefore, a new statistical model was commissioned by JNC from Golder Associates, who sub-contracted the work to the British Geological Survey (BGS). This new model considered all the chemical variability in the data. Several possible alternative combinations of input data were considered, besides the data used in the original M3 modeling.

Finally, a comparison was made between the results of the new modeling and the original M3 modeling.

5.1.5 Summary of M3 Modeling

Statistical processing of analyses of these waters was undertaken by SKB's contractors using the computer code Multivariate Mixing and Mass balance (M3). This modeling has been described in detail elsewhere (Rhén et al. 1997; Laaksoharju, 1999a; Laaksoharju et al. 1999b) and only a brief overview is given here, to allow the following discussion of uncertainties to be understood. The basic approach is illustrated in Figure 5-1.

The M3 code was used to perform PCA, enabling groups of chemically similar waters to be identified. This modeling did not use analytical data for all the groundwaters' constituents, but only data for Na, K, Ca, Mg, HCO_3, Cl, SO_4, D, Tr, and ^{18}O. Most of the chemical variability in the waters (c. 70%) was attributed to just two principal components. These two components were considered to reflect mixing, rather than other potential contributors to chemical variability, such as water/rock reactions, contamination during sampling or, in the case of tritium, radioactive decay.

These other possible contributors to chemical variability were represented by the other principal components. For example, the third principal component was considered to reflect the decay of tritium.

The groundwaters were plotted on a cross-plot, with axes representing the two principal components that represented most of the variability. The plotting position of each water was determined by the corresponding eigen values. When plotted in this way, the groundwaters define a field that can be surrounded by a polygon, having the most extreme groundwater compositions as its apices. Some of these compositions were chosen as "reference" compositions. The proportions of these compositions that would be required to mix to form each of the groundwaters within the polygon were then calculated, by assuming that the reference compositions mix conservatively (that is, without any chemical reactions occurring). A center point within the polygon was used to allow the proportions of more than three reference samples to be calculated. The proportion of any reference water in any other water of interest was assumed to be inversely proportional to the distance between the reference water and the water of interest on this bivariate plot. For each water, the mixing proportions calculated in this way were used together with the actual compositions of the reference waters to calculate theoretical concentrations of the chemical constituents on the water. The resultant theoretical composition was then compared with the actual composition of the water. Deviations from the actual compositions were assumed to be due to chemical reactions between the waters and the rocks.

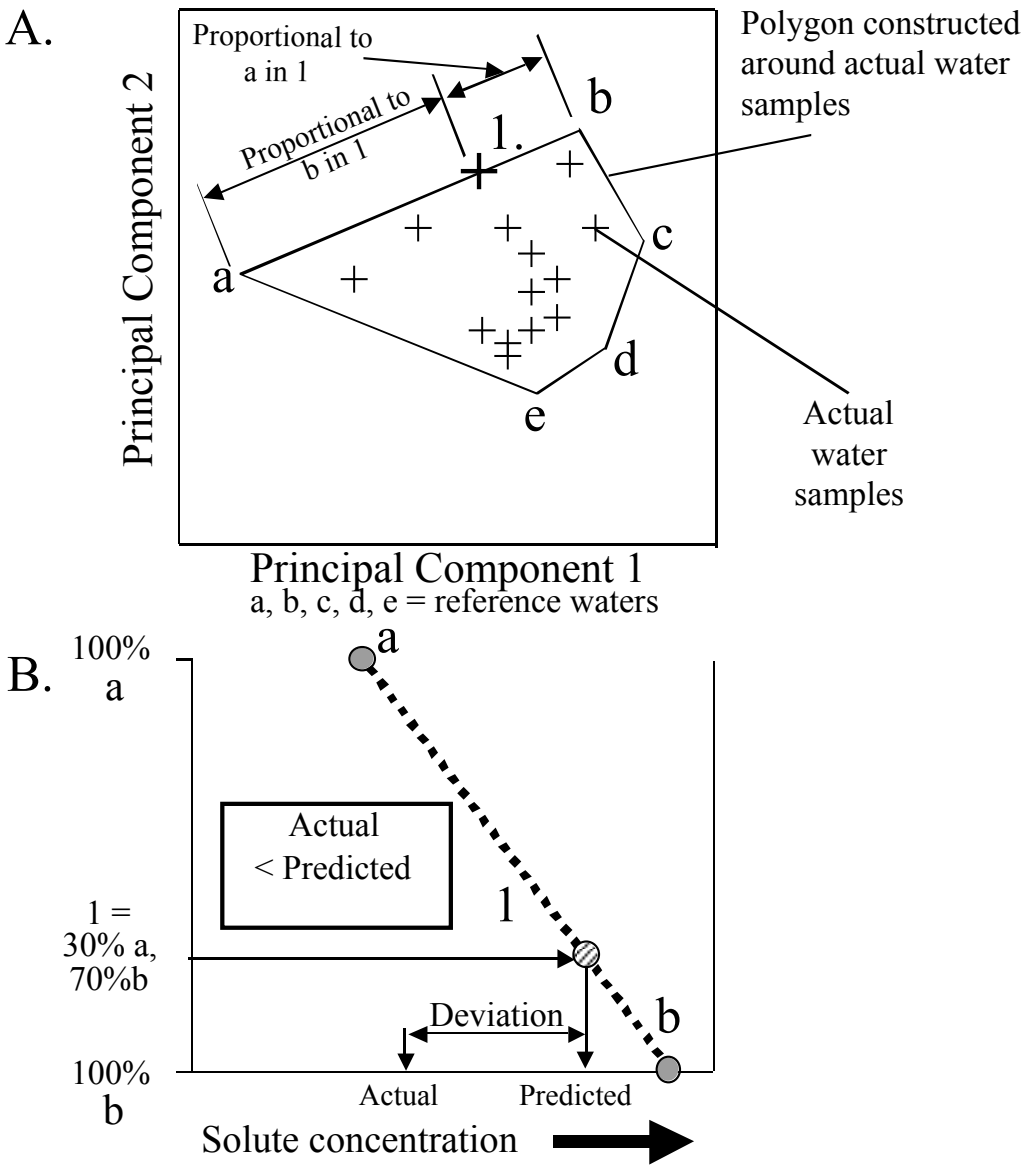

Using the eigen values, waters are plotted on the two most important principal components identified by PCA. The points are enclosed by a polygon with apices representing reference waters that are assumed to mix to form the actual waters. The proportions of the reference waters in each other water are derived geometrically. B. Theoretical concentrations of solutes in each water are calculated from these proportions and compared with actual concentrations. Differences between the values are generally attributed to water/rock interactions, in the case of potentially reactive constituents, like Na. Deviations in relatively non-reactive solutes, like Cl, may imply that that the assumption of mixing between the chosen reference waters is invalid.

Figure 5-1 *Schematic illustration of the M3 approach*

During the Task 5 work, the waters were all reported to be mixtures of the following end-members:

- Brine;
- Glacial water;
- Meteoric water; and
- Baltic Sea water.

5.1.6 Key Assumptions and Uncertainties in the M3 Modeling

The most significant causes of uncertainties in the end-member compositions and mixing proportions calculated by M3 (Laaksoharju, 2000) are:

- Sampling errors due to effects such as borehole drilling, pumping, contamination etc;
- Errors caused due to the analytical methods;
- Conceptual errors, such as the following assumptions being incorrect:

  - the assumption that the number of end-members have been correctly identified;
  - the assumption that all waters are mixtures of all end-members;
- Methodological errors, notably caused by:

  - the model being over-simplified or biased, for example by neglecting trace constituents of the groundwaters from the PCA and assuming that the end-members can be defined adequately by a sub-set of the constituents;
  - the simplifying assumption that the two most important principal components reflect groundwater mixing and that groundwater mixing effects are not represented significantly by any of the other components.

Sampling and analytical errors are unavoidable in any groundwater chemical investigation. These errors will affect not only the M3 modeling, but also any other modeling that uses the same chemical data. The effects of sampling errors were allowed for by evaluating the circumstances of sampling (e.g. rejecting samples collected during hydraulic tests that experienced difficulties). Contamination effects were minimized by using tracers in the drilling fluid and using samples for which contamination from this source was indicated to be less than 1% (Laaksoharju, 2000). The uncertainty from sampling errors was estimated/modeled to be in most cases around ± 10% from the undisturbed, *in-situ* values. Analytical errors for different elements vary but inter-laboratory comparisons indicate generally a deviation of 1-5% in the values (Laaksoharju et al., 1999a, b; Laaksoharju, 2000).

The choice of end-members is inevitably subjective. However, to minimize the chances of inappropriate end-members being chosen, these end-members were selected to be consistent with both distributions of samples on the plot of the two principle components and an independent hydrogeochemical conceptual model. This latter suggested which type of water might have entered the bedrock and employed additional geological information and data from fracture minerals. The model was consistent with the choice of reference waters (glacial meltwater, seawater, meteoric waters) being appropriate for describing mixing in the groundwater system used to guide the minimum number and type of end-members needed to explain the observations.

Alternative mixing proportions were calculated using alternative possible end-members. These alternative end-members were chosen to be consistent with both the independent hydrogeochemical model and the ranges of groundwater compositions on the bivariate plot of the first two principal components (Laaksoharju, 2000). This approach suggested that the error in mixing proportions due to an incorrect selection of end-members was on the order of 10%.

The third principal component accounts for around 10% of the groundwaters' chemical variability. This is small compared with the first and second principal components which contain account for about 70% of the variability; the remaining principal components encompass the other 20% of the variability (Laaksoharju, 2000).

The location of a sample on the plot of the first and second principal components can be inappropriate because of all the errors mentioned above. Laaksoharju et al. (1999a,b) and Laaksoharju (2000) allowed form this by stating the uncertainty in the method to be ± 0.1 mixing proportion units and the detection limit for the method as <10% of a mixing portion.

5.1.7 Summary of Revised Modeling

There are several limitations to applying the M3 modeling in JNC/Golder's approach, notably:

- One goal of JNC/Golder is to evaluate how the basic Task 5 method might be applied in Japan. However, the M3 method was developed for application at Äspö where saline groundwaters and brines are major features of the groundwater system. The method may not be generally applicable. In particular, the reliance of the method on the first two principal components may not be appropriate in fresh groundwater systems. In such cases the first two principle components are more likely to reflect factors other than groundwater mixing. For example, water/rock interactions are likely to be a more significant cause of chemical variation in fresh groundwater systems than in saline groundwater systems. In such cases, it will be necessary to consider other principal components besides the two most important ones, in order to deduce information about groundwater mixing.
- By not considering principal components other than the first two, M3 potentially disregards important information that might be used to evaluate more precisely the validity of the underlying assumptions, such as the assumption that all end-members are present in all waters.
- While sensitivity calculations were conducted by SKB and its contractors to evaluate underlying uncertainties in the M3 method (Laaksoharju, 2000), the results of these calculations have not been reported in detail. Therefore, the precise significance of these uncertainties for JNC/Golder's modeling approach is not clear.
- Even though the end-members used in the M3 modeling were chosen with reference to a hydrogeochemical model for the site, there is still considerable subjectivity in their selection. The chosen end-members, while having extreme compositions near the limits the range of sampled waters compositions, are themselves mixtures of other waters. Additionally, some chemically similar

waters have probably been introduced into the groundwater system at Äspö several times during the site's history. For example, sub-glacial water has presumably been recharged several times during the repeated glaciation of the site within the Quaternary period.

For these reasons, it was decided to carry out revised modeling, using a chemometric algorithm (Cave and Harmon 1997, Cave and Wragg 1997), which makes no initial assumptions about the nature of the end-members present, and which considered all the contributions to chemical variability in the groundwaters.

The basic approach is illustrated in Figure 5-2 and Figure 5-3. Here matrix **A** is the supplied groundwater data matrix and matrices **B** and **C** need to be found. The process for finding matrices **B** and **C** was carried out in a four-stage process:

- PCA and eigenvalue analyses were initially used in a similar fashion to the M3 method.
- The varimax rotated loadings matrix from the PCA of matrix **A**, containing the initial groundwater compositions, were used to produce a first approximation of matrix **B**, which contains the mixing proportions.
- The "pseudoinverse" method for non-square matrices was then applied to matrices **A** and **B**, to produce a first approximation of matrix **C**, which contains chemical components that contribute to the chemical variability in the groundwaters, some of which should correspond approximately to end-members.
- Matrices **B** and **C** were refined iteratively using the "pseudoinverse" method until both matrices contained estimates of mixing proportions and chemical component compositions that are consistent with the groundwater compositions in the original matrix **A.**

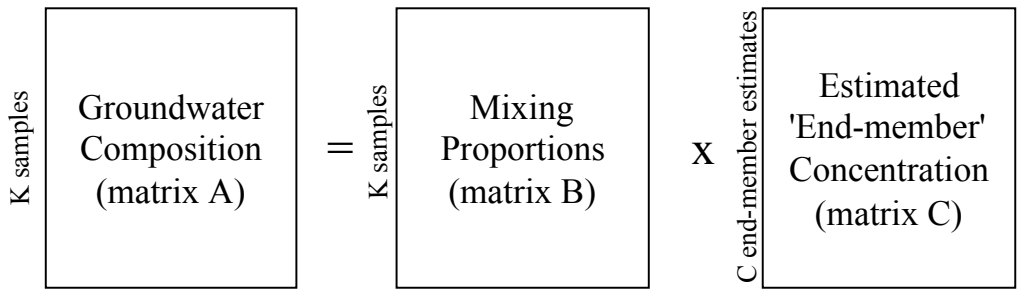

Figure 5-2 *Relationships between matrices used in the revised modeling*

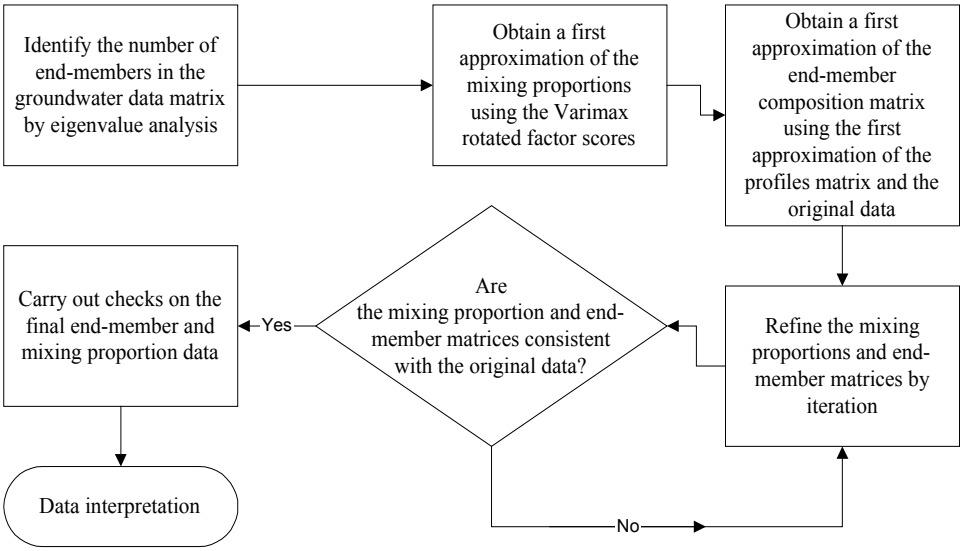

Figure 5-3 *Summary of the procedure adopted in the revised modeling*

It is important to note that the chemical components obtained from the new modeling are not principal components, but are derived from the principal components. Neither are the chemical components "end-members" in the sense of the M3 end-members. However, it is expected that there should be some similarities between compositions of the new chemical components and the M3 components.

To compare the results of the new modeling and the results of the M3 end-member modeling, the new mixing proportions were also expressed in terms of proportions of the original M3 end-members. This was done by a least- square approach, using the proportions of the new chemical components in each of the original M3 end-members and in each of the other waters as follows.

Several alternative cases were evaluated during the new modeling (Table 5-1). Some of these cases used exactly the same data as was used to produce the M3 model results in Data Delivery 9. This approach was to allow comparison of the results between the two methods. Other cases used a sub-set of this data, to explore the significance of departures from this approach.

Table 5-1 Summary of the cases considered in the revised modeling

Case	Determinands Considered	Water Compositions Used	Other Model Details
Model 1	Na, K, Ca, Mg, HCO_3, Cl, SO_4	All waters in Data Delivery 19, except for (Brine, Baltic Sea Water, Glacial Water and Meteoric Water, which were employed as end-members in the M3 modeling, and Sea Water, which was not employed in the latest M3 modeling)	Three separate models, using the different combination of water samples shown at the left Modeling was not carried out separately for high TDS samples as there were insufficient data in this group (6 samples)
		Samples in Data Delivery 19 with medium Total Dissolved Solid (TDS) contents (Cluster 1) (Brine, Baltic Sea Water, Glacial Water Meteoric Water, and Sea Water excluded from consideration)	
		Samples in Data Delivery 19 with low TDS contents (Cluster 2) (Brine, Baltic Sea Water, Glacial Water Meteoric Water, and Sea Water excluded from consideration)	
Model 2	Na, K, Ca, Mg, HCO_3, Cl, SO_4, D, Tr, $\delta^{18}O$	All waters in Data Delivery 19, except for (Brine, Baltic Sea Water, Glacial Water and Meteoric Water, which were employed as end-members in the M3 modeling, and Sea Water, which was not employed in the latest M3 modeling)	δD and δO18 values were multiplied by –1 to make them positive numbers.
Model 2 (v3)	Na, K, Ca, Mg, HCO_3, Cl, SO_4, δD, Tr, $\delta^{18}O$	All waters in Data Delivery 19, except for (Brine, Baltic Sea Water, Glacial Water and Meteoric Water, which were employed as end-members in the M3 modeling, and Sea Water, which was not employed in the latest M3 modeling)	Tritium data were used as reported. δD and $\delta^{18}O$ data were converted from per mil values to D/H and $^{18}O/^{16}O$ ratios for the purposes of the modeling and converted back to per mil values at the end
Model 2 (v5)	Na, K, Ca, Mg, HCO_3, Cl, SO_4, δD, Tr, $\delta^{18}O$ [8]	All waters in Data Delivery 19, INCLUDING Brine, Baltic Sea Water, Glacial Water and Meteoric Water, which were employed as end-members in the M3 modeling. Sea Water, which was not employed in the latest M3 modeling, was not included)	
Model 3	Na, K, Ca, Mg, HCO_3, Cl, SO_4, δD, $\delta^{18}O$	All waters in Data Delivery 19, except for (Brine, Baltic Sea Water, Glacial Water and Meteoric Water, which were employed as end-members in the M3 modeling, and Sea Water, which was not employed in the latest M3 modeling)	The model differs from Model 2(v3) only in that Tritium data were excluded

5.1.8 Key Assumptions and Uncertainties in the Revised Modeling

Unlike the original M3 modeling, the new model makes no prior assumptions about the numbers or compositions of chemical components (analogous to end-members in the M3 modeling). However, other assumptions are made, notably:

- the compositions of at least some of the chemical components derived statistically will approximate real groundwater compositions;
- the assumption that δ–values for ^{18}O and D are additive over the range considered is valid; and
- that all the chemical variability in the groundwaters is expressed by the chemical constituents (Na, Ca, Cl etc) used in the modeling, which form a subset of the actual constituents.

These last two assumptions were also made in the M3 modeling.

5.1.9 Results of the new modeling

All the results of the new modeling are tabulated in Appendix C. The compositions of the chemical components obtained from each model are compared with the compositions of the groundwater end-members used in the M3 modeling in Table 5-2. It is important to note that the chemical components are not placed in order of significance for the overall chemical variations; they are not principal components, though they are derived from principal components. Additionally, chemical components designated by the same number, but produced by different models are not necessarily equivalent.

None of the models in Table 5-2 produced components with the same compositions as the "end-members" used in M3. This result is expected since:

- The new approach makes no *a priori* assumptions about the compositions of waters that mix to form the sampled waters.
- The new approach aims to identify chemical components of the groundwaters, which reflect underlying *processes* rather than actual groundwaters.
- Even if some of the components do represent possible natural waters, it is not unexpected that they differ from the M3 end-members. These latter are simply waters of extreme composition chosen by the user of M3; some of these M3 end-members are themselves mixtures of other waters. It is these "other waters" that could potentially be identified by the new approach.

Several underlying features are common to the results of all models:

- There are usually three or four chemical components that are close to charge balance. Potentially, these could represent the compositions of actual waters.
- The charge-balanced chemical components in any model are - broadly similar to the charge-balanced chemical components produced by the other models (though as noted previously, the numbers used to designate a particular chemical component may change from model to model).

- There are always components that do not charge balance. These chemical components cannot represent actual waters, but instead possibly represent other processes such as water/rock interactions.
- In all the models, there is at least one component that contains HCO_3 and little else. It is possible that this component reflects microbial activity, notably the oxidation of organic matter. Microbial processes were also suggested to be important, based on the M3 modeling (Laaksoharju et al. 1999b).

By comparison between the results of different models, several general conclusions can be drawn:

- Model 1 showed that a single consistent model for the solutes in the water could not be produced without the inclusion of stable oxygen and hydrogen isotope data and tritium data. When these data were not included, the waters had to be divided into three groups to ensure a self-consistent result.
- The inclusion or omission of tritium from the model does make a significant difference to the compositions of all the chemical components, except the most saline component (comparison of Models 2 (v3) and Model 3).
- Addition of a small number of waters of extreme composition to a data set could have a small but significant effect on the compositions (and hence proportions) of the chemical components (comparison of Model 2 and Model 2(v5)).

The relatively large effect of tritium on the results is important, because this isotope is radioactive with a half-life of only 12.43 years. Therefore, considerable decay of tritium must have occurred during the investigations at Äspö, which have lasted more than 10 years. Variations in the reported tritium values will generally not reflect only groundwater mixing. Thus, tritium cannot be considered a conservative tracer for groundwater flow. The fact that the inclusion or omission of tritium significantly affects most of the chemical components in the present model means that errors due to its radioactive decay cannot be allowed for just by neglecting a single component. Thus, it would strictly be more appropriate to exclude tritium from consideration altogether.

Notwithstanding this potential drawback, the results of Model 2 (which includes tritium) were used with the groundwater flow model to predict the compositions of inflows to the tunnel. The reason for using these results was that Model 2 employed the same data as the original M3 modeling (which included tritium). Thus, the predictions based on the revised statistical modeling could be compared more easily with the original M3 modeling results.

Table 5-2 Compositions of end-members used in M3 modeling, reported previously by Laaksoharju et al. (1999b) and the results of JNC/Golder's modeling

Compositions of end-members reported previously (From M3 modeling, reported in SKB's data Delivery 19)											
	Na	K	Ca	Mg	HCO3	Cl	SO4	O18	D	Tr	Bal
Brine ref. w.	8500	45.5	19300	2.1	14.1	47200	906	-8.9	-44.9	4.2	-0.6
Baltic Sea ref. w.	1960	95	93.7	234	90	3760	325	-5.9	-53.3	42	-1.2
Glacial ref. w.	0.2	0.4	0.2	0.1	0.12	0.5	0.5	-21	-158	0	13.6
Meteoric ref. w.	0.4	0.3	0.2	0.1	12.2	0.2	1.4	-10.5	-80	100	-67.9
Model 1											
Chemical Component	Na	K	Ca	Mg	HCO3	Cl	SO4	O18	D	Tr	Bal
All Data											
1	641	23.8	0.00	270	507	0.00	0.00	N.I.	N.I.	N.I.	71.8
2	5663	0.00	10607	0.00	0.00	27529	742	N.I.	N.I.	N.I.	-1.0
3	2342	76.5	1227	214	0.00	6434	448	N.I.	N.I.	N.I.	-2.2
4	0.0	0.0	0.0	0.0	476	0.0	0.0	N.I.	N.I.	N.I.	-100.0
5	767	16.8	0.0	57.5	103	484	466	N.I.	N.I.	N.I.	21.2
Cluster 1 – Medium TDS Samples											
1	3896	0.0	4631	0.0	3367	12845	0.0	N.I.	N.I.	N.I.	-2.1
2	3168	242	0.0	593	242	6241	293	N.I.	N.I.	N.I.	1.8
3	2765	7.5	3759	9.9	0.0	10946	547	N.I.	N.I.	N.I.	-1.8
4	825	0.0	0.0	0.0	0.0	578	747	N.I.	N.I.	N.I.	6.0
5	1225	0.2	0.0	214	131	1615	0.0	N.I.	N.I.	N.I.	19.6
Cluster 2 – High TDS samples											
1	1730	8.5	1089	27.8	0.0	4864	149	N.I.	N.I.	N.I.	-3.0
2	0.00	0.0	0.0	0.0	335	0.0	1.2	N.I.	N.I.	N.I.	-100.0
3	889	2.0	448	0.0	534	1718	422	N.I.	N.I.	N.I.	-3.9
4	70.7	10.7	0.0	27.7	0.0	259	0.0	N.I.	N.I.	N.I.	-13.0
5	179	2.1	0.0	147	682	0.0	0.0	N.I.	N.I.	N.I.	28.2
Model 2											
Chemical Component	Na	K	Ca	Mg	HCO3	Cl	SO4	O18	D	Tr	Bal
1	8508.6	5.1	17235.0	0.0	47.1	44001.5	800.3	-11.8	-75.7	14.6	-1.1
2	2066.3	0.0	1379.1	169.1	225.4	6163.5	0.0	-8.8	-68.5	0.0	-1.4
3	456.9	5.5	258.4	16.7	0.0	1207.9	79.8	-12.4	-94.2	0.0	-2.1
4	0.0	1256.2	0.0	2020.1	505.6	0.0	0.0	0.0	0.0	492.0	92.0
5	0.0	0.0	0.0	0.0	22039.5	0.0	0.0	0.0	0.0	0.0	-100.0
6	0.0	0.0	0.0	0.0	298.8	0.0	0.0	0.0	0.0	391.5	-100.0
7	2021.3	17.8	205.4	8.0	0.0	3230.3	1284.4	-14.3	-107.9	0.0	-8.6

N.I. = Not included. Values that appear to be zero are actually very small numbers.

Table 5-2 Continued

Model 2 V3											
Chemical Component	Na	K	Ca	Mg	HCO3	Cl	SO4	O18	D	Tr	Bal
1	11782.6	26.8	23756.3	0.0	0.0	60832.1	1119.8	-14.5	-92.4	0.0	-1.2
2	5107.0	43.7	0.0	729.7	247.5	7971.5	51.6	1.3	-6.0	0.0	10.4
3	3285.6	227.3	1689.9	371.9	53.1	9018.2	923.6	1.3	3.9	66.5	-2.0
4	20187.6	287.5	44808.2	0.0	58890.3	81067.1	66.0	128.7	1167.0	477.0	-2.1
5	4.0	0.0	0.0	0.0	112.4	0.0	0.0	-11.0	-82.6	8.7	-82.7
6	3135.7	0.0	0.0	185.5	0.0	0.0	1911.2	-15.2	-119.7	0.0	58.4
7	1664.1	24.3	4004.8	131.2	462.3	9300.7	385.0	17.0	114.4	1017.0	1.0
Model 2 V5											
Chemical Component	Na	K	Ca	Mg	HCO3	Cl	SO4	O18	D	Tr	Bal
1	9045.0	33.9	18802.0	0.8	42.0	47544.9	891.7	-10.7	-64.1	0.0	-1.0
2	1975.8	0.0	1228.7	169.6	231.8	5738.2	0.0	-8.5	-66.7	6.1	-1.4
3	433.4	6.0	243.4	15.7	0.0	1140.5	75.3	-12.7	-95.9	0.0	-2.0
4	0.0	0.0	0.0	0.0	9841.4	0.0	0.0	0.0	0.0	0.0	-100.0
5	3841.4	910.2	0.0	1683.6	315.1	0.0	327.6	0.0	0.0	0.0	93.0
6	1949.8	7.1	407.0	0.0	0.0	3528.3	1147.4	-14.3	-107.9	4.2	-7.9
7	0.0	0.0	0.0	0.0	213.1	0.0	0.0	0.0	0.0	436.4	-100.0
Model 3											
Chemical Component	Na	K	Ca	Mg	HCO3	Cl	SO4	O18	D	Tr	Bal
1	11825.3	28.1	23723.5	0.0	0.0	60865.2	1121.2	-13.8	-87.9	N.I.	-1.2
2	3225.9	25.5	0.0	449.5	108.5	5046.4	47.6	-4.1	-40.5	N.I.	10.2
3	3483.6	246.3	2020.5	403.3	107.8	9950.1	960.1	3.9	22.4	N.I.	-1.8
4	39462.1	454.2	30364.5	3113.6	70548.1	90027.7	0.0	208. 7	1732.3	N.I.	-2.7
5	2071.4	0.0	0.0	78.2	0.0	0.0	1595.1	-15.9	-122.3	N.I.	48.8
6	1.7	0.5	0.0	0.0	125.3	0.0	0.0	-10.6	-80.1	N.I.	-91.9

N.I. = Not included. Values that appear to be zero are actually very small numbers.

In Model 2, all the chemical variability could be attributed to 7 principal components (Figure 5-4). This suggested that 7 chemical components could be used to model the groundwater chemistry. When the 7 original principal components were adjusted by iteration, as described in Section 6.1.7, the resulting fit between the reconstructed compositions of the waters (i.e. calculated from matrices B and C above) and the actual compositions was very good for all components except for stable oxygen and hydrogen isotopes (Figure 5-5). This approach demonstrates a high degree of internal consistency in the model. However, the model did not give a good fit for light (relatively heavy-isotope-depleted) water compositions (Figure 5-5: note that the isotopic compositions were converted to positive values for the PCA). One possible explanation is that the waters may not all be mixtures of the same end-members. However, additional processing would be required to evaluate this more fully.

The main features of the chemical components that were calculated by Model 2 are:

- The components in Model 2 do bear some similarity to real waters or to water/rock interactions/contamination effects:
- Chemical component 1 is broadly similar to the brine end-member identified by Laaksoharju et al.;
- Chemical component 2 is broadly similar to the seawater and/or Litorina sea water identified previously by Laaksoharju et al. (1999b);
- Chemical component 3 is broadly similar to a glacial reference water reported previously by Laaksoharju et al. (1999b);
- Chemical components 5 and 6 could potentially represent water/rock interactions and/or microbially mediated reactions;
- Chemical component 7 has some similarities to a sediment pore water identified by Laaksoharju et al. (1999b) previously.
- In support of the hypothesis that microbial action might explain component 5 is that fact that this component tends to be more abundant in waters from the redox zone monitoring boreholes, than in other boreholes. In the redox monitoring boreholes the mean is 1.2445×10^{-2}, std dev 0.0049, whereas in the other boreholes the mean is 3.9475×10^{-3}. std dev 0.0056. Microbial processes have been well documented from the redox zone.
- Component 4, produced by Model 2, is the most difficult to ascribe to a real process. This is because it is not charge-balanced and appears to contain very high concentrations of K and Mg (much higher concentrations than are in fact observed in any actual water). Possibly, component 4 could represent a water/rock interaction, such as cation exchange of Ca and Na for Mg and K. In fact, component 4 composes a maximum of only 1.77% of any actual water (and usually much lower than this). Since water/rock interactions of this kind would be expected to have a relatively small effect on the overall compositions of the predominantly saline waters, this small value is consistent with component 4 representing water/rock interactions.

The general similarity of some of the chemical components and some of the M3 end-members can be approximated by comparing Figure 5-6 and Figure 5-8. There are generally similar patterns in the depth dependence of the new chemical components and the M3 end-members.

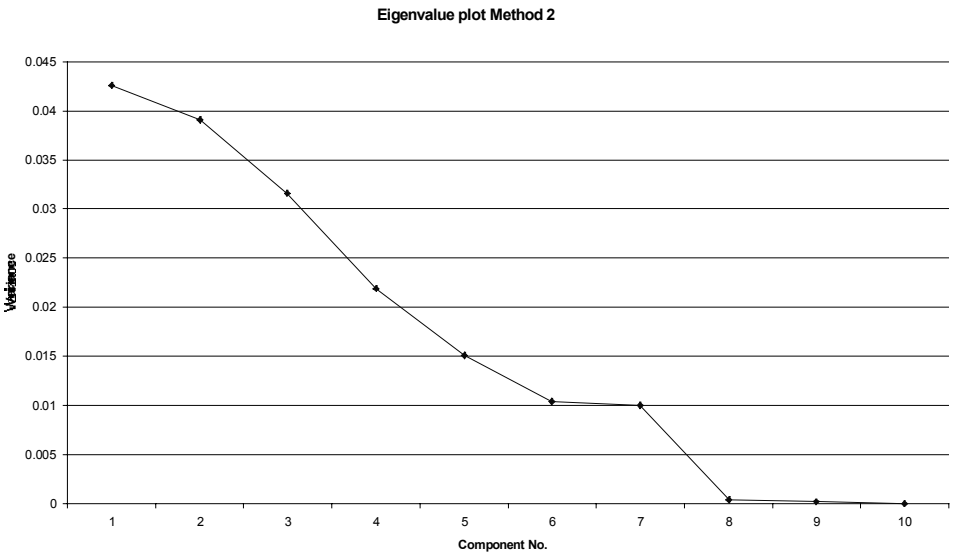

Figure 5-4 *Plot showing eigenvalues, reflecting the contribution of each principal component to the overall chemical variance*

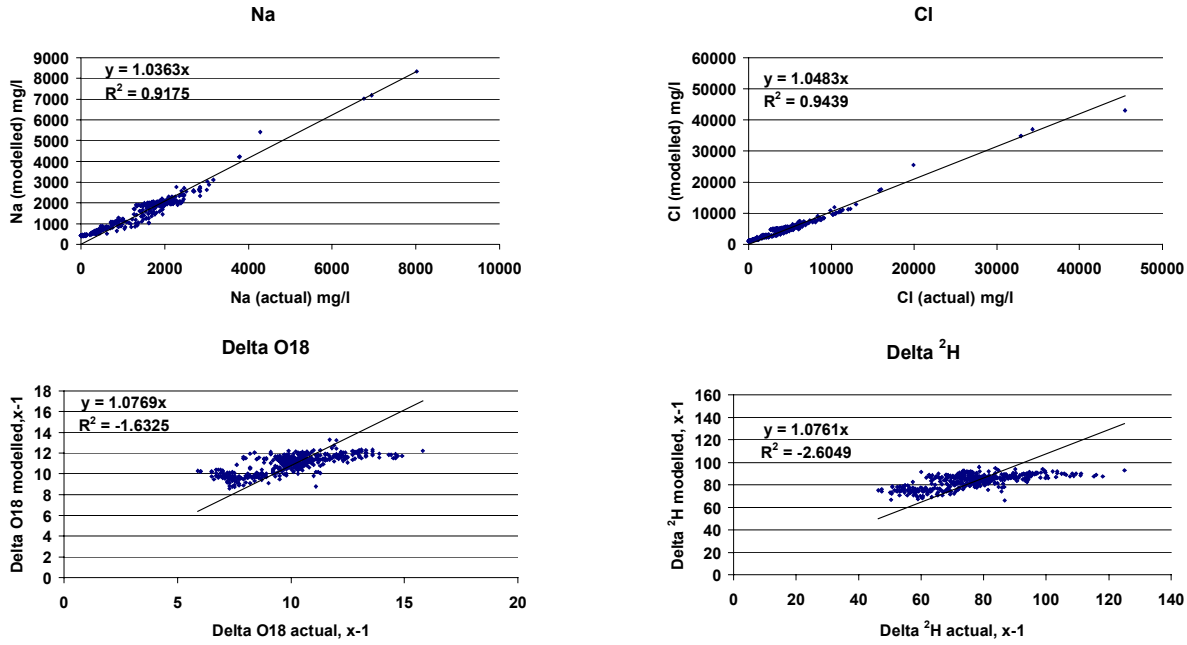

The difference between the line and the data points is a measure of the error. Perfectly correlated results would have coincidence of data and line.

Figure 5-5 *Comparison between concentrations of a relatively reactive solute (Na) and relatively unreactive solutes (Cl, $\delta^{18}O$ and δH) reconstructed from the statistically derived chemical components, and the actual concentrations. Similar plots were produced for all the constituents.*

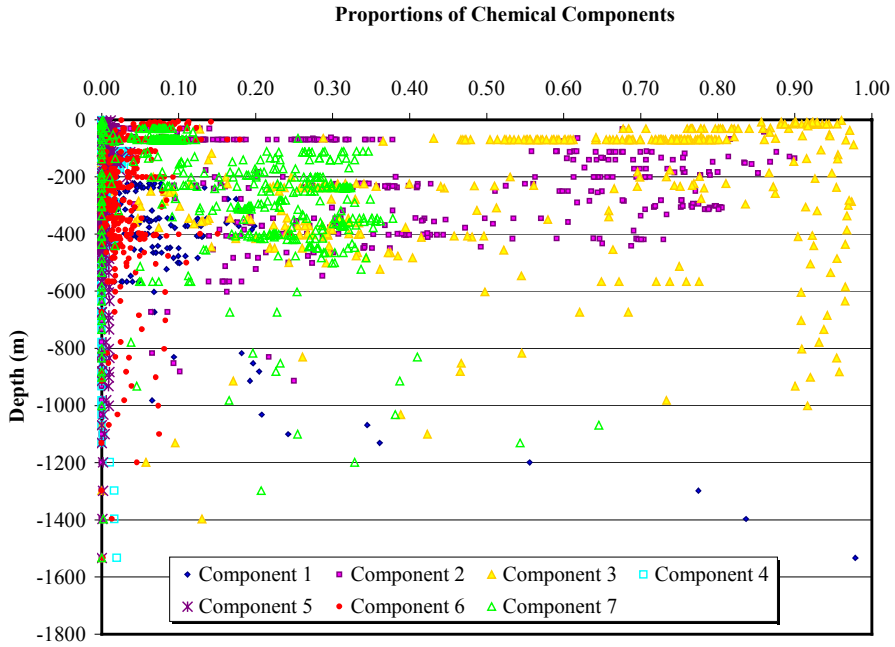

Figure 5-6 *Plot showing variations in proportions of chemical components, calculated using Model 2, with respect to depth.*

5.1.10 Comparison Between Results Of M3 And New Modeling

The results of the new Model 2 are expressed as proportions of the original M3 end-members and plotted versus depth in Figure 5-7. For comparison, Figure 5-8 is similar, but shows the proportions of the same end-members, as calculated in the original M3 modeling and reported by SKB in Data Delivery 19. From these figures, it is apparent that:

- There is generally a positive correlation between proportions of end-members calculated by Model 2 and the proportions calculated by M3 (Figure 5-9).
- There is a particularly good positive correlation between the proportions of brine calculated from Model 2 and the proportions of brine calculated by M3 (Figure 5-9).
- Compared to the M3 modeling, the new modeling calculated generally higher proportions of Baltic sea water at shallower depths (above around 400 m) and generally lower proportions of meteoric water at greater depths (between around 400 m and 1000 m). However, the general depth distribution is similar (Figure 5-7).
- The maximum proportion of the Baltic seawater end-member calculated from Model 2 is around 0.8, whereas the maximum proportion calculated by M3 is close to 1 (Figure 5-9).

However, in contrast to the M3 modeling, the new modeling predicts *negative* proportions of meteoric water for samples of intermediate salinity (Figure 5-7, Figure 5-9 and Figure 5-10). These are clearly unrealistic and initially seem inconsistent with the M3 results. However, a detailed comparison reveals a high degree of underlying consistency, notably:

- The negative proportions given by the new model are almost all given by samples for which M3 also calculated a large deviation between theoretical Cl concentrations (assuming all samples are mixtures of all end-members) and actual Cl concentrations (Figure 5-11).
- The proportions of end-members given by the new calculations can also be used to calculate “deviations” between theoretical and actual concentrations of determinands (Figure 5-1, Section 5.1.5). There is a negative correlation between Cl deviations obtained from the new results and Cl deviations calculated from the M3 results (Figure 5-12).
- The Cl deviations, as a percentage of the total, are largest for waters of low salinity in both the latest modeling and the original modeling.

The reasons why the new model results and the original M3 modeling is consistent are:

- The M3 approach uses calculated mixing proportions and end-member compositions to derive theoretical water compositions, for comparison with actual water compositions. The M3 modeling assumes that all waters contain all end-members. For some waters, this assumption results in calculated Cl concentrations that are lower than the actual concentrations. Since Cl is relatively unreactive in groundwaters, the most logical explanation is that in these, the estimates of meteoric water concentration, based on the assumption of conservative mixing, are too high.
- In contrast, the new modeling adopted the opposite approach. The actual compositions of the waters and the end-members to calculate the mixing proportions. Therefore, the calculation of negative proportions of meteoric water effectively amount to the same thing as the negative deviations for Cl calculated by M3.

A plausible explanation for these discrepancies is that the actual waters are not actually all mixtures of all end-members.

This possibility was also pointed out by Laaksoharju (2000). However, based on the M3 modeling, it was considered that the uncertainty due to this could be encompassed by a ±10% error on the proportion of each component.

The new modeling produced negative proportions of meteoric water as low as around –0.3 (Figure 5-7). An implication is that the uncertainty for individual components could be much greater than the ±10% suggested by Laaksoharju et al (2000).

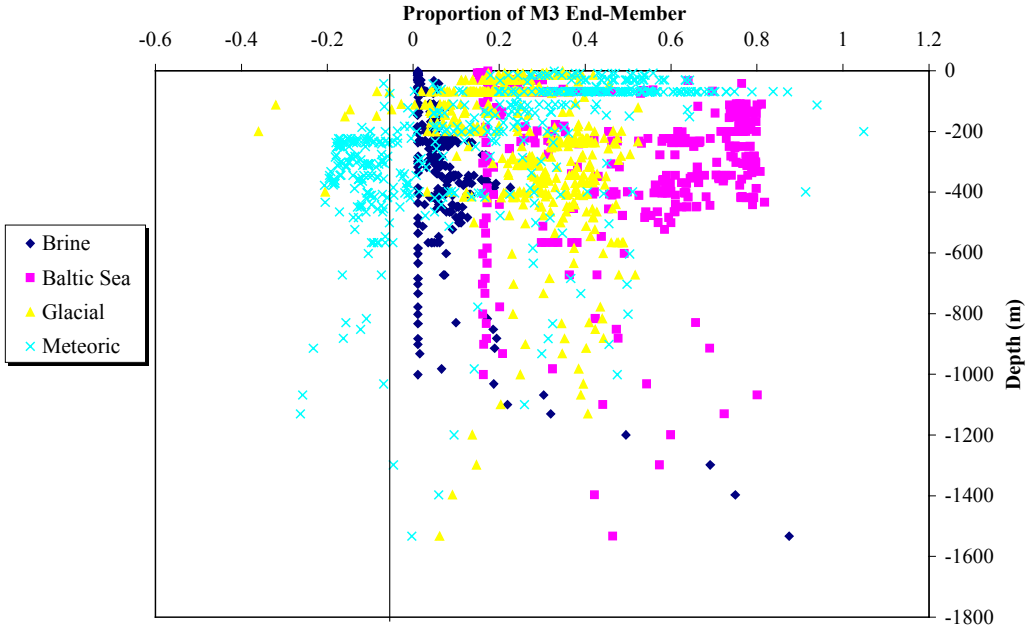

Figure 5-7 *Variations in proportions of end-members used in M3 modeling, calculated from results of the new Model 2, using all 7 chemical components.*

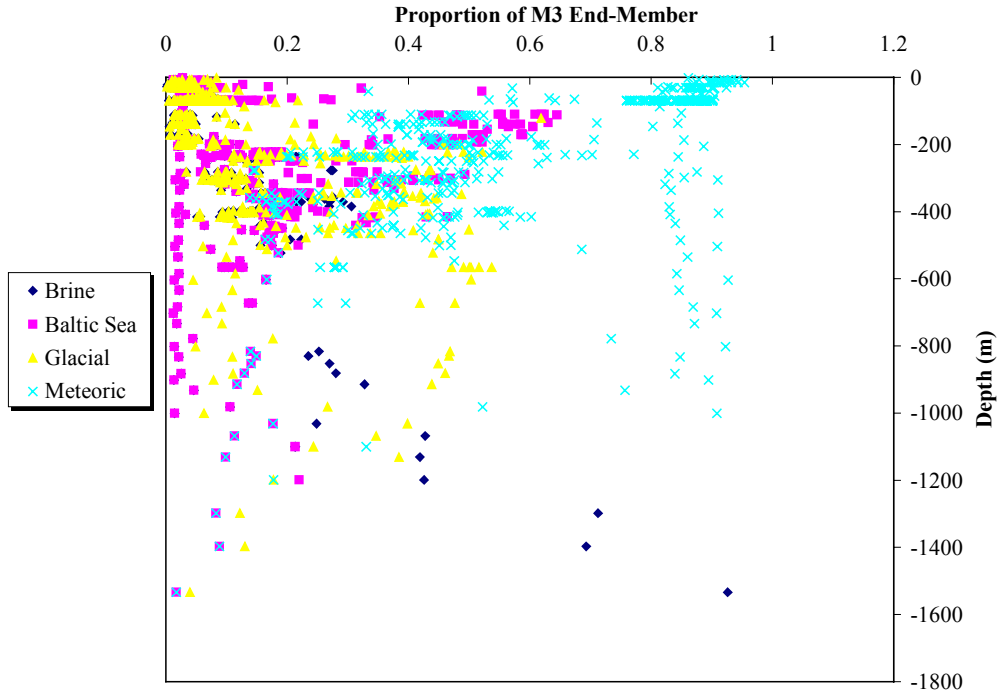

Figure 5-8 *Variations in proportions of end-members used in M3 modeling, as calculated by M3 and reported by SKB in Data Delivery 19*

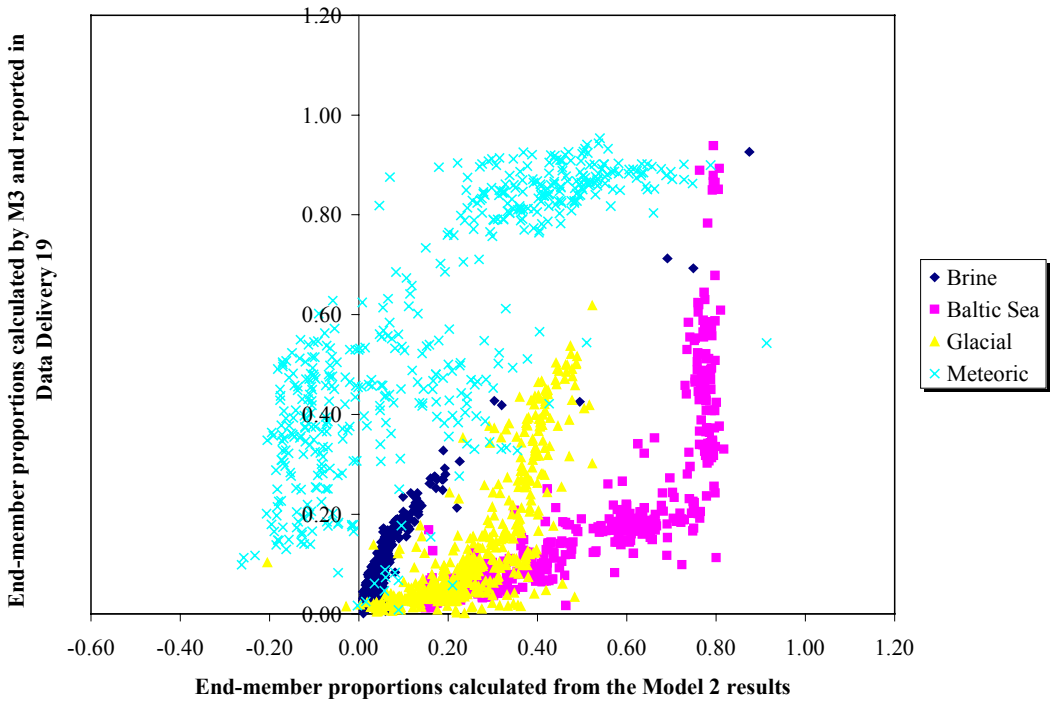

Figure 5-9 *Comparisons between proportions of end-members calculated by M3 and released by SKB in Data Delivery 19, and proportions of the same end-members calculated using the revised Model 2.*

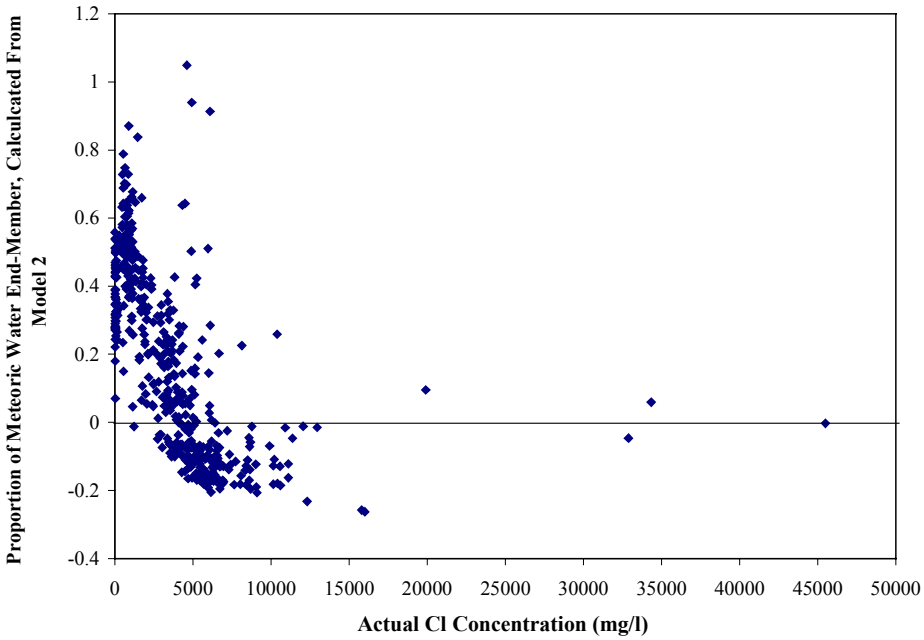

Figure 5-10 *Comparison between the proportion of the meteoric water end-member in each sample, calculated from the Model 2 results, and the actual Cl concentration in each sample.*

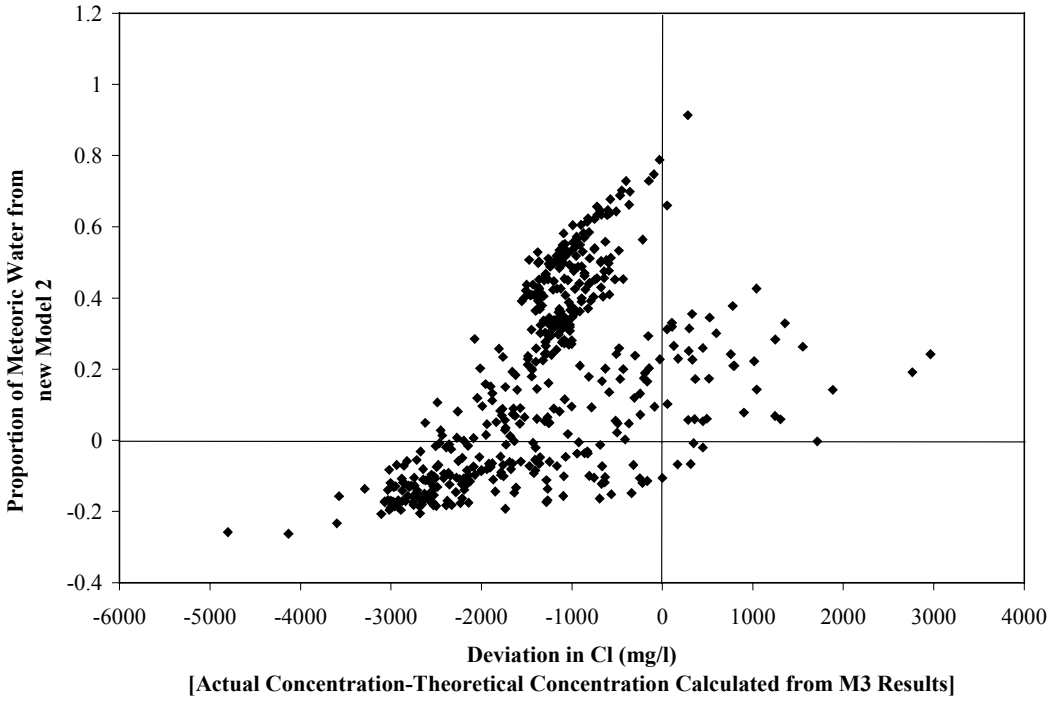

Figure 5-11 *Comparisons between the proportions of the meteoric water end-member, calculated from the new Model 2, and the deviation between theoretical and actual Cl concentrations in each water, from the M3 results.*

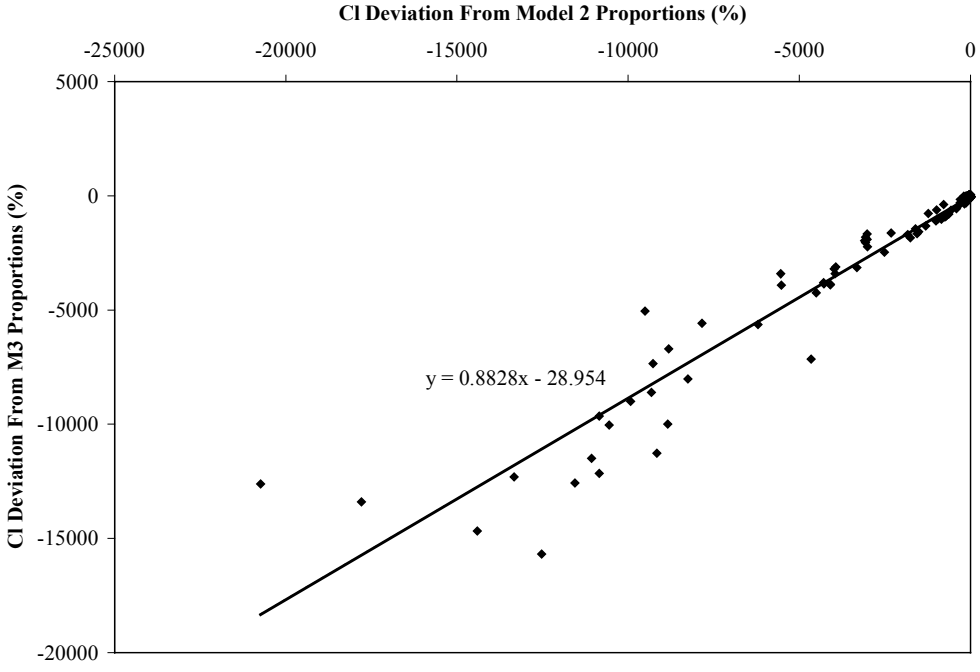

Figure 5-12 *Comparisons between deviations in Cl (calculated - actual), calculated from Model 2 proportions, and deviations in Cl (calculated - actual), calculated from the original M3 proportions.*

5.1.11 Conclusions From The New Modeling

- The new approach should be more generally applicable than the M3 approach, since it takes into account all the chemical variability in the groundwaters.
- The new method allows chemical variability that is due to mixing to be distinguished from components of chemical variability that is due to water/rock interaction. Chemical components that are not attributable to water/rock interactions or other effects can be considered "conservative" tracers for groundwater flow.
- An internally consistent model of all the solute data cannot be obtained if stable oxygen and hydrogen isotope data are not used.
- When stable oxygen and hydrogen isotopic data are included in the model, the internal consistency of the model for solutes is very good. However, the model is not consistent for waters that are relatively depleted in the heavy isotopes. Though the reasons for this could not be evaluated fully, it may be due to the waters not all being mixtures of the same end-members.
- It is possible to express the results of the new method in terms of real groundwaters if so desired, allowing mixing relationships among real groundwaters to be distinguished. In the present study this was done for the original M3 end-members.
- Inclusion or exclusion of groundwater constituents and/or additional waters of extreme composition has a significant effect on the outcome of the method.
- Seven principal components are needed to explain all the chemical variability in the data, when the same data as those used by M3 are employed.
- The M3 results and the new modeling are broadly consistent.
- The proportions brine in any water are most likely to be reliable.
- It is probable that not all the M3 end-members are actually present in the Äspö groundwaters. In particular, meteoric water is probably not present in many groundwaters from intermediate depths.
- Better consistency and more precise mixing proportions could probably be obtained by splitting the data set into several parts and applying the model to each part. In general, an iterative procedure would be needed, involving repeated splitting of the data set and modeling of each part, until the most consistent set of results is obtained. This procedure was outside the scope of the present project.

5.2 PATHWAYS ANALYSIS/MIXING ISSUES

The analyses presented in the preceding sections used a two-stage approach to generating the source locations of the waters flowing into the monitoring sections (JNC, 1999):

1) determine the spatial location of the pathways
2) determine the distance traveled along each pathway each month using the head solution along each path. This head solution was updated every 30 days based on the transient finite element solution.

The individual pathways were defined by graph theory searches through the channel network model using a monitoring section as the source location of each search. The standard PAWorks graph theory search was amended to look for pathways upgradient of the source, hence allowing the sources of the waters infiltrating the monitoring sections to be determined. The graph theory searches used flow weighting, and the search procedure can be summarized by the rules in Figure 5-13. To illustrate this approach an example pipe network is shown in Figure 5-14. The pathways derived using the PAWorks graph theory approach are shown in Figure 5-15. More details of the searching algorithm are provided in the PAWorks Manual (Dershowitz et. al., 1998b).

The pathways found through this graph theory search provide a good representation of the different pathways with the highest flows. However, while the method provides a good measure of the range of locations from which the waters are originating, there is no accurate way to determine the proportion of the waters along a specific pathway. The reason this difficulty arises is that while pathway length and travel time are additive values, the flow along a pathway is not. Weighting of the individual pipe flow may be used to estimate the net flow contribution from a pathway, but this methodology is by necessity approximate. Alternatively, the flow infiltrating a monitoring location may be assumed to be proportional to the flow rate in the pipe from which the water originated. This method was used in the Stage 1 and 2 modeling, but is also approximate.

The other major limitation of the original approach is that although the distance traveled along each pathway is a function of the monthly flow solution, the spatial coordinates of each of the pathways are defined by a single flow solution. A flow solution near the end of the modeled period was used. If the location of the inflows changes with time, due to a marked change in the head solution, these changes in flow direction and true source water coordinates (and water source location) could be significant.

The two major disadvantages of the original pathway analysis, lack of an accurate computation of the proportion of flow coming from each location and specifying pathway coordinates based on a single flow solution, are addressed in the improved approach that uses the newly introduced PAWorks particle tracking algorithm.

For each source (monitoring) location determine the flow in each of the attached pipes.

Select the pipe with the highest inflow into the source (Source Pipe A).
From Source Pipe A:

a) Record the flows in all the upgradient pipes attached to this pipe.
b) Add these inflows to the list of inflows recorded.
c) Select the pipe with the highest inflow.
d) Repeat a) to c) until the specified sink location is reached.
e) Repeat a) through d) until the user specified pathways per source is reached.

For Task 5 modeling, the external head boundaries of the model region were specified as sink locations.

Select the pipe with the second highest inflow into the source (Source Pipe B).
Repeat a) through e) for Source Pipe B until the user specified pathways per source is reached.

Continue for Source Pipes with the next highest inflows until the total number of user specified pathways is reached.

Figure 5-13 *Rules for PAWorks Graph Theory Search used for Task 5 modeling*

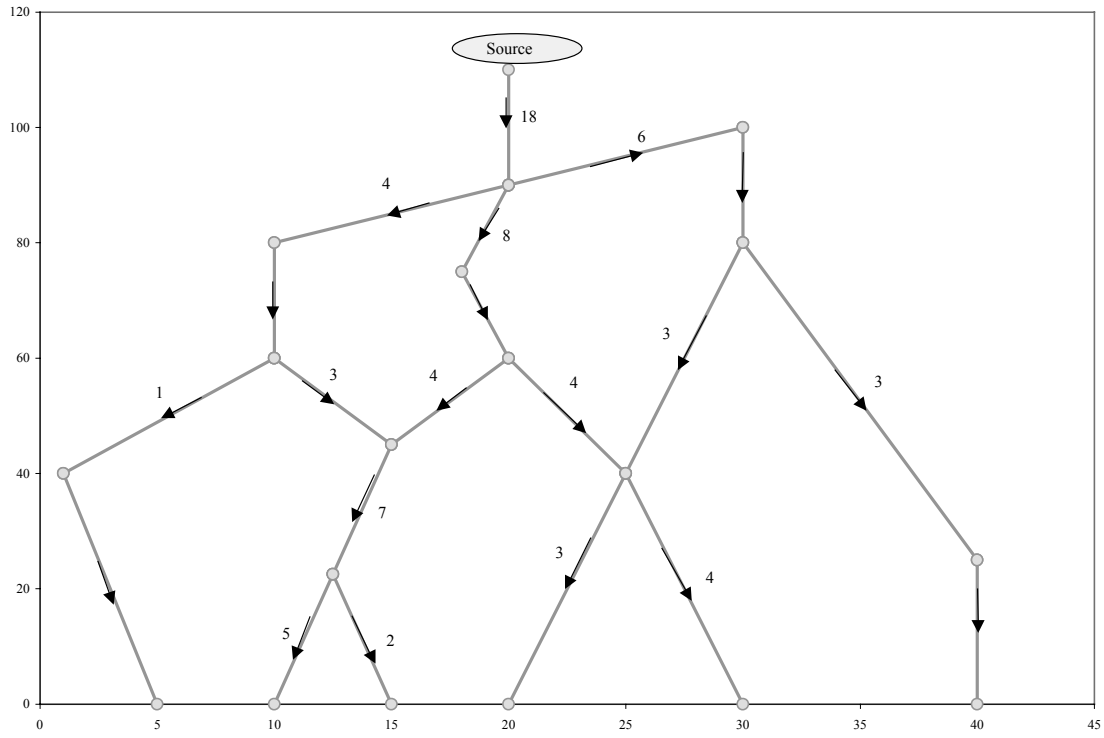

Figure 5-14 *Example Pipe Network*

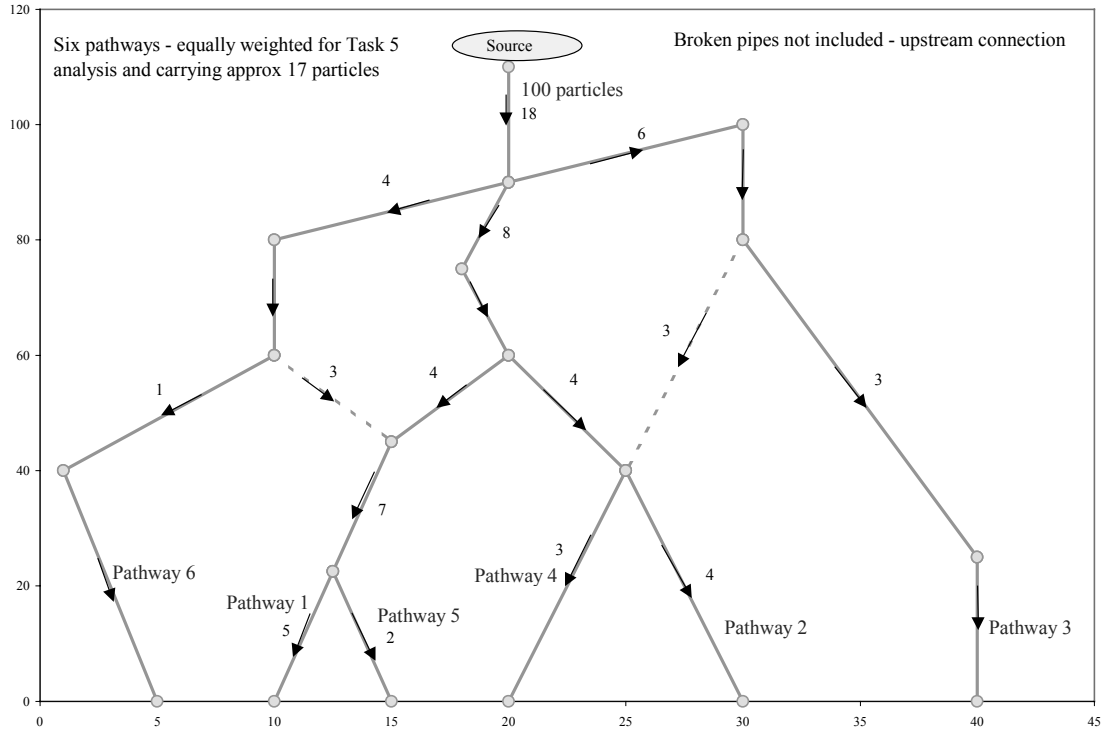

Figure 5-15 *Pathways obtained using PAWorks Graph Theory Search*

The algorithm continues to use the monitoring locations as the sources, the outer head boundaries of the finite element region as the sinks, and searches upgradient to determine where the water originated. At each intersection an individual particle is assigned to the upgradient pipes stochastically, the weighting of each pipe being in proportion to the flow.

For example, if the flows in the three upgradient pipes were:

Pipe	Flow Rate	Weight	Assignment Range
Pipe A	5. x 10^{-5} m^3/s	0.5	0.0 – 0.5
Pipe B	3. x 10^{-5} m^3/s	0.3	>0.5 – 0.8
Pipe C	2. x 10^{-5} m^3/s	0.2	>0.8 – 1.0

A random number between 0.0 and 1.0 is generated and depending on its value the particle is moved into the upgradient pipe depending on an "assignment range" that is proportional to the flow rate. The more particles used in the analyses, the more closely this algorithm matches a flow-weighted solution. The Task 5 analyses used 1000 particles at each source.

To illustrate the approach graphically, the PAWorks particle tracking pathways obtained from the example pipe network illustrated in Figure 5-14 are shown in Figure 5-16.

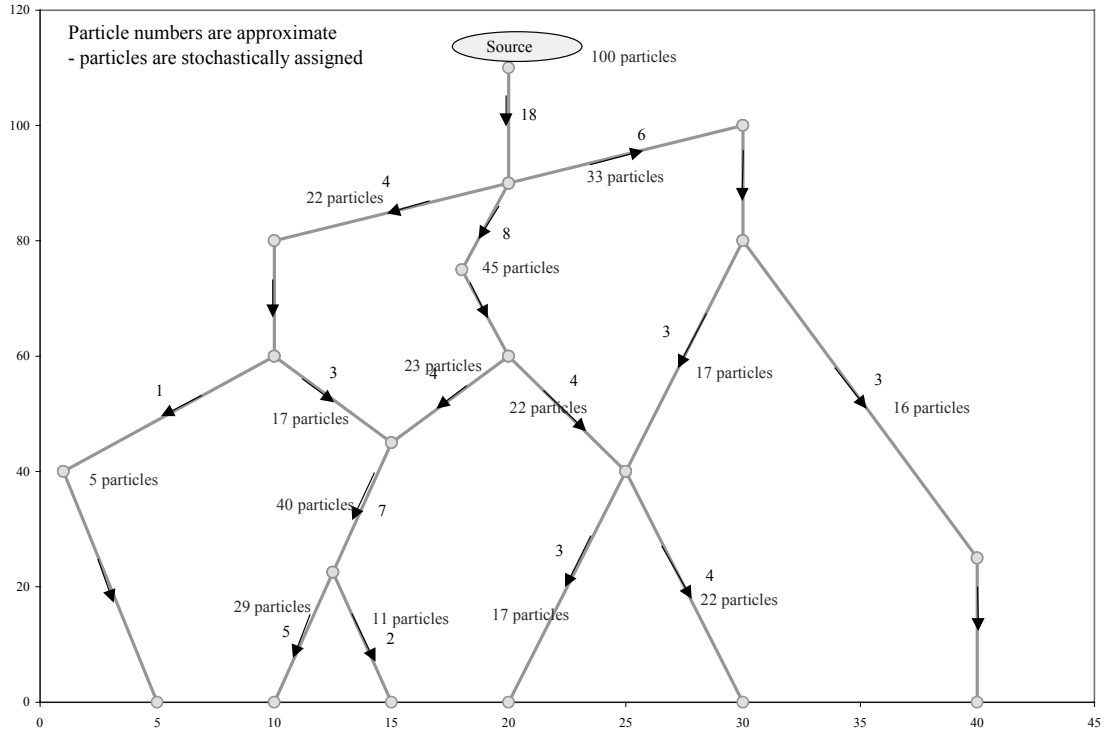

Figure 5-16 *Pathways obtained using PAWorks Particle Tracking Search*

The new particle-tracking algorithm was expanded to allow the code to write particle locations after a user-specified time had elapsed, and to read the initial particle locations from file. Hence, a script file can be used to step through each of the 76 head solutions with the particles moving for 30 days per file. This enables the transient effects of the flow solution to be replicated in time-varying particle pathways.

Example pathways using the original graph theory algorithm and the particle tracking algorithm that is more appropriate to this problem, are presented in 3-D in Figure 5-17 and as a 2-D representation in Figure 5-18 for monitoring section SA2074A. The difference in the derived pathways is marked. The particle-tracking algorithm results in more clustered pathways and more pathways towards the east. This occurs because the flow is preferentially along the large-scale features and hence most of the particles follow these paths. Conversely, although the particle-tracking algorithm shares many of the same paths as the particle-tracking algorithm, it also includes some of the less likely pathways. The pathways also show the effect of the changing head distribution with time, which can be incorporated into the particle tracking results.

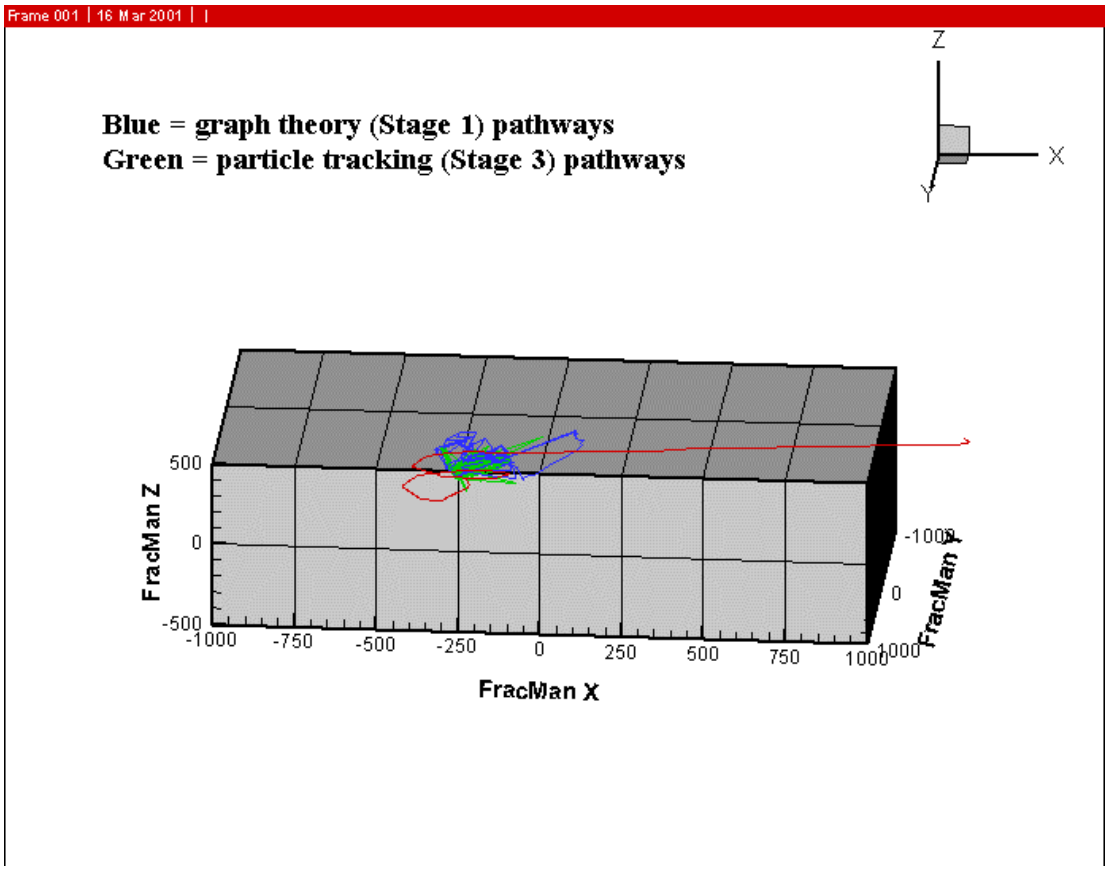

Figure 5-17 *Monitoring section SA2074A graph theory algorithm and particle tracking algorithm pathways (3-D)*

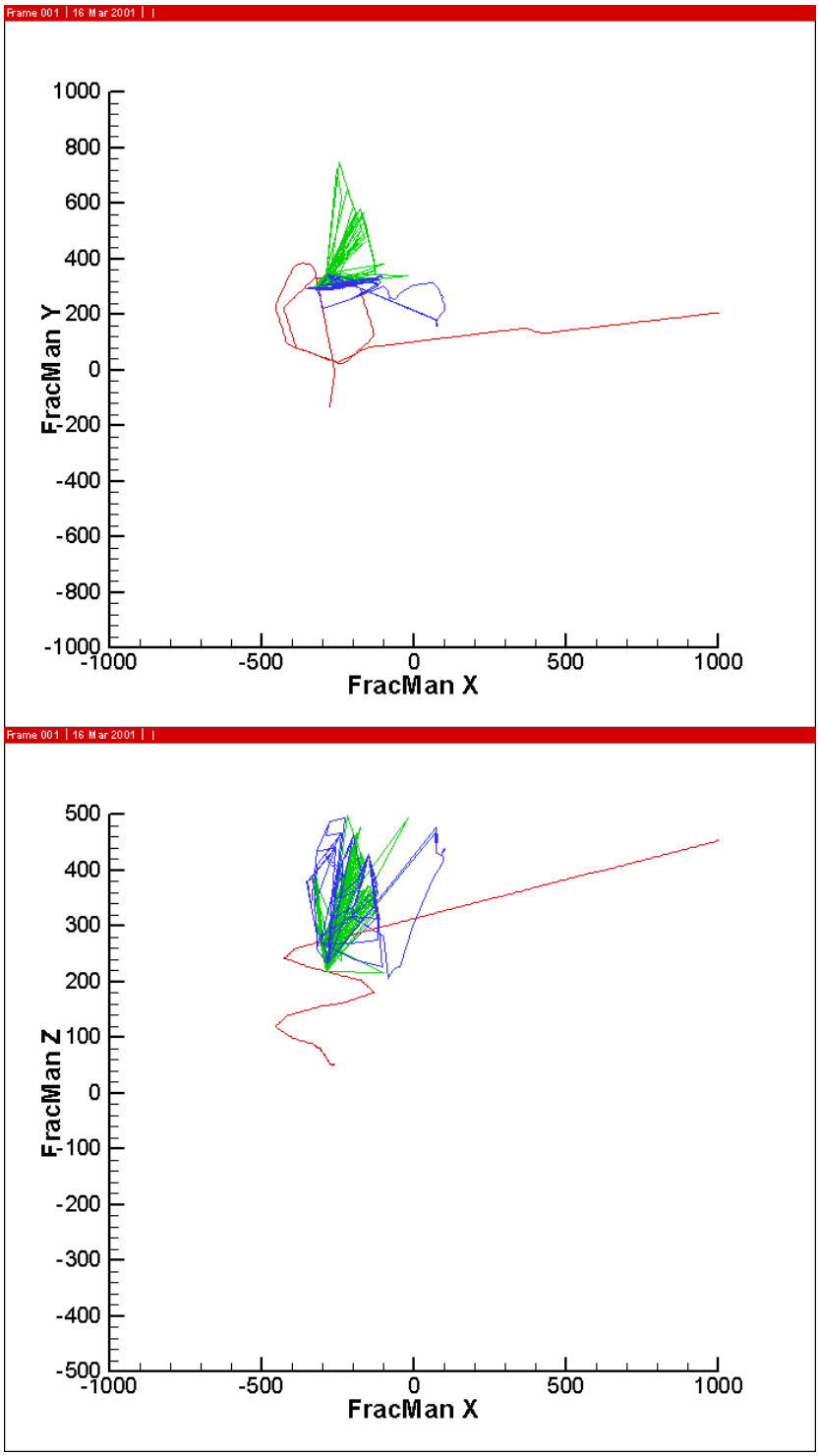

Blue = graph theory algorithm
Green = particle tracking algorithm

Figure 5-18 *Monitoring section SA2074A graph theory algorithm and particle tracking algorithm pathways (2-D)*

5.3 INITAL CONDITION/INTERPOLATION ISSUES

As part of the geochemical analyses it is necessary to make assumptions about how the measured chemistry should be extrapolated to other locations in the vicinity of the Äspö tunnel. The methodology used for the Stage 3 modeling differed from that used for the previous simulations.

For the Stage 2 geochemical analyses the initial geochemical distribution in the vicinity of the Äspö tunnel was based on the spatial grid from the limited borehole sample locations, as developed by SKB and provided as data delivery No. 4. The chemistry at the sample locations was computed using the M3 approach, and the points extrapolated to the grid using a Kriging methodology. The chemistry between the grid points was linearly interpolated between the four surrounding points.

An inherent assumption of this Stage 2 approach was that the chemical composition is unrelated to the hydrogeology in the vicinity. For example, if a fracture is equidistant between a major fracture zone and a background fracture, this approach assumes that the chemistry will be equally affected by the background fracture and the major fracture zone. In effect an average chemical composition should be assumed.

Similarly, any effect of the Baltic Sea on the chemistry is assumed to be completely addressed by the chemistry of the grid points.

The updated analysis uses different assumptions.

- The chemistry at the borehole sampling points is computed using the principal component model described in Section 5.1.
- The chemistry at a specific location is assumed to be dominated by the chemistry on the closest main fracture zone. This assumption is based on the premise that as these features are conductive over a large distance, mixing preferentially occurs between the main features and the background fractures.
- Chemistry is strongly influenced by the vicinity of the Baltic Sea. Therefore whether a location is beneath Äspö Island or the Baltic Sea should be considered as part of the chemical extrapolation process.

In order to use the chemistry on the main fractures as the basis of an interpolation algorithm, the chemistry on these main features needed to be computed. Each main fracture needed sampling points at the four corners of the feature, at the two edges of the feature at a FracMan elevation of 0.0 m, and at the Äspö Island/ Baltic Sea interface, as a minimum. Additional chemistry points were also used where the chemistry showed a distinct non-linear variation with depth.

Determining the main feature chemistry was done in stages. First, any borehole sampling points within 50m of a main fracture zone was projected onto that fracture (see Figure 5-19). Where this did not provide sufficient data points, depth dependent trend lines were computed for each chemistry under/not under Äspö Island and used to compute the chemistry. Measured, extrapolated, or interpreted data points were located at the corners of each main feature plus at either side of the Äspö Island/Baltic Sea interface. This is illustrated in Figure 5-20.

This approach is limited due to the small number of borehole sampling locations. However, it makes optimum use of available data and still allows for the observed chemical dependence of the water to the vicinity of the Baltic.

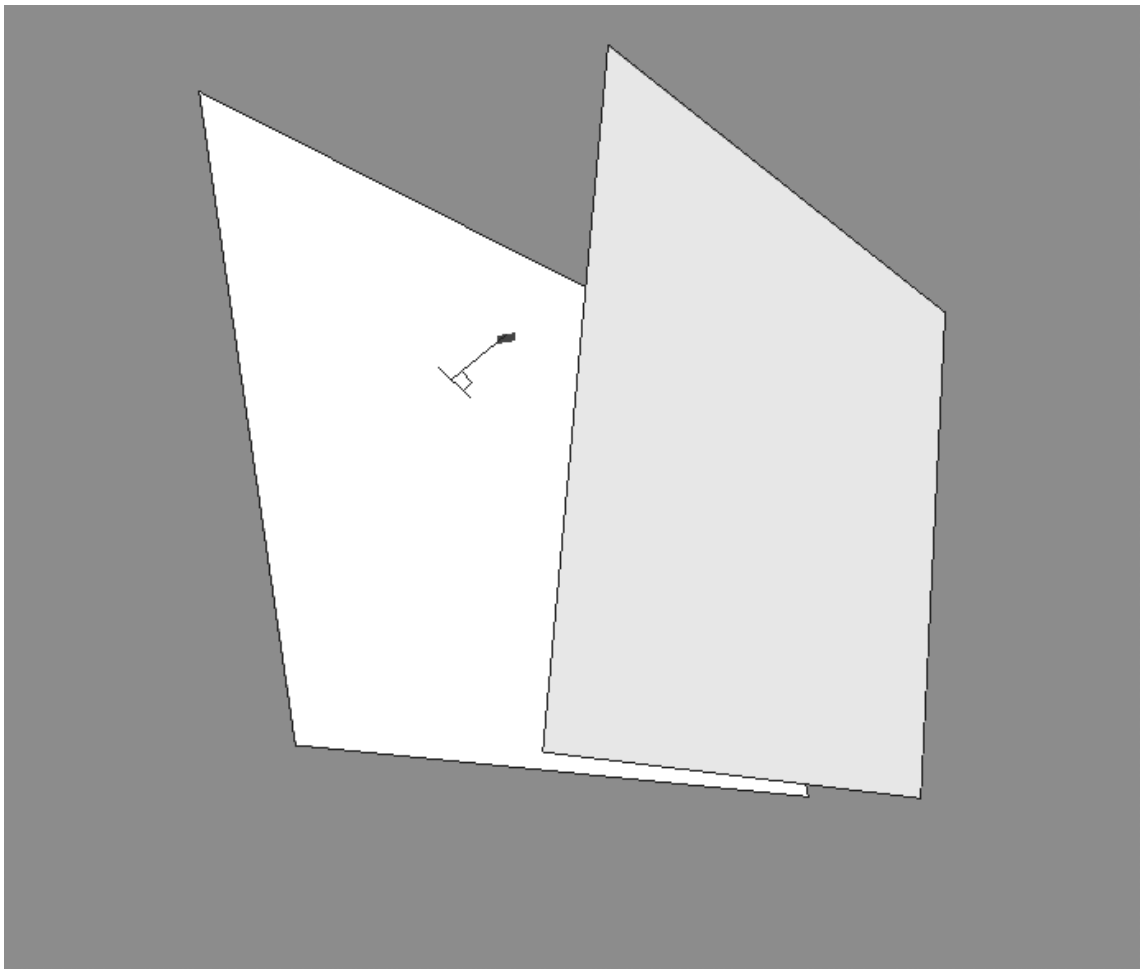

Figure 5-19 *Extrapolation of Measured Chemistry to Adjacent LSFs*

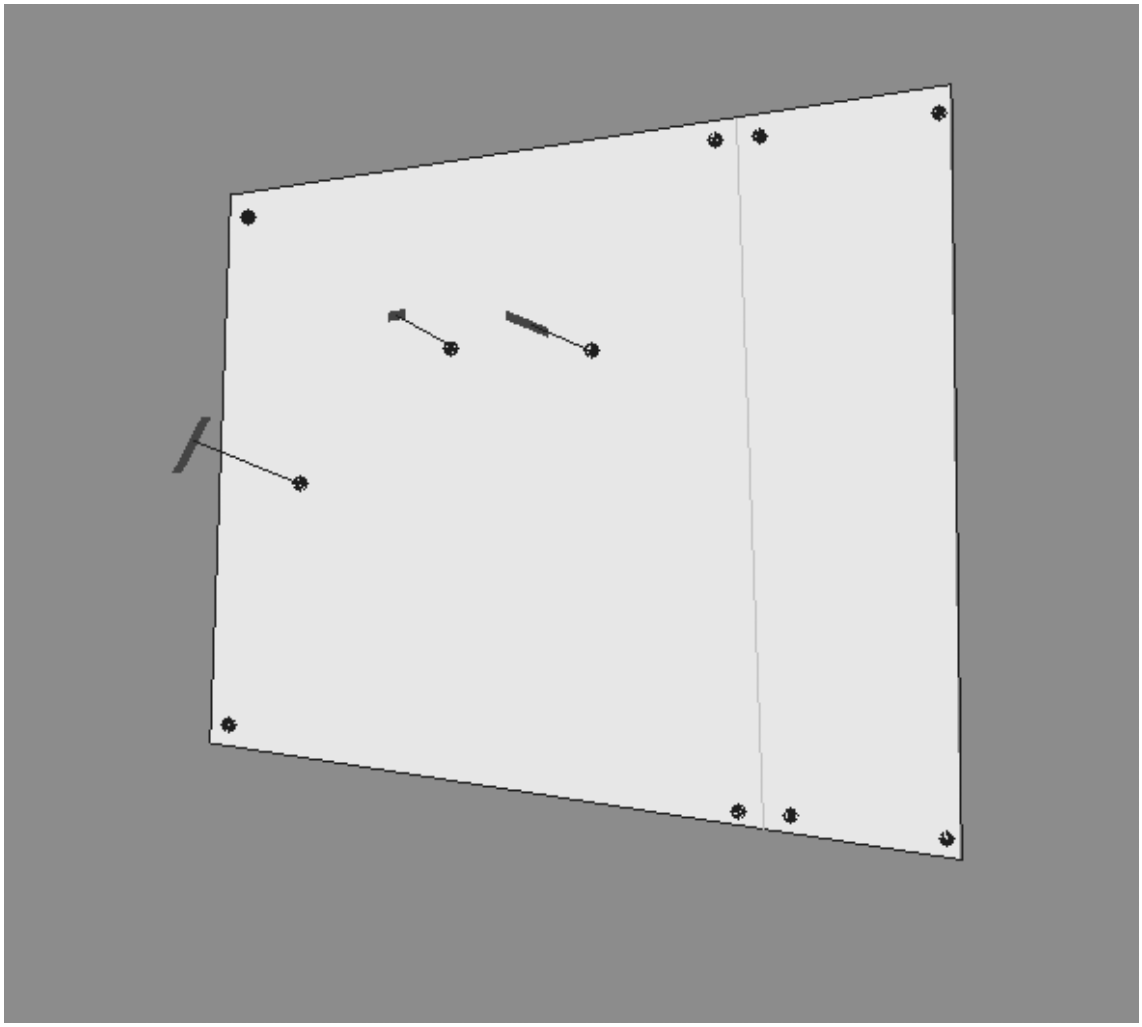

Figure 5-20 *Example of Extrapolated and Interpreted Chemistry on LSF*

Having computed the chemistry on the main features, the following approach was used to determine the time varying chemical composition of the waters in the prediction locations.

Step 1: Obtain location of particle using the PAWorks particle backtracking algorithm
Step 2: If particle is not already within a main fracture zone, project particle to the nearest zone
Step 3: Interpolate chemistry from the chemistry on these fracture zones

The chemistry within a fracture zone was derived using a linear interpolation scheme between the three closest surrounding points.

This interpolation scheme was subsequently found to work well. This implies that the main fracture zones may dominate the chemical compositions of the waters. Additionally, the more general approach to the chemical components enabled the accuracy of the assumptions of pure mixing to be assessed.

5.4 UPDATED MODEL CALIBRATION

This section of the report summarizes the model and results obtained for two related chemistry models:

- Model 2, the 7 chemical component model described in Section 5.1.9 and Table 5-2.
- The end-members (Brine, Baltic, Glacial and Meteoric) computed from the 7 chemical component model.

The model used for both these cases is summarized in Table 5-3.

Table 5-3 Summary of Model for Sensitivity Study

Property	**Description**
Fracture Model	
Major Discrete Features	22 Planar Homogeneous Zones (Rhén et al., 1997). See Table 2-1 for details.
Background Fractures	22704 features described in Table 2-1.
Mystery Feature	Addition an additional feature located between features NNW1and NNW7. Constructed from two fractures as shown in Figure 2-7.
Conditioned fractures intersecting tunnel sections.	Deterministic fractures added at 69 head calibration sections. Transmissivity of these deterministic fractures set at 10^-8 m^2/s to reduce excessive drawdowns.
Transport Aperture	Aperture = 2 * $Transmissivity^{0.5}$
Boundary Conditions	
North, South, East & West sides	Conditioned to the values reported in Svensson (1999).
Base	No flow boundary assigned to each node.
Baltic Sea	Head of 0.0 m.
Äspö Island	No flow boundary assigned to each node.
Geochemistry	
Chemical Composition	Seven chemical components. See Section 5.1 for details.
Interpolation Scheme	Updated interpolation scheme described in Section 5.3

The time varying fit between the measured and numerically modeled 7 chemical component model provides a measure of how well the approach worked. The end member fits are also provided to enable direct comparison to the published SKB solutions.

The best fit hydrogeological model, model H8, described in Section 3.1 and Table 3-1 was used for the analyses. This model was developed using only hydrogeological data. The hydrogeological model was chosen as the base case, in preference to the geochemically fitted models, because it allowed a clearer interpretation of the effect of the addressed uncertainty issues on the derived chemistry. The methodology used for the pathways analysis and the chemistry initial condition/interpolation are given in sections 5.2 and 5.3 respectively.

The time-varying chemistries are presented as computed: no additional calibration has been undertaken.

5.4.1 Results of Seven Component Model Simulations

The calibration borehole section results for the seven component model are presented in Figure 5-21 to Figure 5-29. The two (of three) meshed prediction borehole locations are presented in Figure 5-30 to Figure 5-31.

The calibration sections KR0012B, SA0850B, SA1327B, and the prediction section KA3110A, are not included because these sections were not connected to the general fracture network in the stochastic background fracture realization.

The fits for borehole sections SA2074A, KAS03a, KAS03b and KA3005A were very good. The first three of these sections showed time dependent behavior, indicating the simulation correctly replicated the flow velocities as well as the flow location.

SA0813B showed a good fit for chemical component 2, but component 3 is incorrectly shown as component 3. However, the time dependence of the components is correctly replicated.

SA1229 also indicates time dependent behavior. The fit for component 7 is excellent. The deficiency in the analysis is that component 2 is overestimated due to the absence of component 3 in the simulated results.

The three poorest fits were SA2783A, KAS07, KA1775A and KA3385A. KA1775A indicates very different chemical compositions for the two measured data points, and are therefore possibly inaccurate. The three remaining borehole sections show time dependent responses that would be better modeled if the flow velocities in the finite element model were slower. Slowing the velocity by increasing fracture aperture was not attempted due the good fits to the other sections.

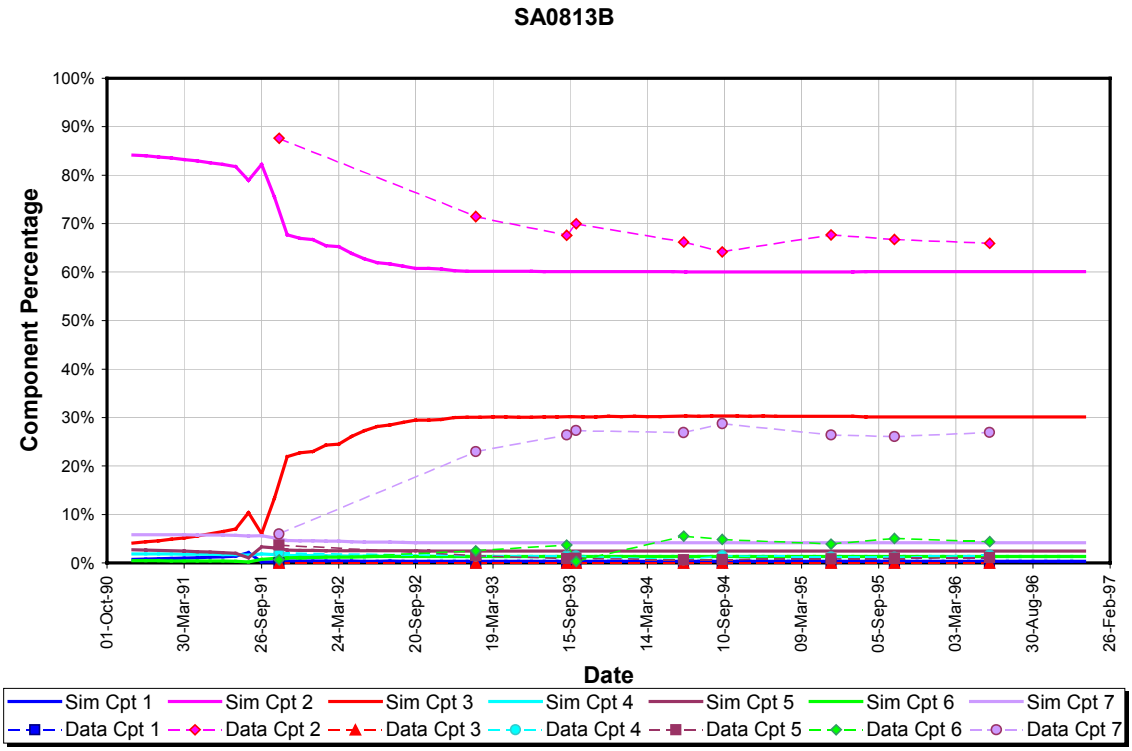

Figure 5-21 *SA0813B geochemical inflows for 7 component model*

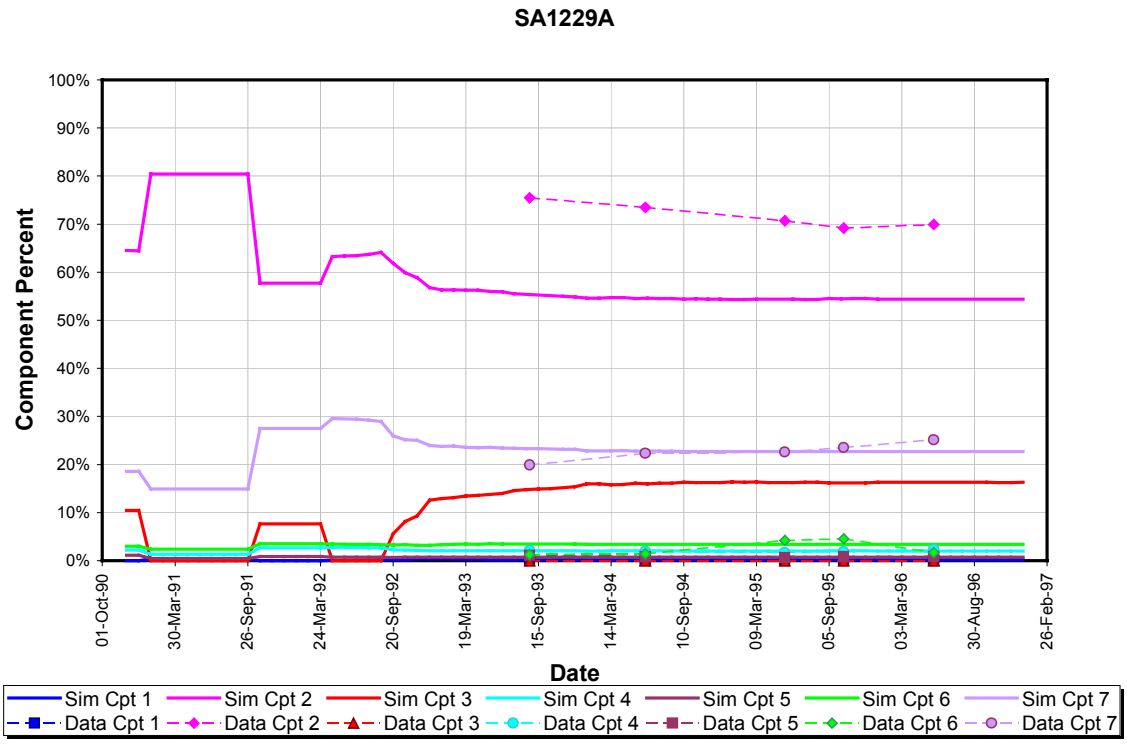

Figure 5-22 *SA1229A geochemical inflows for 7 component model*

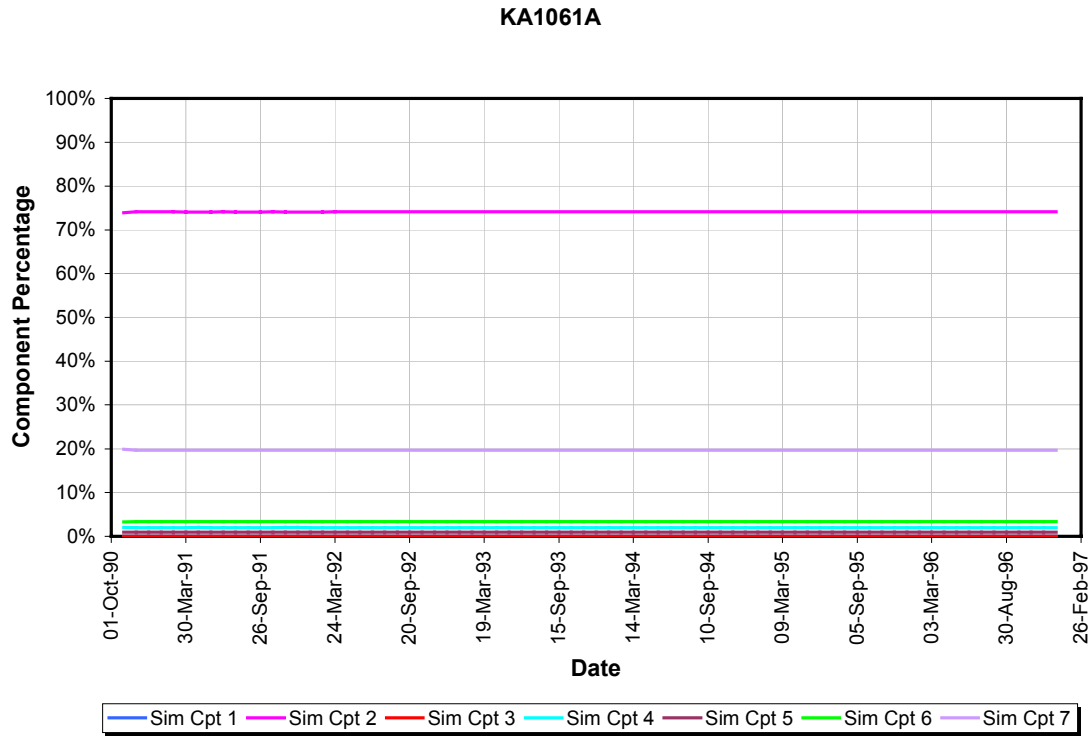

Figure 5-23 *KA1061A geochemical inflows for 7 component model*

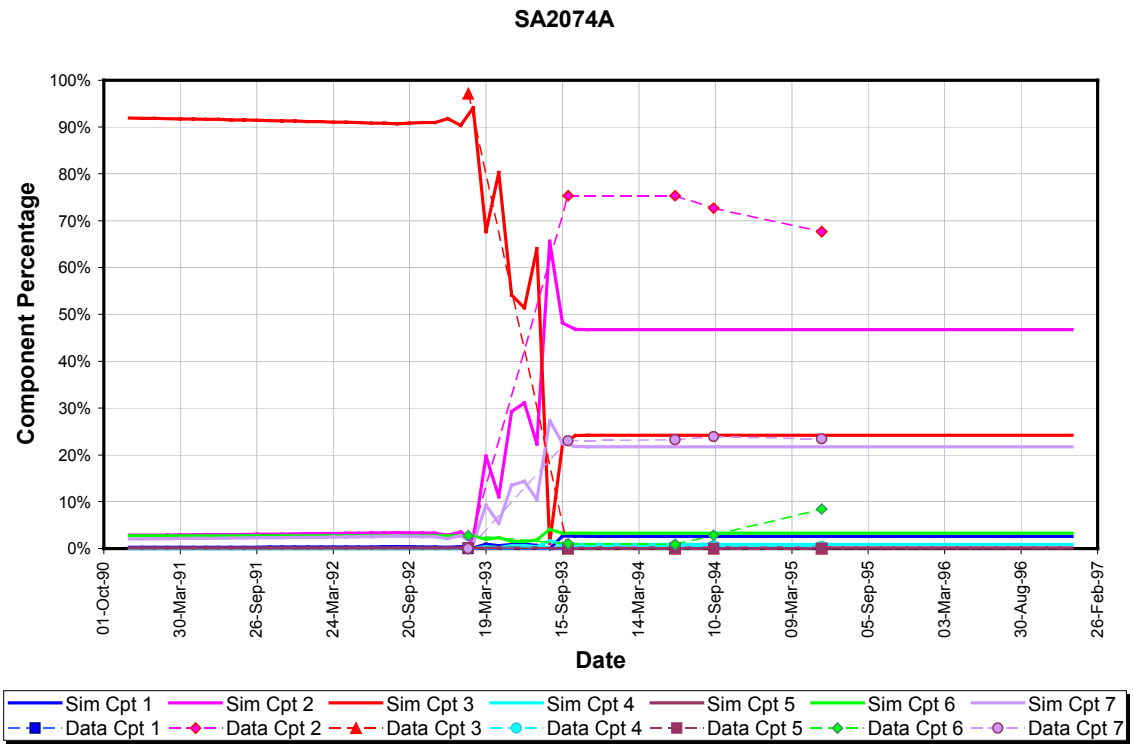

Figure 5-24 *SA2074A geochemical inflows for 7 component model*

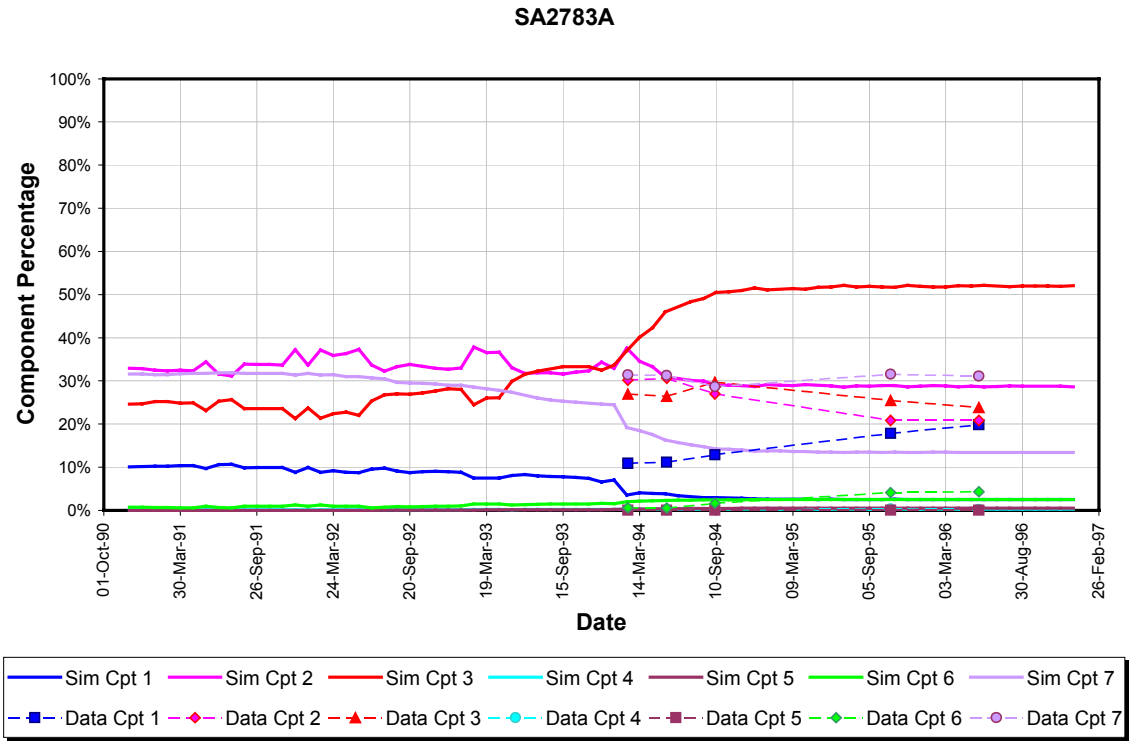

Figure 5-25 *SA2783A geochemical inflows for 7 component model*

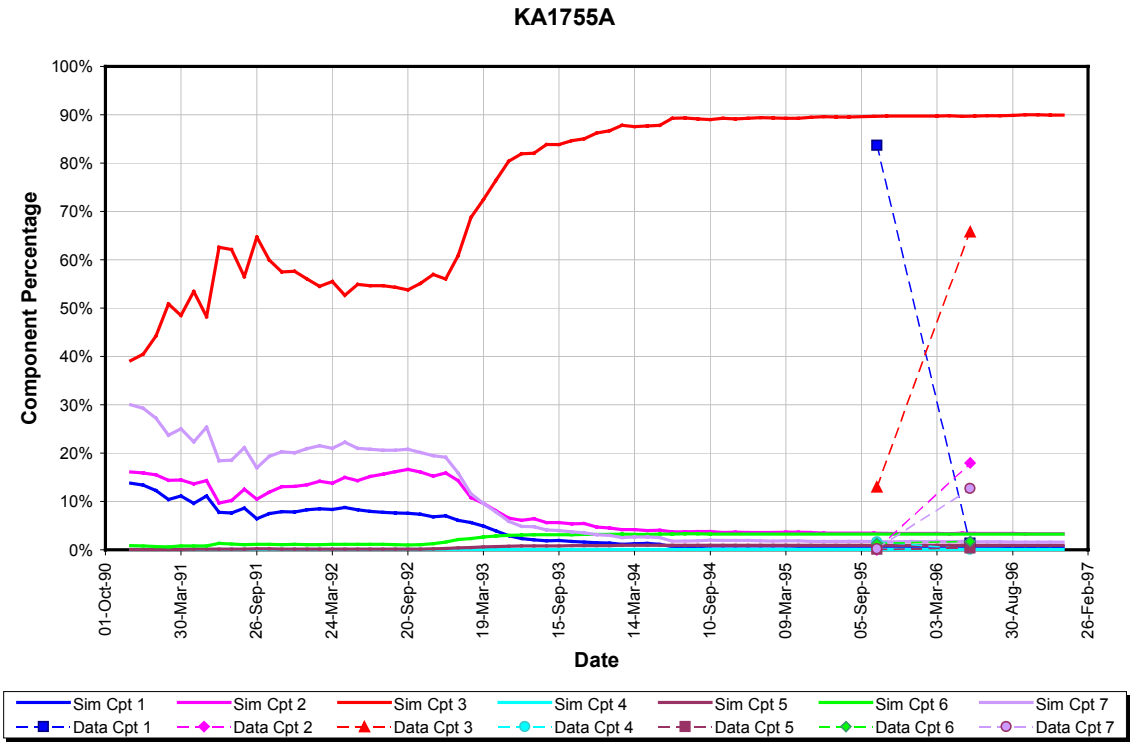

Figure 5-26 *KA1775A geochemical inflows for 7 component model*

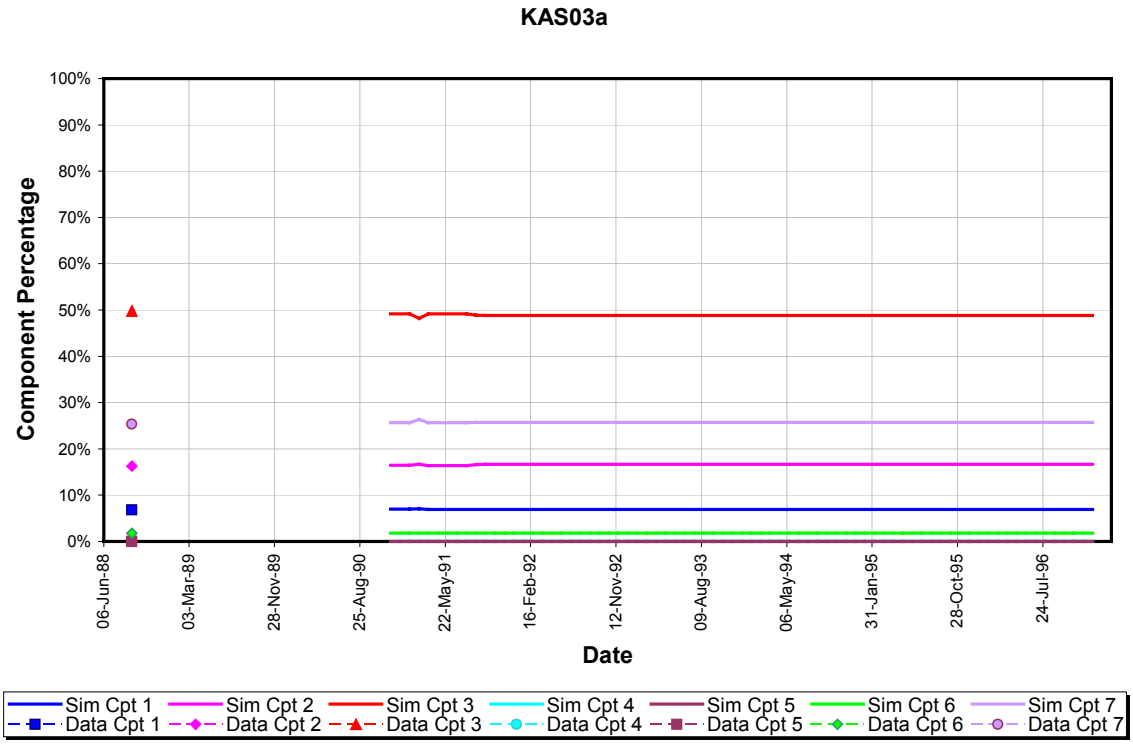

Figure 5-27 *KAS03a geochemical inflows for 7 component model*

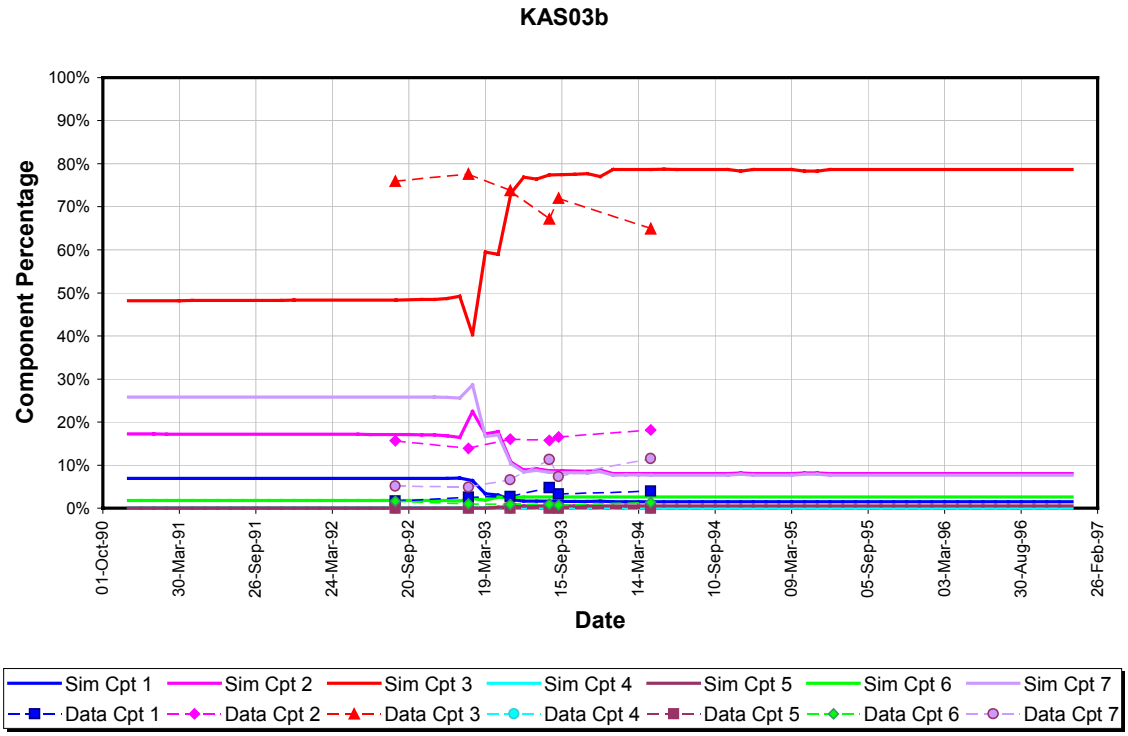

Figure 5-28 *KAS03b geochemical inflows for 7 component model*

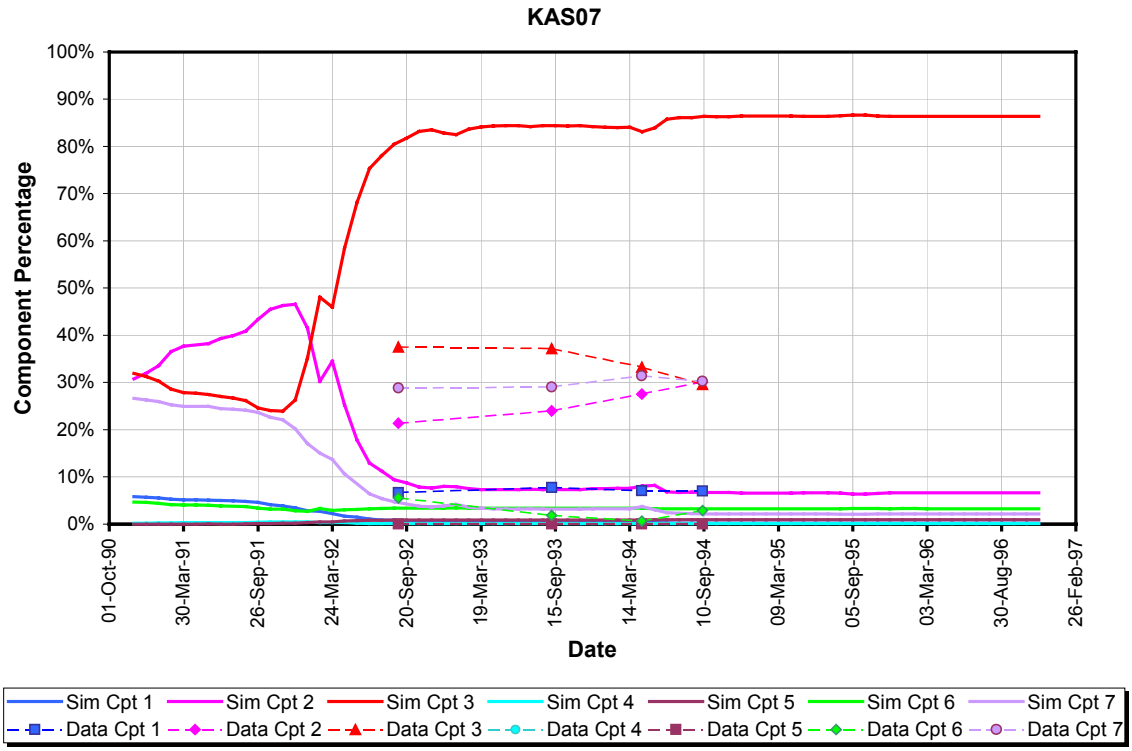

Figure 5-29 *KAS07 geochemical inflows for 7 component model*

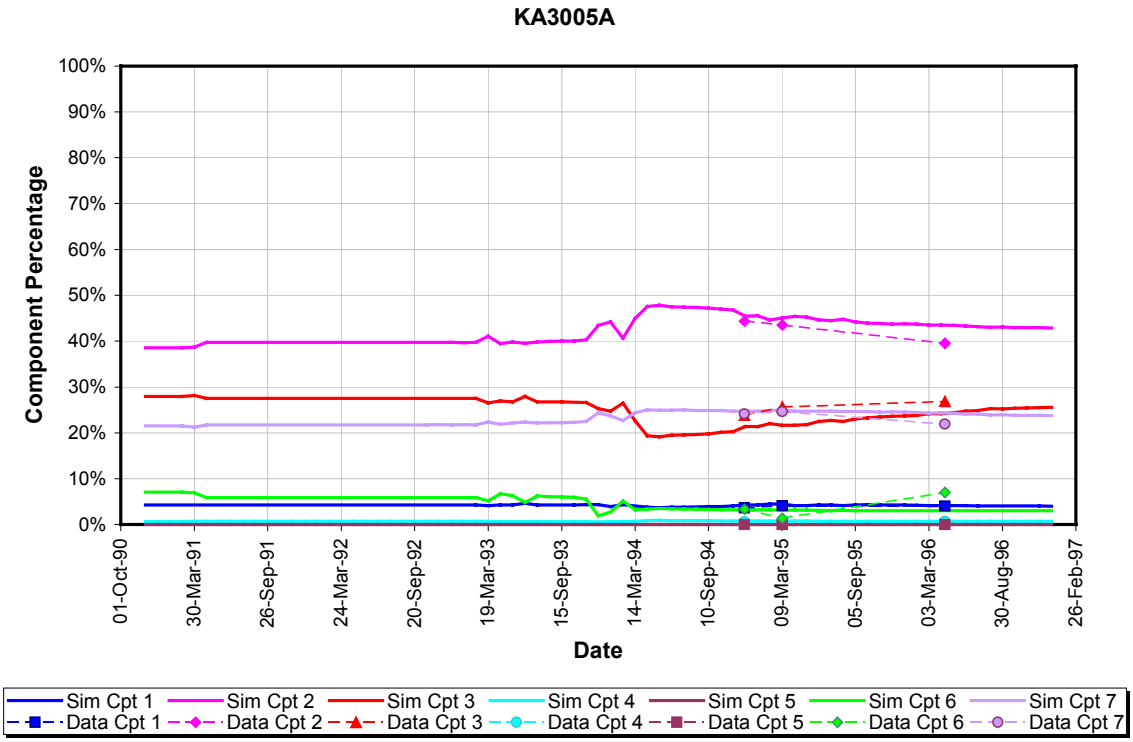

Figure 5-30 *KA3005A geochemical inflows for 7 component model*

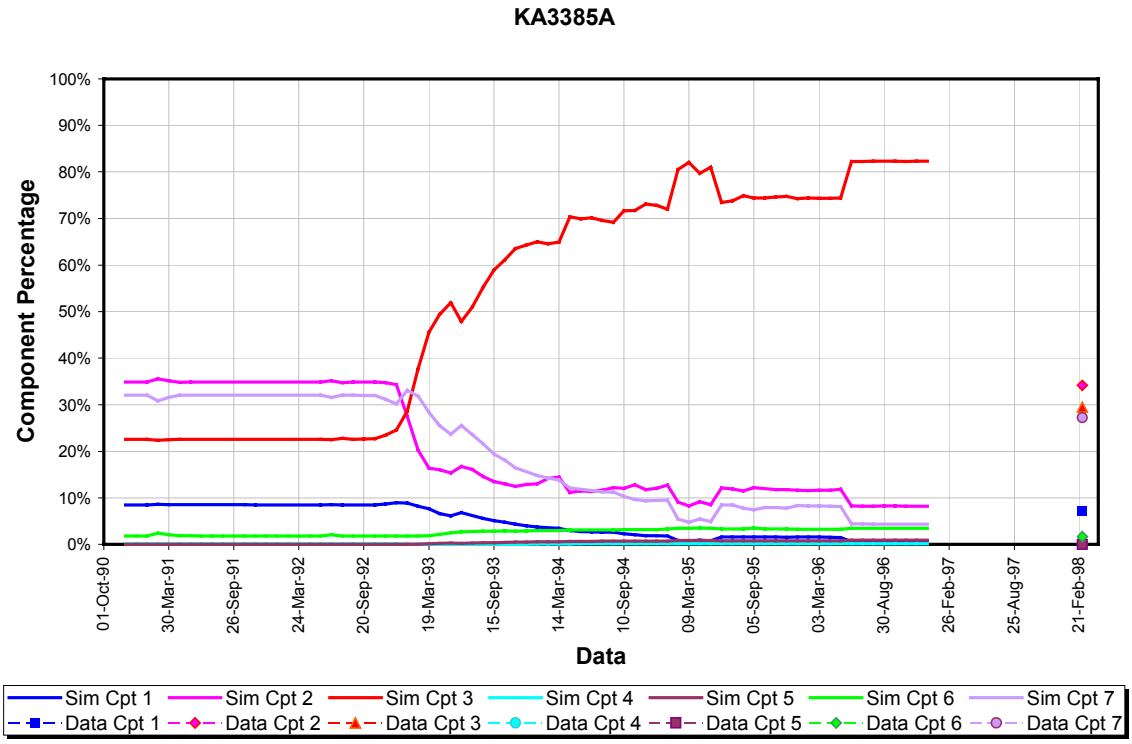

Figure 5-31 *KA3385A geochemical inflows for 7 component model*

5.4.2 Results of End Member Simulations

The results presented for the 7 component model showed discrepancies in the arrival times of the different chemistries, indicating further improvements in the fits could be obtained by changing the storativity values of a few of the LSFs.

The baseline storativity value of all LSFs was obtained using the equation Storativity = 0.001 $T^{1/2}$. The storativity scaling factors used to improve the calibrations are provided in Table 5-4.

Endmember simulation results based on the seven component model are presented in Figure 5-32 to Figure 5-40. The two meshed prediction borehole locations are presented in Figure 5-41 and Figure 5-42.

As explained above, the calibration sections KR0012B, SA0850B, SA1327B, and the prediction section KA3110A, are not included because these sections were not meshed in the finite element simulation.

Table 5-4 Storativity Scaling Factors used for Final Calibration

Fracture	Storativity Scaling Factor
EW-1N	1
EW-1S	3
EW-3 (z=500-200)	1
EW-3 (z<200)	3.2
EW-7	1
NE-1	1
NE-2	3.3
NE-3	1
NE-4N	3.5
NE-4S	1
NW-1	1
NNW-1	1
NNW-2	1.5
NNW-3	1
NNW-4	1
NNW-5	1
NNW-6	1
NNW-7	1
NNW-8	1.7
SFZ11	1
SFZ14a	1
SFZ14b	1

The error term measures for the revised chemistry version of H-8 is provided in Table 5-5.

Table 5-5 New Chemistry Error Estimates

Sim	Stage II: Geochem Calibration	Features	# of Geochem Sections	Geochem Fit Average ABS
NC-1	New Chemistry model.	Based on the H-8 hydrogeological model with revised chemistry definition and recalibrated storativity.	45	8.1 %

It should be noted that the sum of the four end-members does not necessarily add to 1.0. This is a function of the method in which the proportions were computed. The 7 defined chemical components in each of the original end-members (Brine, Baltic, Glacial and Meteoric water) and in each of the other waters is known. By a least-squares method, the coefficients for each of the end-members (brine, Baltic, glacial and meteoric) was calculated such that, when the compositions of these end-members are multiplied by the coefficients, and the results summed, the unknown water composition is obtained.

i.e.

		New Chemical Component						
End-member		1	2	3	4	5	6	7
a	Brine	Br1	Br2	Br3	Br4	Br5	Br6	Br7
b	Baltic	Ba1	Ba2	Ba3	Ba4	Ba5	Ba6	Ba7
c	Glacial	Gl1	Gl2	Gl3	Bl4	Gl5	Gl6	Gl7
d	Meteoric	Me1	Me2	Me3	Me4	Me5	Me6	Me7
	Other Water	OW1	OW2	OW3	OW4	OW5	OW6	OW7

Where Br1, Br2,....Br7 represents the proportions of the new chemical component 1, 2, ...7 in the brine end-member; Ba1, Gl1, Me1 and OW1 represent the proportions of component 1 Baltic sea end-member, glacial end-member and other water, respectively.

By a least-squares method, values for a, b, c and d were calculated, representing proportions such that a x Br1 + b x Ba1 + c x Gl1 + d x Me1 = OW1, and similarly for the other components 1, 2, 3, 4.

The numbers representing the proportions of the end-members are the coefficients a, b, c, d in the table represented above. In theory, they should add up to 1.0.

The reason that they do not is due to the fact that they were derived from least-squares fitting and, quite likely the fact that the underlying assumption that the waters are all mixtures of the 4 end-members is incorrect. For this latter reason, the numbers were not normalized to 1.0.

This conclusion is in fact consistent with the original M3 modeling. The M3 modeling effectively neglects mass from the system, by basing the mixing proportions on geometrical relationships on a plot of eigenvalues corresponding to only the first two principal components. When the M3 proportions calculated in this way are used to calculate concentrations of unreactive groundwater constituents, like Cl, it is found that the numbers calculated do not always correspond to the concentrations in the actual waters. What is striking is that the discrepancies tend to correspond to waters for which negative proportions of meteoric water were calculated by the new modeling.

The results presented in Figure 5-32 to Figure 5-42 are much better than those for the seven individual chemical components. The results for SA2074A, KA3005A, KAS03A and KAS03B are very good. This is consistent with the results of the seven individual chemical components. The match between the measured and modeled end-members for SA1229 is also extremely good. This fit is better than was achieved for the individual chemical components. Unlike the fits for the seven component model, the results for SA2783, KA1755A, KA3385A, and KAS07 are also good. These sections are the most affected by the storativity changes.

SA0813B provides a very good match between measurement and model, especially given the large variations in the measured components. The measurement values include the largest negative fraction of glacial waters. This is obviously unrealistic, and indicates a poorly constrained problem.

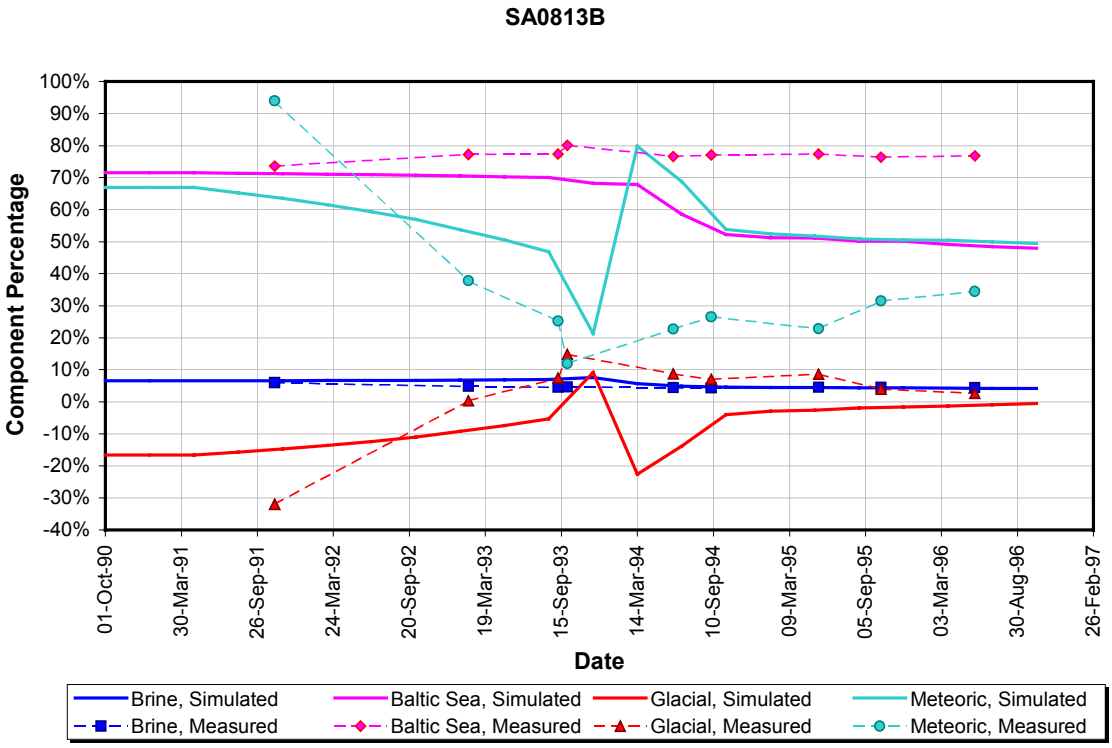

Figure 5-32 *SA0813B geochemical inflows for 4 endmembers*

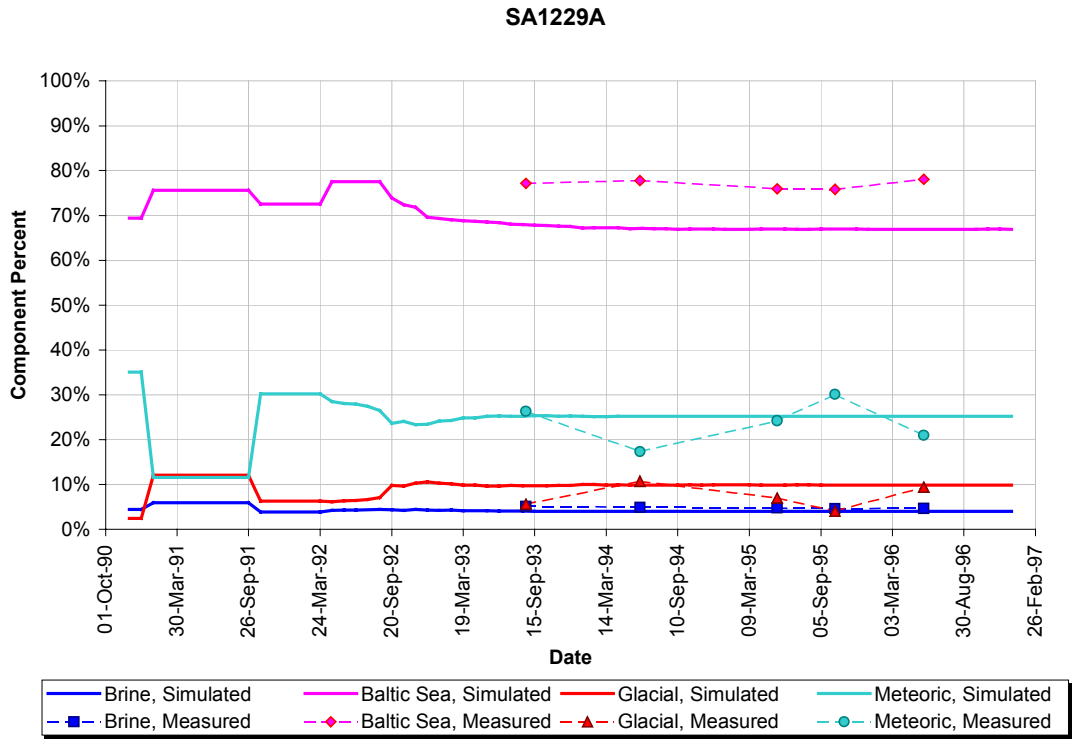

Figure 5-33 *SA1229A geochemical inflows for 4 endmembers*

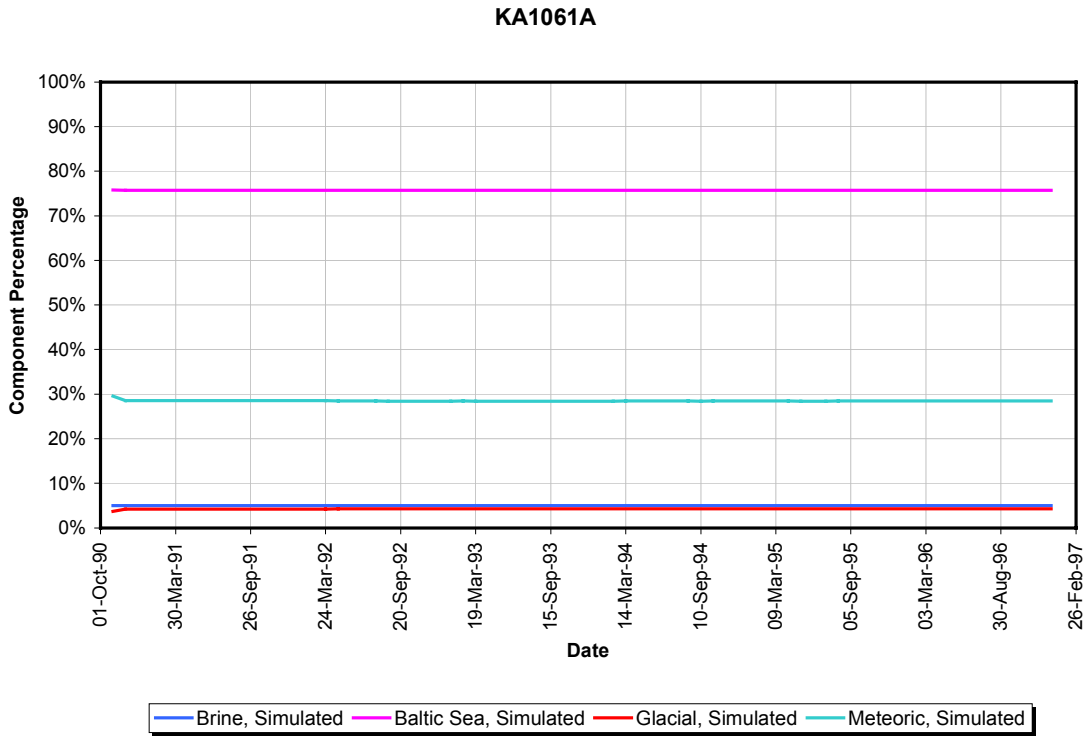

Figure 5-34 *KA1061A geochemical inflows for 4 endmembers*

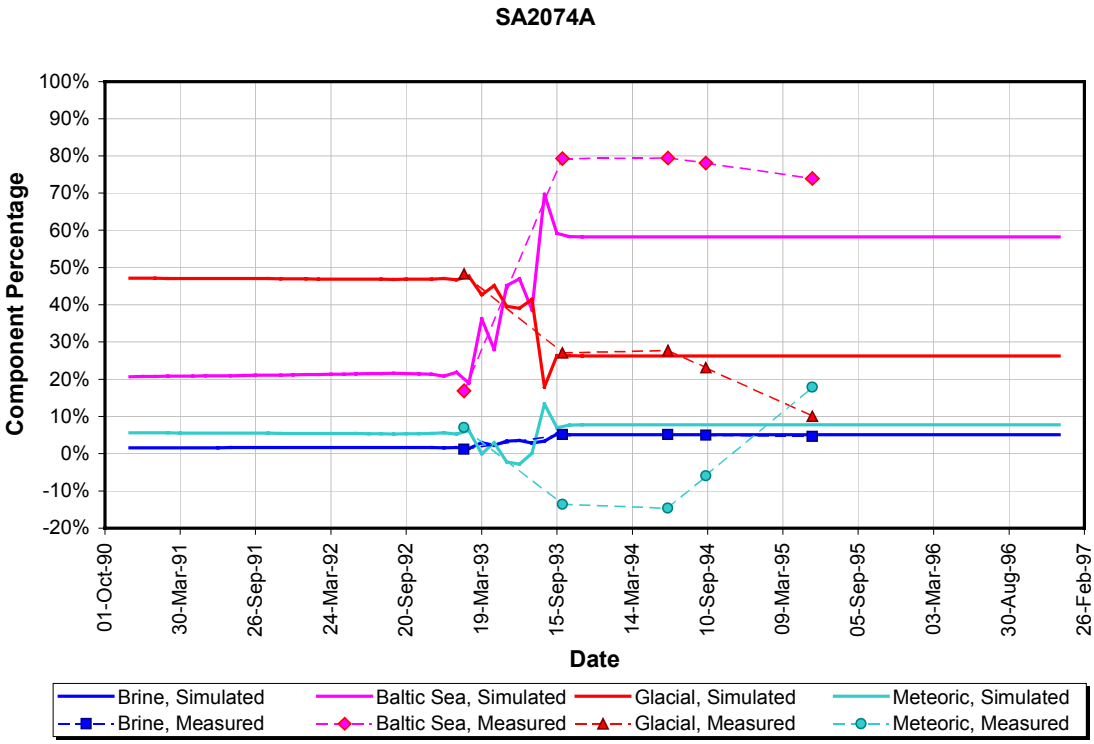

Figure 5-35 *SA2074A geochemical inflows for 4 endmembers*

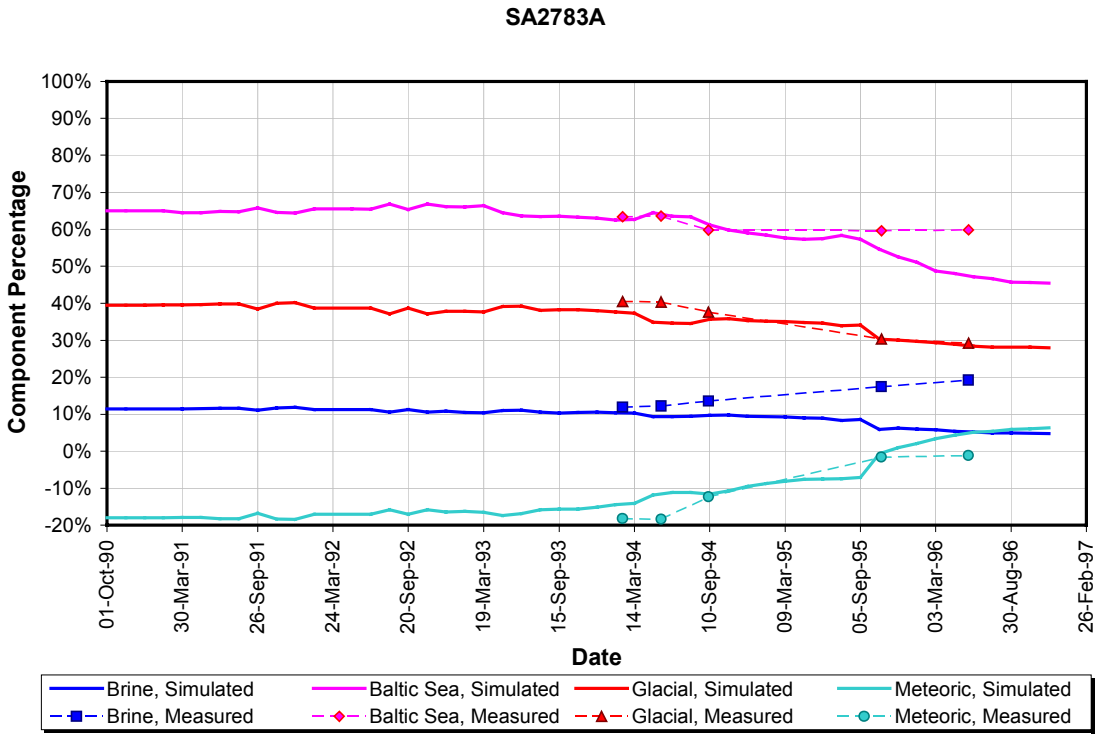

Figure 5-36 *SA2783A geochemical inflows for 4 endmembers*

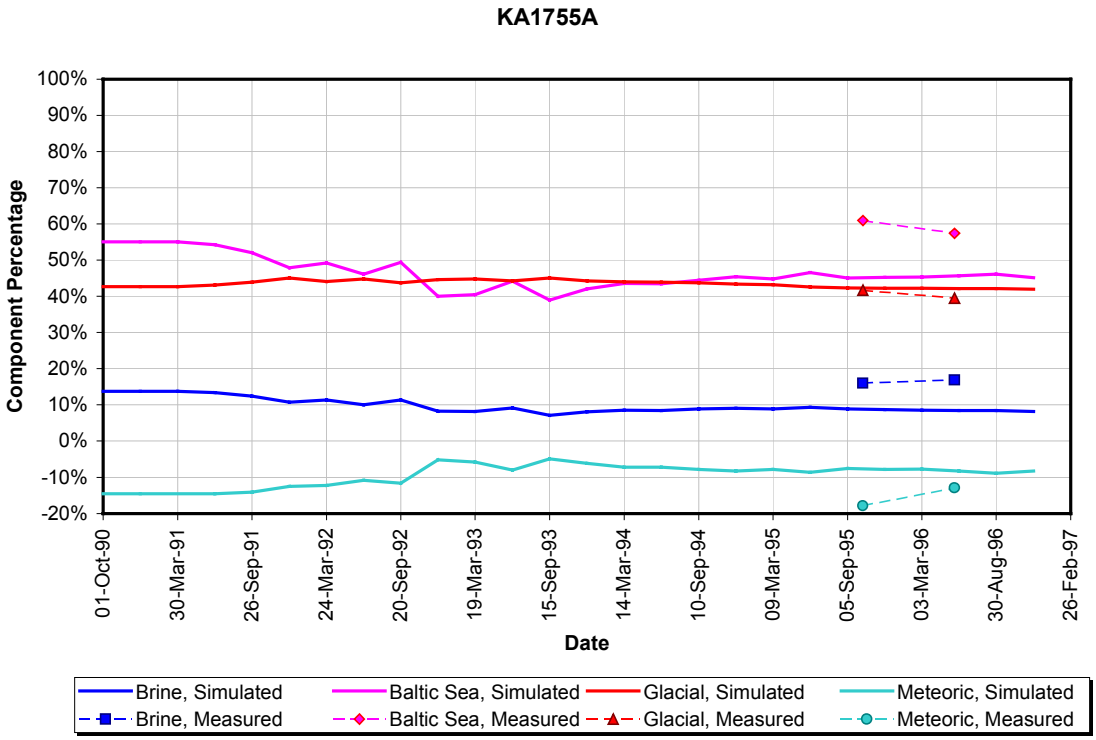

Figure 5-37 *KA1775A geochemical inflows for 4 endmembers*

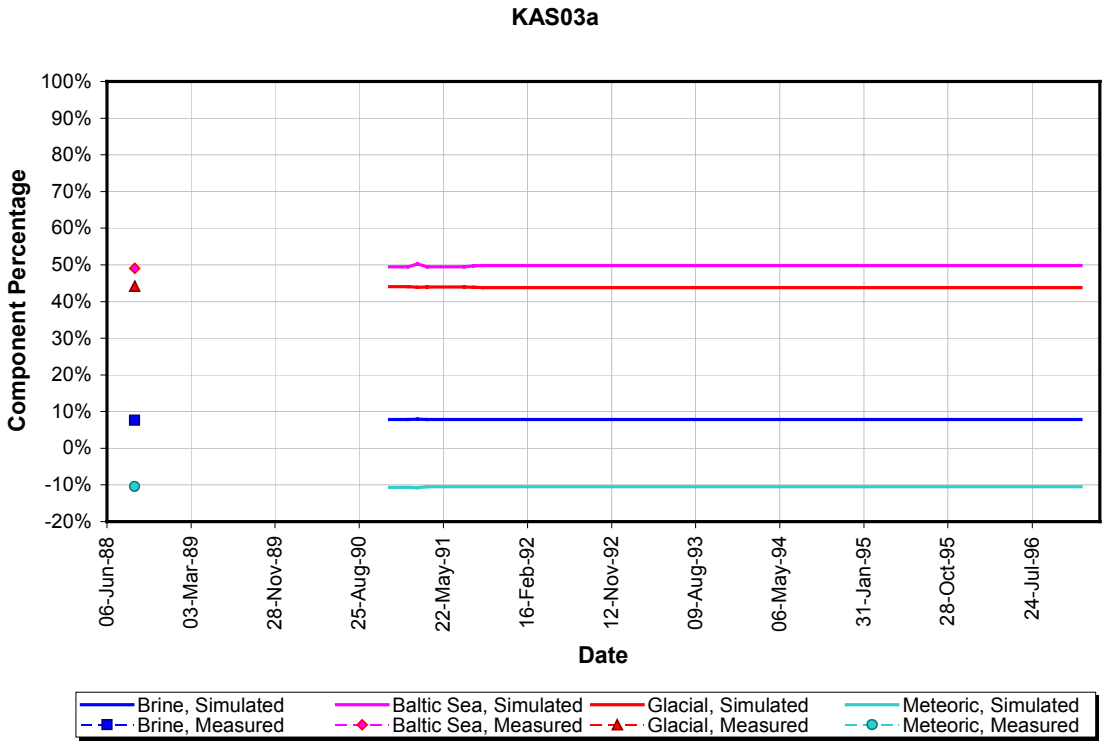

Figure 5-38 *KAS03a geochemical inflows for 4 endmembers*

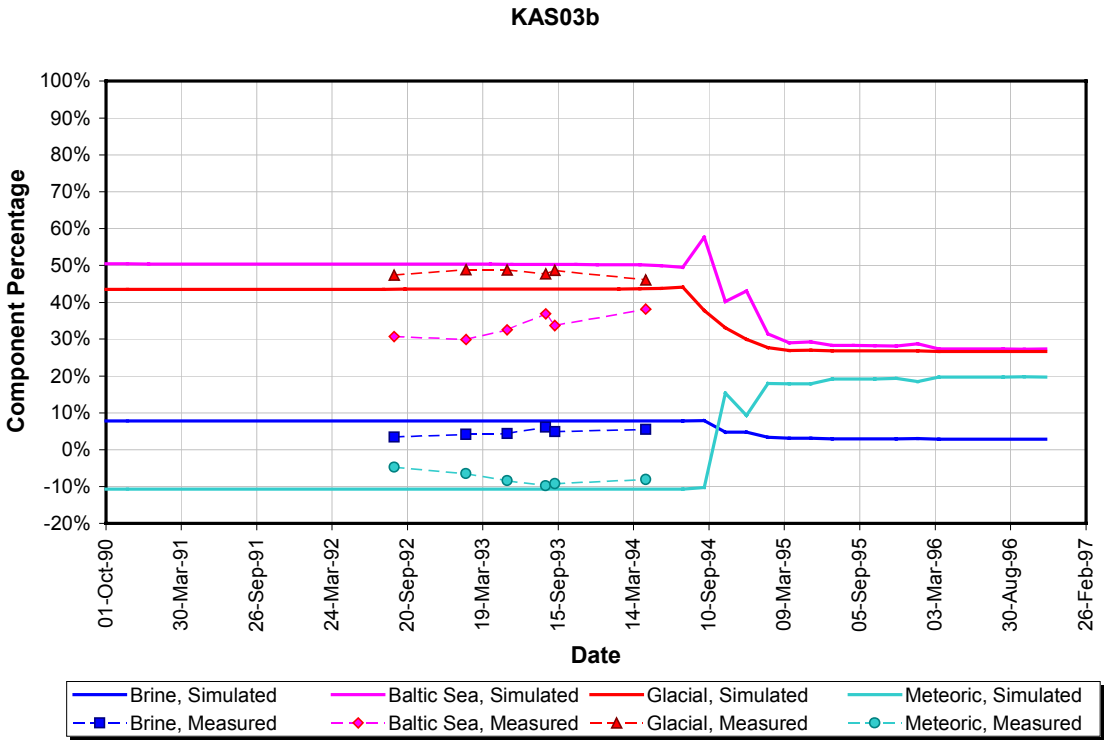

Figure 5-39 *KAS03b geochemical inflows for 4 endmembers*

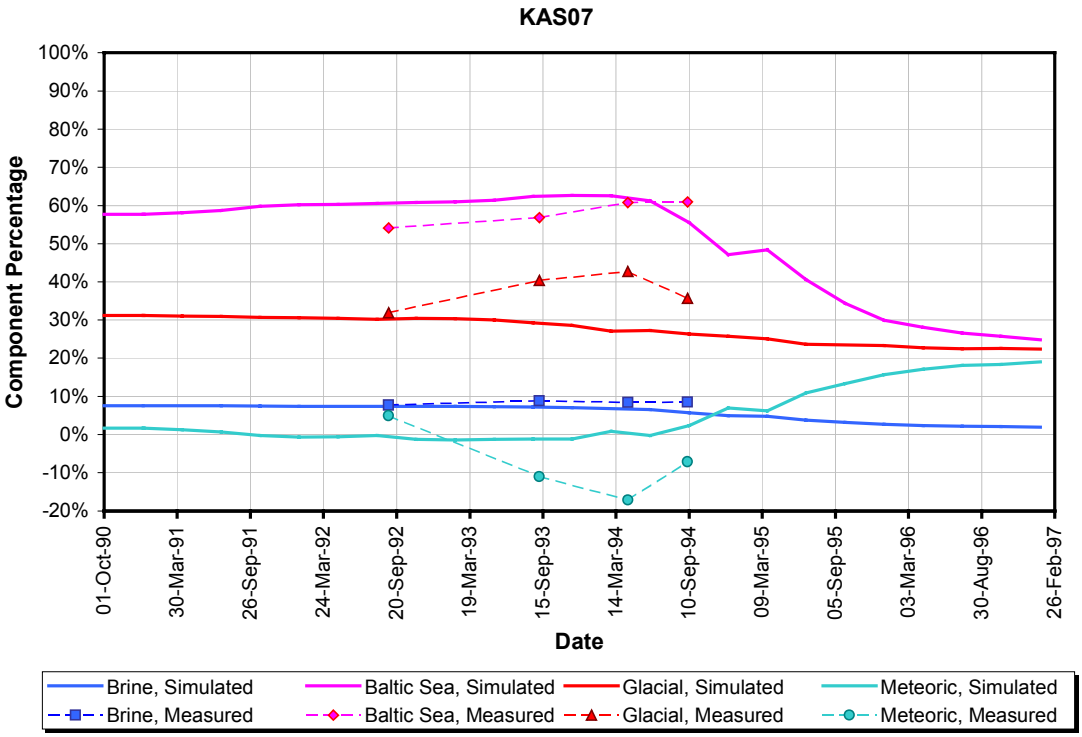

Figure 5-40 *KAS07 geochemical inflows for 4 endmembers*

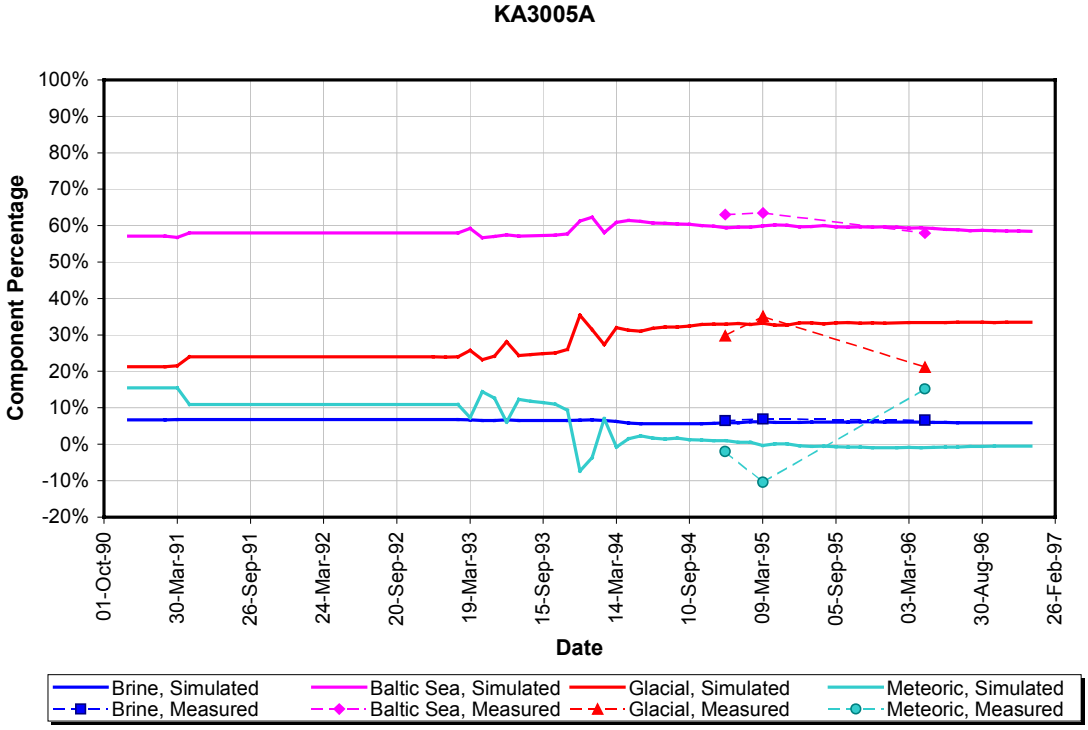

Figure 5-41 *KA3005A geochemical inflows for 4 endmembers*

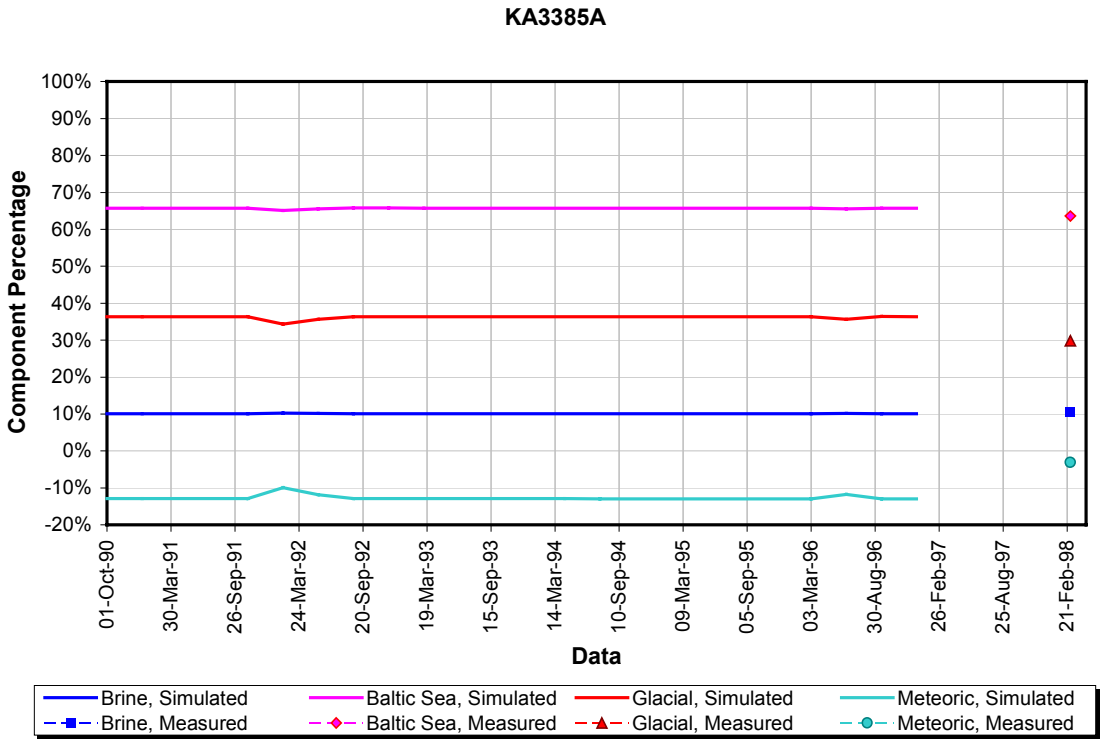

Figure 5-42 *KA3385A geochemical inflows for 4 endmembers*

5.5 VALUE OF TASK 5 FOR JNC

One goal of JNC's participation in the Task 5 project is to evaluate how the methodology used at Äspö might be applied to potential repository sites in Japan. In order to assess the usefulness of the Äspö approach, the methodology was separated into five topics.

1) general conceptual approach
2) applicability of M3 and principal component approaches to geochemistry interpretation
3) spatial chemistry interpretation
4) hydrogeological and hydrochemical constraints on the model
5) site characterization requirements for geology, hydrogeology and geochemistry data

These topics are covered in the following five sub-sections. Concluding remarks are provided in Section 5.5.6.

5.5.1 General Conceptual Approach

The general approach used in the Äspö Task 5 modeling, by the JNC/Golder team and generally by the other Task 5 team members, was sequential. The phases could be summarized as:

- Develop a regional model of the site including only the large scale features
- Develop a conceptual model for the background fractures. For a DFN idealization this included the orientation, size, intensity, and transmissivity of the non-regional features. For porous medium models this would be the equivalent block transmissivities.
- Develop boundary conditions for the modeled region.
- Create a finite element model including the major features, background features, and boundary conditions. Calibrate this model to the measured head distribution by varying the fracture properties and boundary conditions.
- Use this calibrated model to predict chemistry distributions. Calibrate this model to the measured chemistry and head distribution by varying the fracture properties and boundary conditions.

Based on the Task 5 modeling of the Äspö site this approach worked well. It was found that the calibration to measured heads provided a reasonable calibration to the general water sources, but that the travel velocity was poorly predicted. The chemistry data provided a data set from which to refine these velocities. Chemistry data also reduced the non-uniqueness of the system.

It should be noted, however, that the goodness-of-fits achieved were also sensitive to the methodology used to compute the geochemical distribution across the site. The hydrogeology and the geology at the Äspö site are consistent with the major features dominating mixing and flows. Therefore it was necessary to distribute chemistry based on the major features, rather than assuming a continuum. The strong influence of the Baltic / Äspö Island boundary on the chemistry also markedly affected the interpretation. For a different site, this means that the modelers would need to ascertain the structures, geology and/or major processes affecting the chemistry prior to setting up the geochemical spatial distribution. Similarly, the interpretation scheme should also account for the hydrogeological conditions.

5.5.2 Applicability of M3 and Principal Component Approaches

The M3 method was used for the Stage 1 and Stage 2 modeling. The numerically interpreted Principal Components were used to assign chemical properties for the Stage 3 sensitivity modeling. The two approaches have differing advantages and disadvantages.

The M3 method was developed for application at Äspö where saline groundwaters and brines are major features of the groundwater system. The method as applied for Task 5 had the advantage that the four end-members chosen were physically meaningful. However, the M3 method may not be generally applicable. In particular, the reliance of the method on the first two principal components may not be appropriate in fresh groundwater systems. In such cases the first two principle components are more likely to reflect factors other than groundwater mixing. For example, water/rock interactions

are likely to be a more significant cause of chemical variation in fresh groundwater systems than in saline groundwater systems. In such cases, it will be necessary to consider other principal components besides the two most important ones, in order to deduce information about groundwater mixing.

In Model 2, seven chemical component model used for the Stage 3 sensitivity analyses makes no prior assumptions about the numbers or compositions of chemical components (analogous to end-members in the M3 modeling). The advantage of this approach is that the chemical components are based purely on analysis and provide a measure of the applicability of mixing (and by implication chemical reaction) to the groundwater regime. This is extremely important, as if chemical reaction is an important component of the variation in groundwater composition, the geochemical mixing approach used to calibrate the DFN model is invalid. The disadvantage of this approach is that the chemical compositions, and the end-members created from them, are not necessarily physically realistic.

5.5.3 Spatial Chemistry Interpretation

The Task 5 modeling both highlighted the difficulty of extrapolating measured chemistry at a few distinct locations throughout a much larger region, and showed that this could be successfully achieved. Unless the density of measurement locations is sufficiently high, providing good resolution at all chemistry interfaces, a meaningful interpretation requires that the hydrogeology of the area be considered as part of the extrapolation process. Without this interpretation, the number of locations at which chemistry has been measured is typically too small to define chemical boundaries. In particular, the effect of saline interfaces (e.g. the Baltic/Äspö Island boundary), and chemistry depth dependence should be considered.

The dominance of the regional features on the chemistry should also be addressed when choosing an interpolation scheme.

5.5.4 Hydrogeological and Hydrochemical Constraints on the Model

The major constraint on the model should be a good conceptual model for the site prior to modeling. The hydrogeological and hydrochemical data provide invaluable information, but on their own can not be expected to generate anything approaching a unique solution.

The head and geochemical data provides differing constraints on the model. Head data is critical, and ought to be used to calibrate the model prior to geochemical input. The reasons for using the head data first are that this information is less ambiguous. The time-dependent head information is dominated by local connectivity and transmissivities as the tunnel section is being constructed, and by the regional connectivity and boundary conditions later on. Therefore, if the original fracture model accurately reflects the major connectivity, missing connectivity (e.g. the Mystery Feature) and boundary conditions can be calibrated fairly successfully.

The geochemical information provides the only real constraint (or validation) on the source location of waters predicted by a model. This calibration provides information, like the head data, on whether a major connection is missing. However, like the head calibration, it relies on having a good underlying DFN model that already replicates most of the major hydraulic structures.

Additionally, geochemical data can be used to calibrate transport apertures and storage affects. These effects are difficult to calibrate using solely time dependent heads measures at tunnel sections.

5.5.5 Site Characterization Requirements for Geology, Hydrogeology and Geochemistry Data

The site characterization requirements for geology, hydrogeology and geochemistry may be summarized as follows. Note that all three topics are inter-dependent and should be considered together where possible.

Geology:

- Location and size of all major features.
- Orientation, size and intensity of background fracturing.
- Topography, location of streams, etc. required to provide boundary conditions for the edges of the modeled region. Ideally the boundaries should be distant so that the model is not sensitive to the assumptions, and the boundaries should be located where the boundary condition is not sensitive to the model used to generate them. For example, infiltration boundaries based on porous medium results should generally not be assigned to fracture network models.
- Aperture information.

Hydrogeology:

- Hydrogeological properties of the major features. The variation in properties across a feature may be important. Similarly, the effect of the feature on adjacent fractures (e.g. impermeable or permeable zone at edge of fault zone).
- Hydrogeological properties of the background fracturing.
- Time-dependent heads required to provide differing scale of properties
- Both density-corrected and raw information should be collected and reported.
- Measurement locations should be distributed both in main fracture zones and in the background network to allow verification of the relative permeabilities of the DFN. Geology only provides the orientation and size information, intensity and transmissivity should be derived from hydraulic testing.

Geochemistry:

- Time dependent geochemistry both within the major features and the background fracturing.
- Interpretation to provide geochemical overview of the site. This should include the in situ controls on the chemistry variations (e.g. saline – freshwater interface, long term chemical reactions, age of waters, etc.).

5.5.6 Conclusions

The conclusions of the additional Stage 3 analysis are:

- The Stage 3 analysis simulations provided significant improvements in breakthrough calibration.
- The change to an improved interpolation scheme for spatial distribution of end-members was the key to improving the Task 5 predictions
- Seven principal component end-members provide a better match to the actual chemistry and a clearer measure of whether the mixing assumption is appropriate. However, the seven principal components, based solely on numerical analysis, lack physical meaning
- The improved particle-tracking algorithm also contributed to a more accurate breakthrough calculation. This algorithm, which is consistent with the solute allocation in transport codes such as LTG (Dershowitz et al., 1998c), PICNIC (Barten, 1996), etc., is potentially useful for Performance Assessment calculations.

6. CONCLUSIONS

This report presented hydrogeological and pathways modeling of Äspö Island as part of "Task 5" of the Äspö Task Force on Modeling of Groundwater Flow and Transport of Solutes. The report describes model evolution, and the use of hydrogeological and geochemical information to develop predictive models. The SKB Questionnaire, containing a review of the modeling approach used, is included as Appendix D.

The modeling was undertaken in three stages. In Stage 1 the finite element model of the DFN was calibrated to hydrogeological data. Stage 2 used geochemical measurements to improve the calibration. These results were presented as Task 5 predictions. The final stage, Stage 3, documents an additional sensitivity analysis developed to investigate the sensitivity of the results to the interpreted chemical components and particularly the interpolation scheme used to compute the source chemistry within the modeled domain.

Calibration to heads, using a well-defined geological model as the starting point, provided a reasonable estimate of the local connectivity of the system. However, the time dependence of the flows into the tunnel was generally not well modeled.

The inclusion of geochemical data allowed a much better fit to the time dependence of the model. The data also highlighted where additional connections were required to increase the connectivity to a specific area of the model. Inclusion of such features improved the head calibration, as well as the chemistry fit. However, the results proved to be highly sensitive to the methodology used to spatially locate the initial end-members, and to a lesser extent to the choice of chemical components. The Äspö site is dominated by the large-scale features. It was necessary to use the large-scale features as the dominant influence on the chemistry. The Kriged grid of chemistry locations, combined with a linear interpolation scheme to compute the chemistry between the grid points, did a poor job of calculating the chemistry of the inflows. It is believed that the reason for this poor calibration was that the Kriging and interpolation scheme did not incorporate the geology of the model into the interpretation.

The Stage 3 model could have been improved further using the geochemical information. This was not attempted, as the purpose of this modeling stage was to highlight the sensitivity of the results to the data extrapolation/interpretation.

During this Task 5 modeling two main objectives were set:

1) to assess the consistency of groundwater flow models and hydrochemical mixing-reaction models through the integration and comparison of hydraulic and hydrochemical data obtained before, during and after tunnel construction;
2) to develop a procedure for integration of hydrological and hydrochemical information which could be used for assessment of potential repository sites.

The groundwater flow and hydrochemical mixing-reaction models were found to provide consistent results for the Äspö site. This is in part due to the staged approach, with the geological, hydrogeological and chemical data providing differing information.

However, the M3 method was developed for application at Äspö where saline groundwater and brines are major features of the groundwater system. The method as applied for Task 5 had the advantage that the four end-members chosen were physically meaningful. However, the M3 method may not be generally applicable. In particular, the reliance of the method on the first two principal components may not be appropriate in fresh groundwater systems. In such cases the first two principle components are more likely to reflect factors other than groundwater mixing. For example, water/rock interactions are likely to be a more significant cause of chemical variation in fresh groundwater systems than in saline groundwater systems. In such cases, it will be necessary to consider other principal components besides the two most important ones, in order to deduce information about groundwater mixing.

The general procedure for integration of hydrological and hydrochemical information in the Äspö Task 5 modeling was staged. The stages could be summarized as:

- Develop a regional model of the site including only the large scale features
- Develop a conceptual model for the background fractures. For a DFN idealization this included the orientation, size, intensity, and transmissivity of the non-regional features. For porous medium models this would be the equivalent block transmissivities.
- Develop boundary conditions for the modeled region.
- Create a finite element model including the major features, background features, and boundary conditions. Calibrate this model to the measured head distribution by varying the fracture properties and boundary conditions.
- Use this calibrated model to predict chemistry distributions. Calibrate this model to the measured chemistry and head distribution by varying the fracture properties and boundary conditions.

This staged approach is very general, and is therefore applicable to other potential repository sites. The staging was advantageous, because it necessitated constructing a good geology based DFN model of the site prior to calibration. Without such a structure for the DFN, the problem is poorly constrained and the calibration non-unique. A unique calibration likely cannot be obtained in practice, but the staged approach should enable the dominant features to be well replicated.

The head and geochemical data provides differing constraints on the model. Head data is critical, and ought to be used to calibrate the model prior to geochemical input. The reasons for using the head data first are that this information is less ambiguous. The time dependent head information is dominated by local connectivity and transmissivities as the tunnel section is being constructed, and by the regional connectivity and boundary conditions later on. Therefore, if the original fracture model accurately reflects the major connectivity, missing connectivity (e.g. the Mystery Feature) and boundary conditions can be calibrated fairly successfully.

The geochemical information provides the only real constraint (or validation) on the source location of waters predicted by a model. This calibration provides information, like the head data, on whether a major connection is missing. However, like the head calibration, it relies on having a good underlying DFN model that already replicates most of the major hydraulic structures.

Additionally, geochemical data can be used to calibrate transport apertures and storage affects. These effects are difficult to calibrate using solely time dependent heads measures at tunnel sections.

The Äspö Task 5 modeling had access to a wide range of data and generally the quality of these data was very high. The authors feel that the staged approach was advantageous to allowing a systematic assessment of the modeling success. The area where the data could possibly be improved for future performance assessment of repository sites is related to the choice of locations. Generally, the aim of the model validation is to indicate whether the model correctly replicates the overall response of the groundwater system, while still reproducing more local effects. At Äspö the tunnel was a major influence of the groundwater system. Therefore it is important to ensure that any model used for PA correctly replicates these affects. However, the groundwater and pressure regime immediately adjacent to the tunnel is also influenced by the effect of grouting behind the tunnel lining (e.g. reduced inflows into tunnel and head drop across the tunnel lining). For a regional scale model these effects are difficult to include and do not improve understanding of the overall system response. Therefore, where possible, data and calibration locations should be beyond the zone of influence of these activities.

Chemistry measurements prior to tunnel excavation are a more accurate representation of the in situ chemistry distribution, as the tunnel construction was seen to markedly affect the flow regime. Therefore, more early time measurements are advantageous (although difficult to obtain in practice). For the calibration process, chemistry measurements distributed approximately evenly through time would have enabled the flow velocities to be more accurately calibrated. The use of measurement boreholes both within the main fracture zones, and within the background network, are useful in determining the proportion of flow occurring in the different fracture types.

The current modeling was focused on the heads and chemistry measured over several years. For performance assessment the time scale is much longer, typically thousands of years. The usefulness of this modeling to longer time scales should be considered. Tunnel construction likely involves the largest head changes to occur throughout a repository construction and operation. Hence, a good fit to head and chemistry responses gives confidence in the connectivity and transmissivity of the DFN. Prediction of long-term head distributions is more difficult, as the boundary conditions that should be applied to the model are poorly defined over longer time frames. However, this is a deficiency of future knowledge, rather than a deficiency of the DFN model. Potentially, the greater deficiency is the lack of information on the chemistry during tunnel/repository resaturation. It is important to collect chemistry information over a sufficient area to account for longer-term inflows from more remote locations. These inflows, if of differing density and chemistry, may affect the steady state pressure distribution, and possibly chemical reactions within the rock mass adjacent to the tunnels.

Overall, the authors believe the Äspö Task 5 modeling to have been successful, achieving a good fit to both heads and chemistry. The lessons learned are generally applicable to other potential repository sites.

7. REFERENCES

Barten, W., 1996. PICNIC-I test cases: Fracture Case, Paul Scherrer Institut

Bates, R.L. and Jackson, J.A. (eds) 1980. Glossary of Geology. American Geological Institute. Falls Church, Virginia, 1980.

Bear, J., 1972. Dynamics of Fluids in Porous Media. American Elsevier Publishing Co., New York.

Cave, M.R. and Wragg, J, 1997. Measurement of Trace Element Distributions in Soils and Sediments Using Sequential Leach Data and a Non-specific Extraction System With Chemometric Data Processing. *Analyst*, 122, 1211-1221.

Cave, M.R. and Harmon, K, 1997. Determination of Trace Metal Distributions in the Iron Oxide Phases of Red Bed Sandstones by Chemometric Analysis of Whole Rock and Selective Leachate Data. *Analyst*, 122, 501-502.

Davis, J.C. 1986. Statistics and data analysis in geology, 2nd edition. John Wiley and Sons, New York.

Dershowitz, W., D. Shuttle, M. Uchida, and A. Fox, 1998a. Preliminary 2 km Scale Modeling of Geochemical Pathways Äspö Hard Rock Laboratory, Äspö Sweden, Task 5 SKB International Progress Report IPR-02-36. SKB, Stockholm.

Dershowitz, W., G. Lee, P. LaPointe, and J. Geier, 1998b. FracMan Interactive Discrete Fracture Data Analysis, Geometric Modeling, and Exploration Simulation. User Documentation, Version 2.6. Golder Associates Inc., Seattle.

Dershowitz, W., T. Foxford, E. Sudicky, D. Shuttle, and Th. Eiben, 1998c. PAWorks Pathway Analysis for Discrete Fracture Networks with LTG Solute Transport. User Documentation, Version 1.5. Golder Associates Inc, Seattle.

Laaksoharju, M., Tullborg, E-L., Wikberg, P., Wallin, B. and Smellie, J. 1999a. Hydrogeochemical conditions and evolution at the Äspö HRL, Sweden. Applied Geochemistry, 14, 835-859.

Laaksoharju, M., Skårman, C. and Skårman, E. 1999b. Multivariate Mixing and Mass Balance (M^3) Calculations. A New Tool for Decoding Hydrogeochemical Information. Applied Geochemistry. Vol. 14., p 861-871.

Laaksoharju, M. 2000. M3 calculations and their interpretation within task#5. INTERA Report for Task 5 Participants.(Date delivery 14a)

Metcalfe, R., 1999. Geochemical Uncertainty Influences on Äspö Task 5. In preparation. JNC, Tono, Japan.

Miller, I., G. Lee, and W. Dershowitz, 1998. MAFIC Matrix/Fracture Interaction Code with Heat and Solute Transport. User Documentation, Version 1.6. Golder Associates Inc., Seattle.

Nordstrom, D.K. and Munoz, J.L. 1994. Geochemical thermodyanamics 2nd Edition. Blackwell Scientific Publications, Oxford, England. 493pp.

Rhén, I., 1999. Data Distribution. Reference Äspö Structural Model for Task 5. SKB, Stockholm.

Rhen, I., 1998. Data Distribution 4, Boundary Conditions and Initial Conditions. SKB, Stockholm.

Rhén I (ed), Gustafson G, Stanfors R, Wikberg P, 1997a. Äspö HRL - Geoscientific evaluation 1997/5. Models based on site characterization 1986-1995**.** SKB Technical Report TR-97-06. SKB, Stockholm**.**

Rhén, I., Gustafson, G. Stanfors, R. and Wikberg, P. 1997b. Äspö HRL – Geoscientific evaluation 1997/1995: Models based on site characterization 1986-1995. SKB Technical Report 97-06.

Rhén, I., J. Smellie, and P. Smellie, 1998. Äspö HRL Task Force on modeling of groundwater flow and transport of solutes. Task 5, Performance Measures, Version 1. SKB, Stockholm.

Svensson, U., 1999. Äspö HRL Task Force on Modeling of Groundwater Flow and Transport of Solutes, Data delivery No 11. Pressure and salinity boundary conditions. Task No 5 - Integration of hydrology and chemistry.

Uchida, M., W. Dershowitz, A. Sawada, P. Wallmann, and A. Thomas, 1997. FracMan Discrete Fracture Modeling for the Äspö Tunnel Drawdown Experiment. SKB Äspö Project International Cooperation Report ICR-9703. SKB, Stockholm.

Wikberg, P., 1998. Äspö HRL Task Force on modeling of groundwater flow and transport of solutes. Plan for modeling task # 5: Impact of the tunnel construction on the groundwater system at Äspö. A hydrological-hydrochemical model assessment exercise. SKB Report HRL 98-07. SKB, Stockholm.

Appendix A

Detailed Modeling Results Hydraulic Calibration (Stage 1)

Summary of Simulations:

Model	Summary	Features
H-1	LSF Zones Only	Pipe network created from DFN model of 22 deterministic fracture zones. Baltic Sea skin applied to reduce T in upper 10m to a multiple of 0.01 times the original value.
H-2	add Mystery Feature	Two fractures added to explain mystery response
H-3	LSF plus background fractures	First iteration with 22704 background fractures
H-4	Background fractures plus mystery feature	Model includes two fractures to explain mystery response
H-5	Background fractures plus update conditioned features	161 deterministic fractures with T=10^-6 added at head calibration sections in order to ensure that all calibration sections are connected
H-6	Background Fractures, Mystery Feature, Conditioned Fractures	Model includes two fractures to explain mystery response
H-7	Adjust Conditioned Fractures	Number of deterministic fractures at head calibration sections reduced to 69 and transmissivity of remaining fractures decreased to 10^-8 to reduce excessive drawdowns
H-8	Remove Baltic Skin	Baltic Sea skin removed in order to reduce excessive drawdowns

Heads predicted from Models H-8

Model H-8 provided the best head predictions for the calibration carried out using only hydrogeological data. The resulting head predictions are presented in the following pages.

Borehole Section KAS02

KAS02 MA21

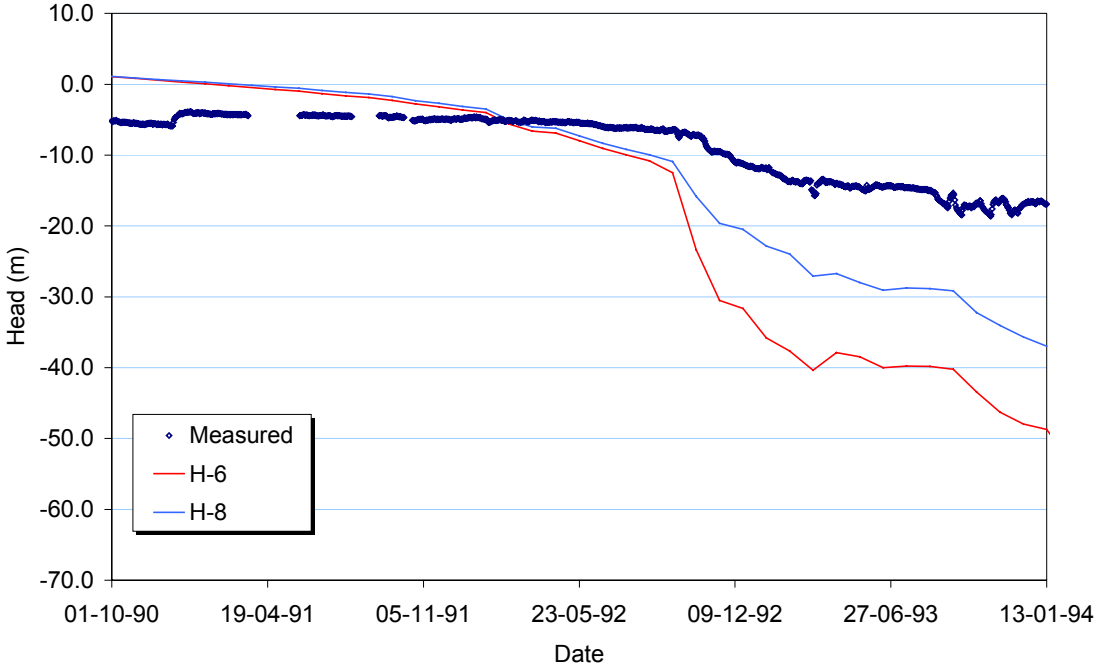

KAS02 MA22

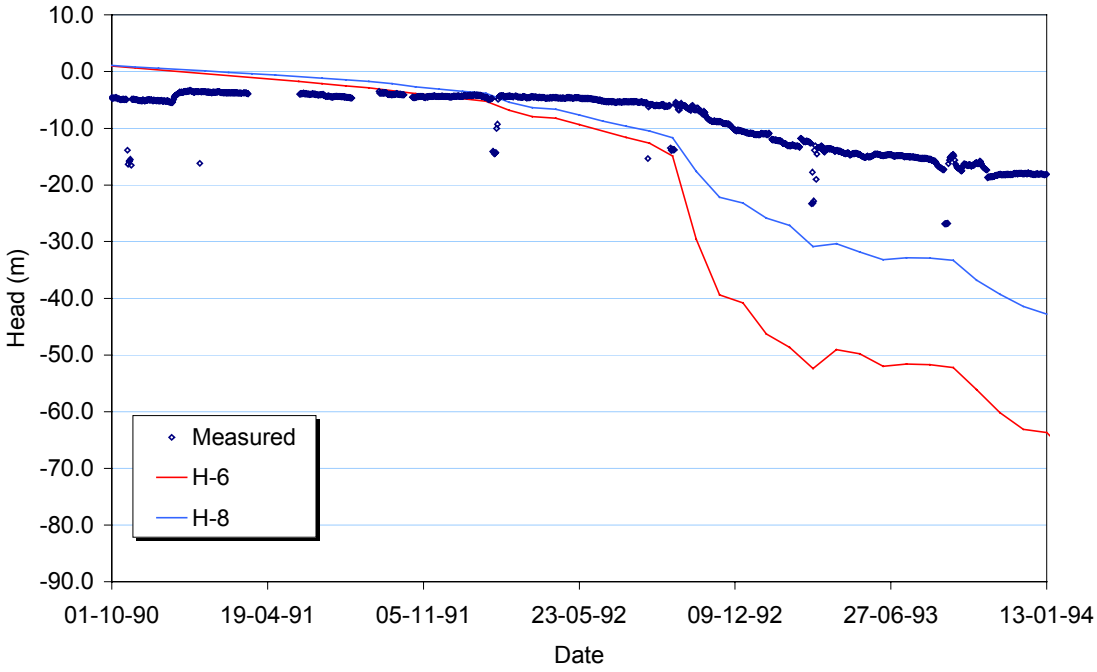

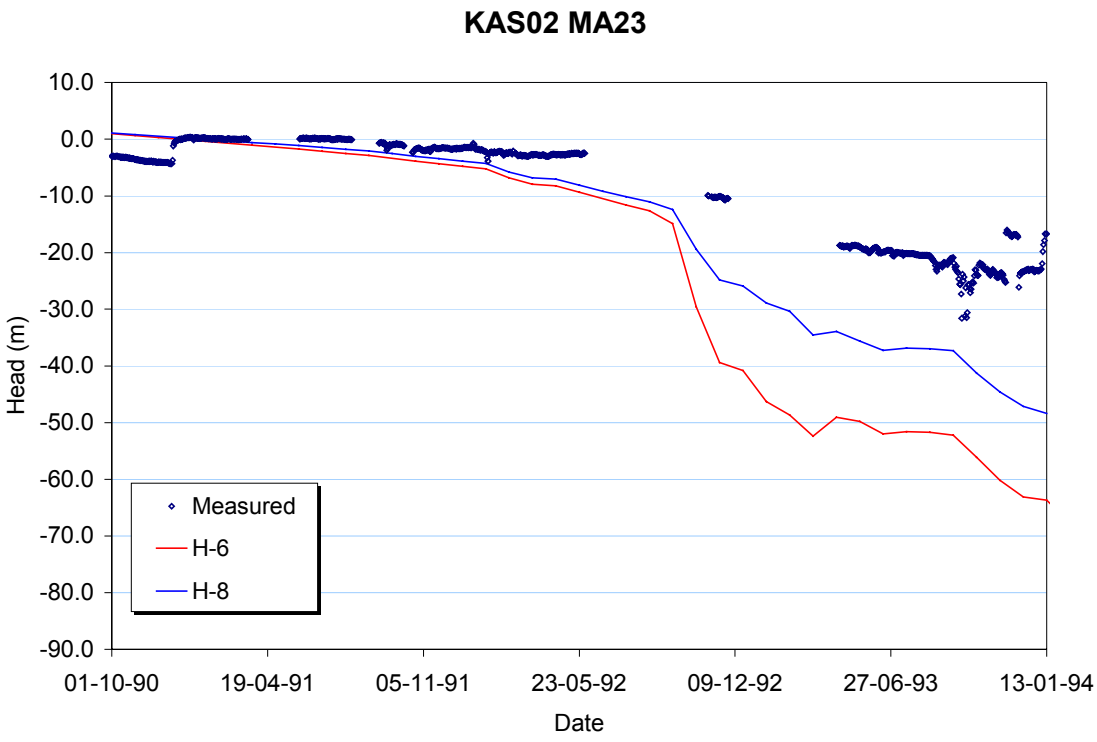
KAS02 MA23
10.0
0.0
-10.0
-20.0
-30.0
-40.0
-50.0
-60.0
-70.0
-80.0
-90.0
Head (m)
Measured
H-6
H-8
01-10-90
19-04-91
05-11-91
23-05-92
09-12-92
27-06-93
13-01-94
Date

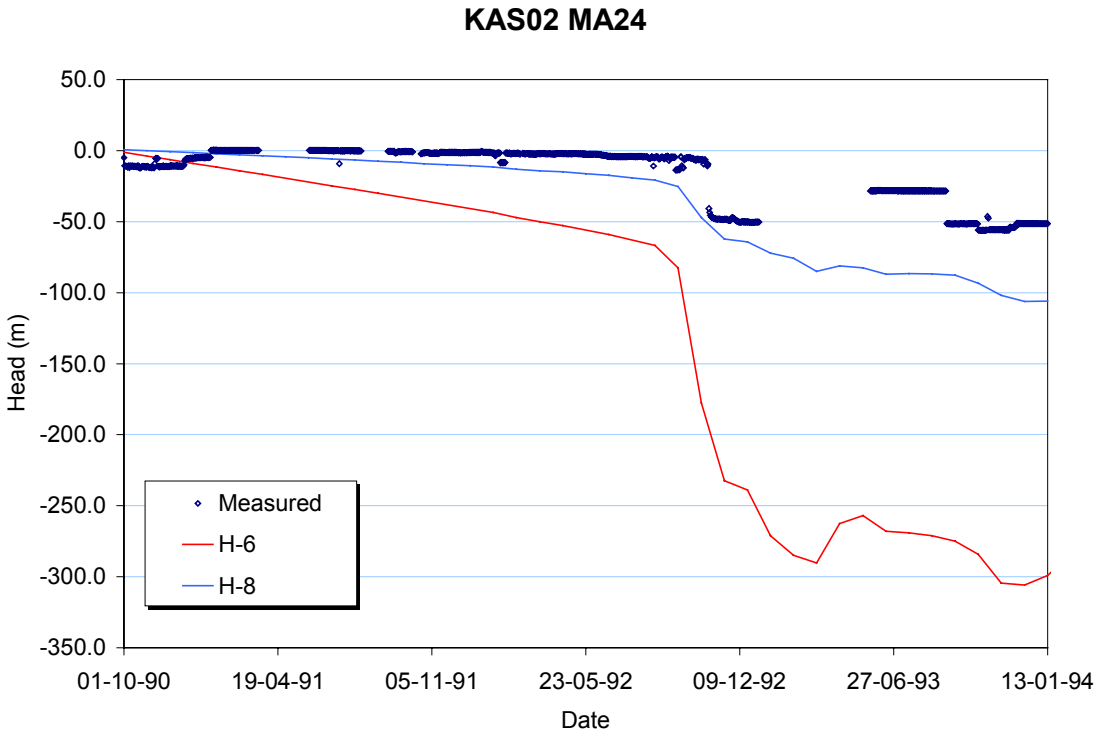
KAS02 MA24
50.0
0.0
-50.0
-100.0
-150.0
-200.0
-250.0
-300.0
-350.0
Head (m)
Measured
H-6
H-8
01-10-90
19-04-91
05-11-91
23-05-92
09-12-92
27-06-93
13-01-94
Date

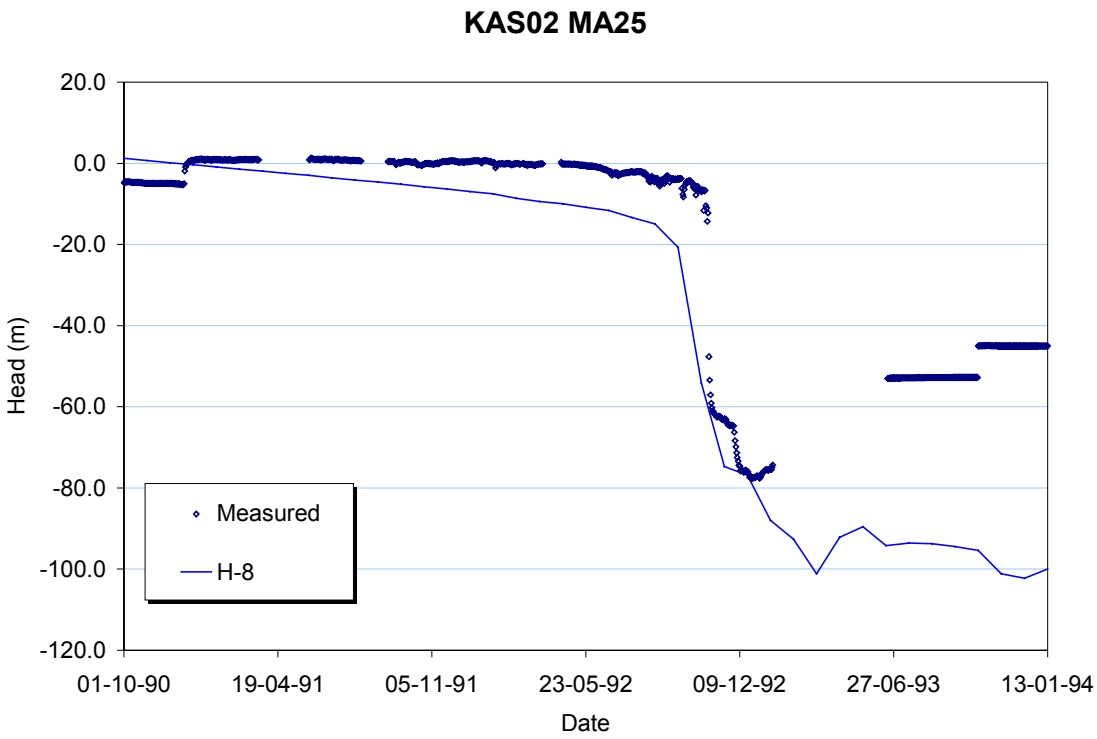
KAS02 MA25
20.0
0.0
-20.0
-40.0
-60.0
-80.0
-100.0
-120.0
Head (m)
Measured
H-8
01-10-90
19-04-91
05-11-91
23-05-92
09-12-92
27-06-93
13-01-94
Date

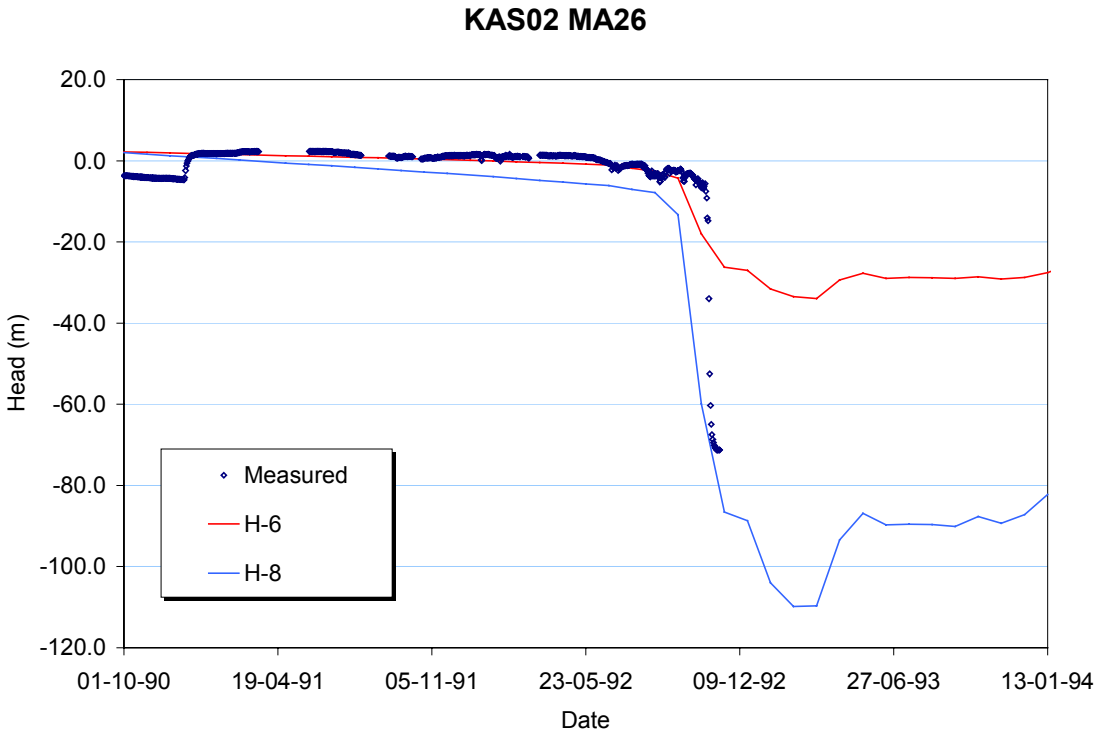
KAS02 MA26
20.0
0.0
-20.0
-40.0
-60.0
-80.0
-100.0
-120.0
Head (m)
Measured
H-6
H-8
01-10-90
19-04-91
05-11-91
23-05-92
09-12-92
27-06-93
13-01-94
Date

Borehole Section KAS03

KAS03 MA31

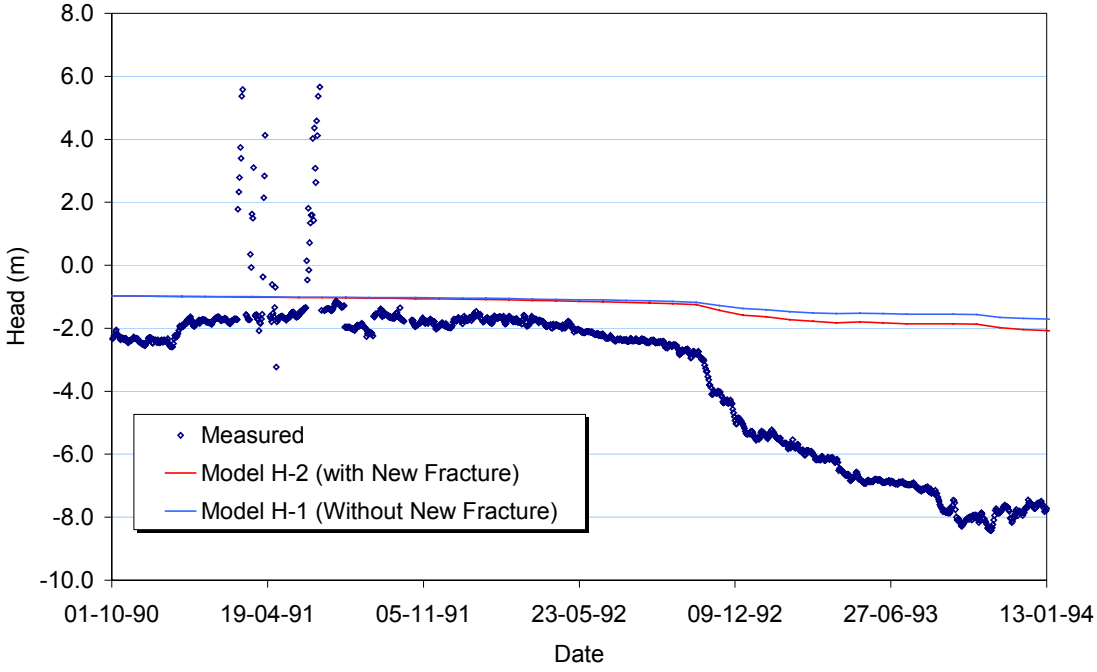

KAS03 MA32

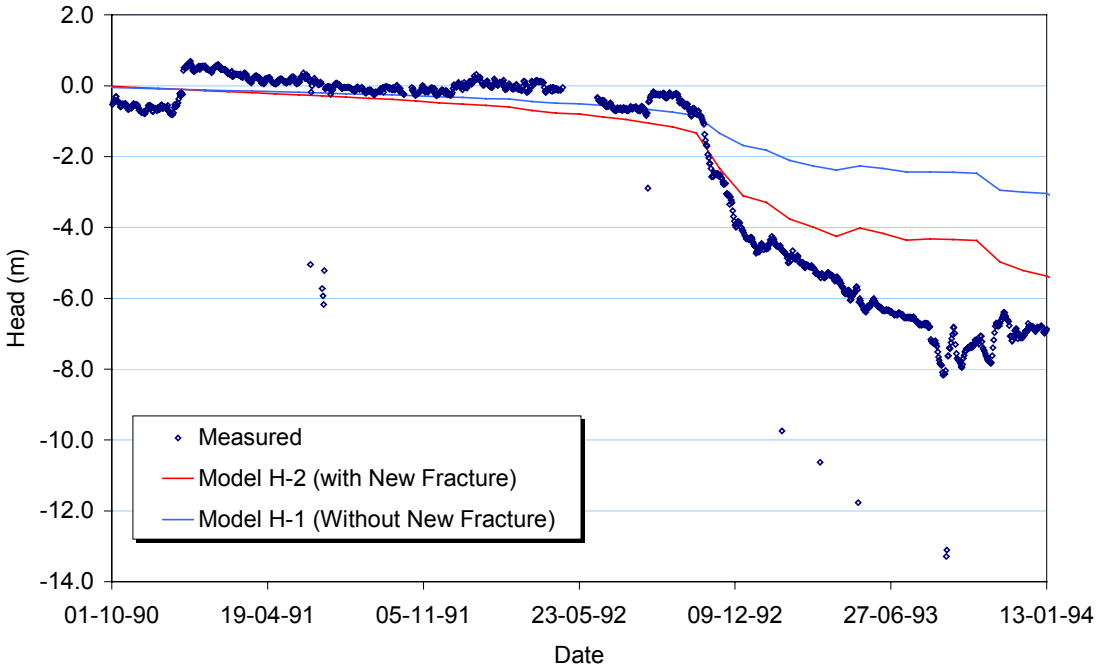

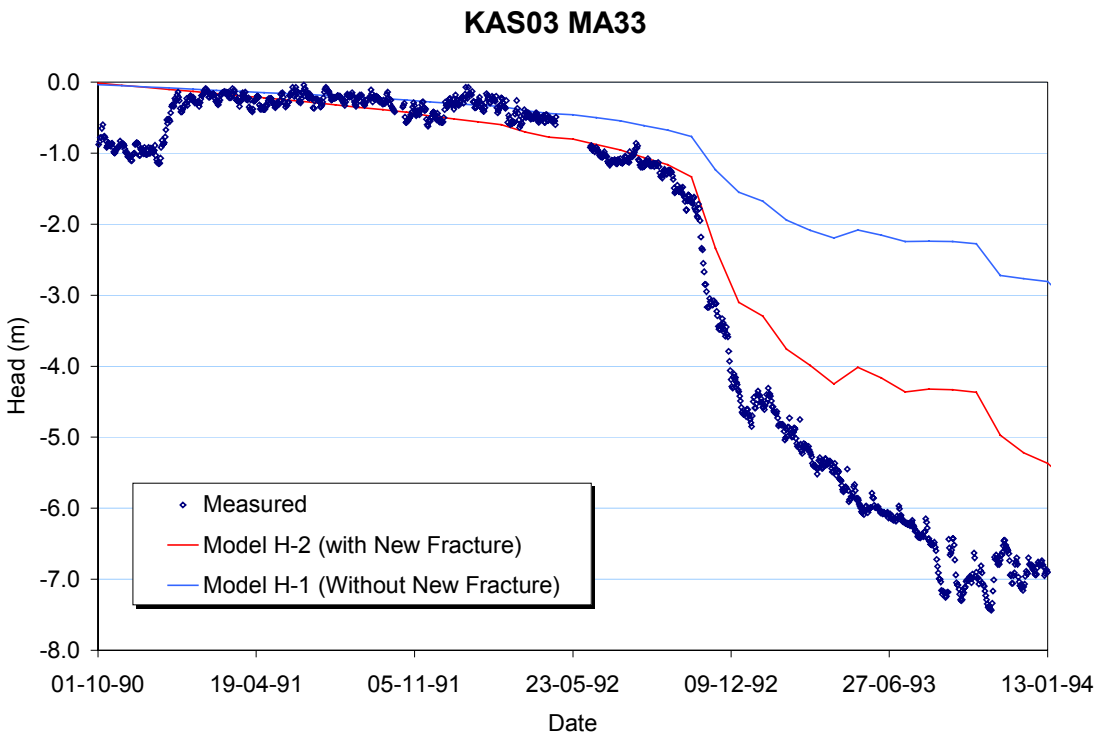
KAS03 MA33
0.0
-1.0
-2.0
-3.0
-4.0
-5.0
-6.0
-7.0
-8.0
Head (m)
Measured
Model H-2 (with New Fracture)
Model H-1 (Without New Fracture)
01-10-90
19-04-91
05-11-91
23-05-92
09-12-92
27-06-93
13-01-94
Date

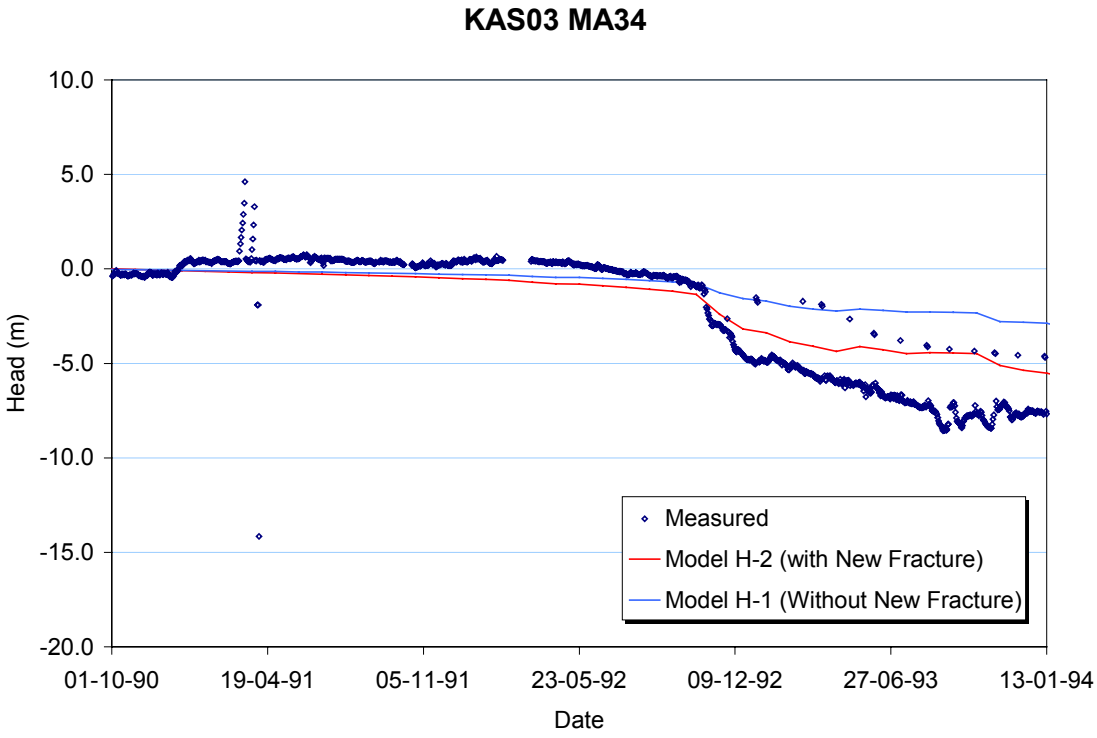
KAS03 MA34
10.0
5.0
0.0
-5.0
-10.0
-15.0
-20.0
Head (m)
Measured
Model H-2 (with New Fracture)
Model H-1 (Without New Fracture)
01-10-90
19-04-91
05-11-91
23-05-92
09-12-92
27-06-93
13-01-94
Date

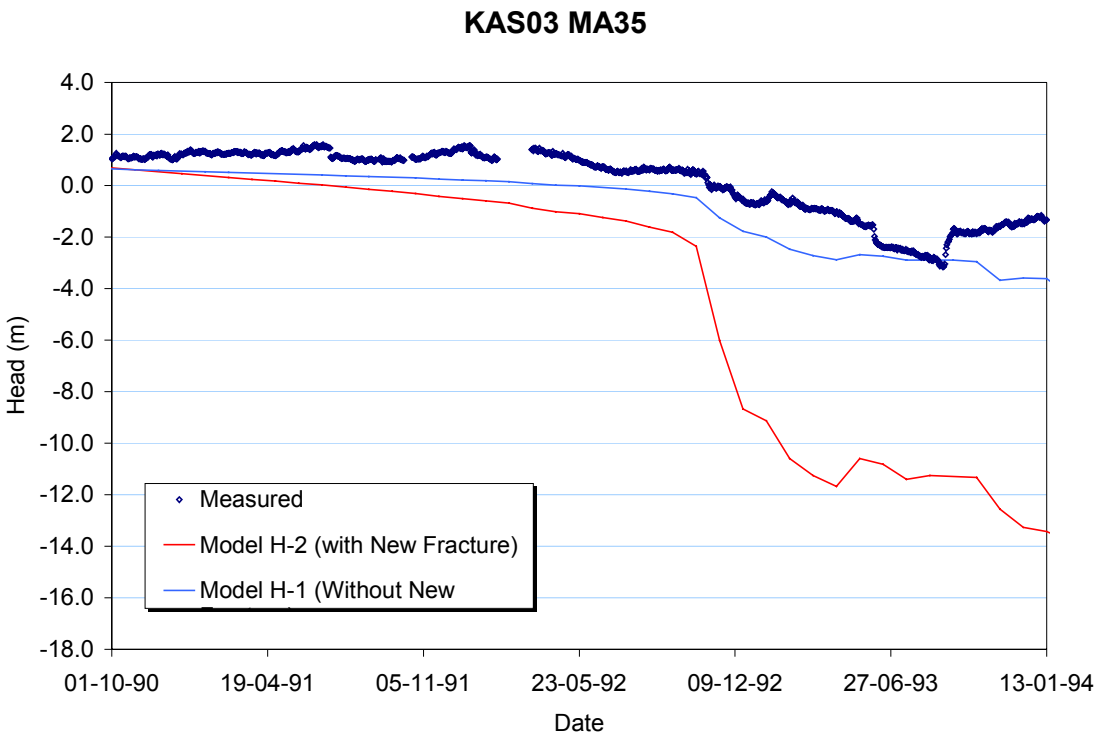
KAS03 MA35
4.0
2.0
0.0
-2.0
-4.0
-6.0
-8.0
-10.0
-12.0
-14.0
-16.0
-18.0
Head (m)
Measured
Model H-2 (with New Fracture)
Model H-1 (Without New
01-10-90
19-04-91
05-11-91
23-05-92
09-12-92
27-06-93
13-01-94
Date

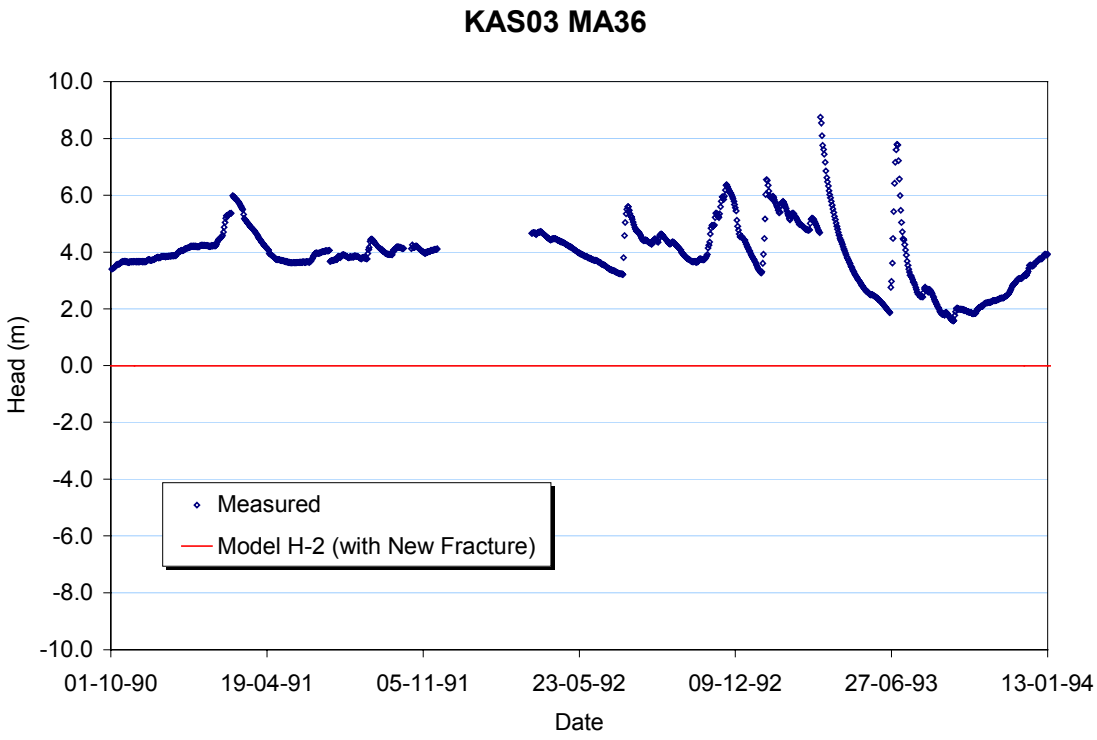
KAS03 MA36
10.0
8.0
6.0
4.0
2.0
0.0
-2.0
-4.0
-6.0
-8.0
-10.0
Head (m)
Measured
Model H-2 (with New Fracture)
01-10-90
19-04-91
05-11-91
23-05-92
09-12-92
27-06-93
13-01-94
Date

Borehole Section KAS06

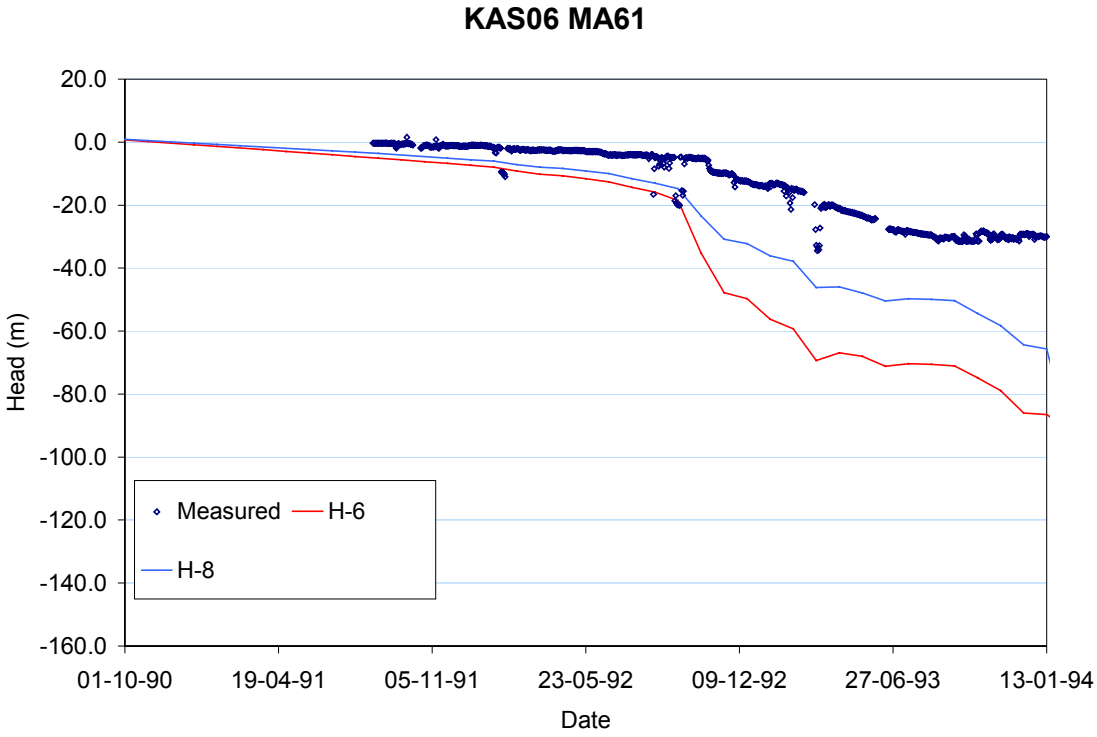

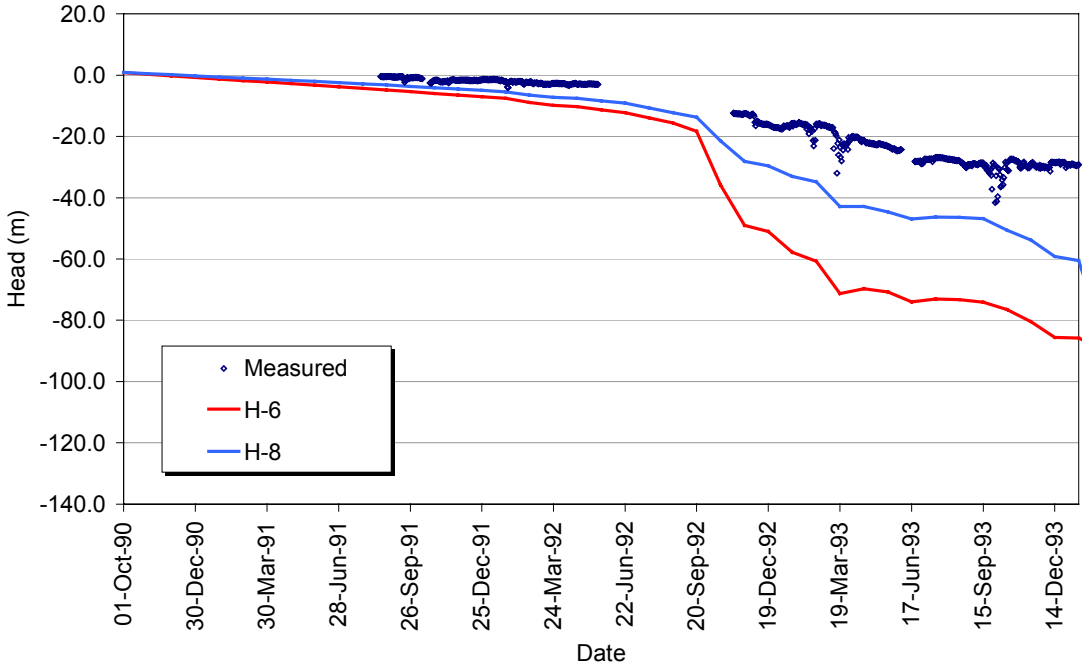

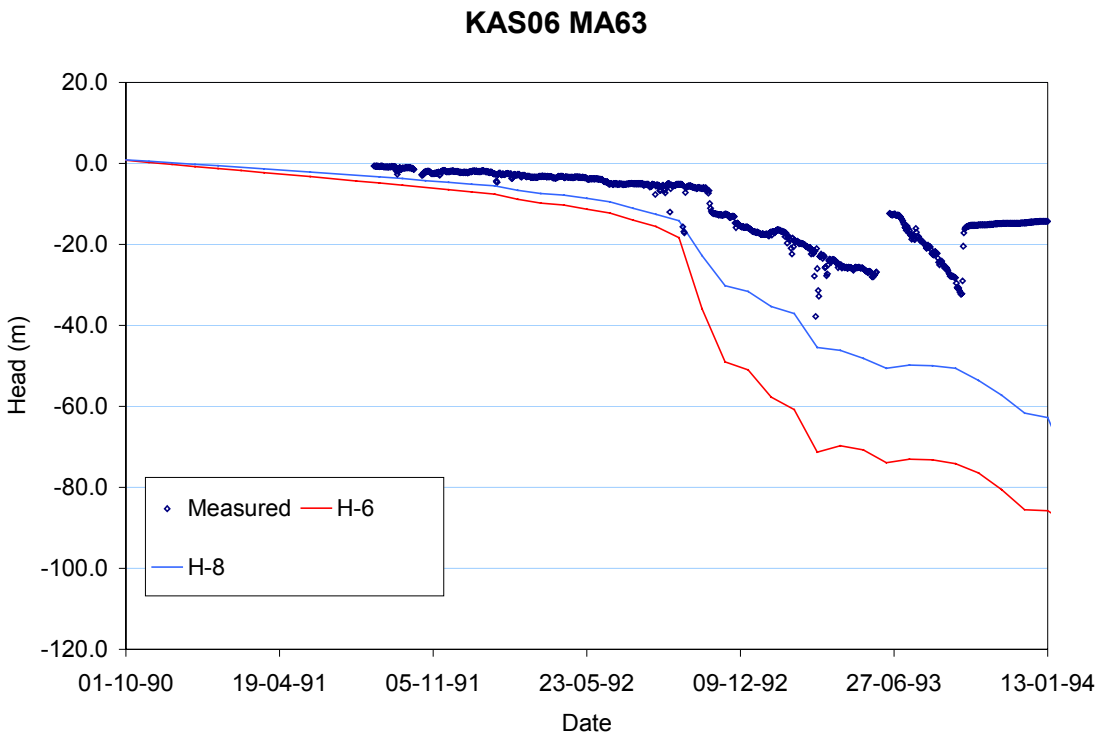
KAS06 MA63
20.0
0.0
-20.0
-40.0
-60.0
-80.0
-100.0
-120.0
Head (m)
Measured
H-6
H-8
01-10-90
19-04-91
05-11-91
23-05-92
09-12-92
27-06-93
13-01-94
Date

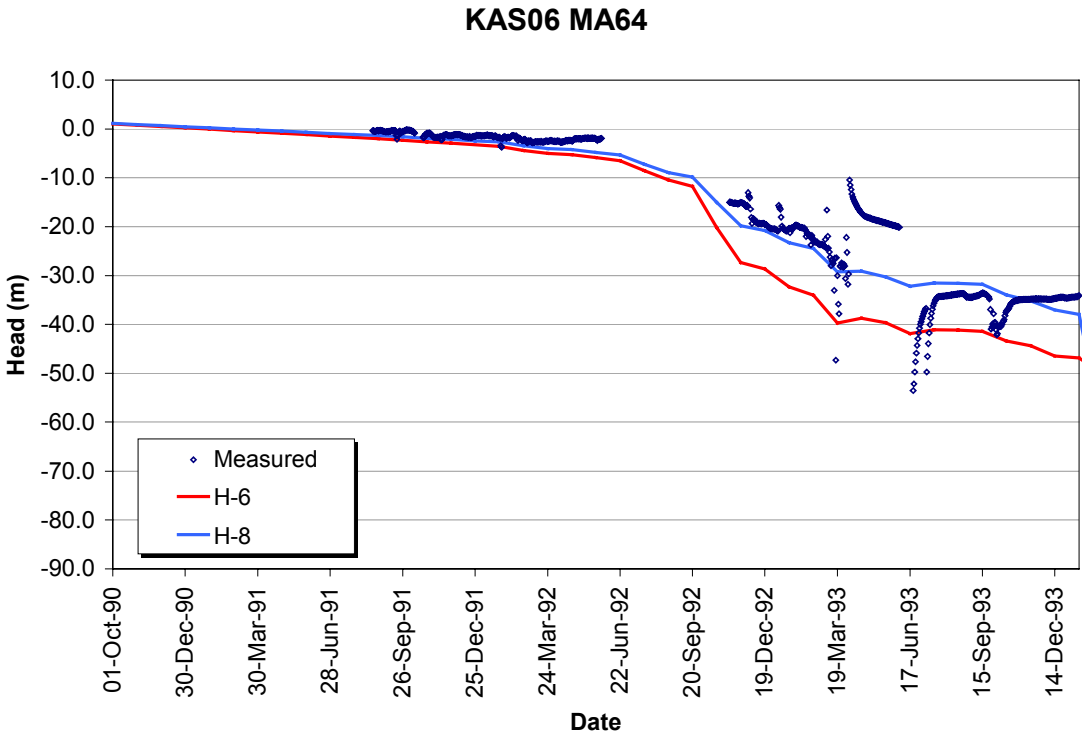
KAS06 MA64
10.0
0.0
-10.0
-20.0
-30.0
-40.0
-50.0
-60.0
-70.0
-80.0
-90.0
Head (m)
Measured
H-6
H-8
01-Oct-90
30-Dec-90
30-Mar-91
28-Jun-91
26-Sep-91
25-Dec-91
24-Mar-92
22-Jun-92
20-Sep-92
19-Dec-92
19-Mar-93
17-Jun-93
15-Sep-93
14-Dec-93
Date

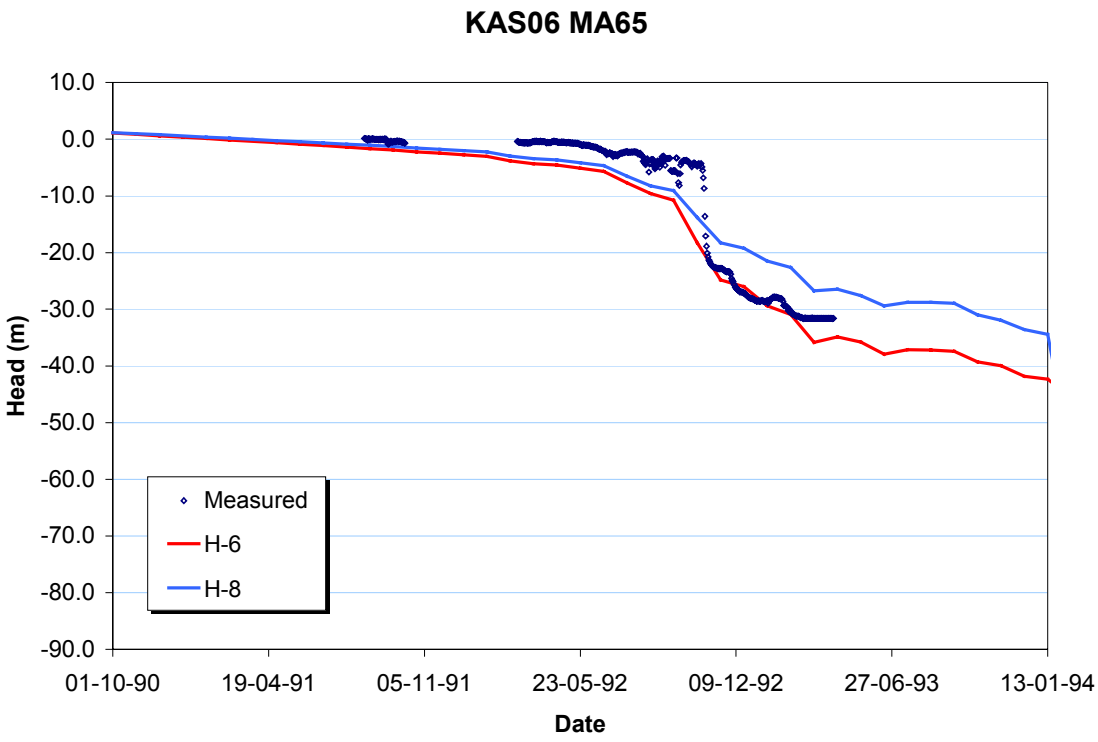
KAS06 MA65
10.0
0.0
-10.0
-20.0
-30.0
-40.0
-50.0
-60.0
-70.0
-80.0
-90.0
Head (m)
Measured
H-6
H-8
01-10-90
19-04-91
05-11-91
23-05-92
09-12-92
27-06-93
13-01-94
Date

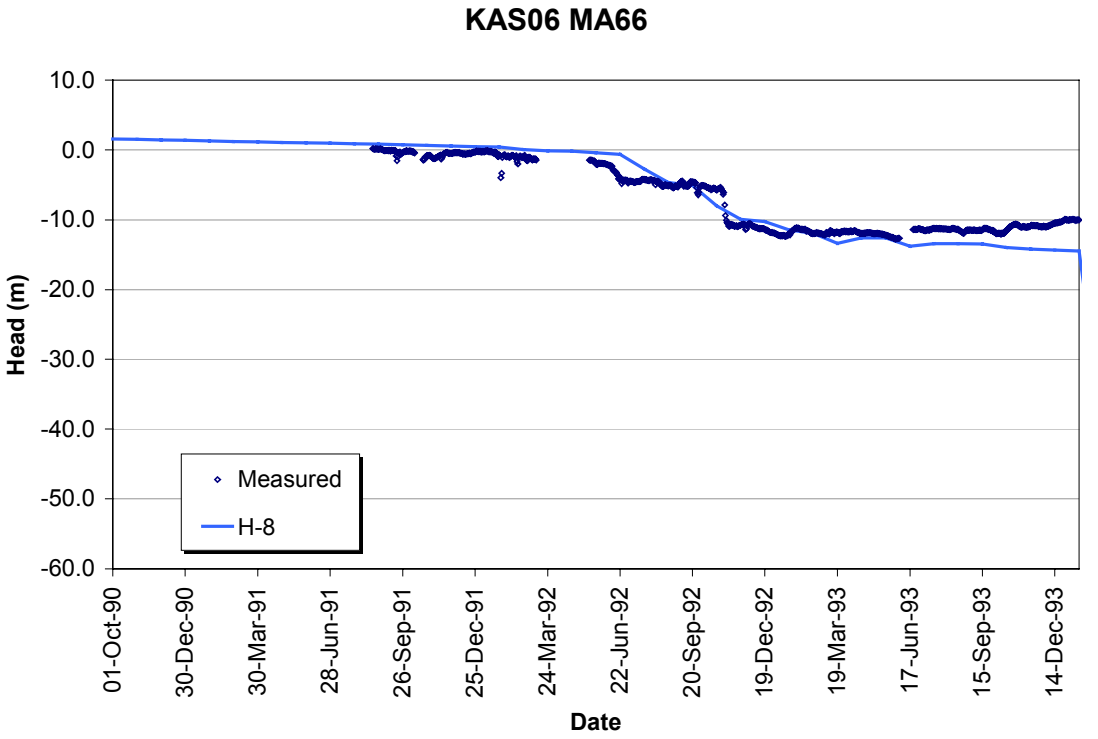
KAS06 MA66
10.0
0.0
-10.0
-20.0
-30.0
-40.0
-50.0
-60.0
Head (m)
Measured
H-8
01-Oct-90
30-Dec-90
30-Mar-91
28-Jun-91
26-Sep-91
25-Dec-91
24-Mar-92
22-Jun-92
20-Sep-92
19-Dec-92
19-Mar-93
17-Jun-93
15-Sep-93
14-Dec-93
Date

Borehole Section KAS08

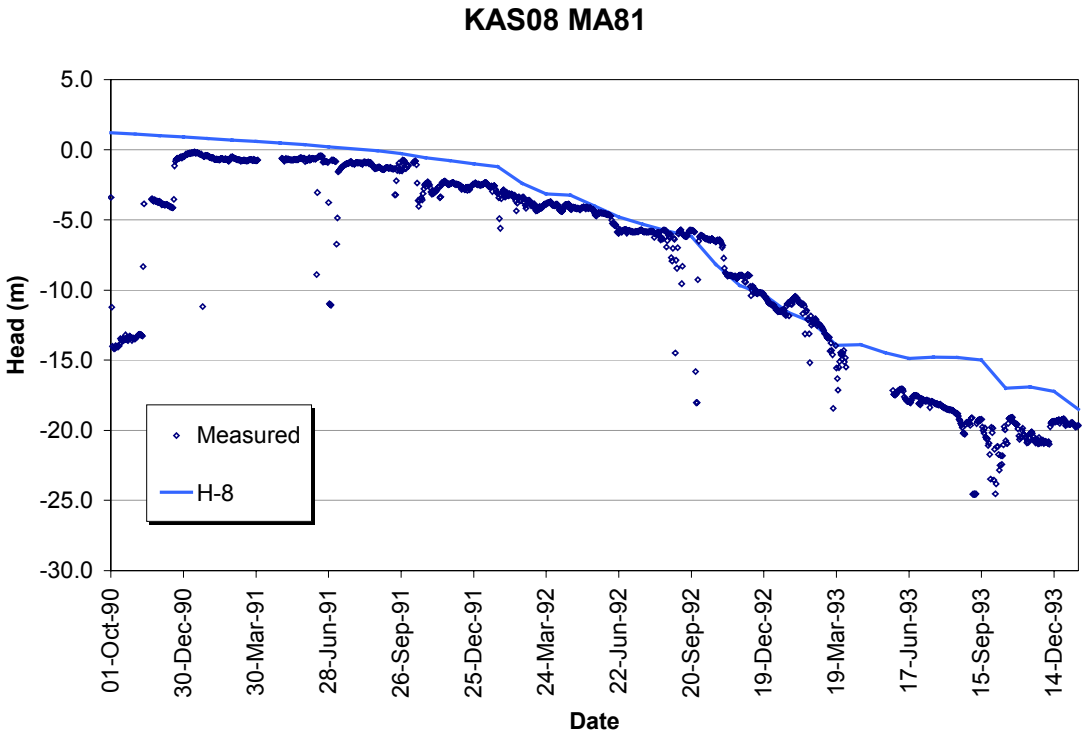

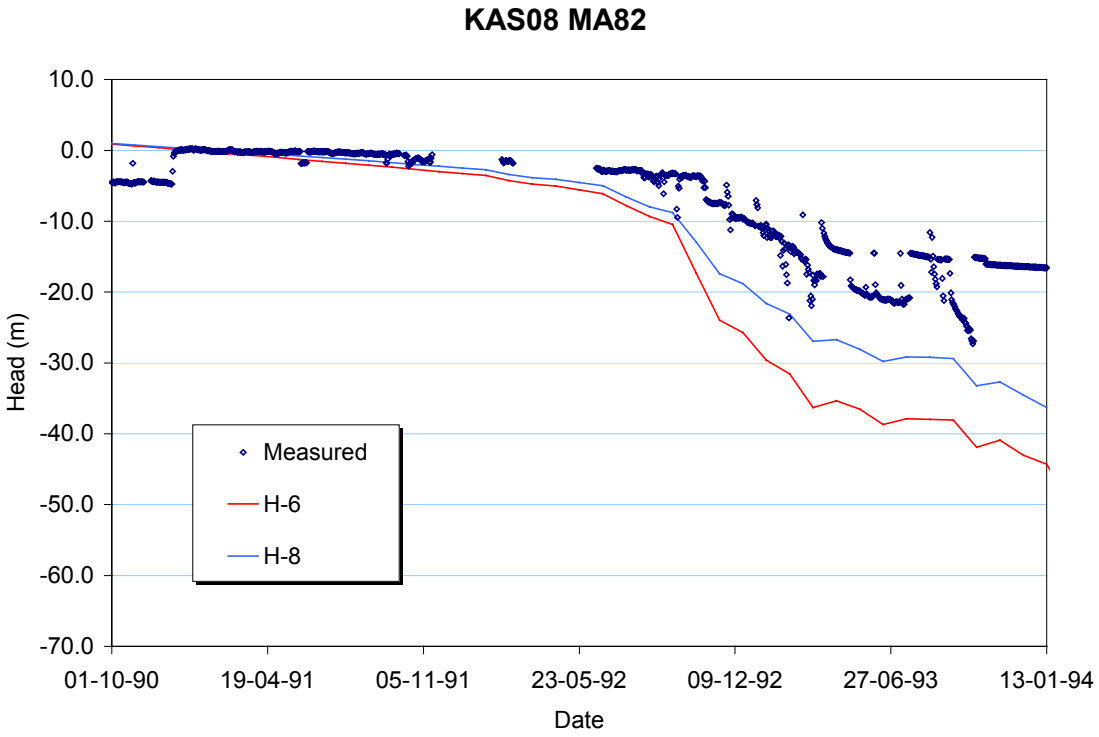

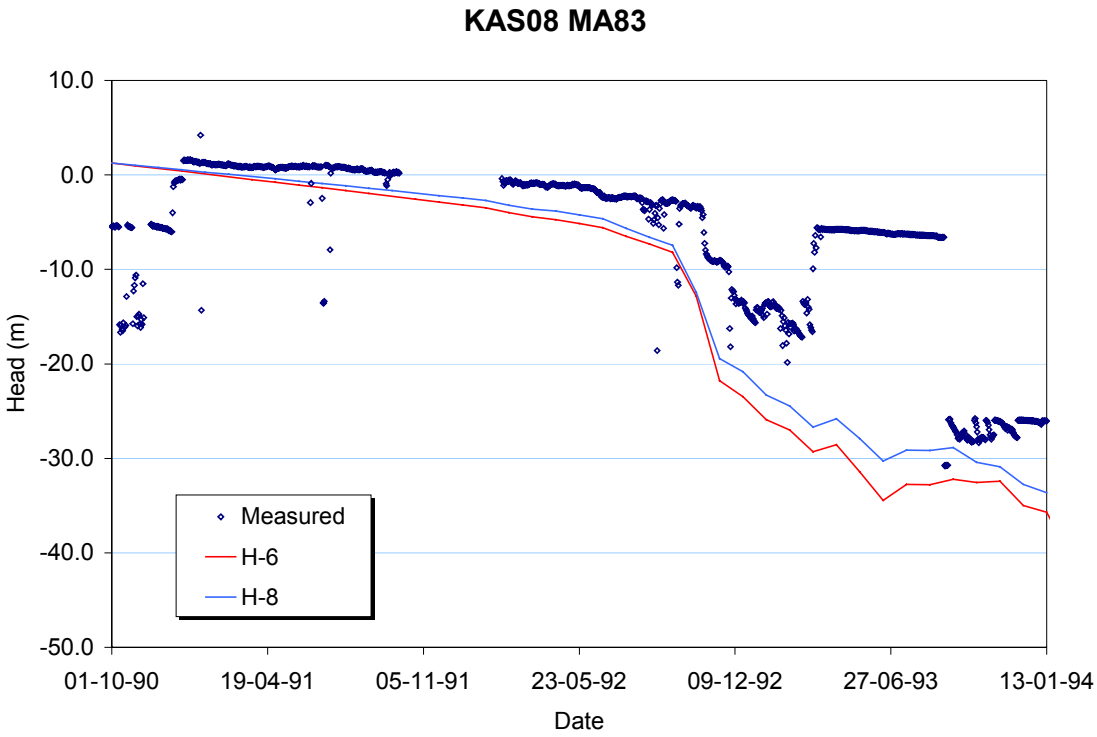
KAS08 MA83
10.0
0.0
-10.0
-20.0
-30.0
-40.0
-50.0
Head (m)
Measured
H-6
H-8
01-10-90
19-04-91
05-11-91
23-05-92
09-12-92
27-06-93
13-01-94
Date

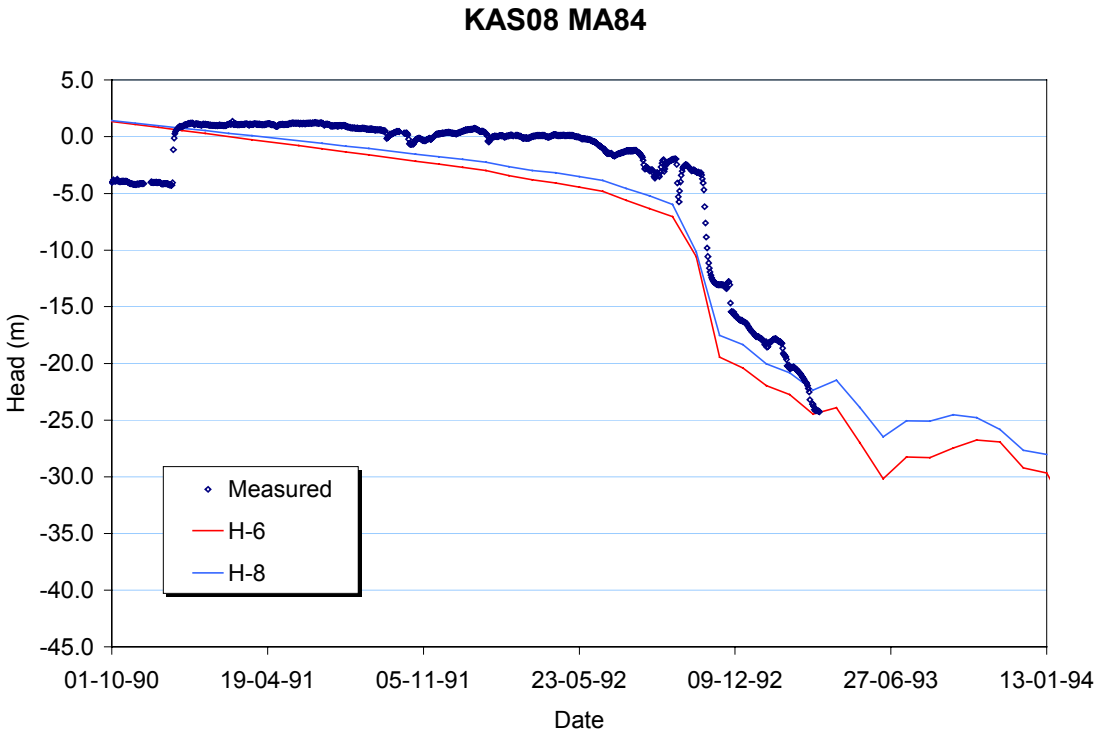
KAS08 MA84
5.0
0.0
-5.0
-10.0
-15.0
-20.0
-25.0
-30.0
-35.0
-40.0
-45.0
Head (m)
Measured
H-6
H-8
01-10-90
19-04-91
05-11-91
23-05-92
09-12-92
27-06-93
13-01-94
Date

Borehole Section KAS14

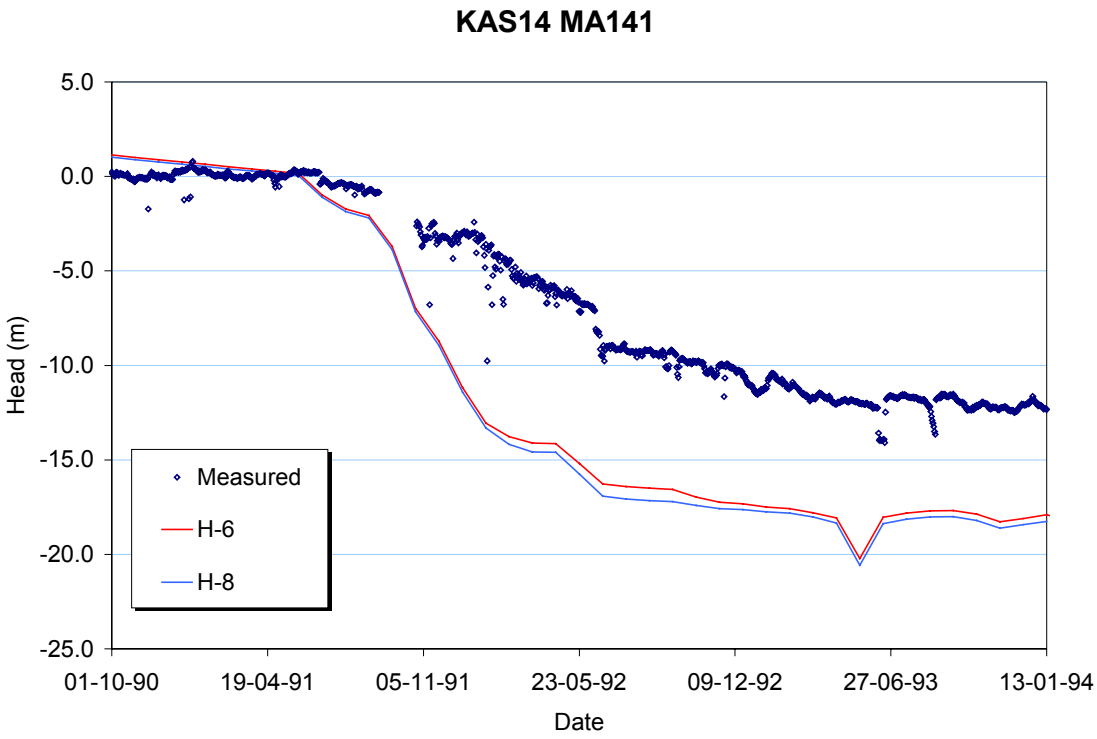

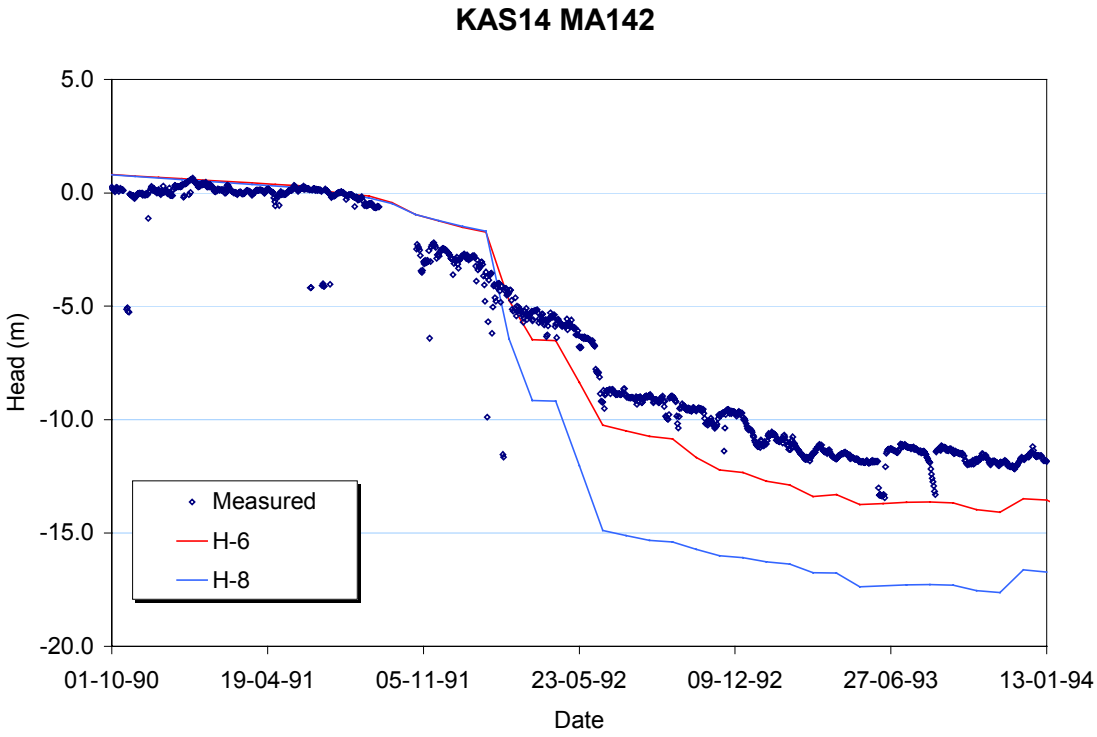

KAS14 MA143

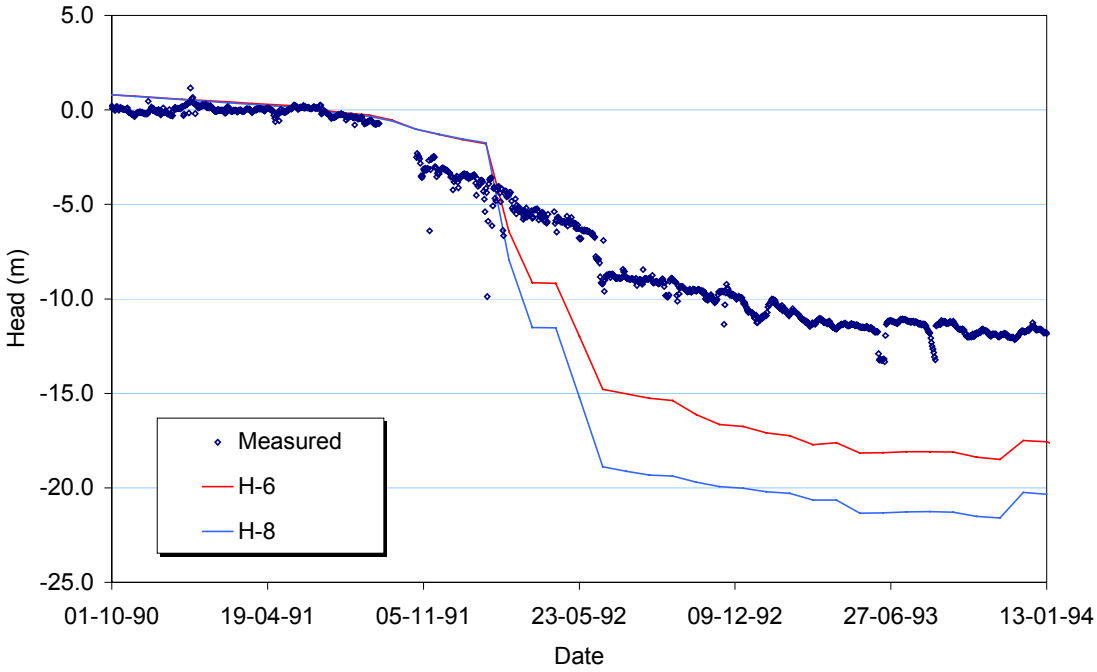

KAS14 MA144

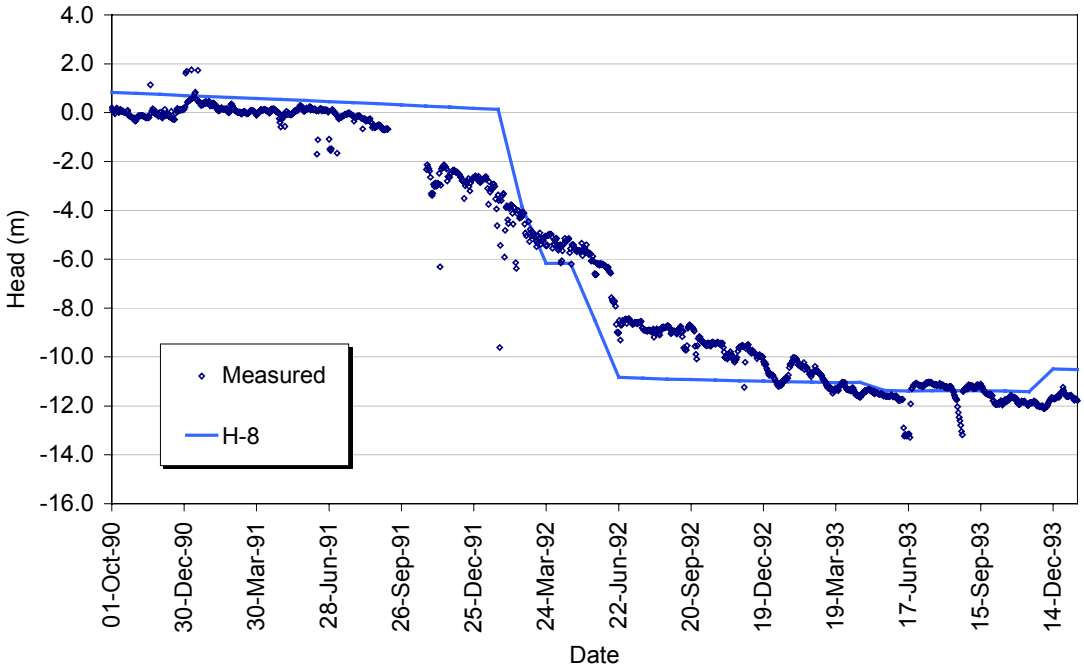

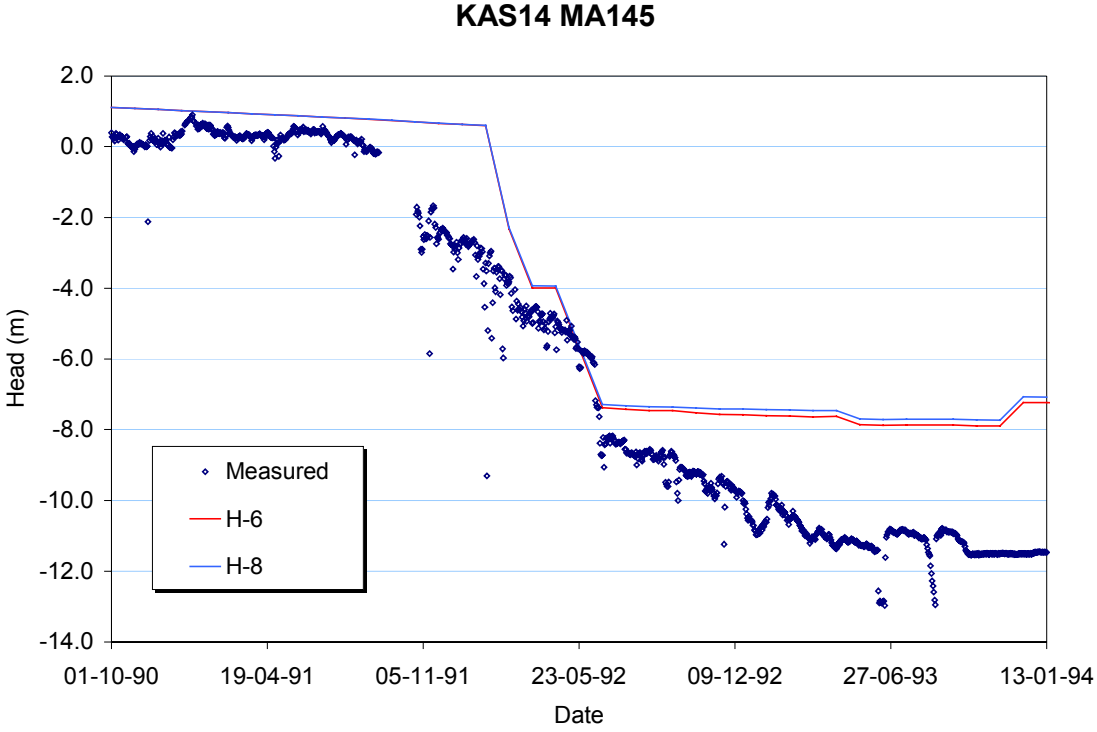
KAS14 MA145
2.0
0.0
-2.0
-4.0
-6.0
-8.0
-10.0
-12.0
-14.0
Head (m)
Measured
H-6
H-8
01-10-90
19-04-91
05-11-91
23-05-92
09-12-92
27-06-93
13-01-94
Date

Appendix B

Detailed Modeling Results Geochemical Calibration (Stage 2)

Summary of Simulations:

Model	Summary	Features
H-8	No geochemical calibration	Final hydrogeological model.
G-1	H-8 model with connection added to north, modify boundary condition on Äspö Island	Connection to north added in order to draw in more Glacial-rich water to deeper control points. Äspö Island boundary condition changed from no flow to 30 mm/year infiltration. No low transmissivity skin over Baltic.
G-2	Baltic skin, change zone transmissivity	Baltic Skin of T=0.01x reintroduced, All fractures (incl. deterministic frac. zones) T= 3x
G-3	update of G-2	G-2, with all fractures (incl. deterministic frac. zones)T=1.6x
G-4	update of G-3	G-3, with transport aperture increased to 5x to increase travel time

Chemistry from Models H-8 and G-4

Model H-8 provided the best head predictions for the calibration carried out using only hydrogeological data. A selection of the resulting geochemistry predictions for this initial fit, and the subsequent geochemical calibrations, are presented in this appendix.

Model H-8

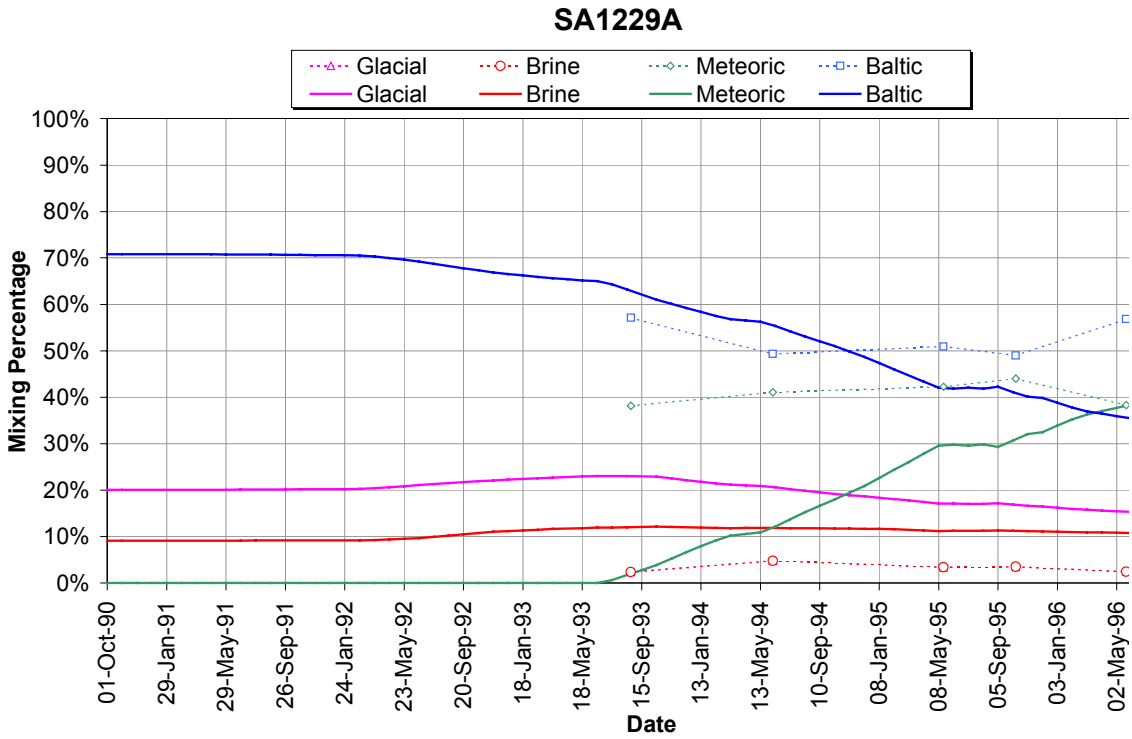
SA1229A
Glacial
Brine
Meteoric
Baltic
Mixing Percentage
100%
90%
80%
70%
60%
50%
40%
30%
20%
10%
0%
01-Oct-90
29-Jan-91
29-May-91
26-Sep-91
24-Jan-92
23-May-92
20-Sep-92
18-Jan-93
18-May-93
15-Sep-93
13-Jan-94
13-May-94
10-Sep-94
08-Jan-95
08-May-95
05-Sep-95
03-Jan-96
02-May-96
Date

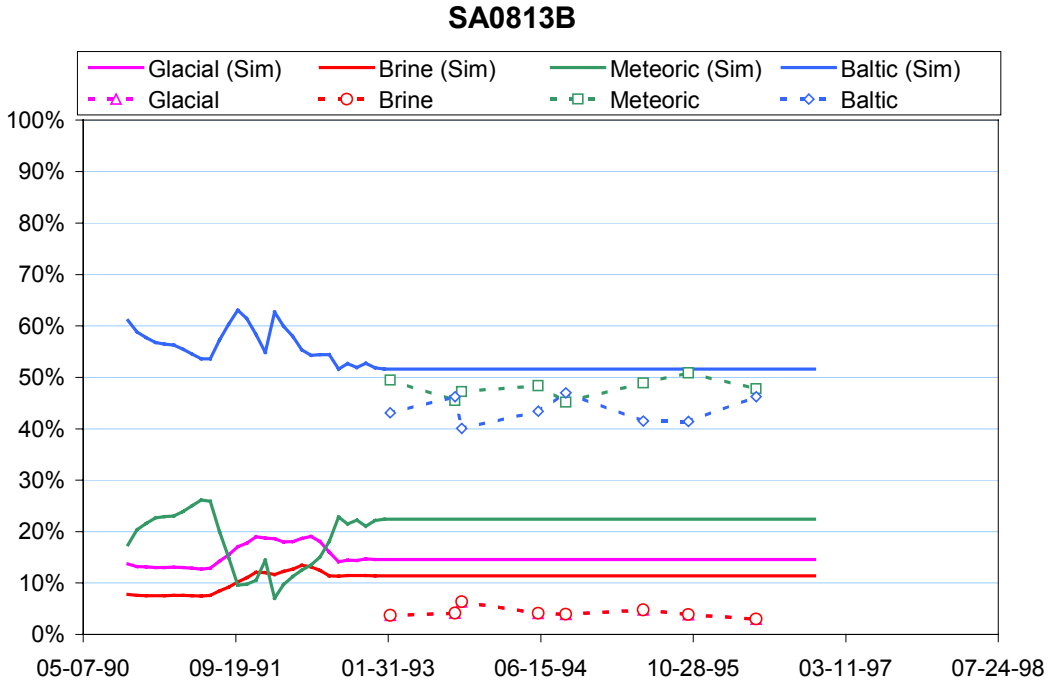
SA0813B
Glacial (Sim)
Brine (Sim)
Meteoric (Sim)
Baltic (Sim)
Glacial
Brine
Meteoric
Baltic
100%
90%
80%
70%
60%
50%
40%
30%
20%
10%
0%
05-07-90
09-19-91
01-31-93
06-15-94
10-28-95
03-11-97
07-24-98

KA1755A

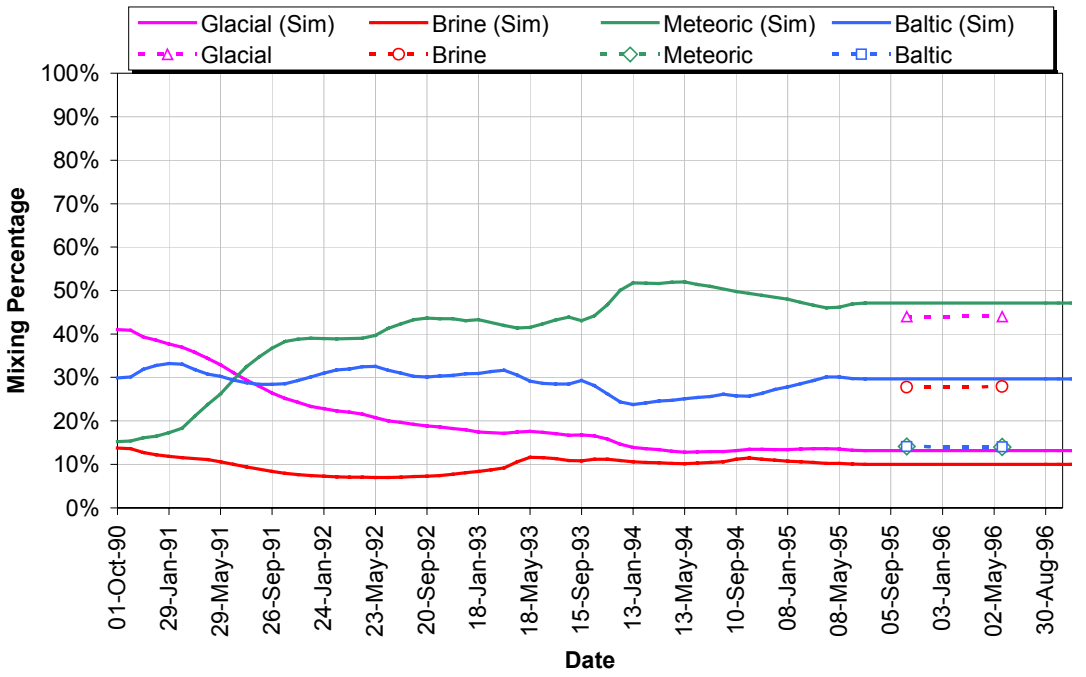

SA2074A

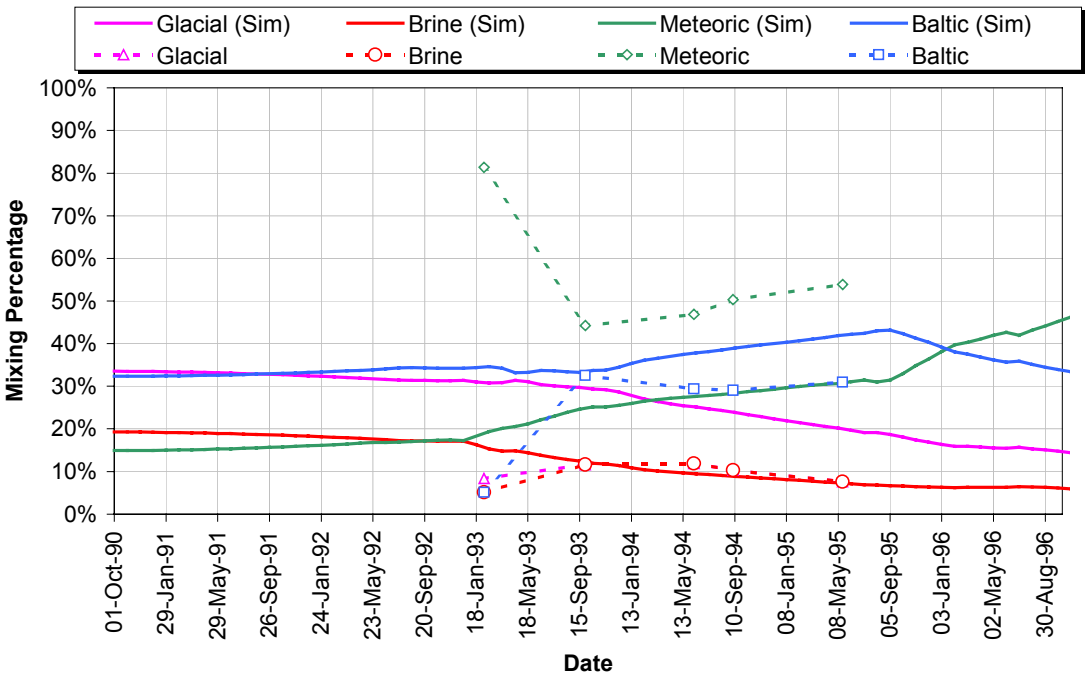

SA2783A

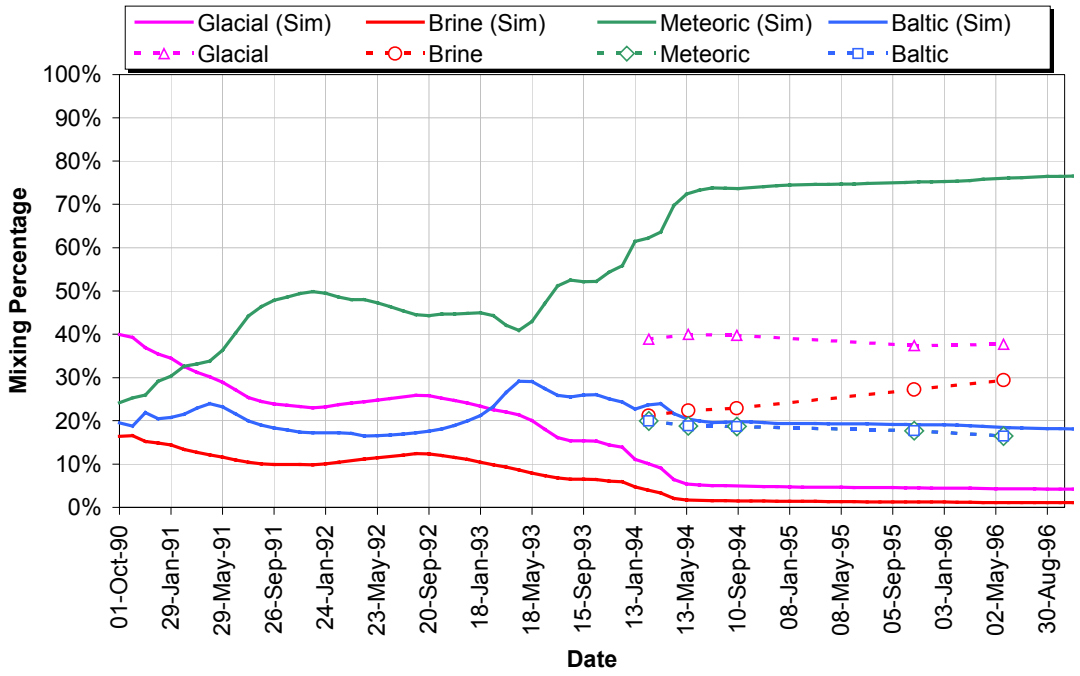

KAS03b

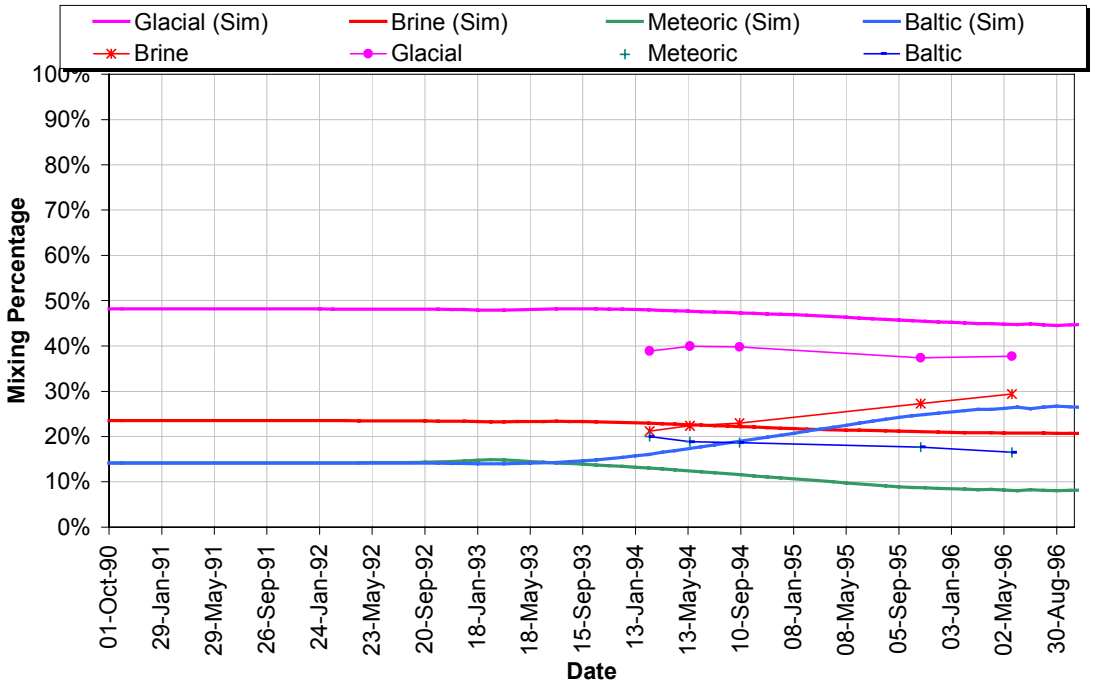

Model G-4

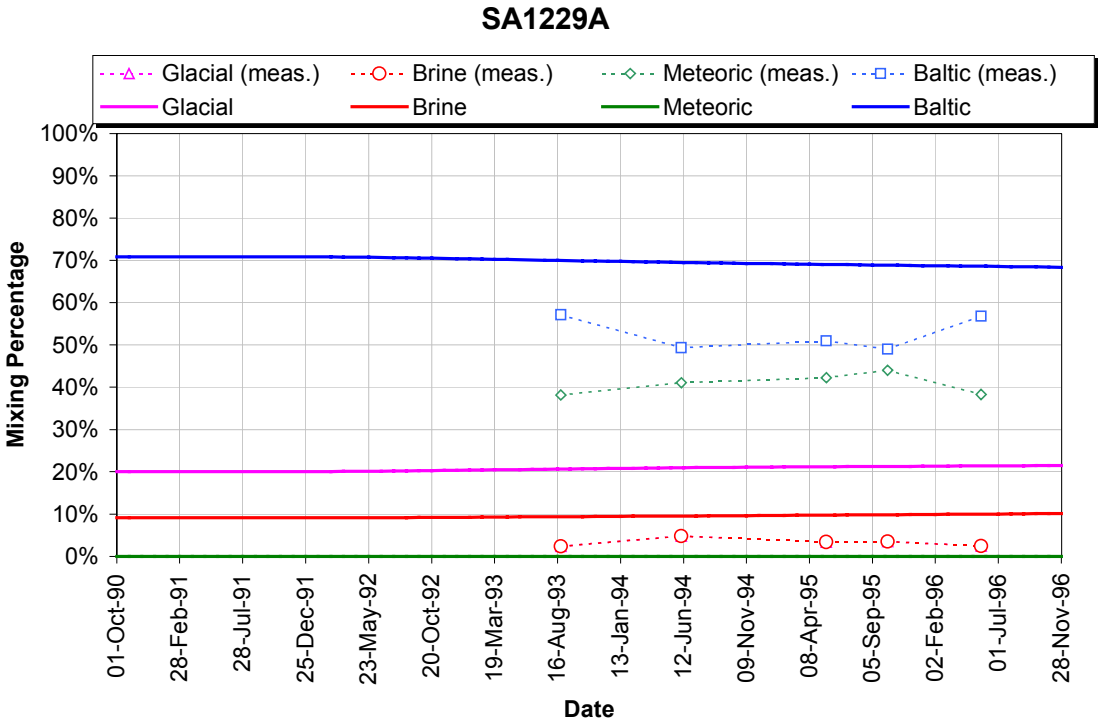
SA1229A
Glacial (meas.)
Brine (meas.)
Meteoric (meas.)
Baltic (meas.)
Glacial
Brine
Meteoric
Baltic
Mixing Percentage
100%
90%
80%
70%
60%
50%
40%
30%
20%
10%
0%
01-Oct-90
28-Feb-91
28-Jul-91
25-Dec-91
23-May-92
20-Oct-92
19-Mar-93
16-Aug-93
13-Jan-94
12-Jun-94
09-Nov-94
08-Apr-95
05-Sep-95
02-Feb-96
01-Jul-96
28-Nov-96
Date

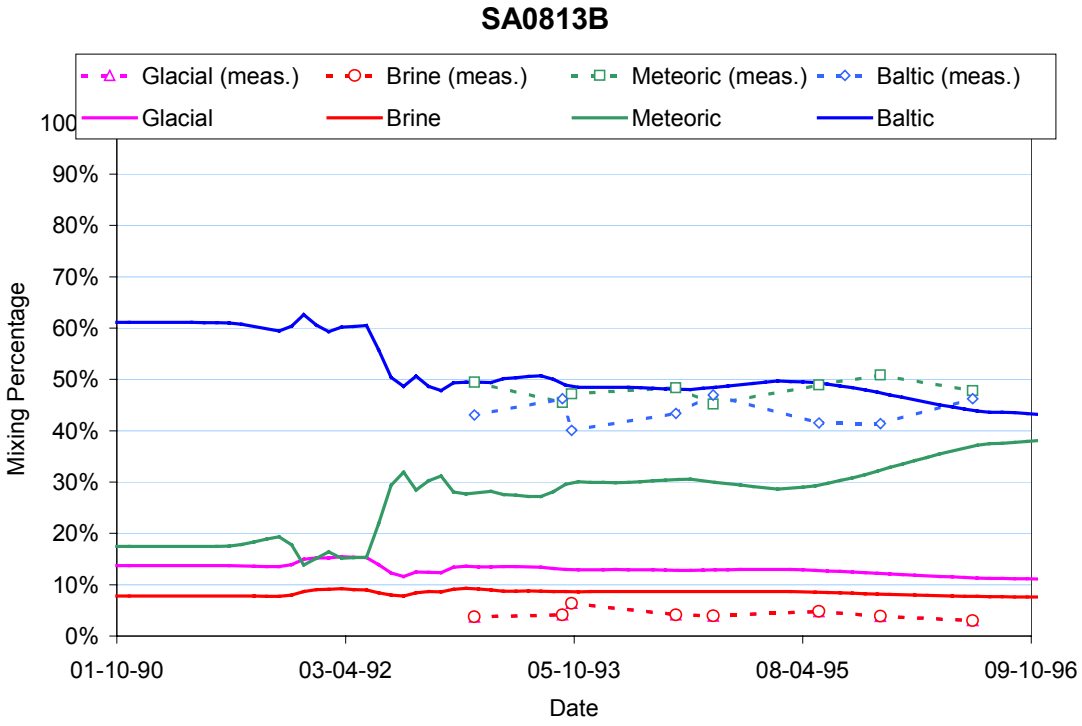
SA0813B
Glacial (meas.)
Brine (meas.)
Meteoric (meas.)
Baltic (meas.)
Glacial
Brine
Meteoric
Baltic
Mixing Percentage
100
90%
80%
70%
60%
50%
40%
30%
20%
10%
0%
01-10-90
03-04-92
05-10-93
08-04-95
09-10-96
Date

KA1755A

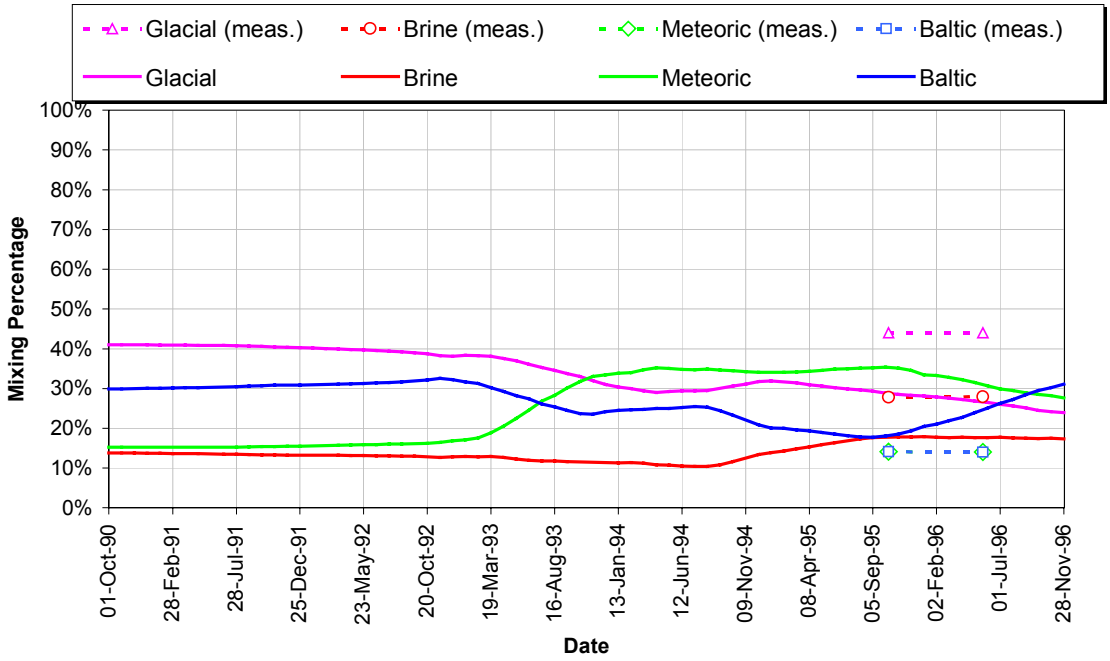

SA2074A

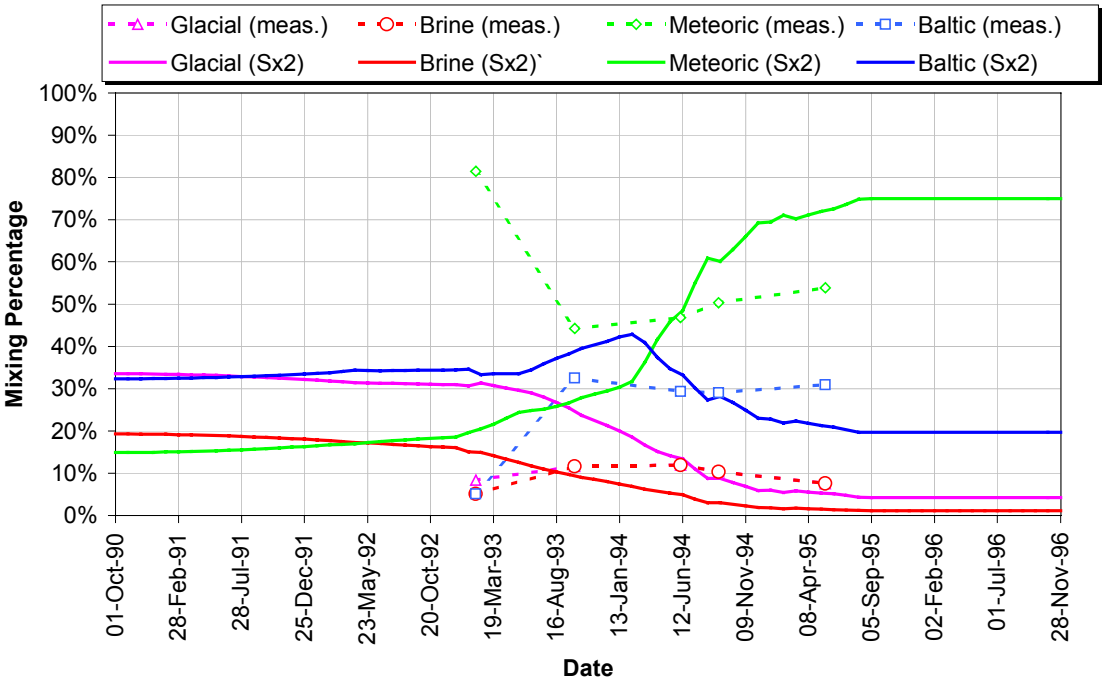

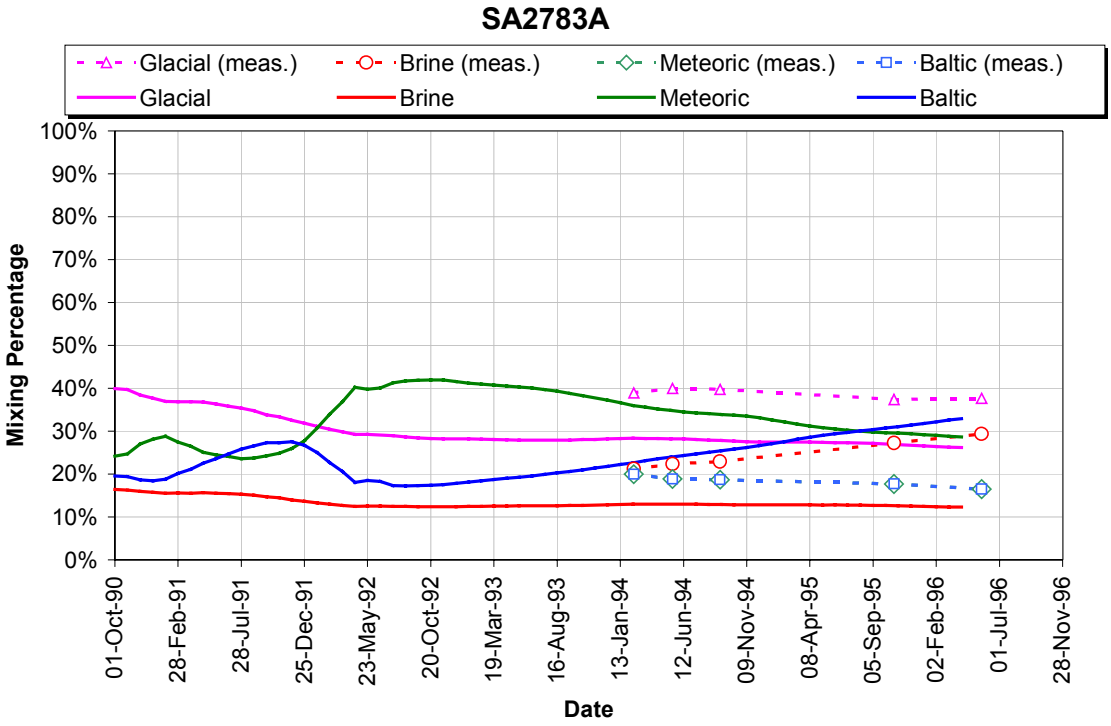
SA2783A
Glacial (meas.)
Brine (meas.)
Meteoric (meas.)
Baltic (meas.)
Glacial
Brine
Meteoric
Baltic
Mixing Percentage
100%
90%
80%
70%
60%
50%
40%
30%
20%
10%
0%
01-Oct-90
28-Feb-91
28-Jul-91
25-Dec-91
23-May-92
20-Oct-92
19-Mar-93
16-Aug-93
13-Jan-94
12-Jun-94
09-Nov-94
08-Apr-95
05-Sep-95
02-Feb-96
01-Jul-96
28-Nov-96
Date

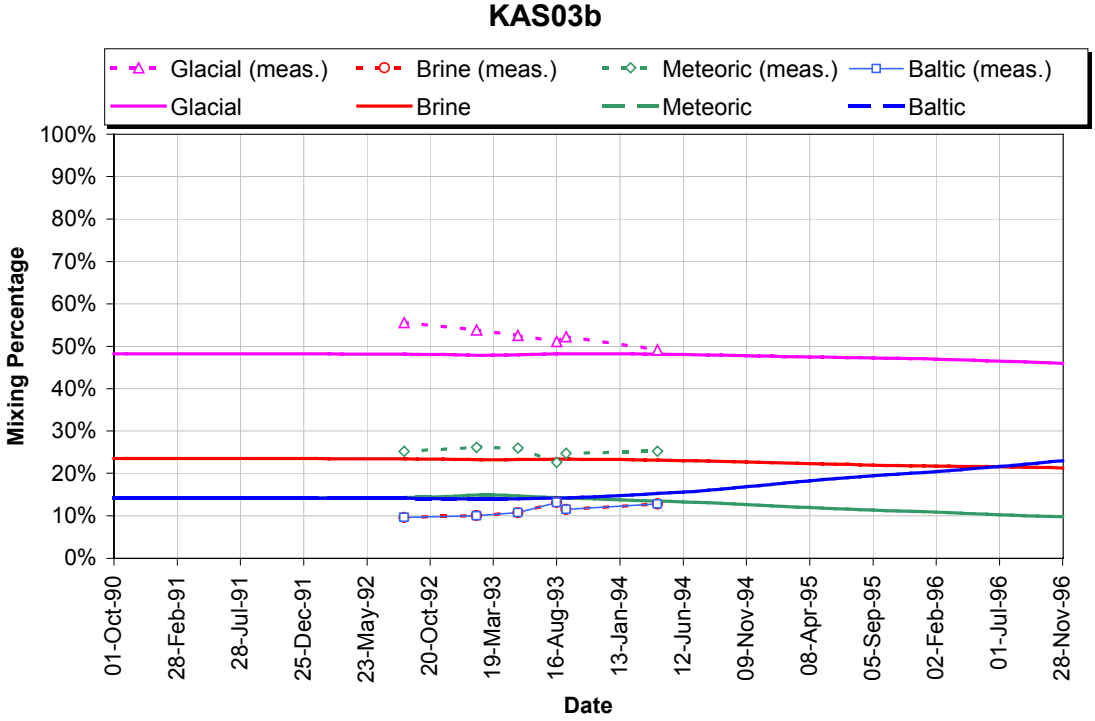
KAS03b
Glacial (meas.)
Brine (meas.)
Meteoric (meas.)
Baltic (meas.)
Glacial
Brine
Meteoric
Baltic
Mixing Percentage
100%
90%
80%
70%
60%
50%
40%
30%
20%
10%
0%
01-Oct-90
28-Feb-91
28-Jul-91
25-Dec-91
23-May-92
20-Oct-92
19-Mar-93
16-Aug-93
13-Jan-94
12-Jun-94
09-Nov-94
08-Apr-95
05-Sep-95
02-Feb-96
01-Jul-96
28-Nov-96
Date

Appendix C

Detailed Modeling Results Additional Sensitivity Calibration (Stage 3)

Summary of Simulations:

This appendix of the report summarizes the chemistry end member results obtained for two related chemistry models:

- Model 2, the 7 chemical component model described in Section 5.1.9 and Table 2 of the main report.
- The end-members (Brine, Baltic, Glacial and Meteoric) computed from the 7 chemical component model.
- The storativity corrected end-members (Brine, Baltic, Glacial and Meteoric) computed from the 7 chemical component model.

Model 2, 7 chemical components

SA0813B

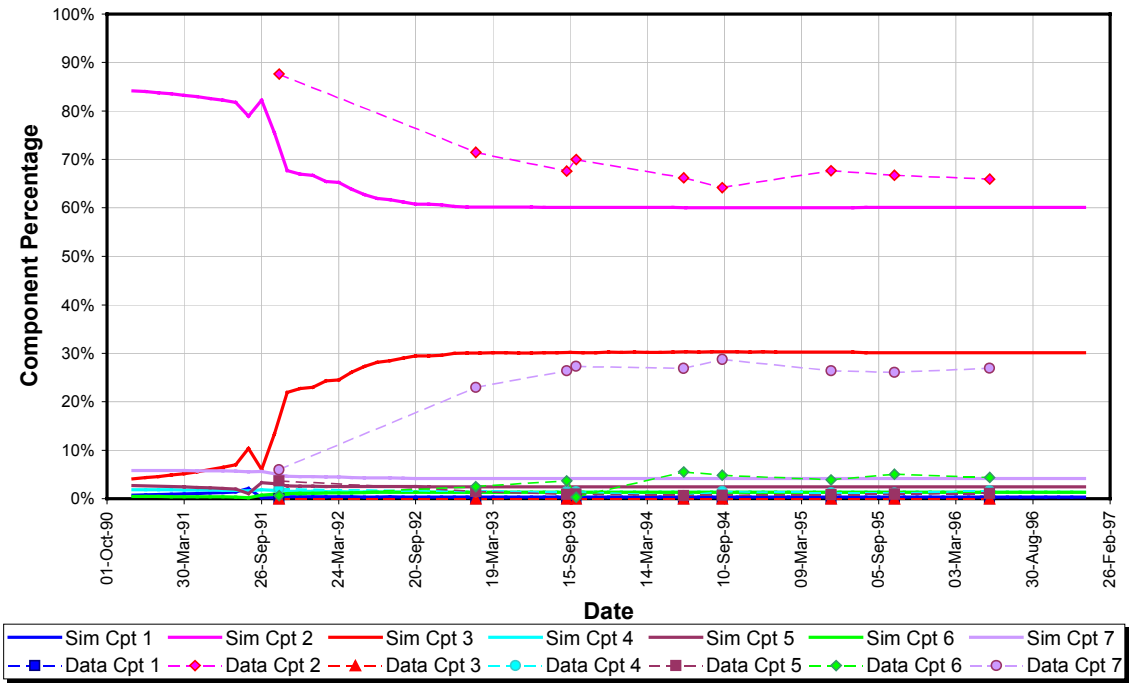

SA1229A

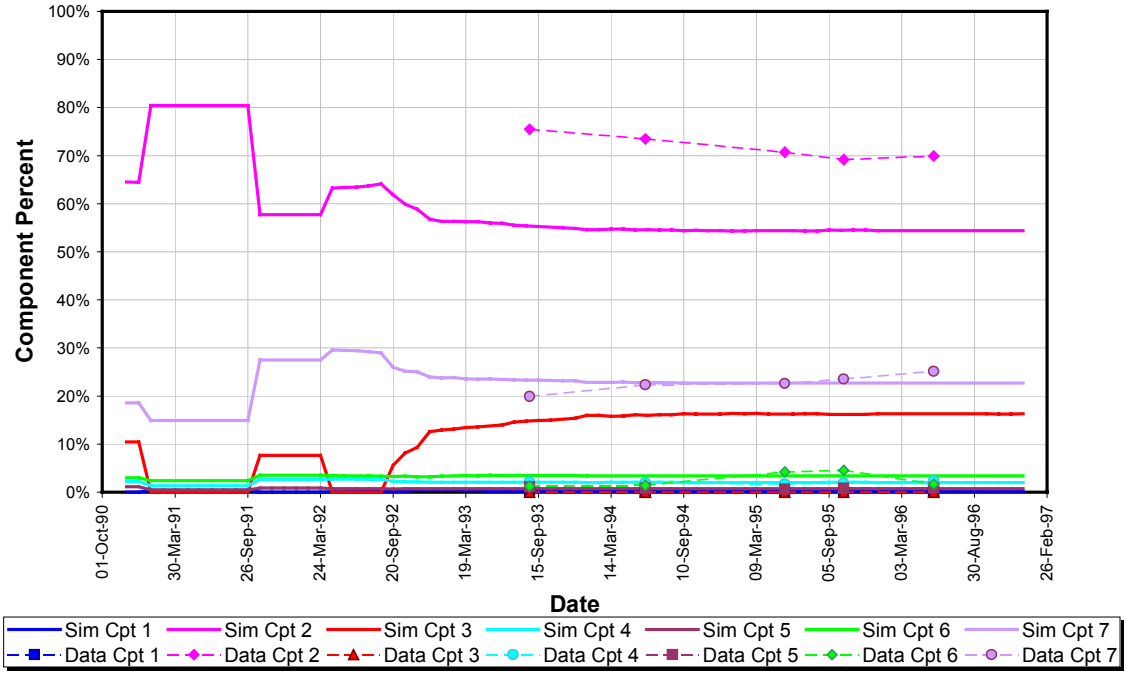

KA1061A

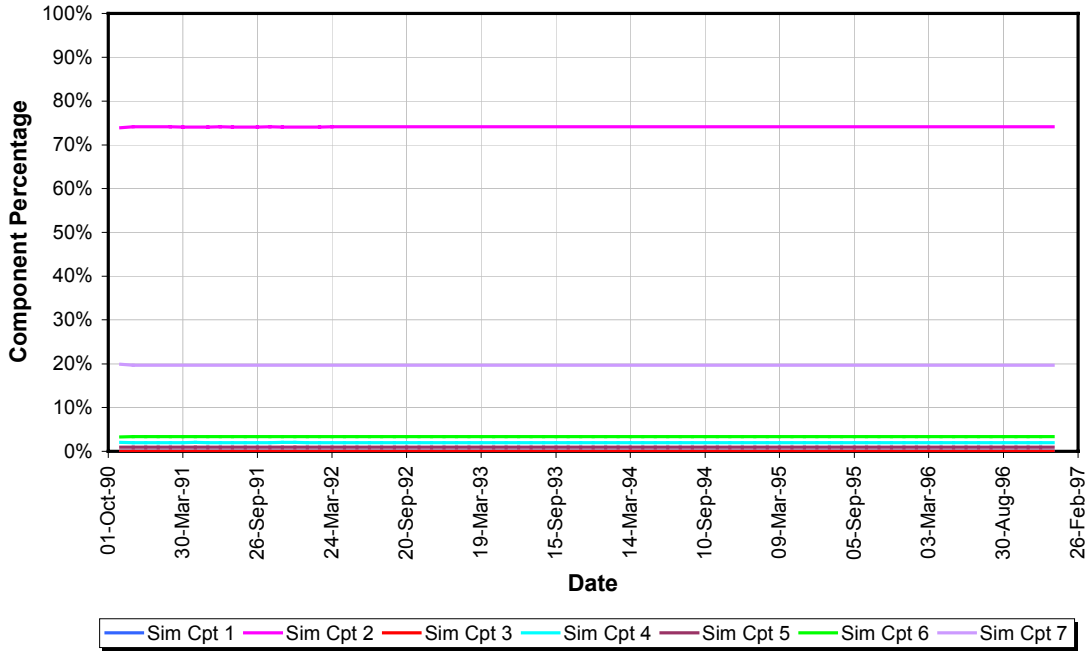

SA2074A

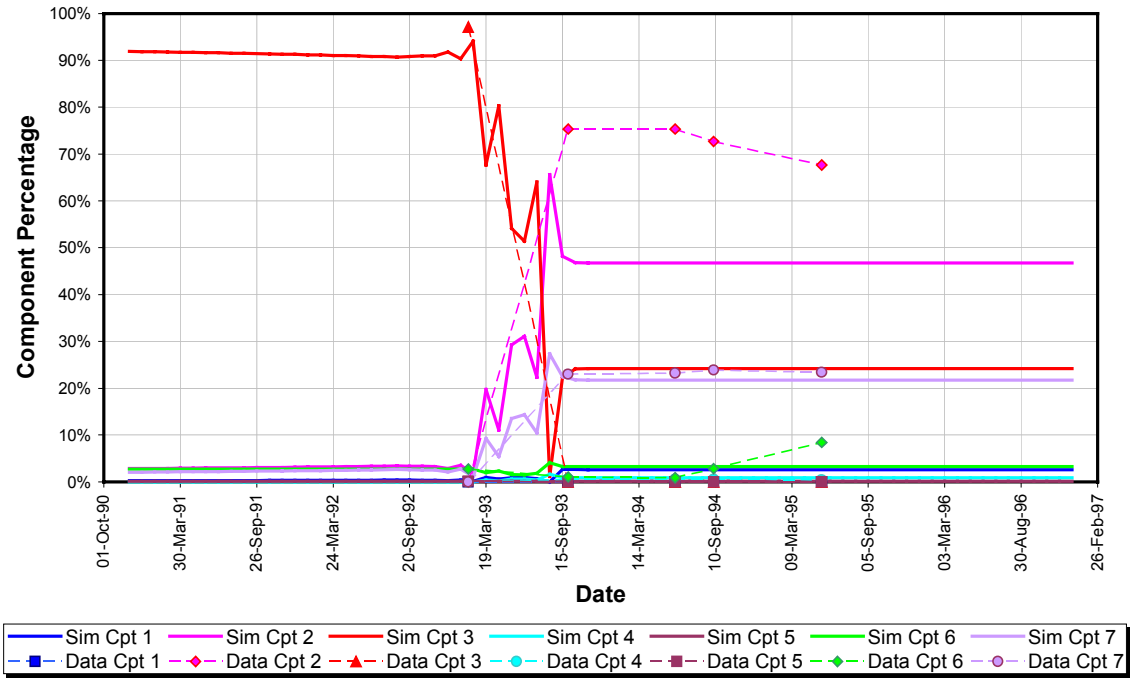

SA2783A

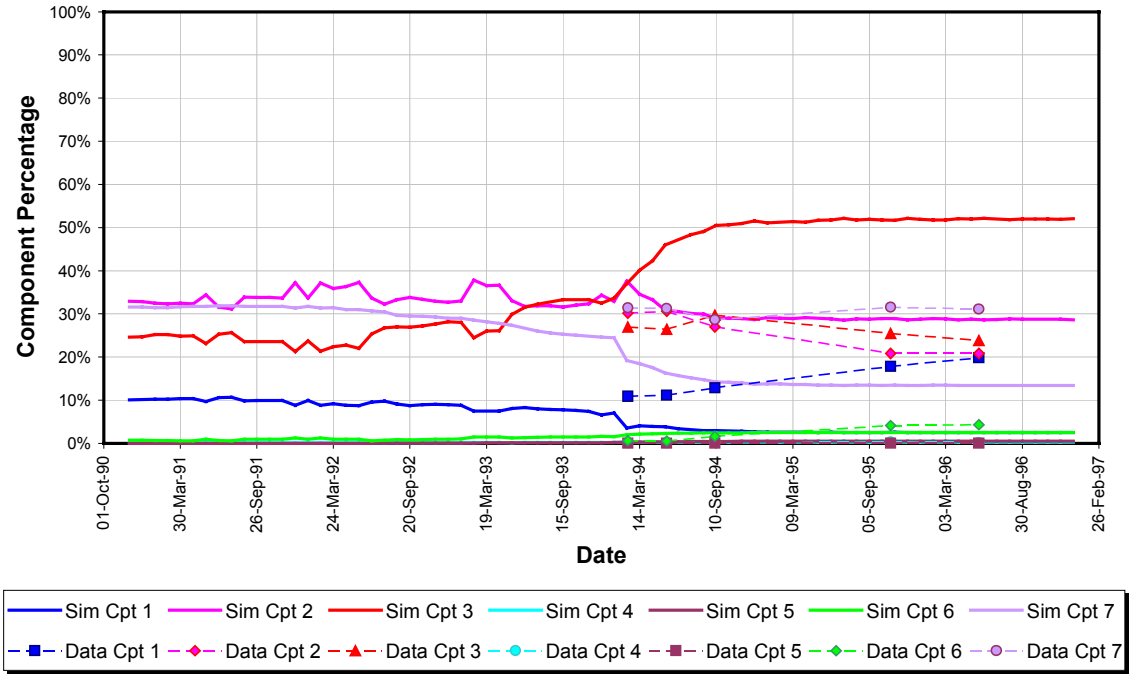

KA1755A

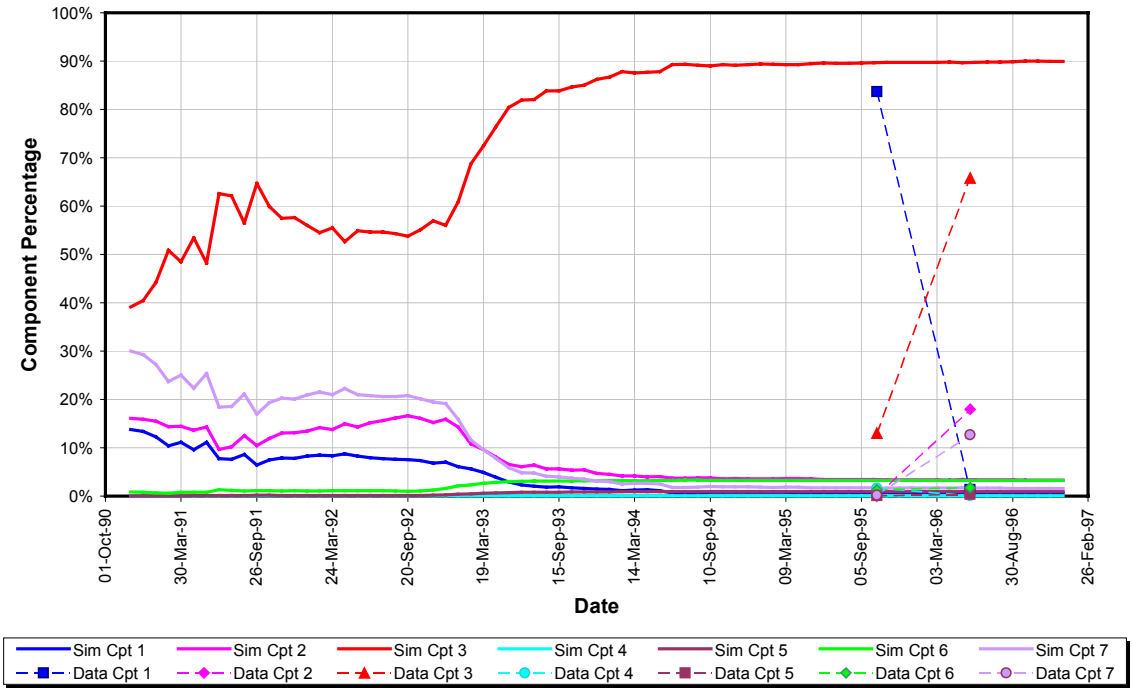

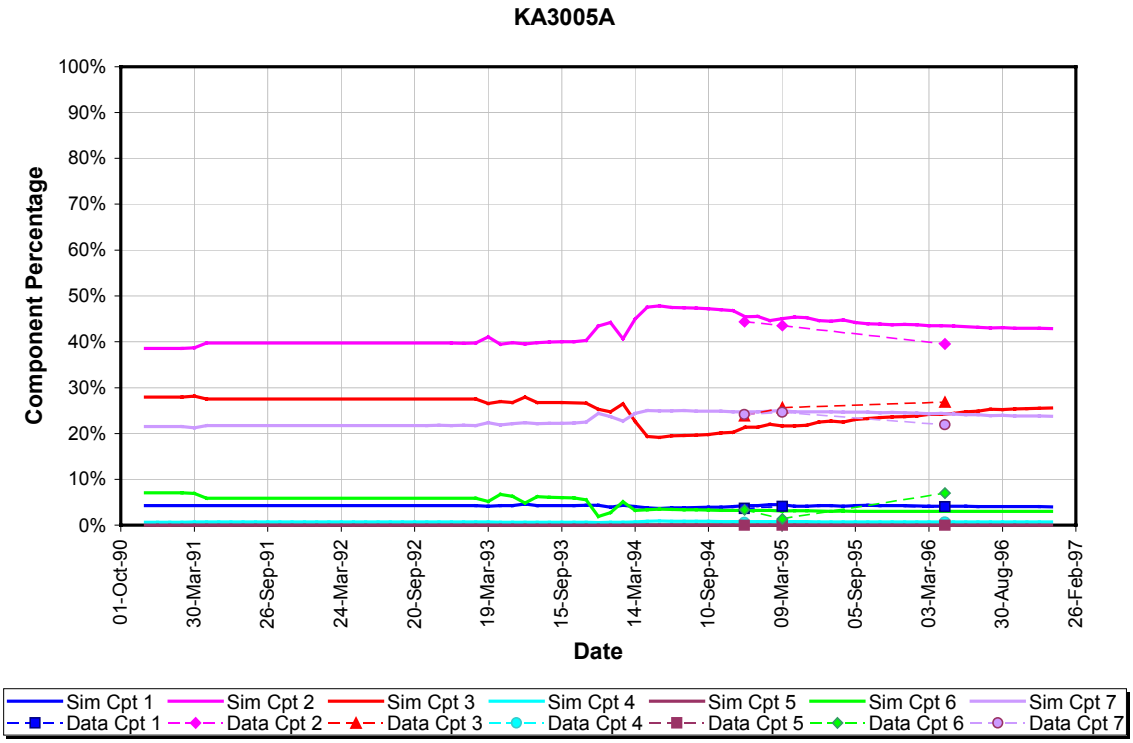
KA3005A
Component Percentage
100%
90%
80%
70%
60%
50%
40%
30%
20%
10%
0%
01-Oct-90
30-Mar-91
26-Sep-91
24-Mar-92
20-Sep-92
19-Mar-93
15-Sep-93
14-Mar-94
10-Sep-94
09-Mar-95
05-Sep-95
03-Mar-96
30-Aug-96
26-Feb-97
Date
Sim Cpt 1
Sim Cpt 2
Sim Cpt 3
Sim Cpt 4
Sim Cpt 5
Sim Cpt 6
Sim Cpt 7
Data Cpt 1
Data Cpt 2
Data Cpt 3
Data Cpt 4
Data Cpt 5
Data Cpt 6
Data Cpt 7

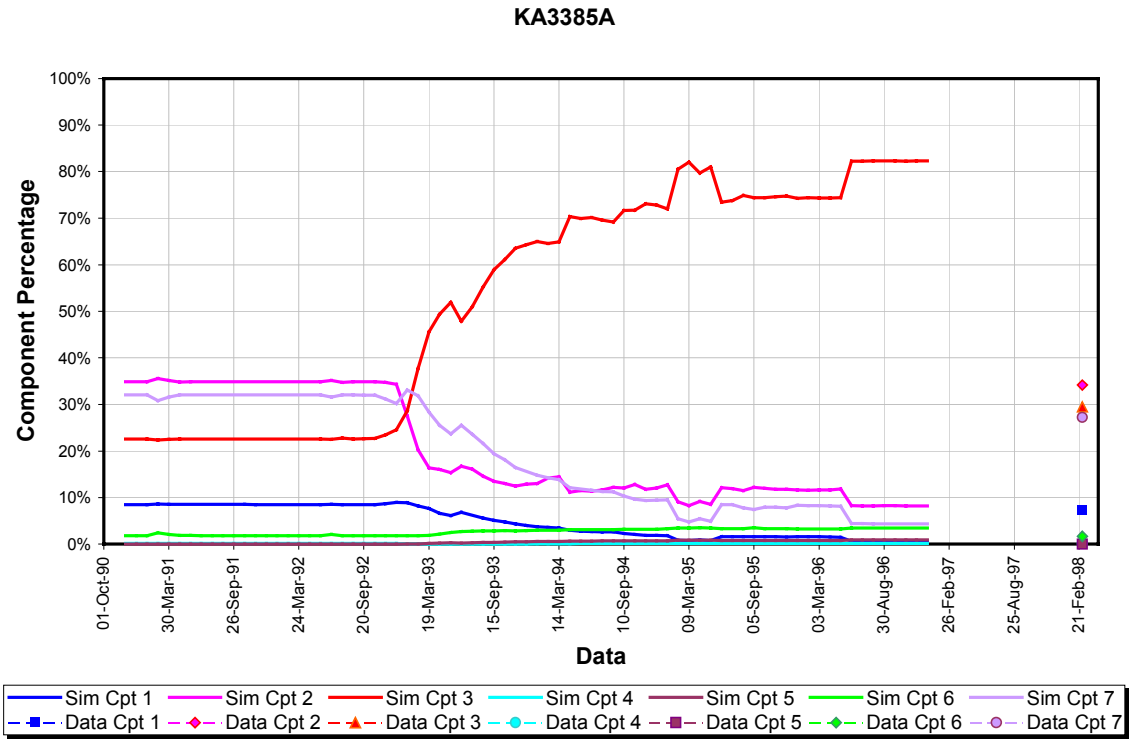
KA3385A
Component Percentage
100%
90%
80%
70%
60%
50%
40%
30%
20%
10%
0%
01-Oct-90
30-Mar-91
26-Sep-91
24-Mar-92
20-Sep-92
19-Mar-93
15-Sep-93
14-Mar-94
10-Sep-94
09-Mar-95
05-Sep-95
03-Mar-96
30-Aug-96
26-Feb-97
25-Aug-97
21-Feb-98
Data
Sim Cpt 1
Sim Cpt 2
Sim Cpt 3
Sim Cpt 4
Sim Cpt 5
Sim Cpt 6
Sim Cpt 7
Data Cpt 1
Data Cpt 2
Data Cpt 3
Data Cpt 4
Data Cpt 5
Data Cpt 6
Data Cpt 7

KAS03a

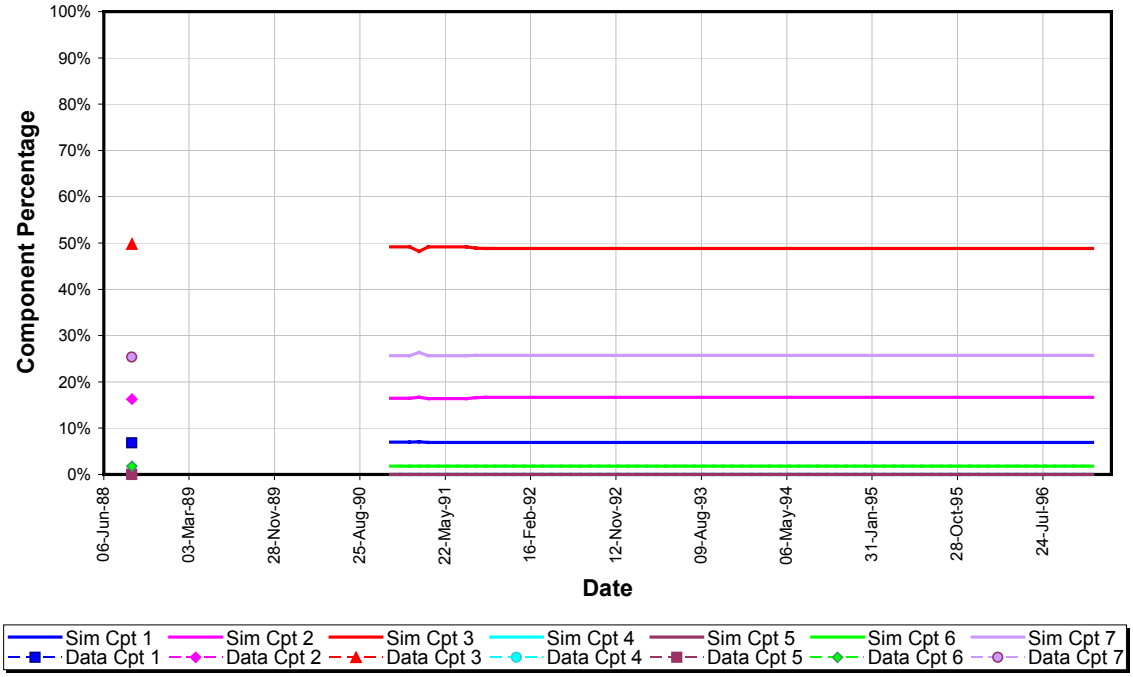

KAS03b

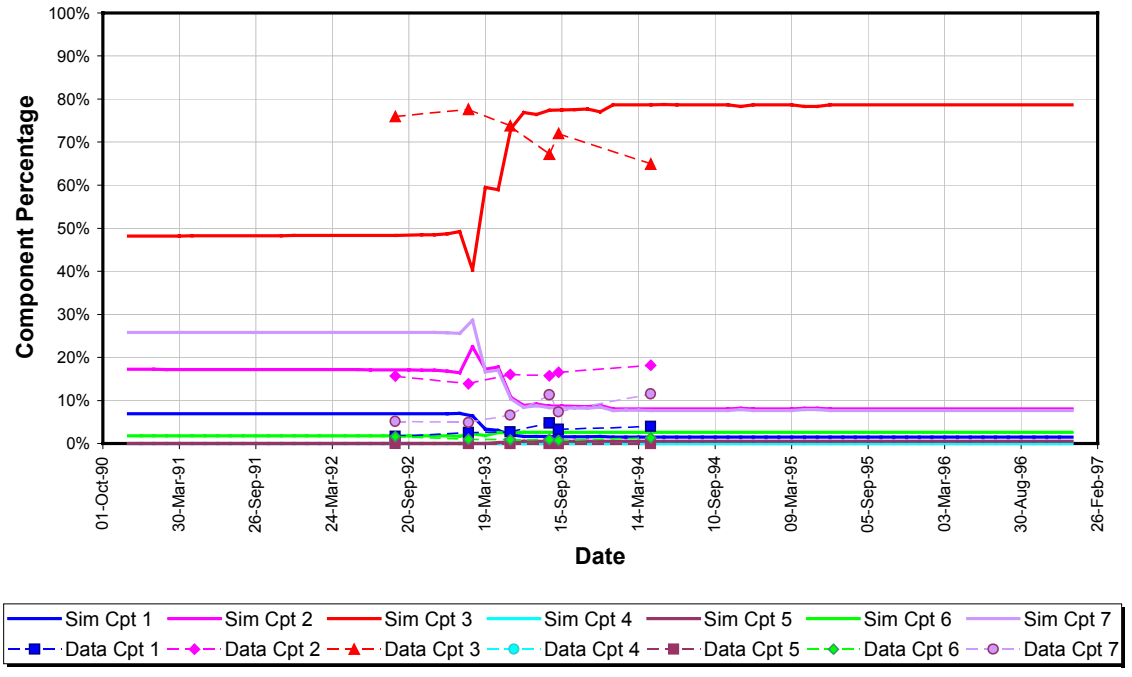

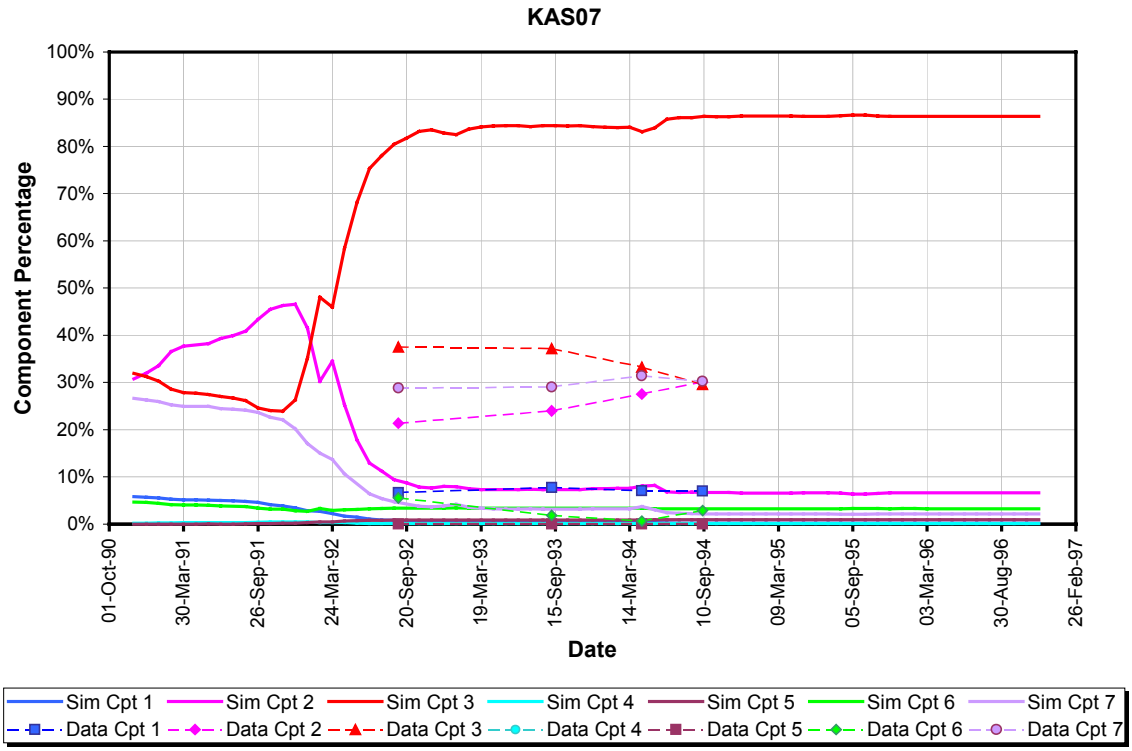
KAS07
Component Percentage
100%
90%
80%
70%
60%
50%
40%
30%
20%
10%
0%
01-Oct-90
30-Mar-91
26-Sep-91
24-Mar-92
20-Sep-92
19-Mar-93
15-Sep-93
14-Mar-94
10-Sep-94
09-Mar-95
05-Sep-95
03-Mar-96
30-Aug-96
26-Feb-97
Date
Sim Cpt 1
Sim Cpt 2
Sim Cpt 3
Sim Cpt 4
Sim Cpt 5
Sim Cpt 6
Sim Cpt 7
Data Cpt 1
Data Cpt 2
Data Cpt 3
Data Cpt 4
Data Cpt 5
Data Cpt 6
Data Cpt 7

End Members based on Model 2 (7 chemical components) – no storativity calibration

SA0813B

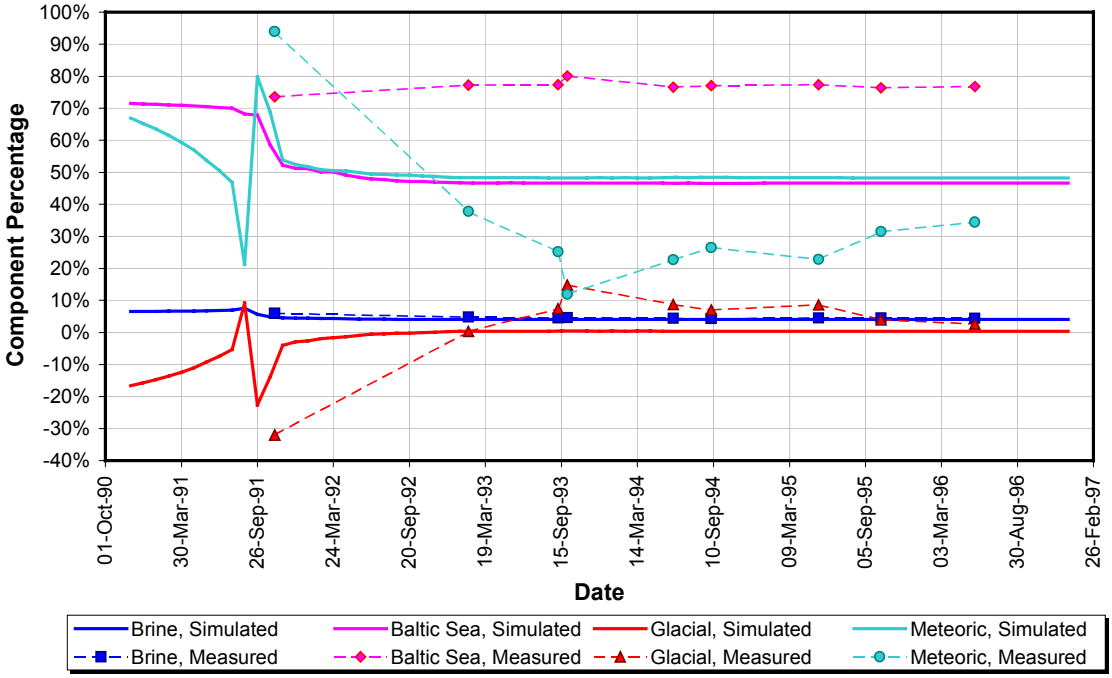

SA1229A

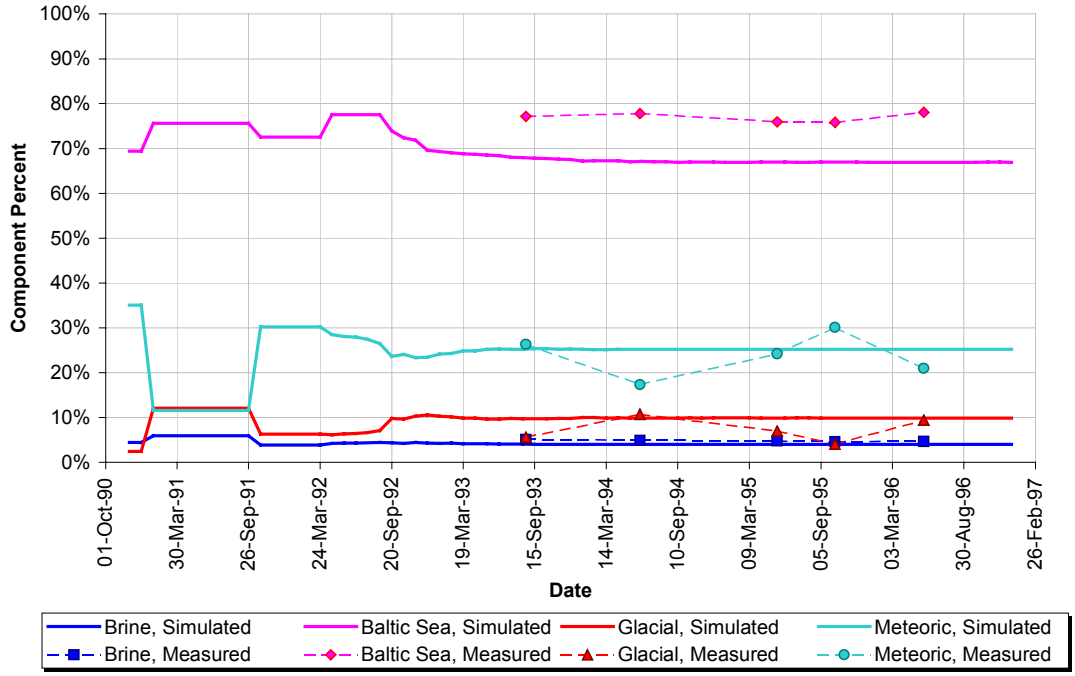

KA1061A

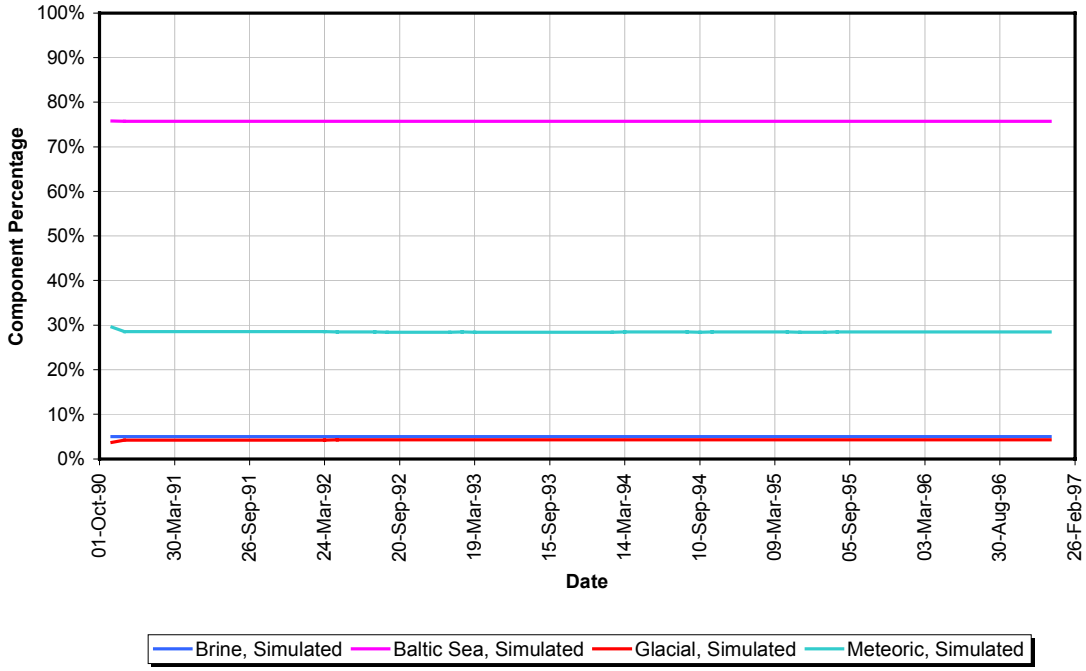

SA2074A

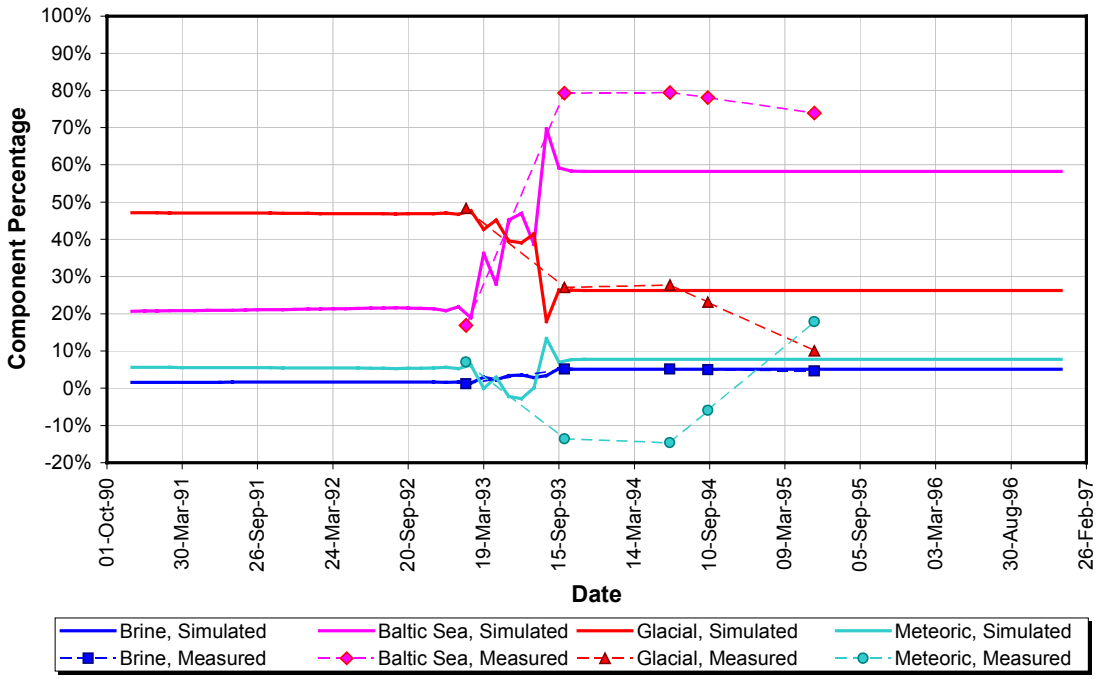

SA2783A

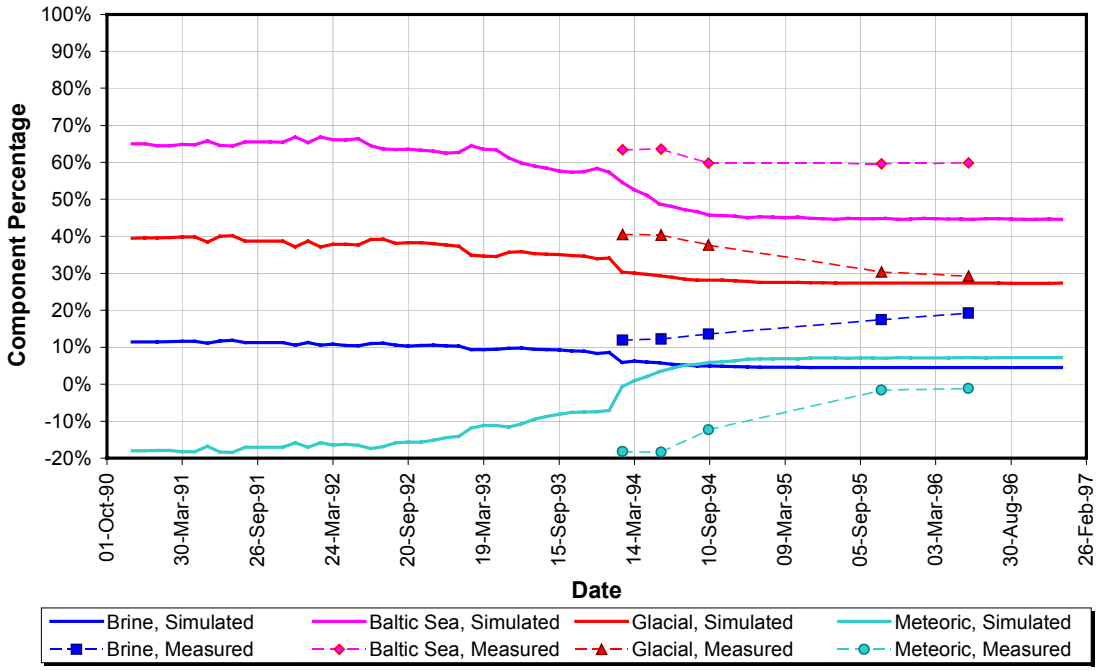

KA1755A

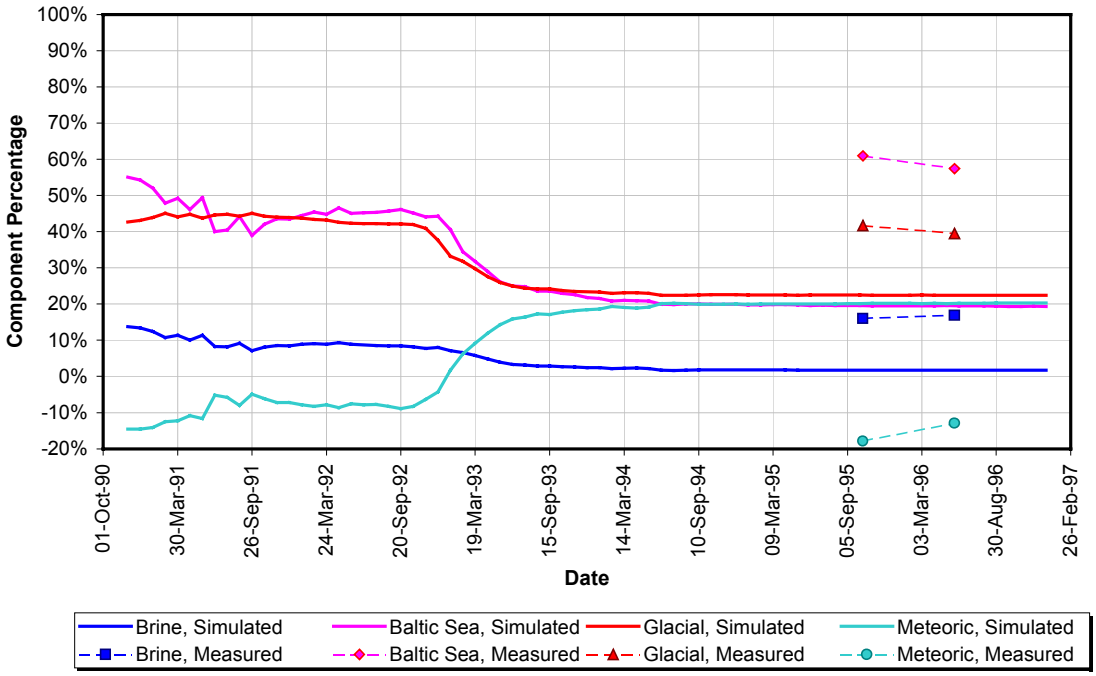

KA3005A

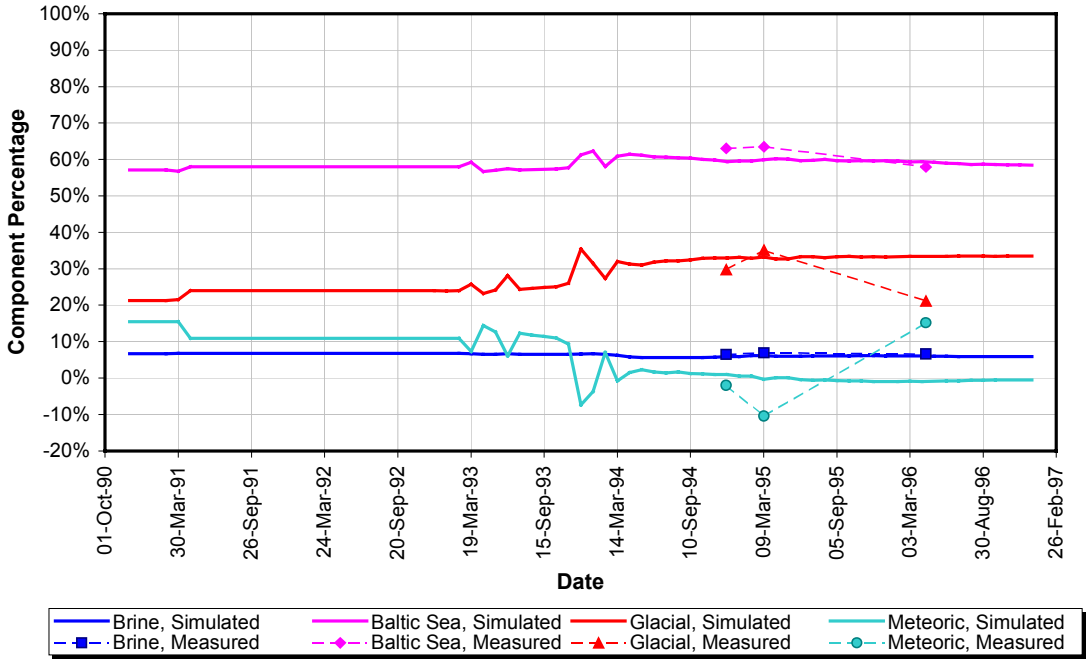

KA3385A

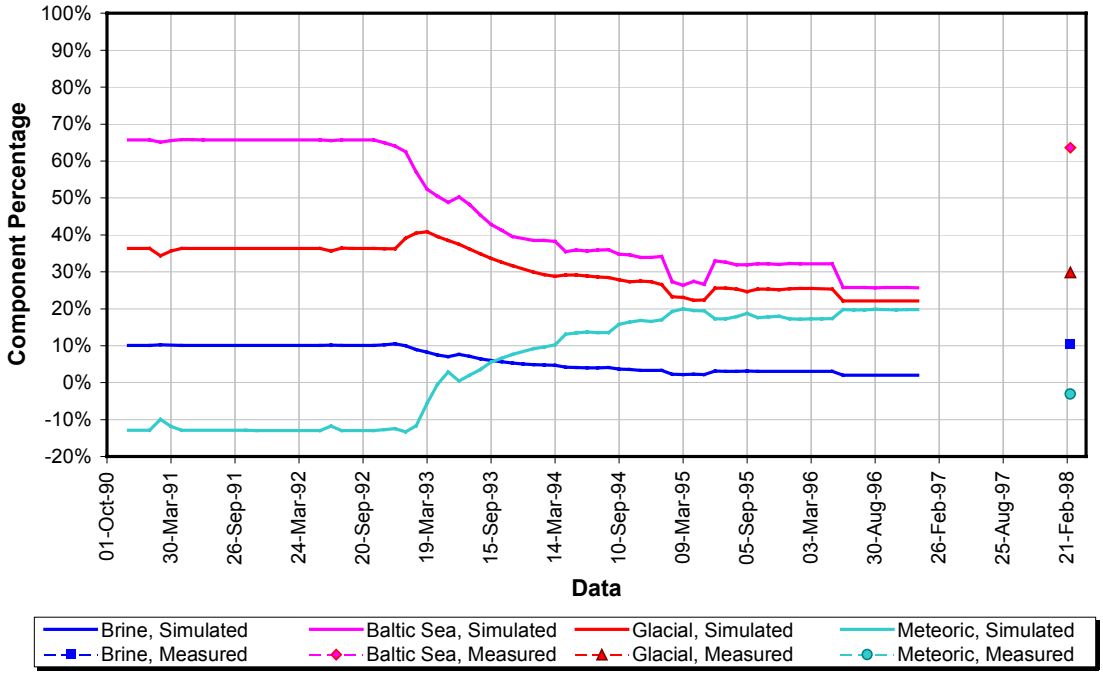

KAS03a

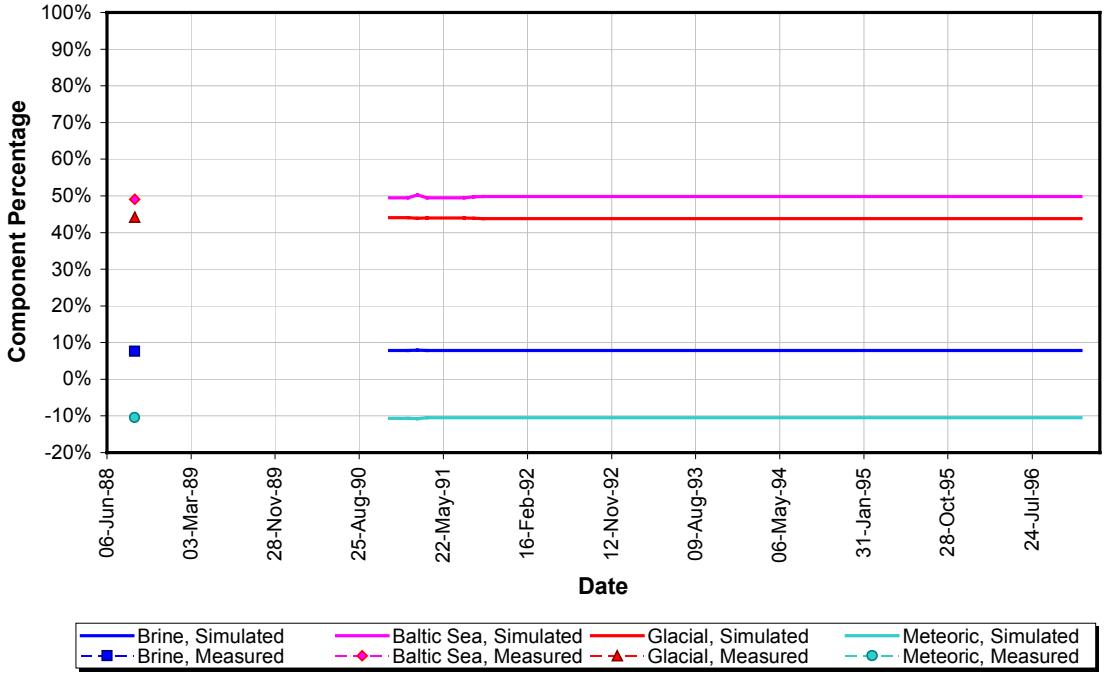

KAS03b

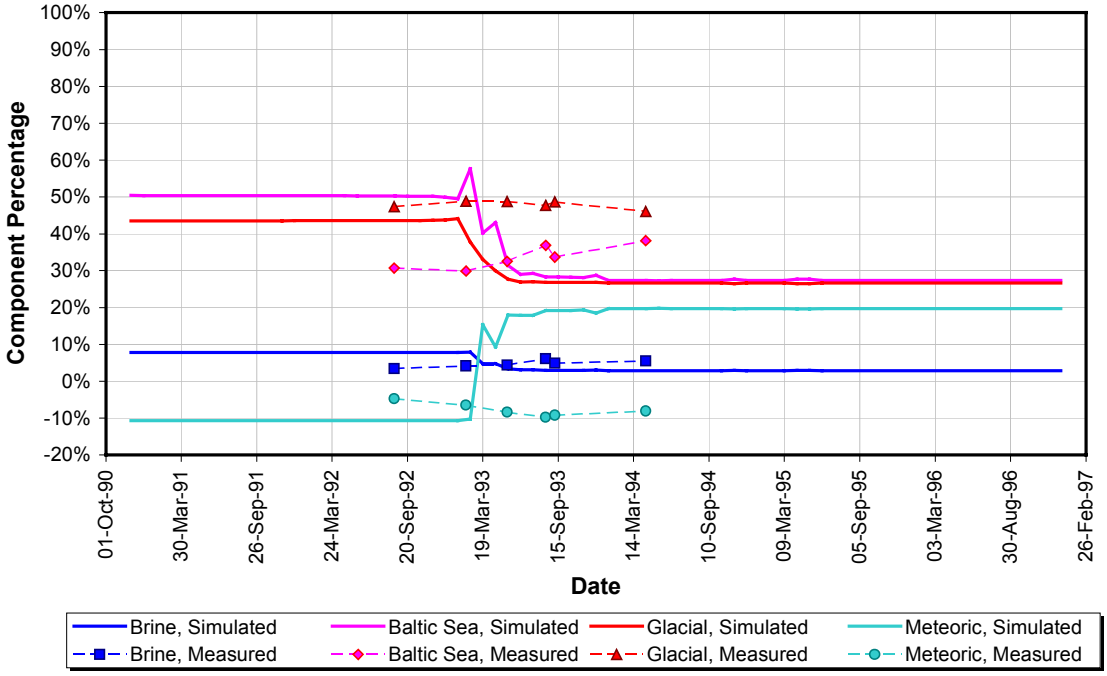

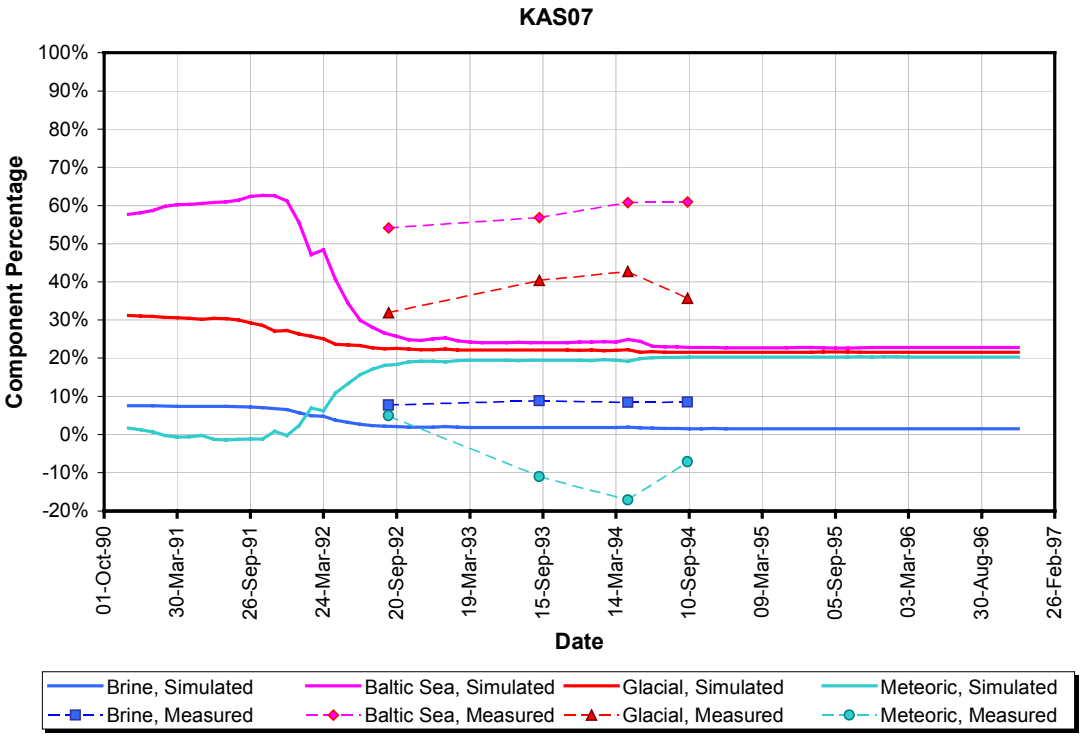
KAS07
Component Percentage
100%
90%
80%
70%
60%
50%
40%
30%
20%
10%
0%
-10%
-20%
01-Oct-90
30-Mar-91
26-Sep-91
24-Mar-92
20-Sep-92
19-Mar-93
15-Sep-93
14-Mar-94
10-Sep-94
09-Mar-95
05-Sep-95
03-Mar-96
30-Aug-96
26-Feb-97
Date
Brine, Simulated
Baltic Sea, Simulated
Glacial, Simulated
Meteoric, Simulated
Brine, Measured
Baltic Sea, Measured
Glacial, Measured
Meteoric, Measured

End Members based on Model 2 (7 chemical components) – including storativity calibration

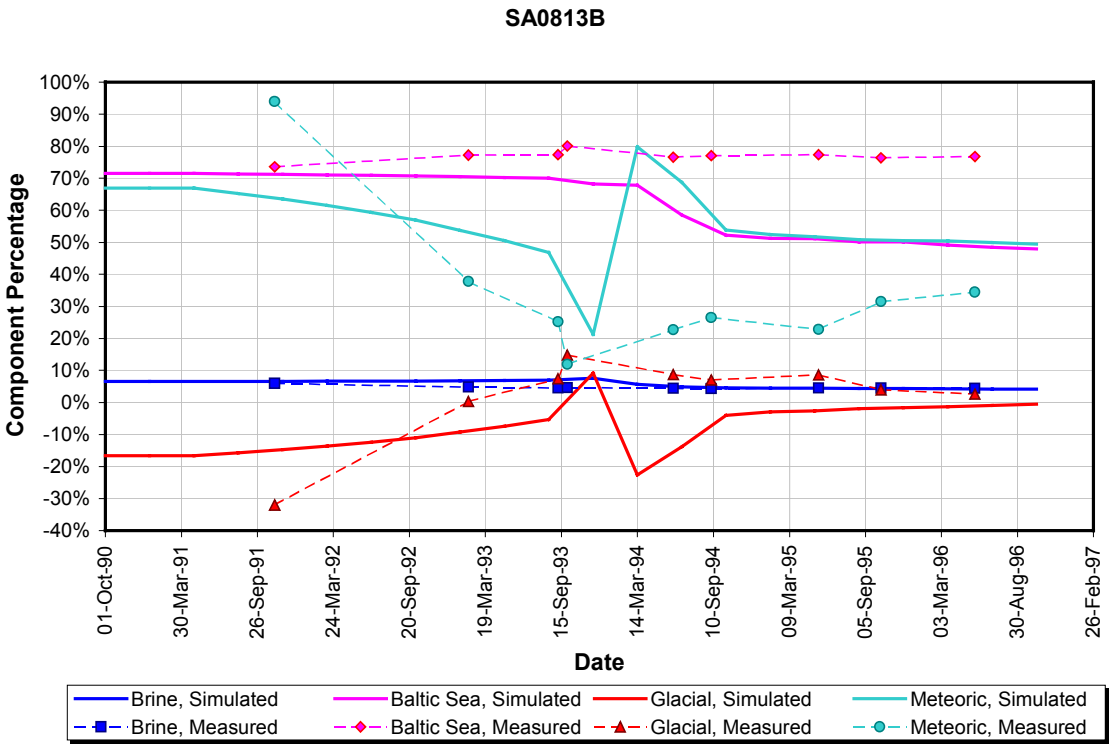

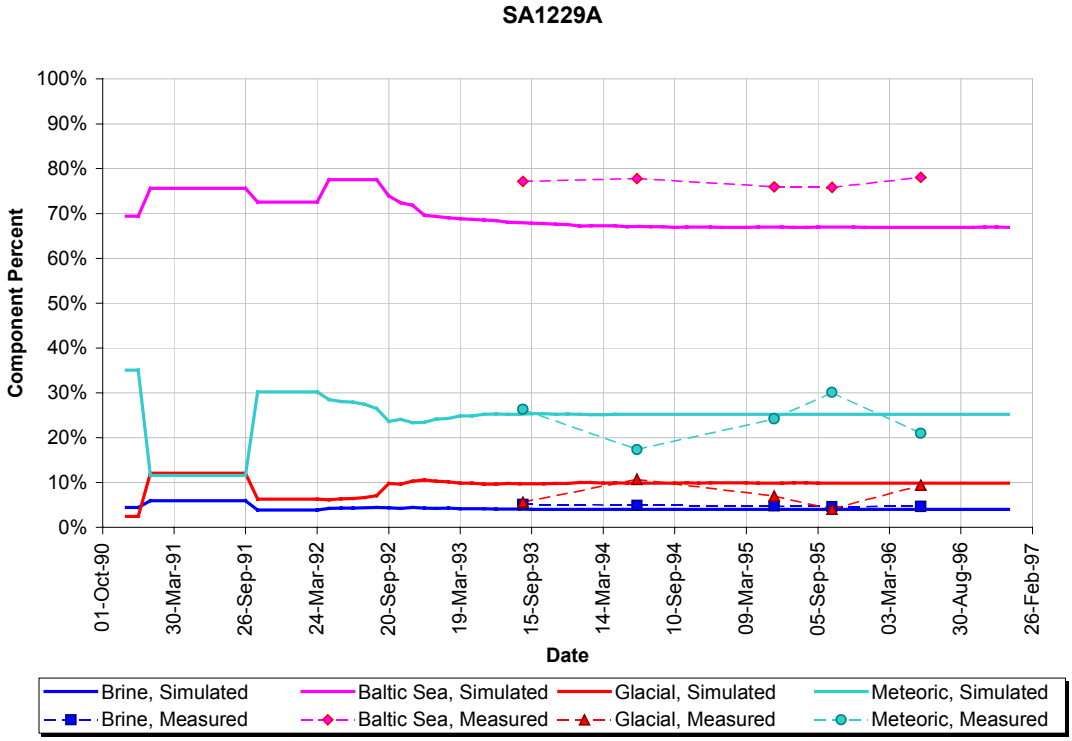

KA1061A

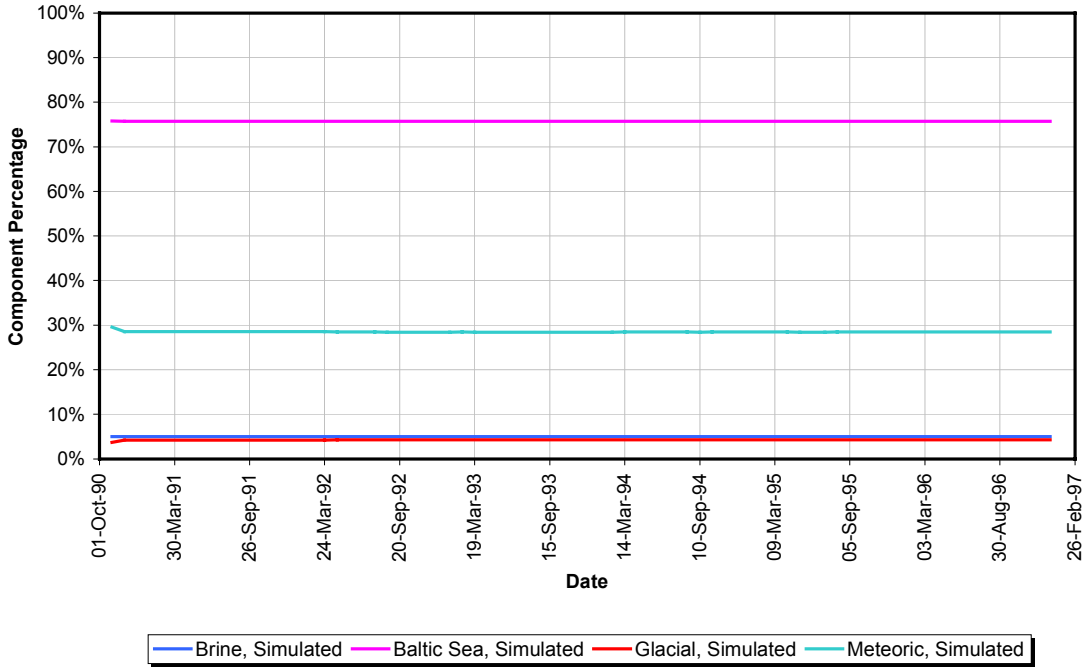

SA2074A

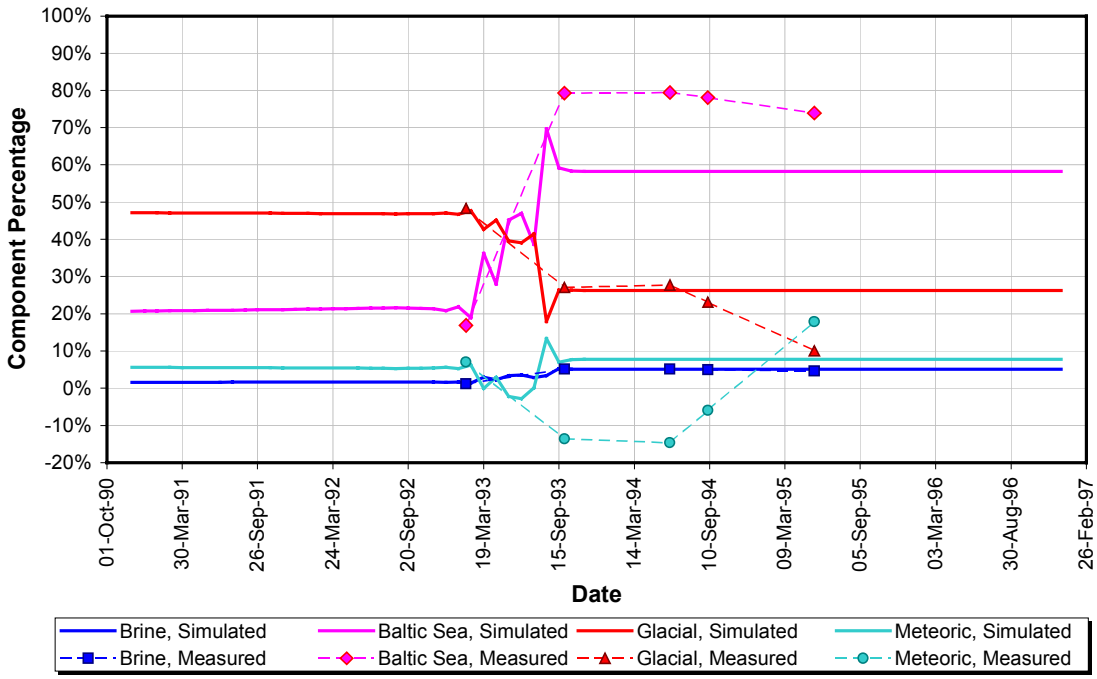

SA2783A

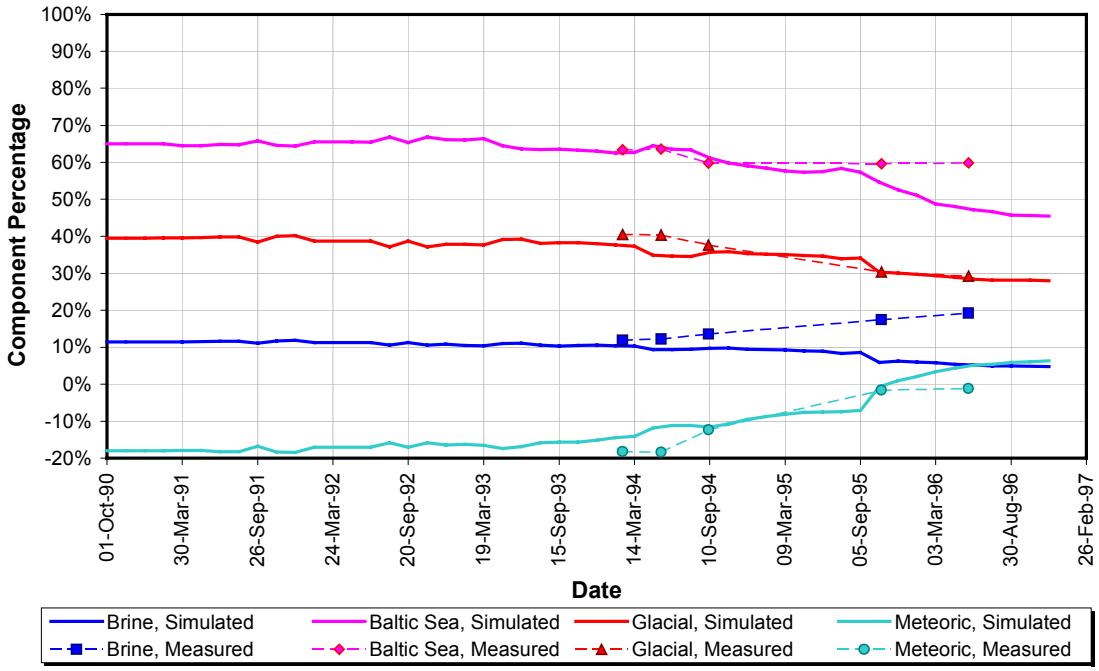

KA1755A

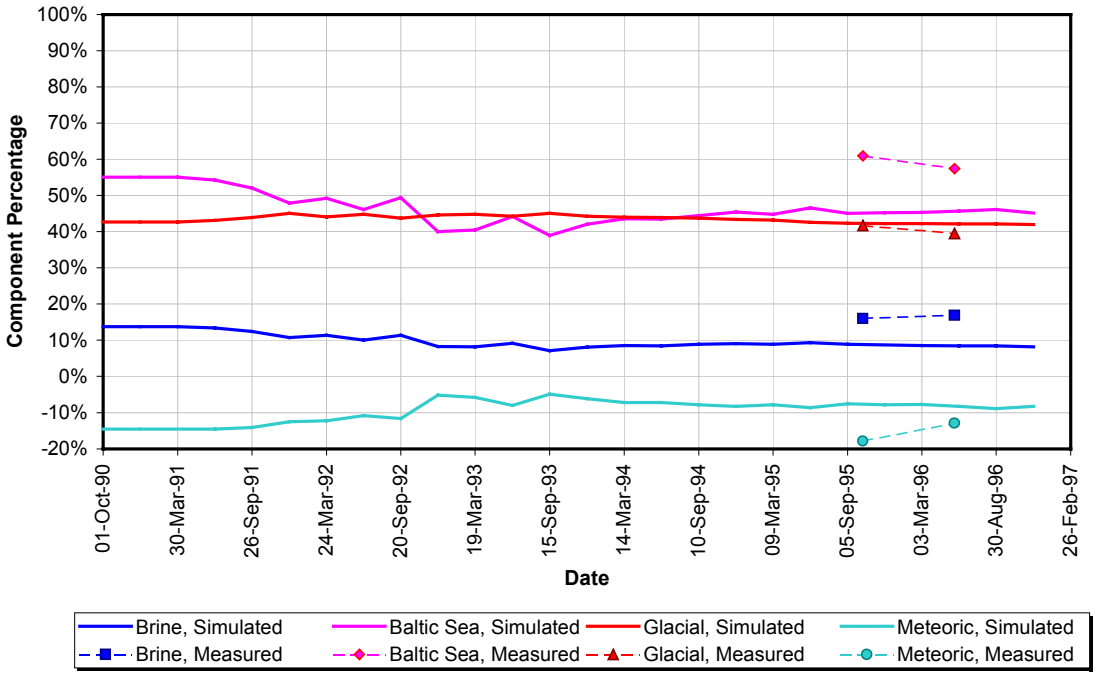

KA3005A

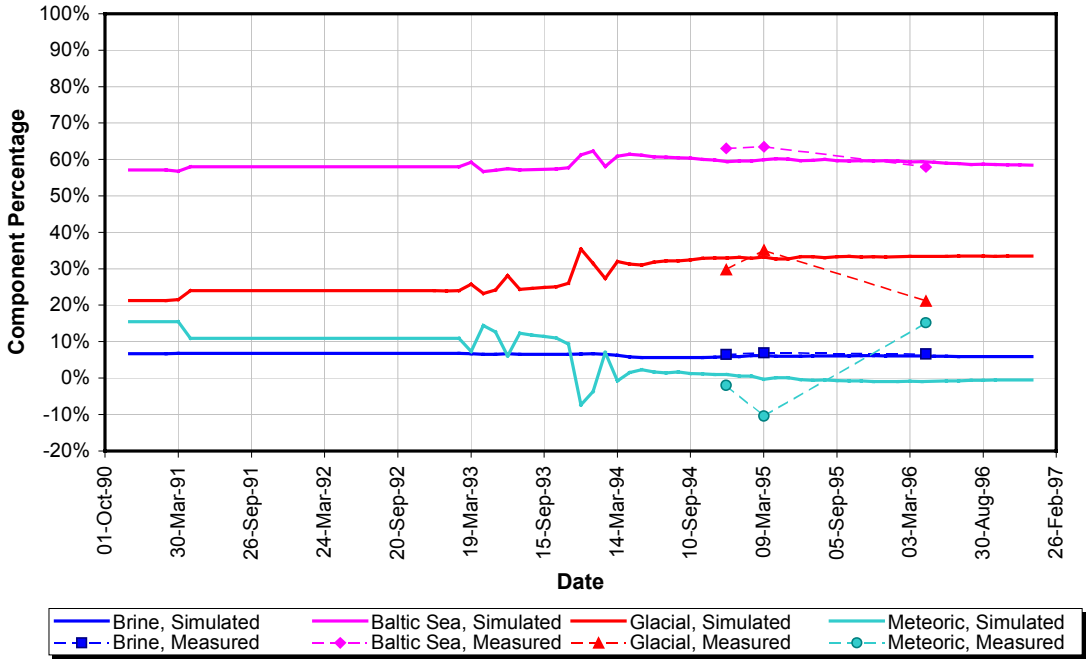

KA3385A

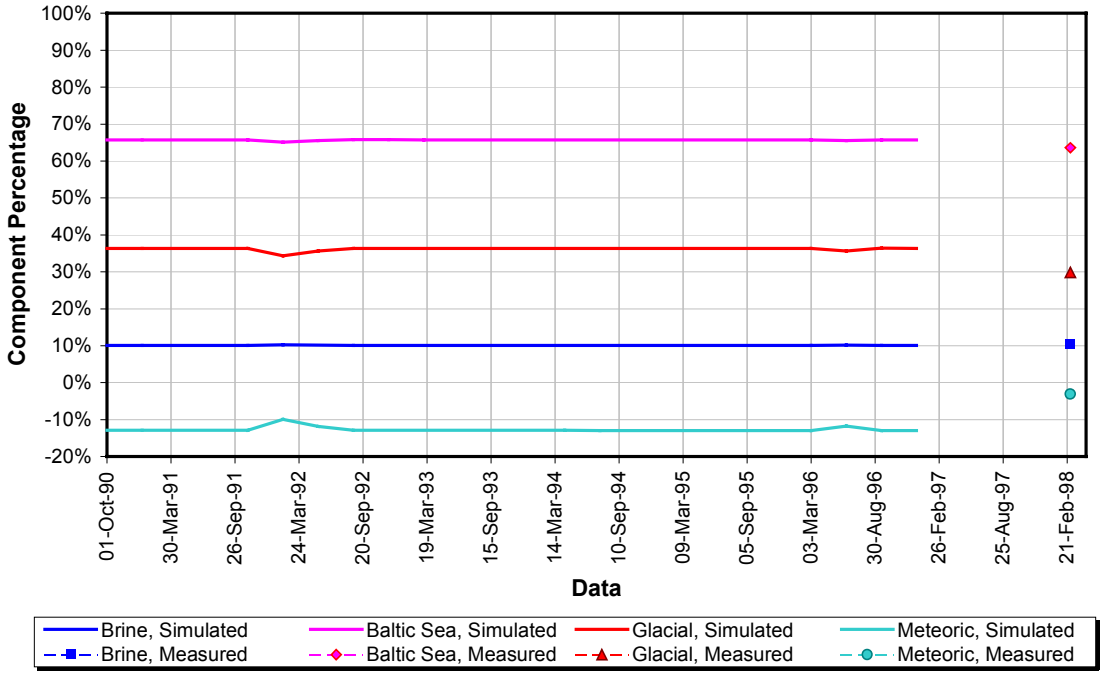

KAS03a

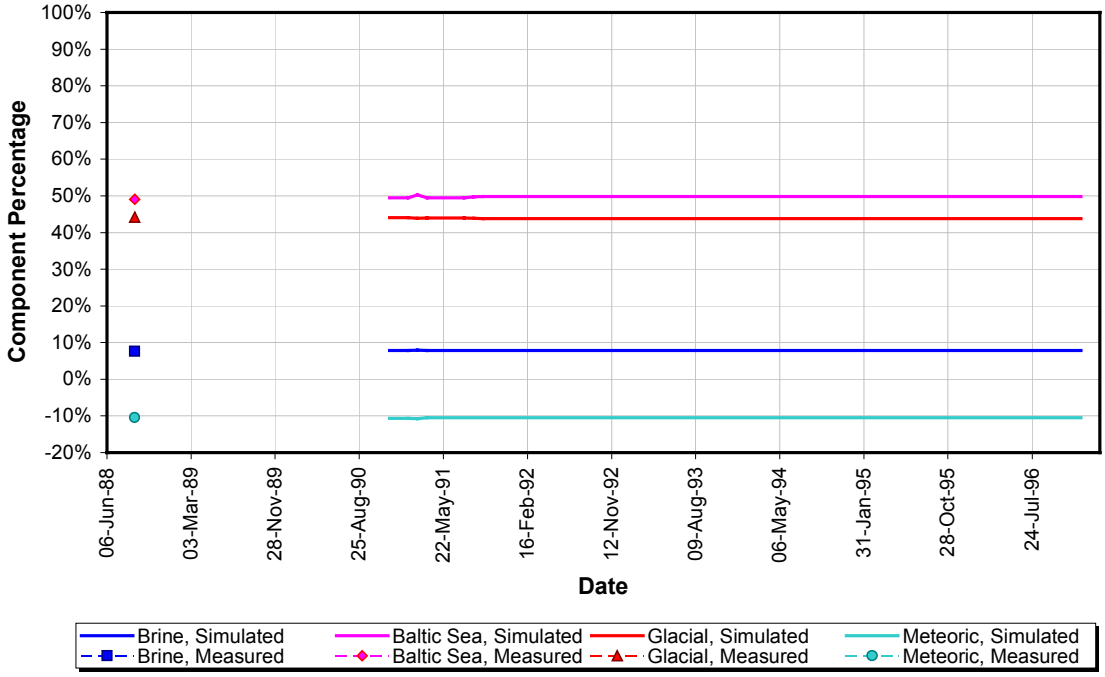

KAS03b

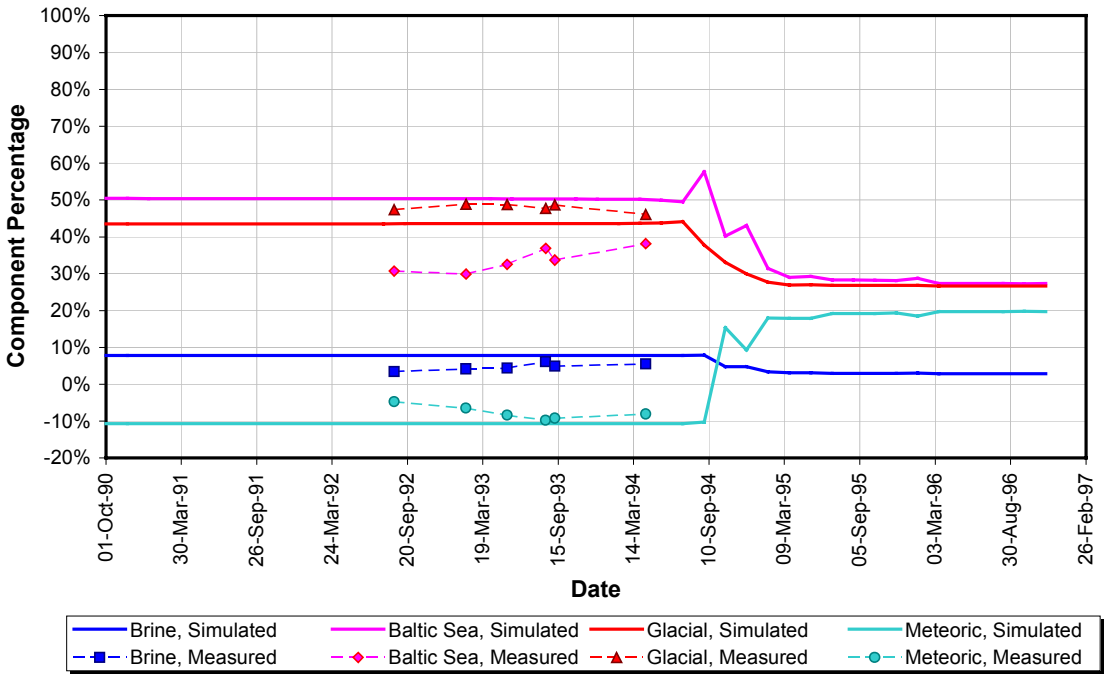

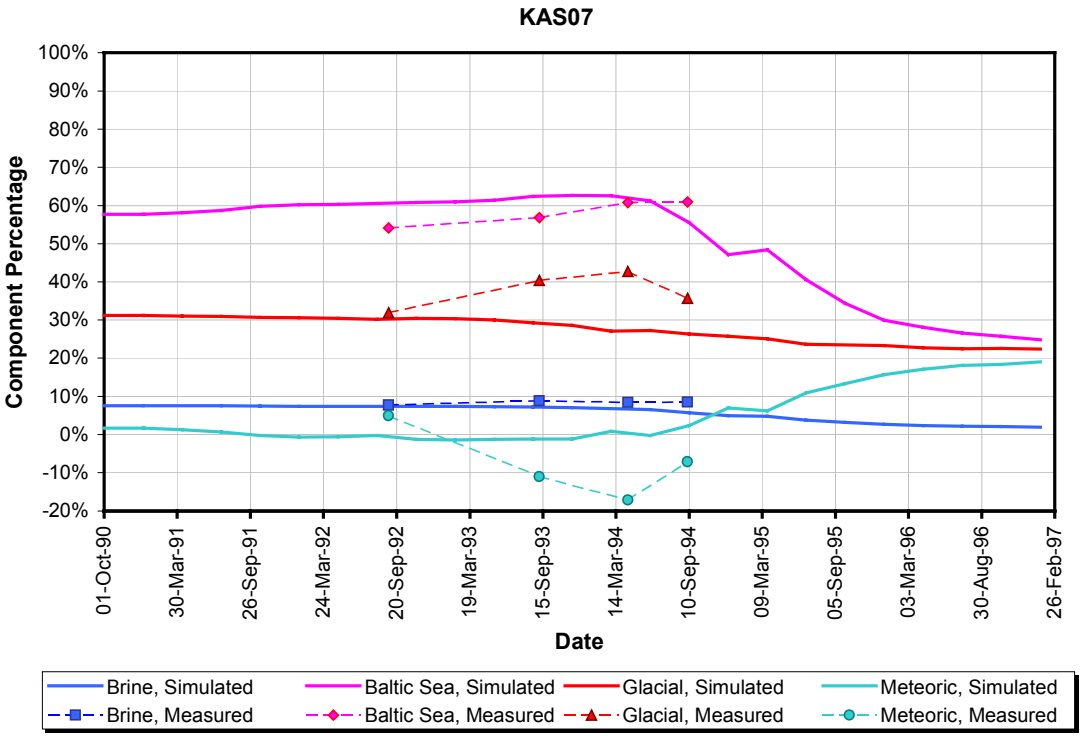
KAS07
Component Percentage
100%
90%
80%
70%
60%
50%
40%
30%
20%
10%
0%
-10%
-20%
01-Oct-90
30-Mar-91
26-Sep-91
24-Mar-92
20-Sep-92
19-Mar-93
15-Sep-93
14-Mar-94
10-Sep-94
09-Mar-95
05-Sep-95
03-Mar-96
30-Aug-96
26-Feb-97
Date
Brine, Simulated
Baltic Sea, Simulated
Glacial, Simulated
Meteoric, Simulated
Brine, Measured
Baltic Sea, Measured
Glacial, Measured
Meteoric, Measured

MODELLING QUESTIONNAIRE FOR TASK 5, JNC/GOLDERS

worked May 2001

This is a Modelling Questionnaire prepared by SKB based on discussions within the Task Force group. It should be answered when reporting Task 5 in order to simplify the evaluation process of the modelling exercise. Preferably, include this response in an appendix to your forthcoming report.

1. SCOPE AND ISSUES

a) *What was the purpose for your participation in Task 5?*
The JNC/Golder team undertook the DFN pipe network modelling. The overall purpose of our involvement was to use the Äspö site as an example of a generic repository location. The lessons learned, in terms of the usefulness of groundwater chemistry data, will be used to constrain future flow models and in developing an approach for optimal use of groundwater chemistry.

b) *What issues did you wish to address through participation in Task 5?*
Issues of interest included relevance of groundwater chemistry data in constraining the flow model and to develop an approach to optimise the use of groundwater chemistry. Other issues include the relevance of data for setting up a regional scale model, importance of LSFs relative to background fractures on different scales, and the effect of the fracture intersection zones.

2. CONCEPTUAL MODEL AND DATA BASE

a) *Please describe your models using the tables 1-3 in the appendix.*
Attached.

b) *To what extent have you used the data sets delivered? Please fill in Table 4 in the appendix.*
Attached.

c) *Specify more exactly what data in the data sets you actually used? Please fill in "Comments" in Table* 4
Attached.

d) *What additional data did you use if any and what assumptions were made to fill in data not provided in the Data Distributions but required by your model? ? Please add in the last part of Table 4.*
Added to table.

e) *Which processes are the most significant for the situation at the Äspö site during the simulation period?*
Connectivity – Modification to NNW-5, extending it towards the north to collect glacial water. Accurate representation of LSF connectivity (required addition of a 'mystery feature') was needed to replicate the advective flow system. This is important to obtain reasonable flow pathways and velocities.
Transmissivity modification beneath Baltic to replicate the effect of lower permeability deposits on the seabed. This was required to replicate the magnitude of the drawdown at the tunnels.
Advective flow – dominates over the chemical reactions.
Storativity – required to obtain reasonable chemistry predictions.

3. MODEL GEOMETRY/STRUCTURAL MODEL

a) *How did you geometrically represent the ÄSPÖ site and its features/zones?*
Region 2 km square by 1 km deep.
The Baltic Sea and Äspö Island were treated differently in terms of applied boundary condition.
All LSFs were explicitly represented as distinct discrete fractures. Background fractures were explicitly represented using a stochastic generation. Additional 'mystery' feature added.

b) *Which features were considered the most significant for the understanding of flow and transport in the ÄSPÖ site, and why?*
The modelling indicated that the chemistry measured at the monitoring locations was dominated by the closest LSFs. Therefore, all LSFs were important. Additionally, the chemistry indicated that feature NNW-5 should be extended towards the north, to increase the proportion of glacially rich groundwater.
In order to generate the correct drawdown responses an additional mystery feature was needed (in reality this may not be a single feature but a fracture zone of higher transmissivity features). This is considered important as it highlighted the need for the hydrogeological model to be both geology and hydrogeologically based.

c) *Motivate selected numerical discretization in relation to used values of correlation length and/or dispersion length.*
The FracMan DFN model did not explicitly include dispersion length – dispersion was a function of the differing tortuous pathways generated by the DFN background fractures. However, the minimum fracture size modelled effectively controls dispersion through the fracturing intensity.

4a. MATERIAL PROPERTIES - HYDROGEOLOGY

a) *How did you represent the material properties in the hydraulic units used to represent the ÄSPÖ SITE?*
The material properties considered were the transmissivity (T), size, orientation, spacing model, storativity (S) and transport aperture (A) of the fractures. Large scale and background fractures were explicitly modelled, with the porosity of the matrix being assumed negligible for advective flow, hence these parameters defined our model.

b) *What is the basis for your assumptions regarding material properties?*
The material properties for the LSF were mainly taken from Rhén et al (1997). Storativity and aperture were assumed based on tracer and interference testing at other sites. The properties of the background fractures were stochastically derived from analysis of measured fracture data.

c) *Which assumptions were the most significant, and why?*
The most significant assumptions relate to aperture and storativity. These are the most difficult to predict prior to chemistry data coming available.

4b. CHEMICAL REACTIONS - HYDROCHEMISTRY

a) *What chemical reactions did you include?*
Pure mixing only.

b) *What is the basis for your assumptions regarding the chosen chemical reactions?*
The error term for our Stage 3 chemistry modelling is a measure of the magnitude of the chemical reactions. It is believed that contributions of reactions to chemical variability is small owing to principal components attributable to reactions having small eigen values, though further work would be needed to confirm this.
The M3 code derived chemistry values at the grid locations used for Stages 1 and 2 are based on mixing.

c) *Which reactions were the most significant, and why?*
n/a

5a. BOUNDARY CONDITIONS FOR HYDROGEOLOGICAL MODEL

a) *What boundary conditions were used in the modelling of the ÄSPÖ site tests?*
See table 1 'boundary conditions' for details.

b) *What was the basis for your assumptions regarding boundary conditions?*
Base – Typical assumption for variable salinity flow with base not close to tunnel.
Sides – The DFN approach provides less sensitivity to fracture intensity for constant head boundary conditions. Therefore a head, not flow, boundary condition was chosen. The values were based on the larger scale model of Svensson (1999).

Baltic Sea – constant head = 0.0. Assumed good connection to the seabed.
Äspö Island – differing net infiltration levels assumed.
Tunnel and shafts – flow rate equal to the measured inflows into the tunnels/shafts.

c) *Which assumptions were the most significant, and why?*
The model is sensitive to the tunnel inflows (set by data provided) and the boundary conditions on the model surface (i.e. Baltic and Äspö Island). The model surface was sensitive because a large proportion of the inflows came from above (due to lower density fluid and the primarily sub-vertical LSFs).

5b. BOUNDARY/INITIAL CONDITIONS FOR HYDROCHEMICAL MODEL

a) *What boundary conditions were used in the modelling of the Äspö site tests?*
Stages 1 and 2 used the end members in Appendix 9 of the data deliveries.
Stage 3 used the 7 principal components derived using the PCA approach and the chemometric code of Cave et al.

b) *What was the basis for your assumptions regarding boundary conditions?*
Stage 1 and 2 models used the previous SKB modelling to provide better coverage of the modelling region. The few data points available limited the chemistry resolution.
Based on earlier modelling, in Stage 3 it was felt that the LSFs dominated the chemistry. Therefore Golder developed an independent scheme for extrapolating measured chemistry throughout the model. The chemistry at the measurement locations was changed from the M3 values to those derived by Cave based on the PCA approach.

c) *Which assumptions were the most significant, and why?*
One major deduction was that the chemistry below Äspö Island and the Baltic Sea was substantially different, and incorporating this into the extrapolation/interpolation scheme was critical.

6. MODEL CALIBRATION

a) *To what extent did you calibrate your model on the provided hydraulic information? (Steady state and transient hydraulic head etc.)*
The heads were used to calibrate the transmissivities and connectivity of the DFN. The timing of the head drops during tunnelling, and the location of the drawdown responses, provide information on transmissivity and connectivity. Head data indicated the existence of a mystery large scale feature.

b) *To what extent did you calibrate your model on the provided "transport data"? (Breakthrough curves etc.)*
The transport data was used to calibrate the storativity and aperture of the fractures. Where appropriate the transmissivities could also be recalibrated if the chemistry indicated that the connectivity was poorly replicated – but at this site negligible changes were required.

c) *To what extent did you calibrate your model on the provided hydrochemical data? (Mixing ratios; density/salinity etc.)*
Model was calibrated to the end members.

d) *What parameters did you vary?*
Transmissivity of the mystery feature. Addition of an extra larger feature. Storativity of the LSFs.

e) *Which parameters were the most significant, and why?*
Transmissivity and storativity.

f) *Compare the calibrated model parameters with the initial database - comments?*
The majority of material properties were similar to those of the base case. The major differences were the addition of a mystery feature, changes to NNW-5 and the increase in storativity in selected large scale fractures.

7. SENSITIVITY ANALYSIS

Identify the sensitivity in your model output to:

a) the discretization used

The model was relatively insensitive to the discretization, due to the dominance of the LSF on the model results.

b) the transmissivity/hydraulic conductivity (distribution) used

The transmissivity was important. It affected the match to the drawdowns during tunnel construction.

c) transport parameters used

The model showed a strong sensitivity to the choice of "particle tracking" algorithm used. Additionally the storativity and aperture effected breakthrough times, and were hard to estimate prior to the chemistry calibration.

d) chemical mixing parameters used

Insensitive, provided the pathways/particles accounted for flow weighting.

e) chemical reaction parameters used

Stage 3 model used the error term to measure the importance of the chemical reactions.

8. LESSONS LEARNED

a) Given your experience in implementing and modelling the ÄSPÖ site, what changes do you recommend with regards to:

- *Experimental site characterisation?*

  Task 5 demonstrated the importance of collecting high quality, well controlled geochemical data from the very start of the project, and collecting that data on a regular basis throughout the project life.

  Radioisotope data would be useful in order to derive water residence time, so that we can assess the applicability of the model to natural conditions/timescales which are more relevant to PA.

- *Presentation of characterisation data?*

  JNC/Golder proposed to address the capability of a model calibrated using only hydrogeological data to predict groundwater chemistry. So, data delivery of groundwater chemistry data should have been delayed.

  Where data delivered for the project had been pre-processed, it would have been valuable to know initially how the processing had been done (e.g. (1) to know exactly how the M3 code calculated end-members (this information was provided prior to stage 3 modelling), e.g. (2) to know how data were interpolated onto the regular grid used as an initial condition).

  Include a legend and units for all provided information.

  Where feasible, provide all the relevant data in one package.

  Summary table of available data, and most recent version (particularly if some data exists under a different task).

  For time dependent data it would have been useful to know whether the chemistry recorded was likely already influenced by the effect of the tunnel drawdowns or is at its initial state.

- *Performance measures and presentation formats?*

  Fewer performance measures as the large number of measures became distracting. A few core measures would result in a more uniform reporting by the groups.

  The presentation formats could also be rationalised to fewer tables but more explicitly defined.

  Perhaps some of the core information could be pasted into provided tables – so that the results from the groups were more uniform. Obviously the output from DFN and EPM models are very different, so the core tables would need to be carefully defined.

  Perhaps we could have a few very well defined "core" or "level 1" objectives and deliverables to be addressed by all modelling teams. Followed by a range of optional "level 2" and "level 3" objectives/deliverables each to be addressed by a few modelling teams.

  Tritium data were provided, but it was learnt that they should not be used in a quantitative way for distinguishing proportions of mixing components. Inclusion or exclusion of tritium data caused the results of PCA to change. Inclusion of tritium data in calculations of mixing proportions is unsound because these data were obtained over a time frame similar to the half life of tritium.

b) *What additional site-specific data would be required to make a more reliable prediction of the tracer experiments?*

The tracer predictions would benefit from stating how the values of porosity, transport aperture, free water diffusion, etc. (if provided) were derived. Are these site specific or generic? Are these values the median of ranges, should we use a distribution of values, and how much confidence do we have in these parameters.

In many cases it is difficult to find out the test specifics (i.e. how the test was actually done on site) because this information is not part of the core data delivery. This has a big effect on the boundary conditions for many of the numerical transport models.

In the light of experience in other programmes it is considered likely that trace element data, especially Br data, would improve the definition of end-members and their mixing proportions.

c) *What conclusions can be made regarding your conceptual model utilised for the exercise?*

The DFN and DFN/CN conceptual models used by the JNC/Golder team appear to be well applicable to the site and we are generally pleased with the results of our predictions. However, this site shows a dominance of LSF responses, and less large scale channelling. The lack of channelling makes the pipe discretization less appealing than the standard DFN approach (although still a reasonable alternative approach for the smaller scale models).

d) *What additional generic research results are required to improve the ability to carry out predictive modelling of transport on the site scale?*

Generally the Task 5 modelling has shown that the larger scale responses are well replicated, typically better than smaller scale tracer tests where local connectivity is harder to predict and the sensitivity to material property heterogeneity greater.

The main limitation to the current model was the uncertainty in the initial spatial distributions of chemically distinct groundwaters. Therefore, it would be beneficial to conduct additional research aimed at defining the initial chemical conditions more accurately throughout the region.

An additional limitation was the separation of uncertainty in chemical predictions due to spatial uncertainty (i.e. are we correctly predicting where it came from) from that due to chemical reactions (i.e. has it chemically changed due to mixing). The PCA method used is thought to distinguish reaction-dependent components from mixing-dependent components and based on the PCA, it was assumed that reaction-dependent uncertainties were small compared to other uncertainties. However, additional research is needed to confirm or refute the validity of this assumption and to refine the PCA methodology for distinguishing reaction-dependent components.

Additional research in the following fields would also be useful:

- A more accurate initial condition for the chemistry throughout the region.
- Long term injection of non-reactive tracers over a longer time frame might allow the true accuracy of the numerical models to be assessed.
- A method to determine transport aperture from aperture measurements in boreholes or excavations.
- Field testing to correlate transport aperture to transmissivity and determine whether the relationship is scale dependent. (Transport aperture has been correlated to tracer tests for specific sites).

9. RESOLUTION OF ISSUES AND UNCERTAINTIES

a) *What inferences did you make regarding the descriptive structural-hydraulic model on the site scale for the ÄSPÖ site?*

The structural model provided by SKB was sufficient to construct a framework for the hydrogeology of the site. The hydrogeological data was required however, to add the additional mystery feature. The additional geochemical data was required to alter the geometry of feature NNW-5, extending it northwards into a region of more glacially rich groundwater.

b) *What inference did you make regarding the active hydochemical processes, hydrochemical data provided and the hydrochemical changes calculated?*

Generally the end member chemistry measured during the modelled period did not change very much. Therefore the prediction of the initial chemistry at any prediction location was important.

Hence the methodology used for the chemistry extrapolation/interpolation was critical. The lack of measured changes provided a lower bound on the required storage in the fractures and matrix in the vicinity of the measurement. However, less constraint on connectivity was obtained than hoped for.

c) *What issues did your model application resolve?*
Strong and fast drawdown responses due to larger scale feature not identified by regional geological model.
Äspö site is dominated on a regional scale by the regional features.

d) *What additional issues were raised by the model application?*
Sensitivity to assumed "initial state" chemistry throughout the region.
An upper bound on the model transport apertures, and to some extent storativity, was not achieved due to the lack of variation in the measured end member chemistries.
We feel that rapid chemical change mostly occurred along LSFs but not within intact rock, which is more relevant to PA.

10. INTEGRATION OF THE HYDOGEOLOGICAL AND HYDROCHEMICAL MODELLING

a) *How did you integrate the hydrogeological and hydro chemical work?*
➔The modelling steps may be summarised as:
1) create a fracture model of the site
2) construct flow model by adding boundary conditions and meshing the fractures
3) calibrate to hydrogeological model data. This was done by optimising the fits to the heads measured at the monitoring sections by adapting the boundary conditions and large discrete fractures (e.g. adding a skin to the Baltic to increase modelled drawdowns, addition of "mystery feature").
4) following head calibration, this model was run with the initial condition groundwater chemistry and a geochemical comparison documented.
5) the differences between the measured and modelled geochemistry were used to calibrate the hydrogeologic model. This calibration resulted in the extension of NNW-5.

The integration was undertaken by decoupling the processes. The chemistry was considered as pure mixing in the particle tracking. However, a PCA methodology was used to redefine the principal components into seven types more representative of the overall chemical system.

b) *How can the integration of the hydrogeological and hydrochemical work be improved?*
Generally the most realistic independent hydrogeological and hydrochemical codes are not fully coupled. Therefore to make best use of both capabilities, the chemistry should be analysed to provide information on the mixing and location of the waters through inverse modelling. e.g. what would the chemistry have been if only advection, dispersion, and diffusion had occurred?

c) *Hydrogeologist: How has the hydrochemistry contributed to your understanding of the hydrogeology around the Äspö site?*
The hydrochemistry provides more detailed information on the directional connectivity and aperture/storativity on a regional scale.

d) *Hydrochemist: How has the hydrogeology contributed to your understanding of the hydrochemistry around the Äspö site?*
The fact that the stage 3 model produced reasonable consistency between predictions and observations improves confidence in the stage 3 model for the initial spatial distributions of chemically distinct waters.
The work emphasised the importance of fracture zones for controlling mixing between chemically distinct waters and hence groundwater chemistry.

Table 1 Description of model for water flow calculations

TOPIC	Example	JNC/Golder Model
Type of model	Stochastic continuum model	Stochastic Discrete Fracture Network (DFN) Model
Process description	Darcy´s flow including density driven flow. (Transport equation for salinity is used for calculation of the density)	Transient flow solution using Darcy's flow equations.
Geometric framework and parameters	Model size: 1.8x1.8x1 km^3 . Deterministic features: All deterministic features provided in the data set. Rock outside the deterministic features modelled as stochastic continuum.	Model Size: N-S 2.0 km; E-W 2km; depth 1 km Deterministic features: All SKB deterministic features provided in the data set. In addition an additional "mystery feature" was added to match the drawdown responses. Deterministic BH features: features added through BH sections to improve connectivity BH to DFN model. Stochastic features: Background features modelled using stochastic discrete features.
Material properties and hydrological properties	Deterministic features: Transmissivity (T), Storativity(S) Rock outside deterministic features: Hydraulic conductivity(K), Specific storage (Ss)	All features: Transmissivity (T) Storativity (S) Aperture (A)
Spatial assignment method	Deterministic features: Constant within each feature (T,S). No changes due to calibration. Rock outside deterministic features: (K,Ss) lognormal distribution with correlation length xx. Mean, standard deviation and correlation based on calibration of the model	Deterministic features: Constant within each feature (T,S,A). No changes in T due to calibration. Transport Aperture set at 2 $T^{0.5}$. Storativity baseline 0.001 $T^{1/2}$. S increased by: EW-1S – factor of 3 EW-3 (z<200) – factor of 3.2 NE-2 - factor of 3.3 NE-4N - factor of 3.5 NNW2 - factor of 1.5 NNW-8 - factor of 1.7 Mystery feature: T = 1.e-5 m^2/s. A = $2T^{0.5}$. S= 0.001 $T^{1/2}$. Background features: Orientation bootstrapped. T – LogNormal (μ = 9 x 10^{-7} m^2/s, σ = 5 x 10^{-6} m^2/s). A = $2T^{0.5}$. S= 0.001 $T^{1/2}$.
Boundary conditions	Surface: Constant flux. Sea: Constant head Vertical-North: Fixed pressure based on vertical salinity distribution. Vertical-East: Fixed pressure based on vertical salinity distribution. Vertical-South: Fixed pressure based on vertical salinity distribution. Vertical-West: Fixed pressure based on vertical salinity distribution. Bottom: No flux. Linear change by time based regional simulations for undisturbed conditions and with Äspö tunnel present.	Base: "no flow" boundary (= constant flux of 0.0 at each node) Sides: The sides of the model were specified as constant head values interpolated from the density corrected values of Svensson (1999). Surface of Äspö Island: was specified to have a constant infiltration rate of either 0.0 mm/year or 30.0 mm/year. Infiltration of 0 mm/year was used for final simulations. Baltic seabed: A constant head boundary condition of 0.0 m. Äspö tunnel: Tunnel prior to construction: group flow rate of 0.0 m3/s. Tunnel following section construction: flow rate equal to the measured inflow rate.
Numerical tool	PHOENICS	FracMan / PAWorks
Numerical method	Finite volume method	Finite Element Method
Output parameters	Head, flow and salinity field.	Head, net flow at nodes, particle location with time.

Table 2 Description of model for tracer transport calculations

TOPIC	EXAMPLE	JNC/Golder model
Type of model	Stochastic continuum model	Stochastic Discrete Fracture Network (DFN) Model
Process description	Advection and diffusion, spreading due to spatially variable velocity and molecular diffusion.	Tasks 1 and 2: Advection corrected for fluid density. Task 3: Advection with stochastic dispersion along flow lines.
Geometric framework and parameters	Model size: 1.8x1.8x1 km^3 . Deterministic features: All deterministic features provided in the data set. Rock outside the deterministic features modelled as stochastic continuum.	Model Size: N-S 2.0 km; E-W 2km; depth 1 km Deterministic features: All SKB deterministic features provided in the data set. In addition an additional "mystery feature" was added to match the drawdown responses. NNW-5 was extended north to collect more glacial water. Deterministic BH features: features added through BH sections to improve connectivity BH to DFN model. Stochastic features: Background features modelled using stochastic discrete features.
Material properties	Flow porosity (ne)	Transport aperture
Spatial assignment method	ne based on hydraulic conductivity value (TR 97-06) for each cell in model, including deterministic features and rock outside these features.	Aperture $A = 2T^{0.5}$.
Boundary conditions	Mixing ratios for end-members as provided as initial conditions in data sets.	Stage 1 and 2 : Initial geochemical conditions were provided at 98 locations, in Appendix 14 of Data Delivery 7 using M3. These values were extrapolated by SKB (Rhén, 1998) using Kriging to a grid of 1000 locations. Stage 3: Chemistry at monitoring locations extrapolated to LSFs within 50m. Chemistry on LSF derived based on monitoring points, proximity to Baltic, chemical depth profiles. All particles projected to nearest LSF prior to interpolation of chemistry.
Numerical tool	PHOENICS	FracMan / PAWorks
Numerical method	Particle tracking method or tracking components by solving the advection/diffusion equation for each component	Stage 1 and 2: Graph theory searches through the channel network model. Stage 3: Particle tracking using 76 time varying head solutions.
Output parameters	Breakthrough curves	Location of particles at 30 day intervals.

Table 3 Description of model for chemical reactions calculations

TOPIC	EXAMPLE	JNC/Golder model
Type of model	xxx	Stage 1 and 2 : Mixing using M3 chemistry Stage 3 : Principal Component Analysis (PCA)
Process description	Mixing. Reactions: Xx, Yy,Zz,Dd…..	Stage 1 and 2: Mixing. Stage 3: Mixing – deviation indicates chemical reactions.
Geometric framework and parameters	Modelling reactions within one fracture zone, NE-1.	
Reaction parameters	Xx: a=ff, b=gg,… Yy: c=. Zz: d=...	
Spatial distribution of reactions assumed	Xx: seafloor sediments Yz: Bedrock below sea, superficial Dd: Bedrock ground surface, superficial Yz: Bedrock below sea, at depth Zz: Bedrock ground surface, at depth Yy, Zz: near tunnel	
Boundary/initial conditions for the reactions	Xx: aaa… Yy: bbb…	The measured chemical components at the monitoring locations.
Numerical tool	Phreeque	Chemometric algorithm of Cave and Harmon, 1997/Cave and Wragg, 1997.
Numerical method	xx	PCA
Output parameters	xx	Principal components and their distribution.

Table 4a Summary of data usage

Data del. No	Data	Importance of data (see notes)	Comment
1	Hydrochemical data 1		
1a	Surface bore holes- undisturbed conditions, Äspö-Laxemar	*m*	Superseded interpretations of these data were used for the initial conditions and in the calibration.
1b	Surface bore holes- disturbed conditions (by tunnel excavation), Äspö	*m*	as above
1c	Surface bore holes- undisturbed conditions, Ävrö	*m*	as above
1d	Surface bore holes- sampled during drilling, Äspö	*m*	as above
1e	Data related to the Redox experiment	-	
1f	Tunnel and tunnel bore holes- disturbed conditions	*m*	as above
2	Hydogeological data 1		
2a1	Annual mean air temperature	-	
2a2	Annual mean precipitation	*p*	Used to determine the probably net infiltration rate over Äspö Island.
2a3	Annual mean evapotranspiration	*p*	Used to determine the probably net infiltration rate over Äspö Island.
2b1	Tunnel front position by time	**P**	Geometry and construction time used as part of the tunnel boundary condition.
2b2	Shaft position by time	**P**	Geometry and construction time used as part of the shaft boundary condition.
2c1	Geometry of main tunnel	**P**	Required for the explicit modelling of the tunnels and shafts.
2c2	Geometry of shafts	**P**	Required for the explicit modelling of the tunnels and shafts.
2d	Hydrochemistry at weirs (Cloride, pH, Electrical conductivity, period: July 1993- Aug 1993)	-	
2e	Geometry of the deterministic large hydraulic features (Most of them are fracture zones)	**P**	Required to explicitly model the LSFs.

Table 4b Summary of data usage

Data del. No	Data	Importance of data (see notes)	Comment
3	Hydrogeological data 2		
3a	Monthly mean flow rates measured at weirs. Tunnel section 0-2900m, period May 1991 – January 1994	**P**	Used as the group flow rate boundary conditions for the tunnel sections.
3b	Piezometric levels for period June 1st 1991 – May 21st 1993. Values with 30 days interval (Task 3 data set)	**P**	Provided heads for the hydrogeological calibration.
3c	Salinity levels in bore hole sections for period -Sept 1993. (Task 3 data set)	-	
3d	Undisturbed piezometric levels	*p*	
3e	Co-ordinates for bore hole sections	**P**	Used to explicitly model the BH sections in the DFN model.
3f	Piezometric levels for period July 1st 1990 – January 24st 1994. Daily values.	**P**	Used to provide 30 days interval heads for the hydrogeological calibration.
4	Hydochemical data 2		
4a	Chemical components, mixing proportions and deviations for all bore hole sections used in the M3 calculations	X	
4b	Bore holes with time series, > 3 samples (part of 4a)	*p*	Information used for the geochemical calibration (superseded by later data).
4c	Bore holes sections interpreted to intersect deterministic large hydraulic features (Most of them are fracture zones) (part of 4a)	X	This information is useful, but the data was independently computed for the Stage 3 modelling as we required the distance of all boreholes from the LSFs.
4d	Chemical components, mixing proportions and deviations. Grid data based on interpolation. Undisturbed conditions	*p*	Information used for the Stage 1 and 2 geochemical initial conditions (superseded by the improved methodology of Stage 3).
4e	Chemical components, mixing proportions and deviations. Grid data based on interpolation. Disturbed conditions (by tunnel excavation)	X	Not explicitly used because the geochemistry change was modelled by the FracMan/PAWorks code. But interesting for comparison with the final condition.
4f	Boundary and initial conditions. Chemical components, mixing proportions and deviations (1989). Grid data for vertical boundaries based on interpolation. Undisturbed conditions	*p*	Information used for the Stage 1 and 2 geochemical initial conditions (superseded by the improved methodology of Stage 3).
4g	Boundary conditions after tunnel construction (1996) Chemical components, mixing proportions and deviations. Grid data for vertical boundaries based on interpolation. Disturbed conditions (by tunnel excavation)	X	Not explicitly used because the geochemistry change was modelled by the FracMan/PAWorks code. But interesting for comparison with the final condition.

Table 4c Summary of data usage

Data del. No	Data	Importance of data (see notes)	Comment
5	Geographic data 1		
5a	Äspö coast line	**P**	Simplified version of Äspö coastline was used in Stage 3 to differentiate between chemistry under Baltic and Äspö Island.
5b	Topography of Äspö and the nearby surroundings	*m*	Topography of Äspö not used. However, at a different sites this information might have been explicitly used.
6	Hydro tests and tracer tests		
6a	Large scale interference tests (19 tests)	X	This data was not explicitly used due to the availability of long term measurements in the boreholes.
6b	Long time pump and tracer test, LPT2	-	as above
7	Hydochemical data 3, update of data delivery 4 based on new end-members. Recommended to be used instead of 4.		
7a	Chemical components, mixing proportions and deviations for all bore hole sections used in the M3 calculations	**P**	Information used for the geochemical initial conditions in Stage 3 and all geochemical calibration.
7b	Bore holes with time series, > 3 samples (part of 7a)	**P**	Information used for the geochemical initial conditions in Stage 3 and all geochemical calibration.
7c	Bore holes sections interpreted to intersect deterministic large hydraulic features (Most of them are fracture zones) (part of 7a)	X	This information is useful, but the data was independently computed for the Stage 3 modelling as we required the distance of all boreholes from the LSFs.
7d	Chemical components, mixing proportions and deviations. Grid data based on interpolation. Undisturbed conditions	*p*	Information used for the Stage 1 and 2 geochemical initial conditions (superseded by the improved methodology of Stage 3).
7e	Chemical components, mixing proportions and deviations. Grid data based on interpolation. Disturbed conditions (by tunnel excavation)	X	Not explicitly used because the geochemistry change was modelled by the FracMan/PAWorks code. But interesting for comparison with the final condition.
7f	Boundary and initial conditions. Chemical components, mixing proportions and deviations (1989). Grid data for vertical boundaries based on interpolation. Undisturbed conditions	*p*	Information used for the Stage 1 and 2 geochemical initial conditions (superseded by the improved methodology of Stage 3).
7g	Boundary conditions after tunnel construction (1996) Chemical components, mixing proportions and deviations. Grid data for vertical boundaries based on interpolation. Disturbed conditions (by tunnel excavation)	X	Not explicitly used because the geochemistry change was modelled by the FracMan/PAWorks code. But interesting for comparison with the final condition.

Table 4d Summary of data usage

Data del. No	Data	Importance of data (see notes)	Comment
8	Performance measures and reporting 1		
8a	Performance measures	**M**	Useful to have specific measures and locations to enable relative performance of models to be measured.
8b	Suggested control points. 6 points in tunnel section 0-2900m and 3 point in tunnel section 2900-3600m.	**M**	
8c	Suggested flowchart for illustration of modelling	*m*	
9	Hydrogeological data 3		
9a	Monthly mean flow rates measured at weirs. Tunnel section 0-3600m, period: May 1991- Dec 1996.	**P**	Required for tunnel boundary condition.
10	Geographic data 2		
10a	Topography of Äspö and the nearby surroundings (larger area than 5b)	-	Not used for Äspö, however at a different site these features may be explicitly modelled. Therefore data is important.
10b	Co-ordinates for wetlands	-	Not used for Äspö, however at a different site these features may be explicitly modelled. Therefore data is important.
10c	Co-ordinates for lakes	-	Not used for Äspö, however at a different site these features may be explicitly modelled. Therefore data is important.
10d	Co-ordinates for catchments	-	Not used for Äspö, however at a different site these features may be explicitly modelled. Therefore data is important.
10e	Co-ordinates for streams	-	Not used for Äspö, however at a different site these features may be explicitly modelled. Therefore data is important.
10f	Co-ordinate transformation Äspö system- RAK	-	
11	Boundary and initial conditions		
11a	Pressure before tunnel construction, from the regional SKB model (TR 97-09)	**M**	
11b	Salinity before tunnel construction, from the regional SKB model (TR 97-09)	**P**	Information used for the Stage 1 and 2 density correction used for the velocity within the graph theory derived pathways. The density correction was not used for the Stage 3 modelling.
11c	Pressure after tunnel construction, from the regional SKB model (TR 97-09)	X	
11d	Salinity after tunnel construction, from the regional SKB model (TR 97-09)	*m*	

Table 4e Summary of data usage

Data del. No	Data	Importance of data (see notes)	Comment
13	Performance measures and reporting 2		
13a	Suggested control points. 6 points in tunnel section 0-2900m and 3 point in tunnel section 2900-3600m (same as 8b) and 2 outside the tunnel.	**P**	Used for the focus of the later calibration.
12	Transport parameters compiled		
12a	LPT2 tracer tests	X	
12b	Tracer test during passage of fracture zone NE-1	X	
12c	Redox tracer tests	-	
12d	TRUE-1 tracer tests	X	
14	Hydrochemical data 4		
14a	Groundwater reactions to consider within TASK5 modelling (Description of how M3 calculates the contribution of reactions and identifying dominating reactions based on the M3 calculations.	X	Useful for getting an overview of the geochemistry.
15	Co-ordinates for the test sections defining the control points	**P**	required for calibration. Coordinates required to explicitly model the monitoring section.
16	Co-ordinates for bore holes drilled from the tunnel	X	Arrived too late to be fully incorporated into the modelling.

Table 4f Summary of data usage

Data del. No	Data	Importance of data (see notes)	Comment
17	Hydogeological data - prediction period		
17a	Hydrochemistry at weirs (Cloride, pH, Electrical conductivity, period: July 1993- Dec 1995)	X	
17b	Piezometric levels for period July 1st 1990 – Dec 1996. Daily values.	X	
18	Hydochemical data - prediction period.		
18a	Chemical components, mixing proportions and deviations for all bore hole sections used in the M3 calculations. Data for tunnel section 2900-3600m.	**P**	Provides information to check validity of the model calibration and gain greater insight into how the groundwater system is operating
18b	Bore holes with time series, > 3 samples (part of 18a)	**P**	Provides information to check validity of the model calibration and gain greater insight into how the groundwater system is operating
18c	Bore holes sections interpreted to intersect deterministic large hydraulic features (Most of them are fracture zones) (part of 18a)	X	Important information. This was independently calculated as part of the modelling procedure.
	Other data (part of data to Task 1, 3 and 4)		
	Fracture orientation, fracture spacing and trace length – tunnel data	**P**	The JNC/Golder model explicitly models the fractures. Hence the size and orientation of the features is important, effecting the connectivity and flow volume through the background features. Terzaghi affect means that measurements at different orientations provides a better data set. Similarly, truncation and plane angle affects size measurement – different scales provide the greatest data range.
	Fracture orientation, fracture spacing– mapping of cores	**P**	as above
	Fracture orientation, fracture spacing and trace length – mapping of outcrops	**P**	as above

P = data of great importance for quantitative estimation of model parameters
p = data of less importance for quantitative estimation of model parameters
M = data of great importance used qualitatively for setting up model
m = data of less importance used qualitatively for setting up model
X = data useful as general background information
- = data not used